

AD-A184 864

# NAVAL POSTGRADUATE SCHOOL

Monterey, California

DTIC FILE COPY

2



DTIC  
ELECTE  
OCT 0 2 1987  
S D  
Ch D

## THESIS

THE USE OF COAXIAL TRANSMISSION LINE  
ELEMENTS  
IN LOG-PERIODIC DIPOLE ARRAYS

by

Robert E. Tarleton, Jr.

June 1987

Thesis Advisor

Richard W. Adler

Approved for public release; distribution is unlimited.

87 9 25 123

REPORT DOCUMENTATION PAGE

<b>1a</b> REPORT SECURITY CLASSIFICATION UNCLASSIFIED		<b>1b</b> RESTRICTIVE MARKINGS													
<b>2a</b> SECURITY CLASSIFICATION AUTHORITY		<b>3</b> DISTRIBUTION / AVAILABILITY OF REPORT Approved for public release; distribution unlimited													
<b>2b</b> DECLASSIFICATION / DOWNGRADING SCHEDULE															
<b>4</b> PERFORMING ORGANIZATION REPORT NUMBER(S)		<b>5</b> MONITORING ORGANIZATION REPORT NUMBER(S)													
<b>6a</b> NAME OF PERFORMING ORGANIZATION Naval Postgraduate School	<b>6b</b> OFFICE SYMBOL <i>(if applicable)</i> Code 62	<b>7a</b> NAME OF MONITORING ORGANIZATION Naval Postgraduate School													
<b>6c</b> ADDRESS (City, State, and ZIP Code) Monterey, California 93943-5000		<b>7b</b> ADDRESS (City, State, and ZIP Code) Monterey, California 93943-5000													
<b>8a</b> NAME OF FUNDING / SPONSORING ORGANIZATION	<b>8b</b> OFFICE SYMBOL <i>(if applicable)</i>	<b>9</b> PROCUREMENT INSTRUMENT IDENTIFICATION NUMBER													
<b>10a</b> ADDRESS (City, State, and ZIP Code)		<b>10</b> SOURCE OF FUNDING NUMBERS <table border="1" style="width:100%; border-collapse: collapse;"> <tr> <td style="width:25%;">PROGRAM ELEMENT NO.</td> <td style="width:25%;">PROJECT NO.</td> <td style="width:25%;">TASK NO.</td> <td style="width:25%;">WORK UNIT / ACCESSION NO.</td> </tr> <tr> <td> </td> <td> </td> <td> </td> <td> </td> </tr> </table>		PROGRAM ELEMENT NO.	PROJECT NO.	TASK NO.	WORK UNIT / ACCESSION NO.								
PROGRAM ELEMENT NO.	PROJECT NO.	TASK NO.	WORK UNIT / ACCESSION NO.												
<b>11</b> TITLE (Include Security Classification) THE USE OF COAXIAL TRANSMISSION LINE ELEMENTS IN LOG-PERIODIC DIPOLE ARRAYS															
<b>12</b> PERSONAL AUTHOR(S) Warleton, Robert E., Jr.															
<b>13</b> TYPE OF REPORT Master's Thesis	<b>14</b> TIME COVERED FROM _____ TO _____	<b>15</b> DATE OF REPORT (Year Month Day) 1987 June	<b>16</b> PAGES (Total) 170												
<b>17</b> REPRESENTATIVE NOTATION															
<table border="1" style="width:100%; border-collapse: collapse;"> <thead> <tr> <th colspan="3">COSATI CODES</th> </tr> <tr> <th>FIELD</th> <th>GROUP</th> <th>SUB GROUP</th> </tr> </thead> <tbody> <tr> <td> </td> <td> </td> <td> </td> </tr> <tr> <td> </td> <td> </td> <td> </td> </tr> </tbody> </table>		COSATI CODES			FIELD	GROUP	SUB GROUP							<b>18</b> SUBJECT TERMS (Continue on reverse if necessary and identify by block number) Log-periodic dipole array, k-beta diagram, Snyder dipole, Numerical Electromagnetics Code	
COSATI CODES															
FIELD	GROUP	SUB GROUP													
<b>19</b> ABSTRACT (Continue on reverse if necessary and identify by block number) This thesis examines the feasibility of designing a log-periodic dipole array (LPDA) with coaxial transmission line elements and comparing the resulting operational bandwidth with that of a conventional LPDA. Using the Numerical Electromagnetics Code (NEC), a coaxial dipole was modeled to optimize the bandwidth and then used as the element in a variety of uniform arrays. Different types of element connections were examined including switched series, switched parallel, and unswitched parallel. The results of NEC for each of the arrays are plotted as k- $\beta$ diagrams to compare to the standard arrays. The results of the investigation show that the Snyder dipole provides more operational bandwidth than a standard dipole, but when placed in a uniform array there is no more bandwidth than that of a conventional uniform array.															
<b>20</b> DISTRIBUTION STATEMENT OF ABSTRACT <input checked="" type="checkbox"/> UNCLASSIFIED / UNLIMITED <input type="checkbox"/> SAME AS RPT <input type="checkbox"/> DTIC USERS		<b>21</b> ABSTRACT SECURITY CLASSIFICATION UNCLASSIFIED													
<b>22a</b> NAME OF RESPONSIBLE PERSON Richard W. Adler		<b>22b</b> TELEPHONE (include Area Code) (408) 646-2352	<b>22c</b> DTIC REPORT NUMBER 62Ab												

Approved for public release; distribution is unlimited.

The Use of Coaxial Transmission Line Elements  
in Log-periodic Dipole Arrays

by

Robert E. Tarleton, Jr.  
Electronic Engineer, Department of Defense  
B.S.E., Arizona State University, 1980

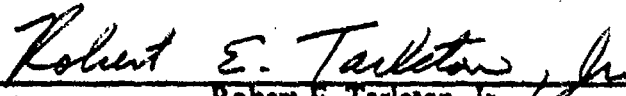
Submitted in partial fulfillment of the  
requirements for the degree of

MASTER OF SCIENCE IN ELECTRICAL ENGINEERING

from the

NAVAL POSTGRADUATE SCHOOL  
June 1987


Author:


  
Robert E. Tarleton, Jr.

Approved by:

  
Richard W. Adler, Thesis Advisor

  
W. Ray Vincent, Second Reader

  
John P. Powers, Chairman,  
Department of Electrical and Computer Engineering

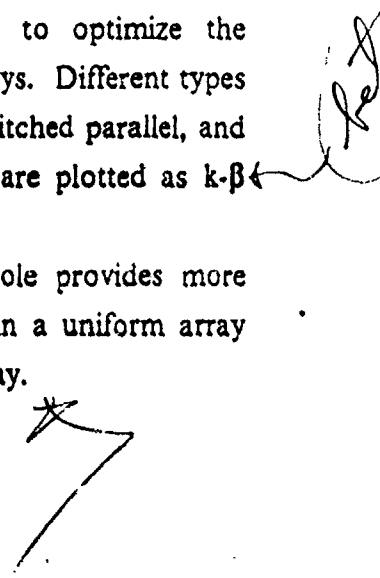
  
Gordon E. Schacher,  
Dean of Science and Engineering



# ABSTRACT

This thesis examines the feasibility of designing a log-periodic dipole array (LPDA) with coaxial transmission line elements and comparing the resulting operational bandwidth with that of a conventional LPDA. Using the Numerical Electromagnetics Code (NEC), a coaxial dipole was modeled to optimize the bandwidth and then used as the element in a variety of uniform arrays. Different types of element connections were examined including switched series, switched parallel, and unswitched parallel. The results of NEC for each of the arrays are plotted as  $k-\beta$  diagrams to compare to the standard arrays.

The results of the investigation show that the Snyder dipole provides more operational bandwidth than a standard dipole, but when placed in a uniform array there is no more bandwidth than that of a conventional uniform array.



Accession For	
NTIS	CRA&I
DTIC	TAB
Unannounced	<input type="checkbox"/>
Justification	<input type="checkbox"/>
By .....	
Distribution/ .....	
Availability Codes	
Dist	Avail and/or Special
A-1	

## TABLE OF CONTENTS

I.	INTRODUCTION .....	8
A.	THE LOG-PERIODIC ANTENNA .....	8
B.	THE LOG-PERIODIC DIPOLE ARRAY .....	9
C.	CHARACTERISTICS OF SUCCESSFUL LOG-PERIODIC ANTENNAS .....	11
D.	THE LPDA WITH COAXIAL ELEMENTS .....	11
II.	DEVELOPMENT OF THE SNYDER DIPOLE .....	13
A.	THE NUMERICAL ELECTROMAGNETICS CODE .....	13
B.	PROCEDURE FOR OBTAINING OPTIMUM SNYDER DIPOLE .....	13
III.	K-BETA DIAGRAMS .....	17
A.	K-BETA DIAGRAM DESCRIPTION .....	17
B.	OBTAINING THE K-BETA DIAGRAM DATA USING NEC .....	18
IV.	EXPERIMENTAL PROCEDURES AND RESULTS .....	20
A.	CHARACTERISTICS OF UNTAPERED ARRAYS .....	20
B.	DEVELOPMENT OF THE SNYDER LPDA .....	20
C.	EXPERIMENTAL RESULTS .....	21
1.	Switched Series Array .....	21
2.	Switched Parallel Array .....	23
3.	Unswitched Parallel Array .....	32
D.	COMPARISON OF SNYDER ARRAY TO CONVENTIONAL ARRAY .....	32
V.	CONCLUSIONS AND RECOMMENDATIONS .....	44
APPENDIX A:	NEC DATA SETS .....	46

APPENDIX B:	NEAR-MAGNETIC FIELD PLOTS FOR SNYDER SWITCHED SERIES ARRAYS .....	48
APPENDIX C:	NEAR-MAGNETIC FIELD PLOTS FOR SNYDER SWITCHED PARALLEL ARRAYS .....	87
APPENDIX D:	NEAR-MAGNETIC FIELD PLOTS FOR SNYDER UNSWITCHED PARALLEL ARRAY .....	132
APPENDIX E:	NEAR-MAGNETIC FIELD PLOTS FOR STANDARD ELEMENT ARRAYS .....	147
LIST OF REFERENCES .....		162
INITIAL DISTRIBUTION LIST .....		163

## LIST OF FIGURES

1.1	Log-periodic Toothed Planar Antenna (from Ref. 2) .....	9
1.2	Log-periodic Dipole Array (from Ref. 2) .....	10
1.3	Connection of LPDA Elements (from Ref. 3) .....	10
1.4	The Snyder Dipole (from Ref. 5) .....	12
2.1	Dipole and Transmission Line Susceptances .....	15
2.2	Standard Dipole and Snyder Dipole Bandwidths .....	16
3.1	$k$ - $\beta$ Diagram (from Ref. 8) .....	17
4.1	Types of Voltage Feed .....	22
4.2	$k$ - $\beta$ Diagram for a Snyder Switched Series Array. Element Spacing = 1/8 Wavelength .....	24
4.3	Attenuation of a Snyder Switched Series Array. Element Spacing = 1/8 Wavelength .....	25
4.4	$k$ - $\beta$ Diagram for a Snyder Switched Series Array. Element Spacing = 1/4 Wavelength .....	26
4.5	Attenuation of a Snyder Switched Series Array. Element Spacing = 1/4 Wavelength .....	27
4.6	$k$ - $\beta$ Diagram for a Snyder Switched Series Array. Element Spacing = 3/8 Wavelength .....	28
4.7	Attenuation of a Snyder Switched Series Array. Element Spacing = 3/8 Wavelength .....	29
4.8	$k$ - $\beta$ Diagram for a Snyder Switched Parallel Array. Element Spacing = 1/8 Wavelength .....	30
4.9	Attenuation of a Snyder Switched Parallel Array. Element Spacing = 1/8 Wavelength .....	31
4.10	$k$ - $\beta$ Diagram for a Snyder Switched Parallel Array. Element Spacing = 1/4 Wavelength .....	33
4.11	Attenuation of a Snyder Switched Parallel Array. Element Spacing = 1/4 Wavelength .....	34
4.12	$k$ - $\beta$ Diagram for a Snyder Switched Parallel Array. Element Spacing = 3/8 Wavelength .....	35
4.13	Attenuation of a Snyder Switched Parallel Array. Element Spacing = 3/8 Wavelength .....	36

4.14	k- $\beta$ Diagram for a Snyder Unswitched Parallel Array. Element Spacing = 1/4 Wavelength . . . . .	37
4.15	Attenuation of a Snyder Unswitched Parallel Array. Element Spacing = 1/4 Wavelength . . . . .	38
4.16	k- $\beta$ Diagram for a Standard Switched Parallel Array. Element Spacing = 3/8 Wavelength . . . . .	40
4.17	Attenuation of a Standard Switched Parallel Array. Element Spacing = 3/8 Wavelength . . . . .	41
4.18	k- $\beta$ Diagram Comparison . . . . .	42
4.19	Attenuation Comparison . . . . .	43



## I. INTRODUCTION

### A. THE LOG-PERIODIC ANTENNA

The log-periodic antenna (LPA) is structured so that its impedance and radiation characteristics repeat periodically as the logarithm of frequency. The variations over the operational frequency are minor so that the LPA is considered to be frequency independent.

The LPA design is based on relatively simple ideas that produce bandwidths of operation that were considered impossible several decades ago. One of these ideas is the angle condition which specifies an antenna array by angles only and not by specific dimensions. In this case the antenna is self-scaling and eliminates the dependence on its characteristic length and operating frequency. The second idea is that if an antenna array's dimensions are scaled by a factor  $\tau$ , it will exhibit the same properties at one frequency as at  $\tau$  times that frequency. These properties are a periodic function of the logarithm of frequency with the period of  $\log \tau$ . Thus the term log-periodic is used to describe these types of antennas. [Ref. 1]

The first successful LPAs were discovered by R.H. DuHamel and D.E. Isbell in the late 1950s. Many unsuccessful attempts were log-periodic but produced unacceptable variations of pattern and impedance over a period. One of the first successful LPAs was the log-periodic toothed planar antenna (Figure 1.1). Current flows out along the teeth and is insignificant at the ends. The ratio of edge distance is a constant factor given by:

$$\tau = R_{n+1}/R_n < 1 \quad (\text{eqn 1.1})$$

The slot width is:

$$\sigma = a_n/R_n < 1 \quad (\text{eqn 1.2})$$

The scaling factor  $\tau$  gives the period of the antenna. The frequencies  $f_{n+1}$  and  $f_n$  lead to identical performance so the antenna is logarithmically periodic. [Ref. 2: p.290]

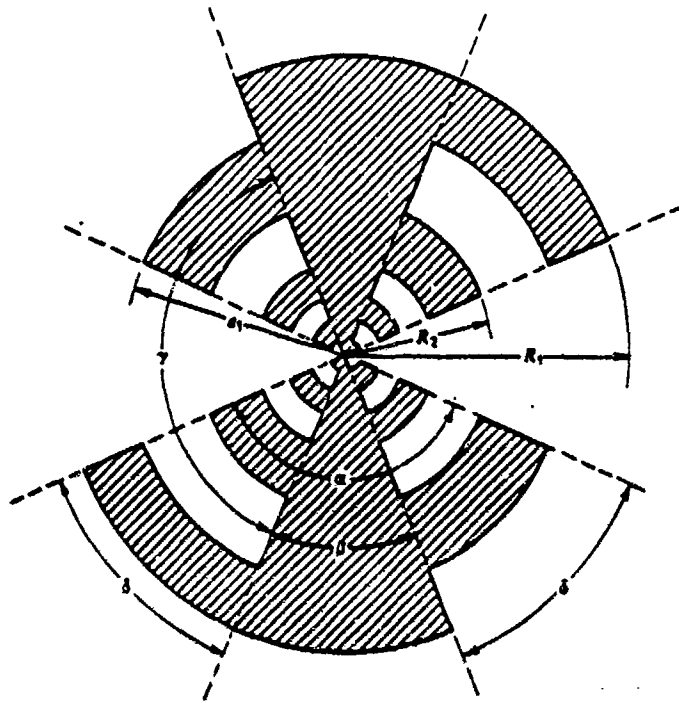


Figure 1.1 Log-periodic Toothed Planar Antenna (from Ref. 2).

## B. THE LOG-PERIODIC DIPOLE ARRAY

After a few years of experimenting, Isbell developed the log-periodic dipole array (LPDA), an array of parallel wire dipole elements of increasing length outward from the apex feed point (Figure 1.2). He used a parallel load with switched phase from one element to the next. This is still the most common method used, although other feed types have also been used successfully. [Ref. 3: p. 55]

The switched feed in Isbell's LPDA produces a 180 degree phase shift between elements. The elements near the input nearly cancel since they are close together and almost out of phase. As the spacing between elements ( $d$ ) increases, the phase delay in the transmission line combined with the 180 degree phase shift gives a total of  $360(1-d/\lambda)$  degrees. The radiated fields of the two dipoles are then  $d$  apart in phase in the backward direction. Moving further out increases the phase delay, causing the in-phase direction to move from backward to broadside to forward radiation. If the elements are resonant with the total phase delay from one element to the next equal to about  $360(1-d/\lambda)$  degrees, a good beam is generated off the apex. Due to this condition, the transmission line power is exhausted before the phase changes very much.

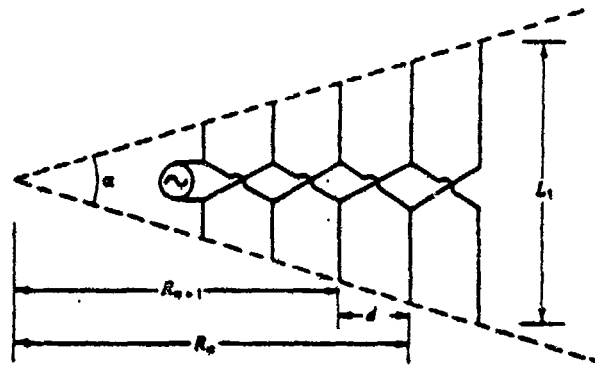


Figure 1.2 Log-periodic Dipole Array (from Ref. 2).

The antenna is fed by running a coaxial line inside one side of the boom and connecting its inner conductor to the other side at the input (Figure 1.3) [Ref. 3: p. 71]. This forms a parallel feed with switched phasing between the elements. This method of current feed will be investigated and applied in this thesis as will series switched and parallel unswitched feeds.

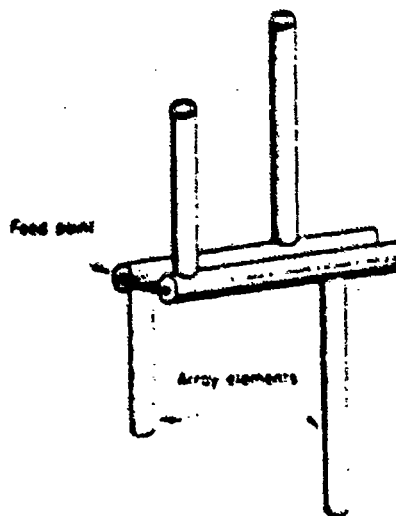


Figure 1.3 Connection of LPDA Elements (from Ref. 3).

### C. CHARACTERISTICS OF SUCCESSFUL LOG-PERIODIC ANTENNAS

There are several characteristics associated with log-periodic antennas. By definition, the electrical properties must repeat periodically with the logarithm of the frequency to help ensure broadband performance. To maintain frequency independence, the electrical properties must vary only slightly over a period, and the current must decay rapidly over an active region to eliminate end effects caused by truncation of the electrical length of the antenna. The log-periodic antenna must also produce backward wave radiation (towards the feed point). Backward radiation can be determined by observing an antenna array with the feed point on the left. As the wave travels to the right, backward radiation occurs if the magnitude of the current is sharply attenuated as it moves across the left most element of the active region and the phase increases in the element on the right. This will cause the antenna to radiate at the feed point to the left with a null to the right. Thus the wave has propagated in the backward direction. [Ref. 4]

### D. THE LPDA WITH COAXIAL ELEMENTS

Many LPDAs have been designed and built over the last thirty years. What makes this research unique is the use of dipoles made of coaxial transmission line. The coax dipole was patented in 1984 by Mr. Richard D. Snyder and will be referred to as the "Snyder dipole" throughout the remainder of this text to differentiate it from the conventional wire dipole. The Snyder dipole (Figure 1.4) is constructed using coaxial transmission line for the inner portions of its segments, connected so that the outer conductor acts as part of the radiator, and the inner and outer conductors of the coax form compensation stubs. The stubs' impedances vary with frequency in such a way as to cancel the dipole reactance normally exhibited with frequency change, and can be connected in series or parallel. The coax conductors are shorted together at one end of the line so that the non-radiating conductor combines with the second conductor to form an impedance modifying stub and the second conductor forms part of the antenna segment [Ref. 5]. This leads to a larger operational bandwidth than in the conventional dipole.

If an LPDA using Snyder elements proves successful, it will have many advantages in field use over the conventional LPDA, particularly at lower frequencies with long wavelengths. Advantages include allowing a larger deviation from the operating frequency, lighter weight, more rugged, and more easily transportable since the conventional LPDA would require much thicker (and therefore heavier) elements to

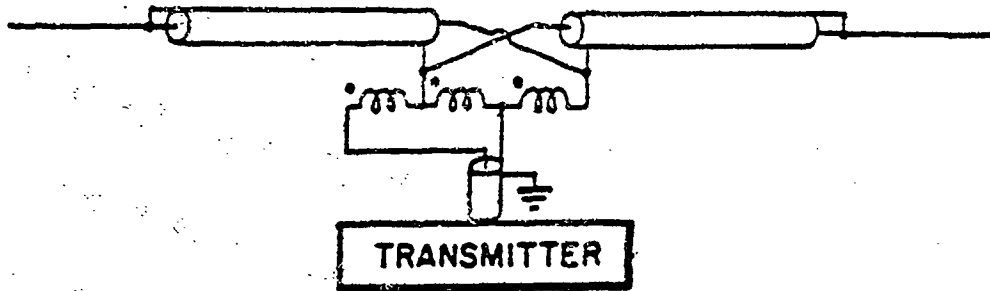


Figure 1.4 The Snyder Dipole (from Ref. 5).

achieve the same bandwidth. Since many of the advantages are size and weight related, the analysis presented herein will be performed on antenna arrays operating in the high frequency (HF) band at 3.88 Megahertz (MHz) with a wavelength of 77.3 meters.

## II. DEVELOPMENT OF THE SNYDER DIPOLE

### A. THE NUMERICAL ELECTROMAGNETICS CODE

All antennas in this research were modeled on an IBM main-frame computer using the Numerical Electromagnetics Code (NEC) version three. NEC was developed by the Lawrence Livermore Laboratory for the Naval Ocean Systems Center (NOSC). It is a user-oriented computer code used to analyze antennas or other metal structures based on the use of numerical solutions of integral equations for currents induced on the structure by an incident plane wave or a voltage source [Ref. 6]. Outputs from NEC include current and charge density, voltage standing wave ratio (VSWR), near electric or magnetic fields, and radiated fields. Single and double precision versions are available for better accuracy as well as versions that allow for large numbers of networks or wires.

### B. PROCEDURE FOR OBTAINING OPTIMUM SNYDER DIPOLE

The goal for the optimum Snyder dipole was to achieve the widest bandwidth possible with a VSWR no greater than 2:1 without exceeding size constraints. Since the operational bandwidth of a dipole increases as the diameter increases, this effort was restricted to 0.3 inches in diameter, about the size of standard coaxial transmission cable. This way the design is consistent with the stated advantages of light weight, ruggedness, and transportability.

The Snyder dipole was modeled on NEC as a standard dipole with two transmission lines in parallel to simulate the coax segments of the antenna. The first step was to model a standard half-wave dipole. It was based on a frequency of 3.88 MHz which has a wavelength of 77.3 meters. The dipole was modeled for free space propagation with no ground plane and the transmission line segments were modeled as one-fourth wavelength stubs. Both the dipole and the transmission lines were swept through a frequency range of 3.5 to 4.2 MHz with a resulting output of admittance at each frequency. The susceptance (imaginary part of the admittance) for the dipole was capacitive below resonance and inductive above resonance. The susceptance for the parallel transmission lines was inductive below resonance and capacitive above resonance, the opposite of the dipole. The impedance of the transmission lines were then varied until a value was found which provided maximum cancellation of the

dipole susceptance. The addition of the transmission line and dipole impedances are shown in Figure 2.1. A value of 50 ohms for each of the parallel transmission lines was found to best counter the susceptance characteristics of the dipole. The transmission lines and dipole were then combined to model the Snyder dipole with the transmission lines acting as the compensation stubs that cancel the antenna reactance normally associated with frequency change. This is what makes the Snyder dipole more broadband than the conventional dipole.

The next step entailed the modeling of the Snyder dipole using NEC, and tweaking the input impedance, or balun load, so as to produce the largest bandwidth possible with a VSWR not greater than 2:1. The model used for the Snyder dipole is given in Appendix A, and the comparison of bandwidth for the Snyder dipole and the standard dipole is shown in Figure 2.2. The standard dipole bandwidth is about 6 percent while the Snyder dipole bandwidth is over 16 percent. The standard dipole diameter shown is equal to the thin segments of the Snyder dipole. A standard dipole diameter equal to the thick portions of the Snyder dipole produced a bandwidth of about 9 percent, so even in the worst case the Snyder dipole still gives a bandwidth gain of well over 50 percent compared to a conventional dipole. The bandwidths are based on the formula:

$$BW = 2(f_2 - f_1)/(f_2 + f_1) \quad (\text{eqn 2.1})$$

where  $f_2$  and  $f_1$  are the upper and lower points where each frequency curve crosses the line equal to a VSWR of 2:1. Hansen [Ref. 7] shows larger bandwidths in both cases, but he used a much higher antenna diameter-to-length ratio. As mentioned earlier, this effort was confined to coaxial transmission line diameter, but as a check a NEC run was made using Hansen's diameter-to-length ratio. The resulting bandwidth was close to that calculated by Hansen with NEC giving a slightly larger bandwidth. The Snyder dipole was also run with a double precision version of NEC to check accuracy. The results varied by less than two percent, so the remaining NEC runs used only single precision to conserve computer resources and costs. The bandwidth displayed by the NEC model of the Snyder dipole was consistent with Mr. Snyder's claim.

The next step in the analysis was to see if an LPDA built with Snyder dipole elements would either increase the bandwidth or provide the same bandwidth with fewer elements than the conventional LPDA. Before presenting the experimental procedures, it is appropriate to discuss the characteristics of LPDAs.

# SUSCEPTANCE CURVES

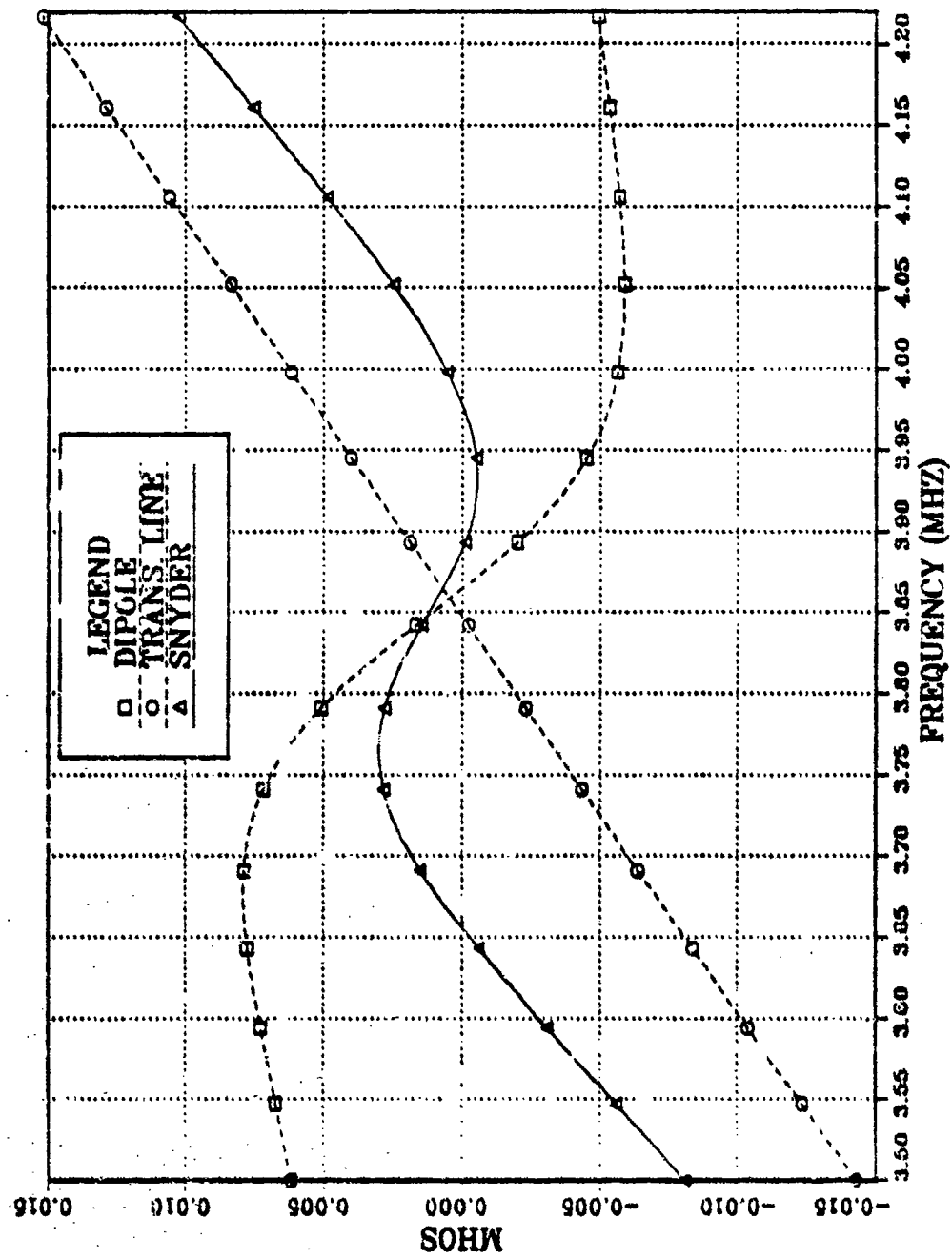


Figure 2.1 Dipole and Transmission Line Susceptances.



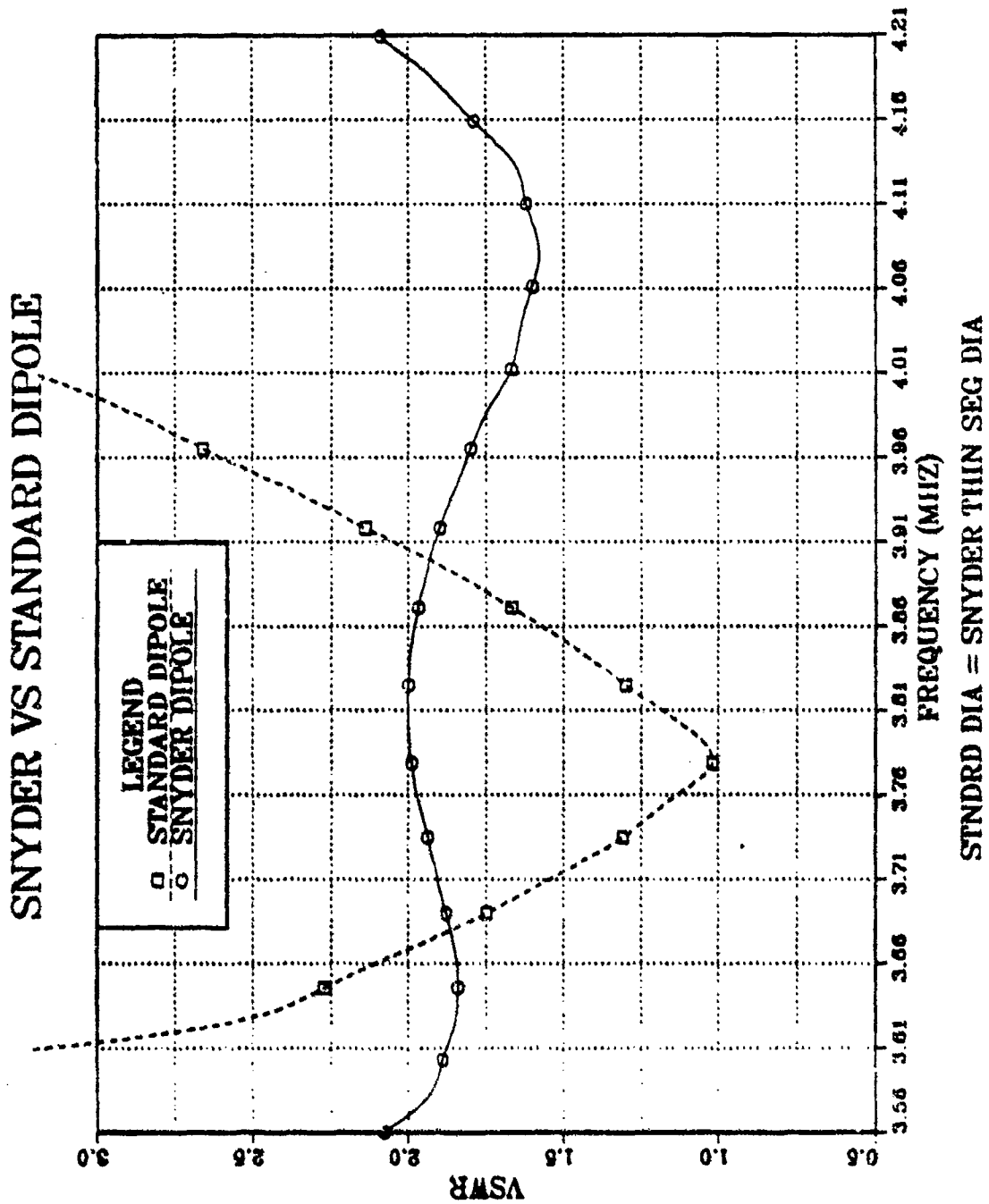


Figure 2.2 Standard Dipole and Snyder Dipole Bandwidths.

### III. K-BETA DIAGRAMS

#### A. K-BETA DIAGRAM DESCRIPTION

One of the characteristics of an LPDA mentioned in chapter one is that of backward radiation. It is possible to tell whether or not an array possesses the capacity for backward radiation by the use of a  $k$ - $\beta$  diagram, also called a dispersion or Brillouin diagram (Figure 3.1).

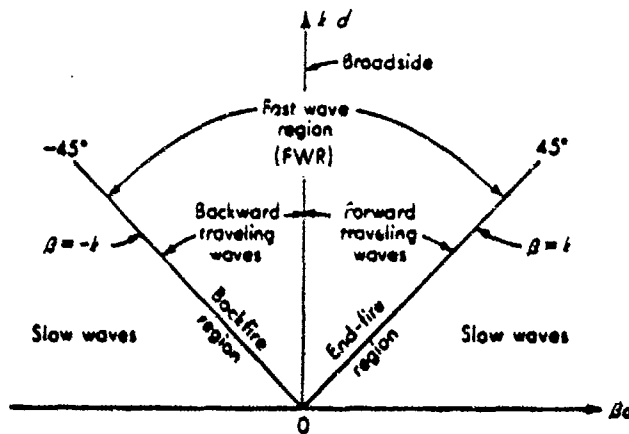


Figure 3.1  $k$ - $\beta$  Diagram (from Ref. 8).

This diagram is obtained by plotting the free space constant  $k$  versus the propagation constant  $\beta$  (or  $kd$  versus  $\beta d$  where  $d$  is the antenna element spacing). It is only necessary to show one period since the log-periodic antenna characteristics repeat every  $2\pi$ . For free space propagation:

$$k = \beta = 2\pi/\lambda \quad (\text{eqn 3.1})$$

According to Mittra and Jones [Ref. 9: p. 20], the  $k$ - $\beta$  diagram can be separated into three different frequency regions. These are the propagation (P) region, the complex (C) region, and the radiation (R) region. The propagation region corresponds to the feed excitation region in the antenna and has little or no attenuation. The

complex region occurs at  $\beta = \pm\pi$  and acts as a stopband where the attenuation is high but coupling to space is poor, so the complex region does not facilitate radiation. The third region, the radiation region, is where an antenna is an efficient radiator. It is also where fast waves occur, that is, where  $k$  is greater than  $\beta$ . The radiation region can be divided into an  $R_f$  region, for forward radiation (away from the feed), and the  $R_b$  region, for backward radiation (towards the feed). The most successful log-periodic antennas have radiation occurring in the  $R_b$  region near the line where  $\beta = -k$ . The  $R_b$  region should also have a large amount of attenuation to facilitate radiation into space. It is these characteristics of the  $k$ - $\beta$  diagram that will be used to determine if the Snyder LPDA has the possibility of producing backward radiation with high attenuation and becoming a good log-periodic antenna.

## B. OBTAINING THE K-BETA DIAGRAM DATA USING NEC

To determine  $\beta$ , the amplitude and phase of the current along the transmission feed line can be measured in the near field of the antenna array at different frequencies. Early experimenters used a current loop placed in the near magnetic field of the antenna elements and measured actual values for the current phase and amplitude in relation to a reference point. For this thesis, "experimental data" was gathered by the use of NEC to determine the amplitude and phase of the near magnetic fields. The near field is usually considered to extend to  $0.1\lambda$ . NEC requires near field calculations be taken at no closer than  $0.001\lambda$ , so several runs were performed taking magnetic field calculations at distances of  $0.002\lambda$  and  $0.01\lambda$ . A comparison of the two distances gave a magnitude difference of less than two percent and a phase difference of less than ten percent. All NEC information used in the final analysis was near field calculations taken at a distance of  $0.01\lambda$ .

When NEC is programmed for near magnetic fields at one frequency, the output is the magnitude in amps per meter and the phase in degrees. These values are given for the X, Y, and Z directions at each antenna element. The X direction magnetic fields were used for the analysis since the antenna array was placed in the X-Y plane with the wave propagating in the X direction. Using a plotting program, the phase values were plotted for each type of antenna feed at several different frequencies and element spacings. The slope of each plot was then multiplied by the element spacing ( $d$ ) and converted to radians to produce one point on the  $k$ - $\beta$  (or more specifically,  $kd$ - $\beta d$ ) diagram. The current magnitude output was used to derive  $\alpha$  in the complex propagation equation:

$$\gamma = \alpha + j\beta$$

(eqn 3.2)

These values were plotted using the same plotting program as before. The ratio of maximum to minimum amplitude was converted to decibels per meter, divided by the distance over which it varied, and then multiplied by the antenna element spacing to produce one point on the attenuation plot.

The  $k\text{-}\beta$  and attenuation diagrams for the Snyder uniform array are presented and discussed in the next chapter. By comparing the diagrams of the Snyder array with those of a conventional array, it will be possible to determine whether or not the Snyder array shows any improvement over the conventional uniform array.

## IV. EXPERIMENTAL PROCEDURES AND RESULTS

### A. CHARACTERISTICS OF UNTAPERED ARRAYS

The LPDA is made up of elements tapering in length from the longer, low frequency elements to the shorter, high frequency elements at the feed point. An untapered version of the LPDA, called a uniform array, was used to simplify the modeling necessary for NEC. Mittra and Jones [Ref. 9: p. 21] describe the  $k$ - $\beta$  characteristics required of the untapered counterpart of a potentially successful tapered log-periodic antenna.

Starting from small values of  $k$ , the untapered antenna shall have a continuous P region, immediately beyond which it moves into an  $R_b$  region. If the  $R_b$  region is quite efficient (if the coupling to space for the wave in this region is fairly (sic) effective), it is immaterial what the  $k$ - $\beta$  properties of the structure are beyond the R region. However, if the P region is interrupted by a C or  $R_r$  region ahead of the  $R_b$  region, the tapered structure derived from it will be a potentially unsuccessful broadband antenna. It is therefore quite important to distinguish between the C and R regions as previously defined.

It is also important to have high attenuation in the  $R_b$  region for proper coupling of the wave to space. These guidelines will be applied to the  $k$ - $\beta$  diagrams derived from the NEC runs for the various antenna array configurations.

### B. DEVELOPMENT OF THE SNYDER LPDA

The antenna modeled as the Snyder uniform array contains 10 elements, each identical to the Snyder dipole (see the NEC code in Appendix A). Each element consists of a  $1/4$  wavelength (at 3.88 MHz) center section and a  $1/8$  wavelength section on each end. The center section is 0.296 inches in diameter and simulates the coaxial transmission line section of the Snyder dipole by connecting the middle segment to  $1/4$  wavelength stubs. These are the stubs that were described earlier that cancel the dipole reactance in the Snyder dipole. They are open-circuited at the element end and short-circuited at the stub end to produce the desired results. The  $1/8$  wavelength end sections are 0.144 inches in diameter, barely stretching the NEC requirement that adjacent wire segments not vary in size by more than two to one. A 300 ohm transmission line connects each element and the voltage source.

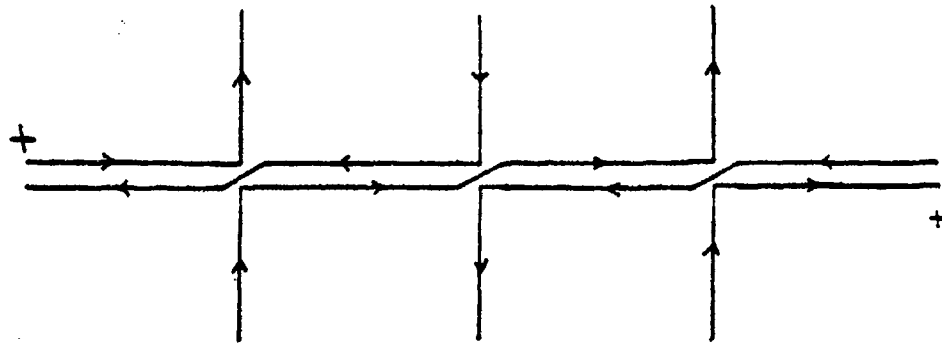
The elements were laid horizontally in the X-Y plane with the voltage source  $1/4$  wavelength from the array in the minus X direction, and the 300 ohm transmission line terminated in a matched impedance  $1/4$  wavelength from the array in the plus X direction. The near magnetic fields were calculated in the Z direction at 0.8 meters, approximately equal to  $0.01\lambda$ , above the center of each element. The near field values were calculated for several different frequencies for each array configuration. As mentioned in the section on  $k-\beta$  diagram data, the plotted values for each frequency form one point on the  $k-\beta$  and attenuation diagrams. Other sets of  $k-\beta$  and attenuation diagrams were formed by changing the distance between the elements in the array. If the elements can be spaced further apart in the Snyder LPDA without losing any bandwidth, then maybe fewer elements would be necessary than in the conventional LPDA. Different types of voltage feed were also modeled on NEC for comparison and discussion in the next section (Figure 4.1). The use of the word "feed" may be a poor choice since it refers to the way the elements are loaded, not the order in which the voltage is supplied to the elements. All of the antenna configurations modeled in this thesis receive excitation by means of a coaxial transmission line running between adjacent elements.

## C. EXPERIMENTAL RESULTS

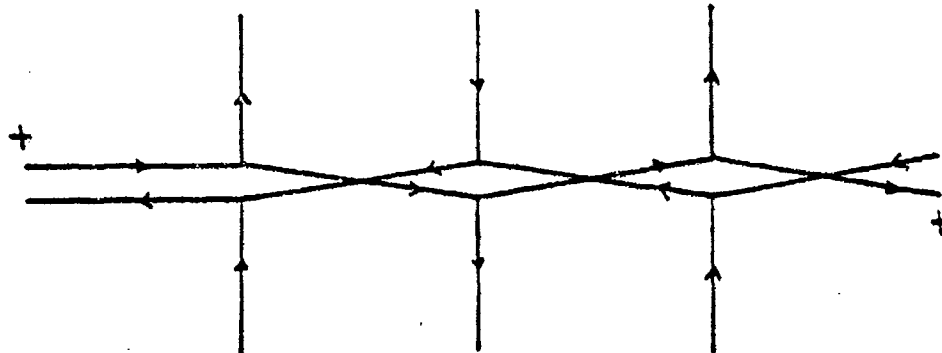
### 1. Switched Series Array

The switched series feed connects the antenna array elements in series with a 180 degree phase shift between each element. This method is not commonly used for LPDAs, but was tried since suggestions in various conversations led to the idea that the switched series feed might produce good results when using Snyder dipole elements.

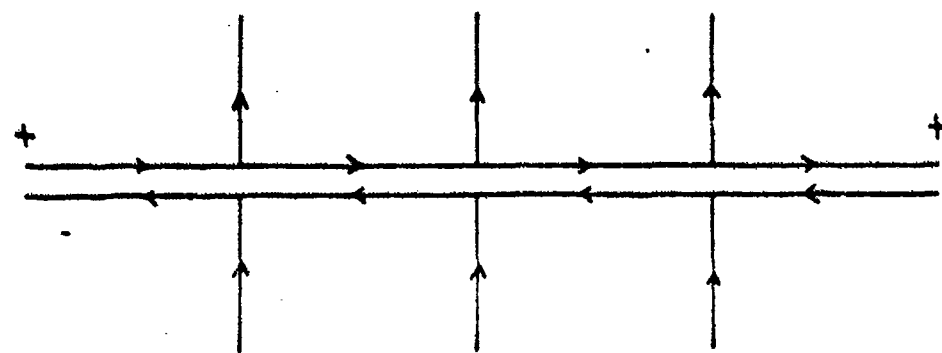
The  $k-\beta$  and attenuation diagrams for a switched series fed array are presented in Figures 4.2 and 4.3. The element spacing ( $d$ ) is  $1/8$  wavelength for a frequency of 3.88 MHz, which is the resonant frequency of the dipole element. All array element spacings in the remainder of this study will also be in reference to the resonant frequency of the dipole element. Following the guidelines of the previous section, these figures show two areas of backward radiation, one extending from the low  $kd$  values up to 0.77 and the second from 0.82 to high  $kd$  values. The  $kd$  value of 0.77 corresponds to a frequency of 3.81 MHz and 0.82 equals 4.04 MHz. Even though both of the backward radiation ( $R_b$ ) regions are preceded by a propagation region, the attenuation never goes above 5 decibels (dB), which is not enough to facilitate coupling of the wave into space. An attenuation of about 15 dB or higher in the  $R_b$  region is necessary for



Switched Series



Switched Parallel



Unswitched Parallel

Figure 4.1 Types of Voltage Feed.

propagation. The highest attenuation of 7.5 dB occurs in the forward radiation ( $R_f$ ) region which will not allow proper radiation from the antenna.

Figures 4.4 and 4.5 show results for a switched series fed array with the element spacing equal to  $1/4$  wavelength. The  $k$ - $\beta$  diagram is basically the same as for  $1/8$  wavelength except it is shifted up in frequency (up the  $kd$  axis). The major difference here is that the attenuation is occurring in the  $R_b$  region where it is needed, but it is too low to readily induce radiation into space. It should be noted that the NEC run at 3.81 MHz ( $kd=1.54$ ) was not used in the diagrams since the NEC calculations showed characteristics of a standing wave or improper impedance that is nonconducive to a successful LPDA.

In the  $k$ - $\beta$  and attenuation diagrams for an element spacing of  $3/8$  wavelength (Figures 4.6 and 4.7), the attenuation is fairly strong in the  $R_b$  regions, particularly between 2.4 and 2.6 (3.96 to 4.29 MHz). This is still a relatively low attenuation value with a narrow bandwidth. The results of the switched series feed models show very little potential for a successful log-periodic antenna. The near field NEC plots for the various switched series arrays are shown in Appendix B.

## 2. Switched Parallel Array

The switched parallel voltage feed is the most common method used to excite LPDAs. This method consists of loading the array elements in parallel and inducing a 180 degree phase shift between each element. The switched parallel feed was the one used by Isbell to produce the first successful LPDA.

The diagrams for a switched parallel feed with an element spacing of  $1/8$  wavelength (Figures 4.8 and 4.9) show a broad  $R_b$  region, but the attenuation is never any greater than about 5 decibels. Prospects for a successful LPDA are poor in this case due to the low attenuation.



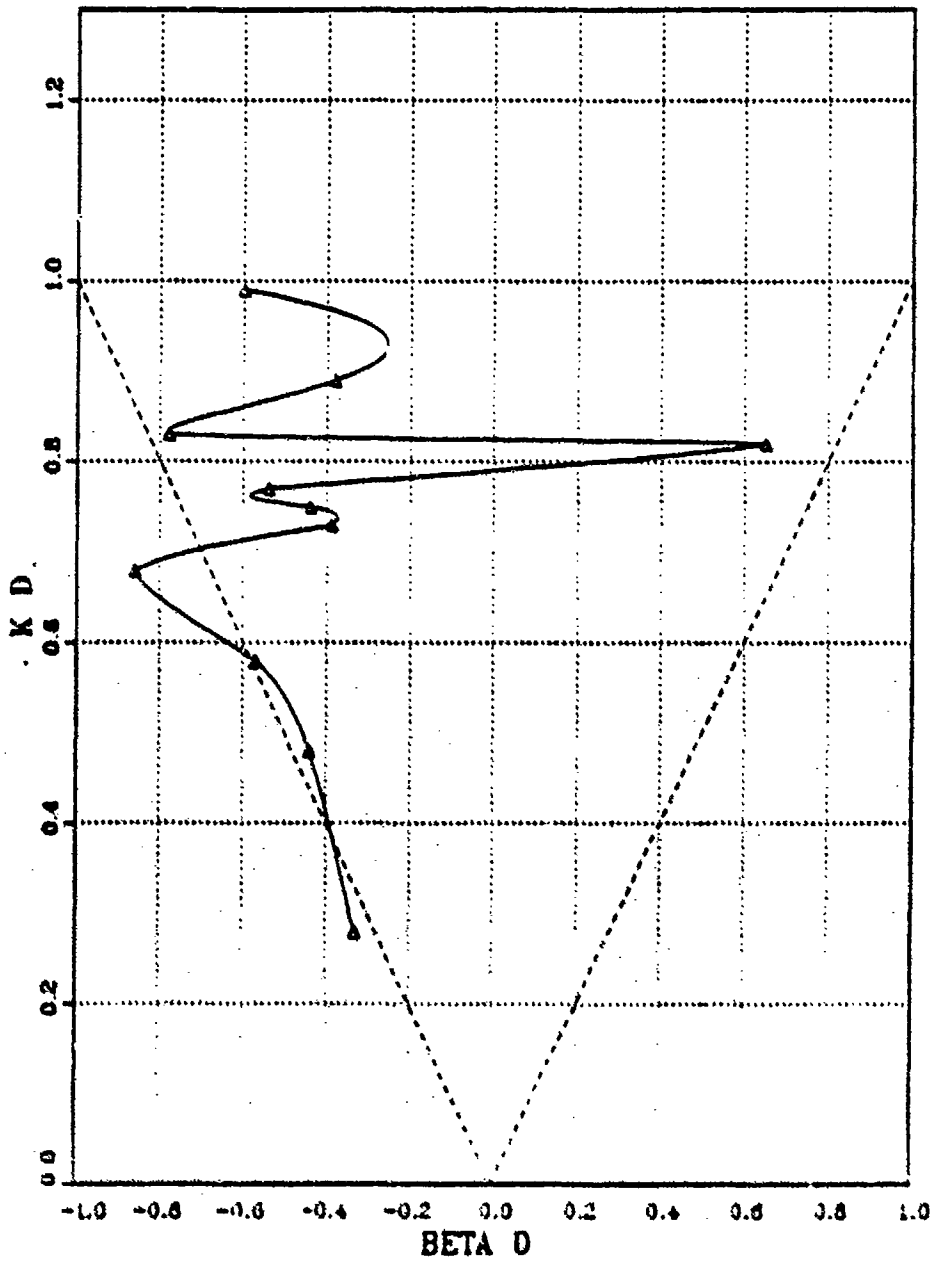


Figure 4.2  $k$ - $\beta$  Diagram for a Snyder Switched Series Array.  
Element Spacing =  $1/8$  Wavelength.

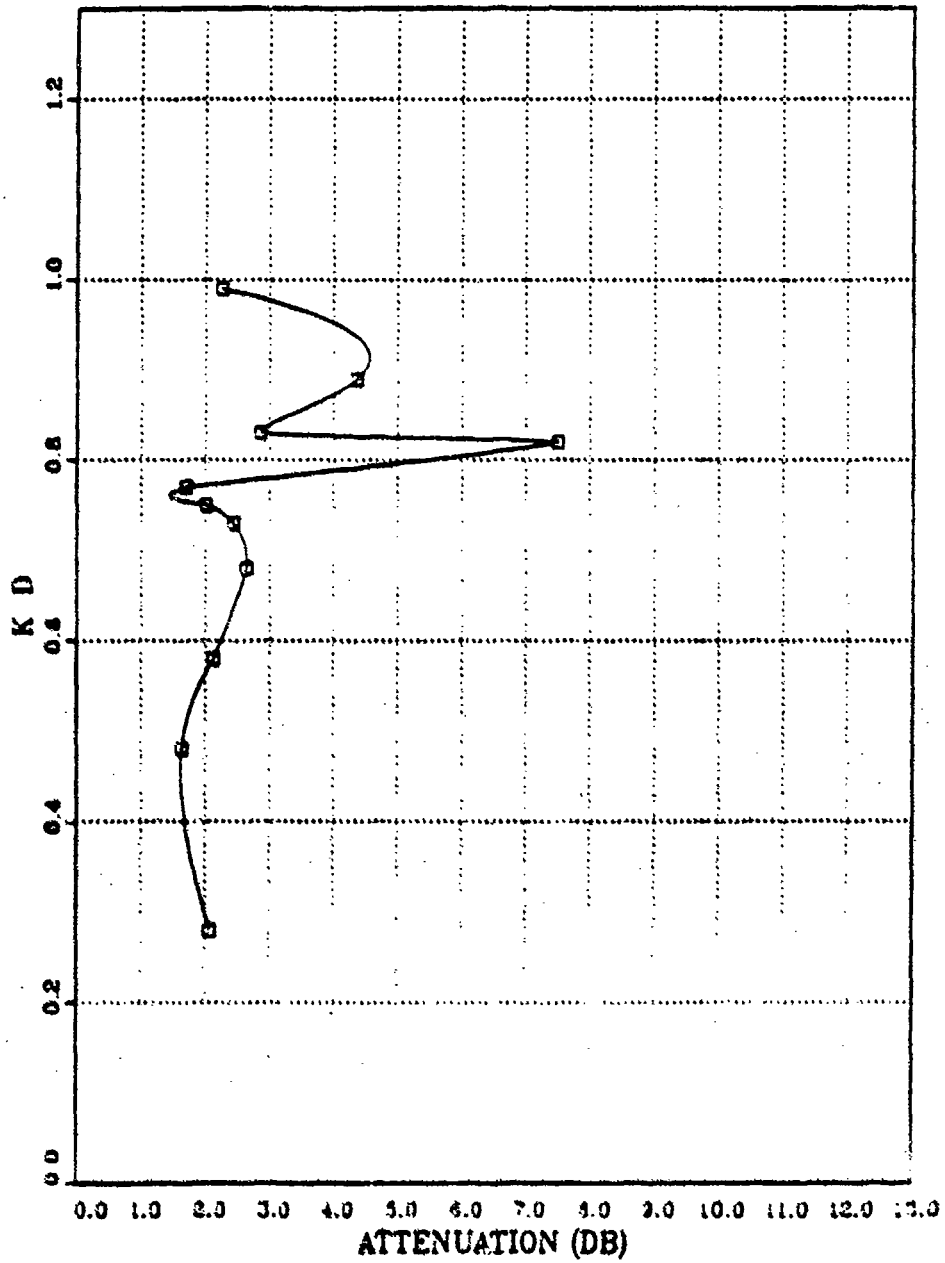


Figure 4.3 Attenuation of a Snyder Switched Series Array.  
Element Spacing = 1/8 Wavelength.

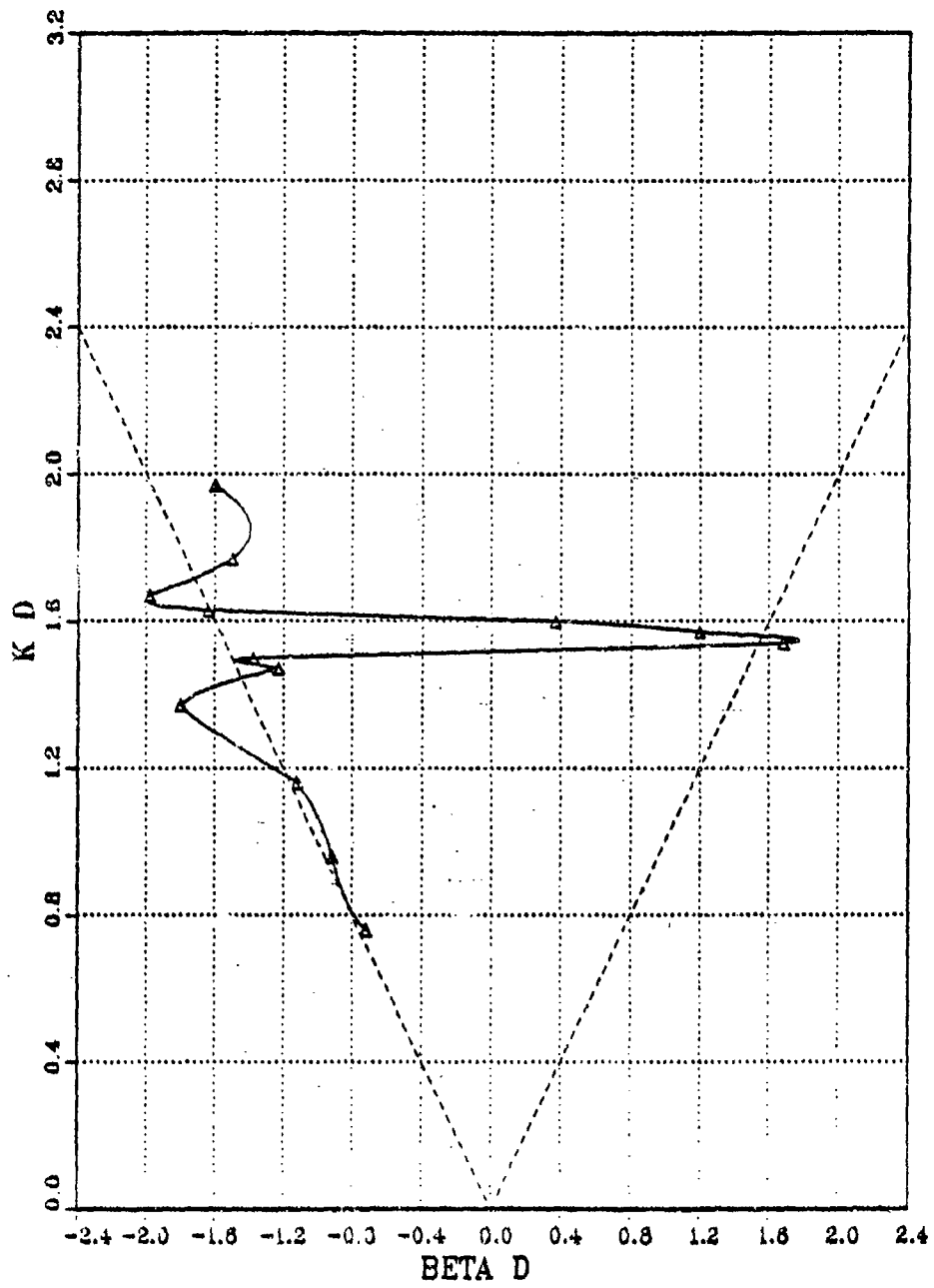


Figure 4.4  $k$ - $\beta$  Diagram for a Snyder Switched Series Array.  
Element Spacing =  $1/4$  Wavelength.

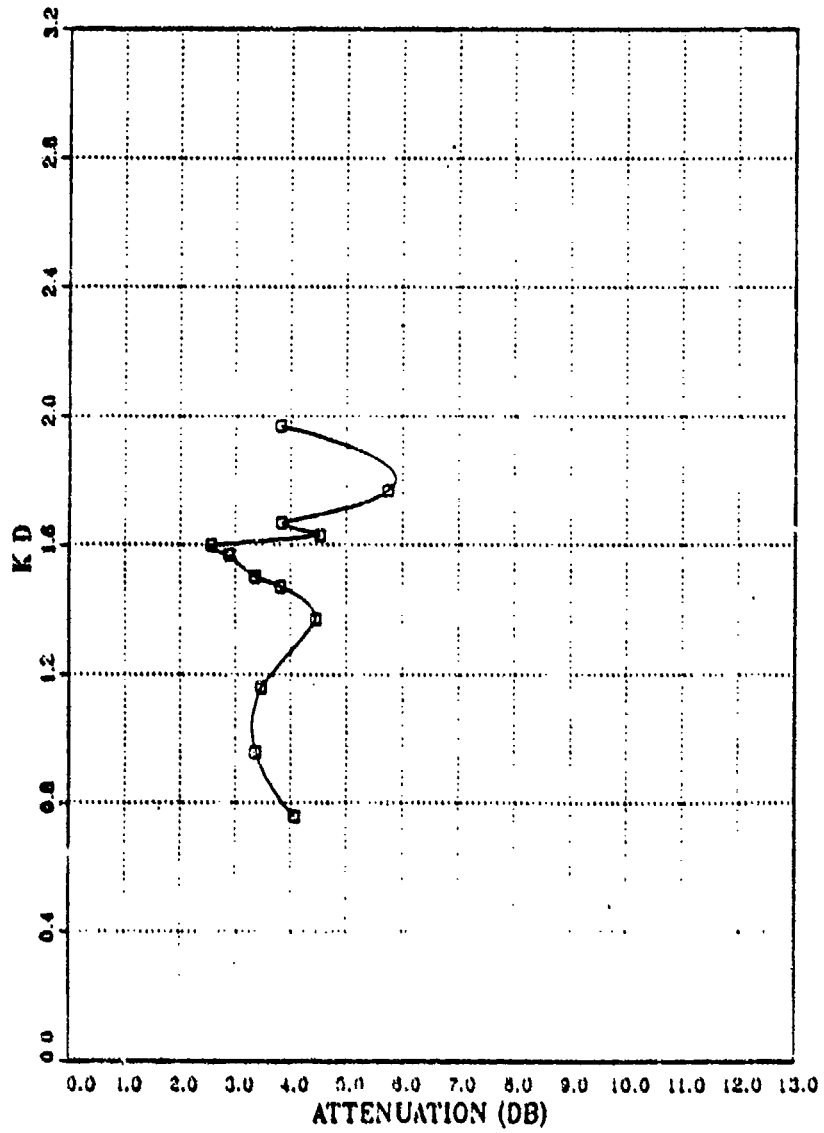


Figure 4.5 Attenuation of a Snyder Switched Series Array.  
 Element Spacing = 1/4 Wavelength.

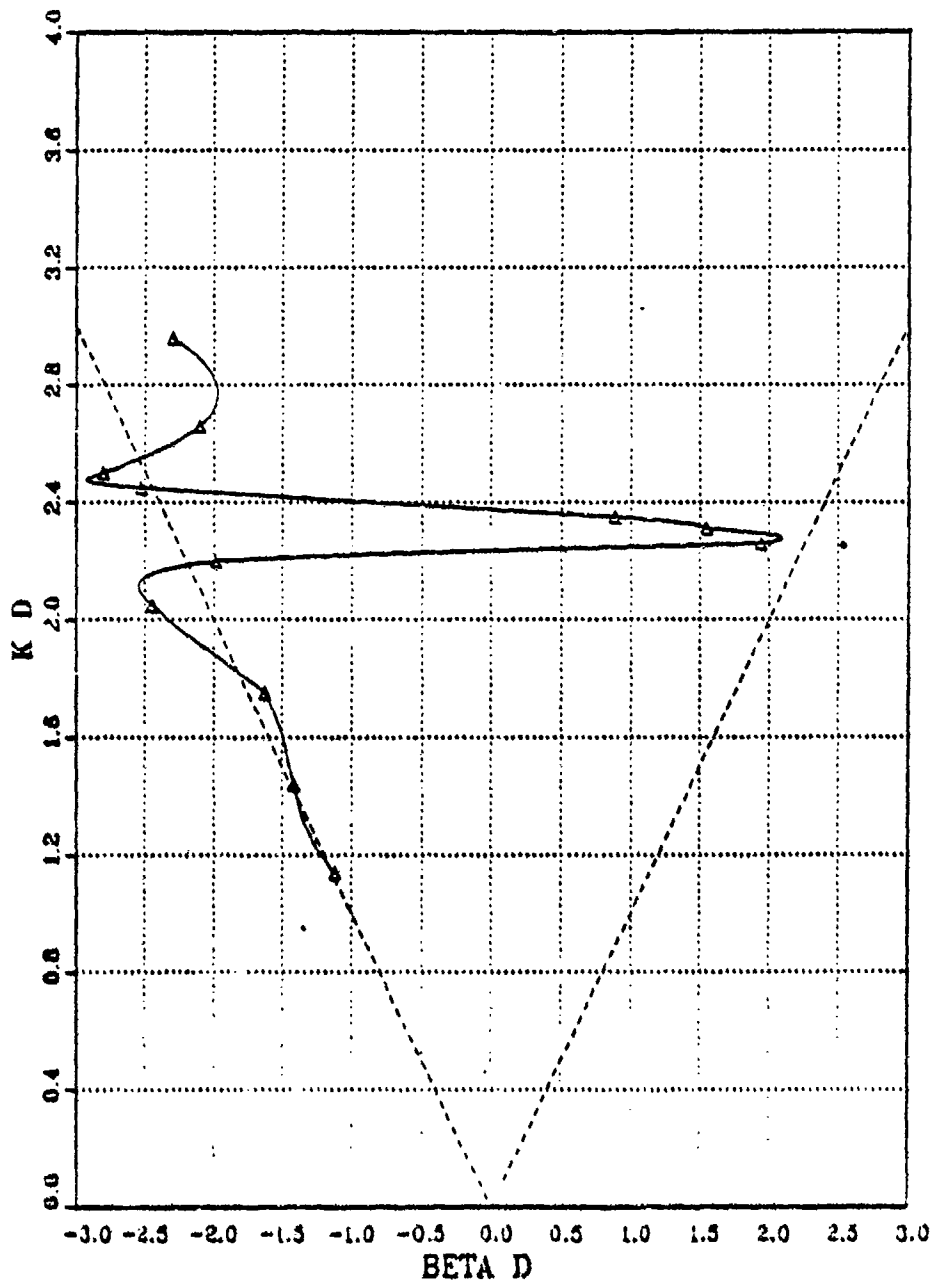


Figure 4.6  $k$ - $\beta$  Diagram for a Snyder Switched Series Array.  
Element Spacing =  $3/8$  Wavelength.

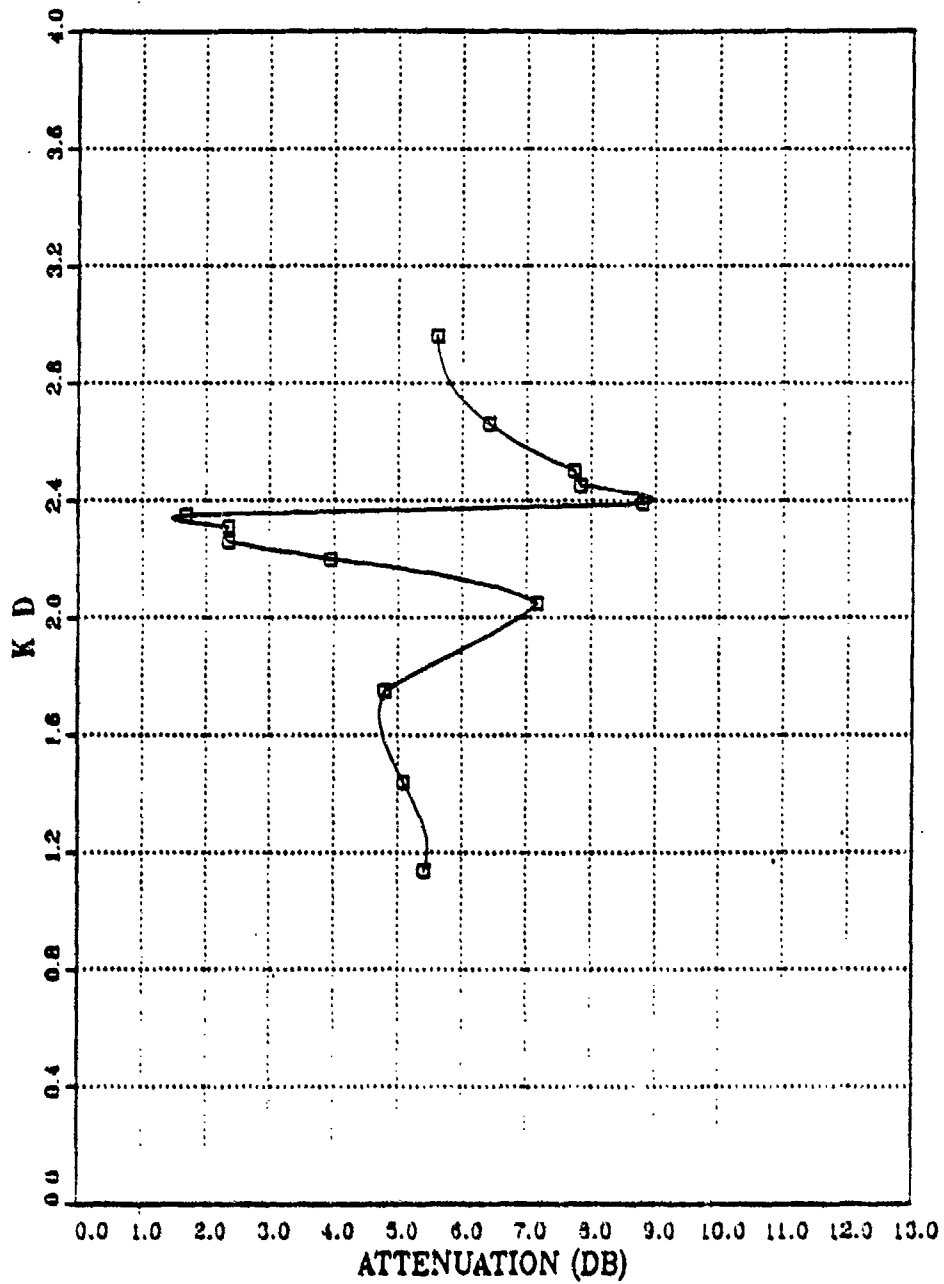


Figure 4.7 Attenuation of a Snyder Switched Series Array.  
Element Spacing =  $3/8$  Wavelength.

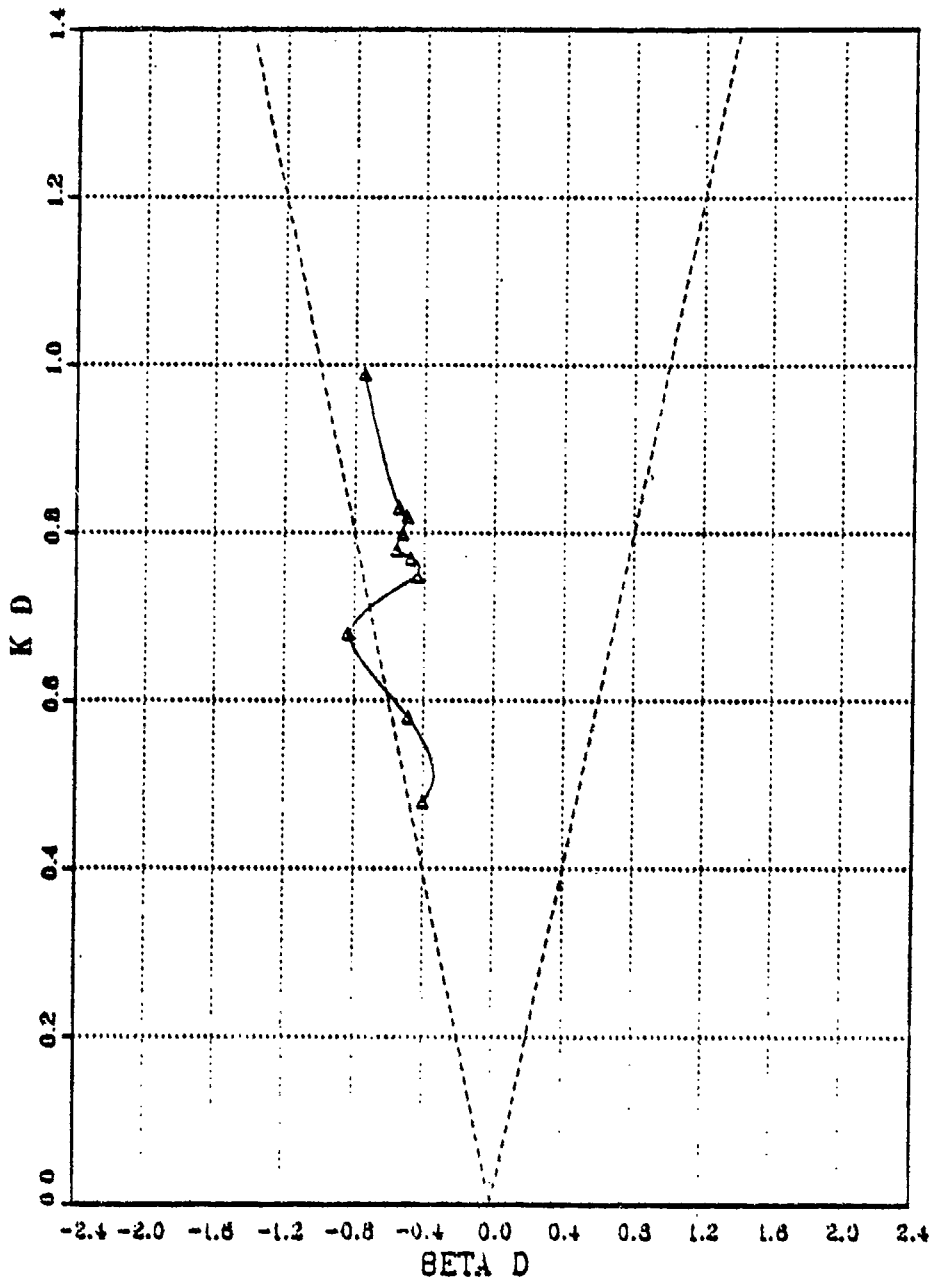


Figure 4.8  $k$ - $\beta$  Diagram for a Snyder Switched Parallel Array.  
Element Spacing =  $1/8$  Wavelength.

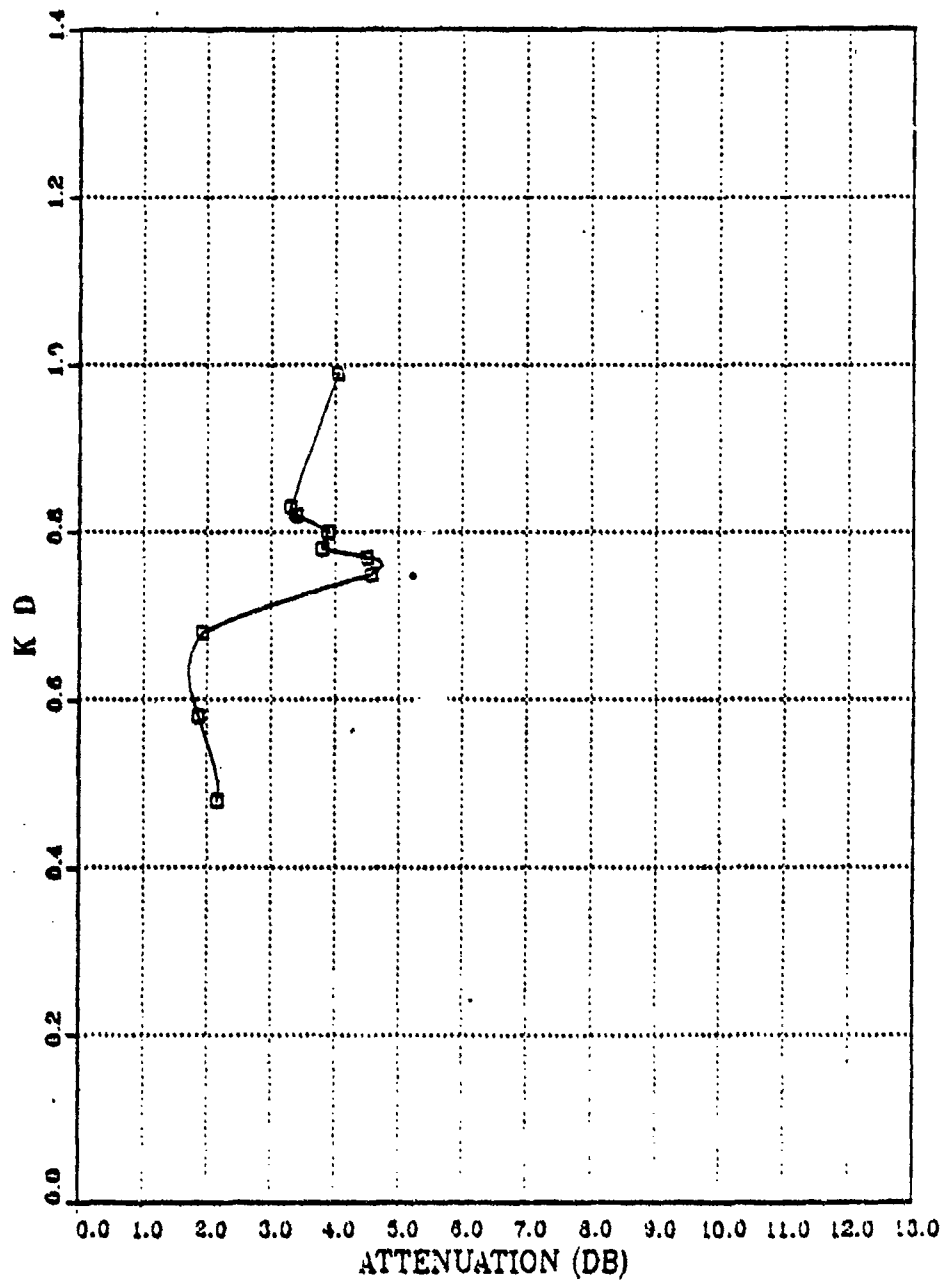


Figure 4.9 Attenuation of a Snyder Switched Parallel Array.  
Element Spacing =  $1/8$  Wavelength.



The  $k\text{-}\beta$  and attenuation diagrams for a  $1/4$  wavelength element spacing (Figures 4.10 and 4.11) show much improvement over those of the  $1/8$  wavelength spacing. A broad  $R_b$  region exists up to  $kd$  equal 1.65 (4.10 MHz) with high attenuation in at least part of that region. This is conducive to backward radiation, a key characteristic of successful log-periodic antennas. The second area of high attenuation occurs in an  $R_f$  region and thus that portion of the frequency band would not radiate well.

Figures 4.12 and 4.13 show a switched parallel array with the elements spaced  $3/8$  wavelengths apart. This configuration produced the highest attenuation in an  $R_b$  region indicating good coupling to space, but the backward radiation region is only from 2.2 to 2.45 which corresponds to 3.63 to 4.04 MHz. This antenna meets the requirements of being a backward radiator with high attenuation but does not meet the design goal of having a broad operating frequency.

A switched parallel feed NEC run was made with the elements spaced at  $1/2$  wavelength with poor results. Almost every frequency contained characteristics of a standing wave or improper input impedance to the elements. There were no  $k\text{-}\beta$  or attenuation diagrams produced for this configuration, but plots of the NEC results are included in Appendix C with the other switched parallel antennas.

### 3. Unswitched Parallel Array

An unswitched parallel or straight feed configuration at  $1/4$  wavelength element spacing (Figures 4.14 and 4.15) did not produce good results. In this case, there is no phase shift between the elements. Phase shift seems to be a necessary characteristic of a good log-periodic antenna as Isbell found out when he designed his first LPDAs. The  $k\text{-}\beta$  diagram shows a very broad band  $R_b$  region but the attenuation is too low to accomplish radiation. The results in this case were as expected. The near field plots for this array make up Appendix D.

## D. COMPARISON OF SNYDER ARRAY TO CONVENTIONAL ARRAY

The results of the previous section indicate the switched parallel array with  $3/8$  wavelength element spacing holds the most potential for becoming a successful LPDA. It produced high attenuation in the  $R_b$  region as is required for a log-periodic antenna. To determine if the design goal of producing more bandwidth than a conventional LPDA has been met, a uniform array with standard elements was modeled in NEC. All characteristics were modeled exactly the same as the Snyder dipole except that

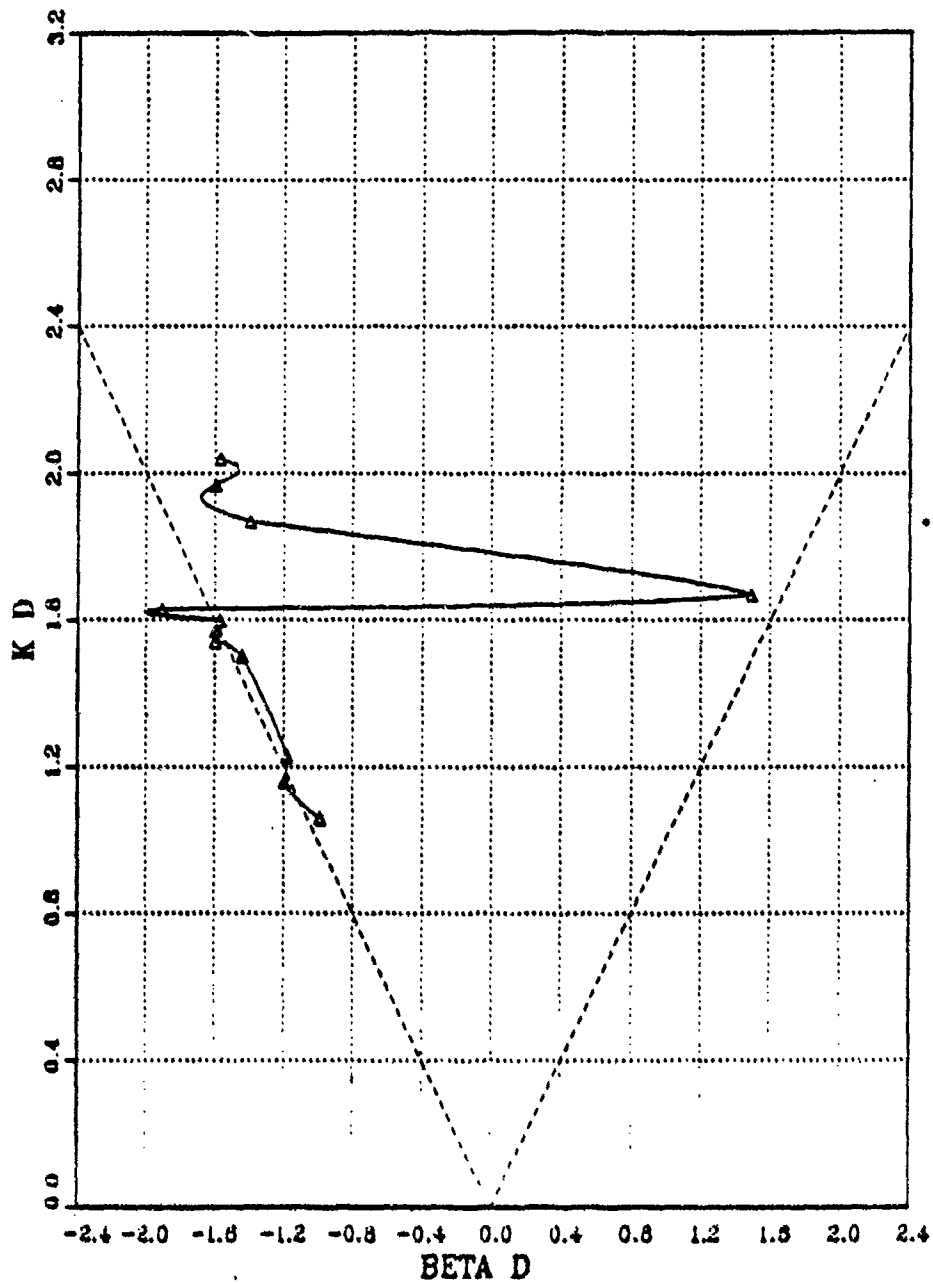


Figure 4.10  $k$ - $\beta$  Diagram for a Snyder Switched Parallel Array.  
Element Spacing =  $1/4$  Wavelength.

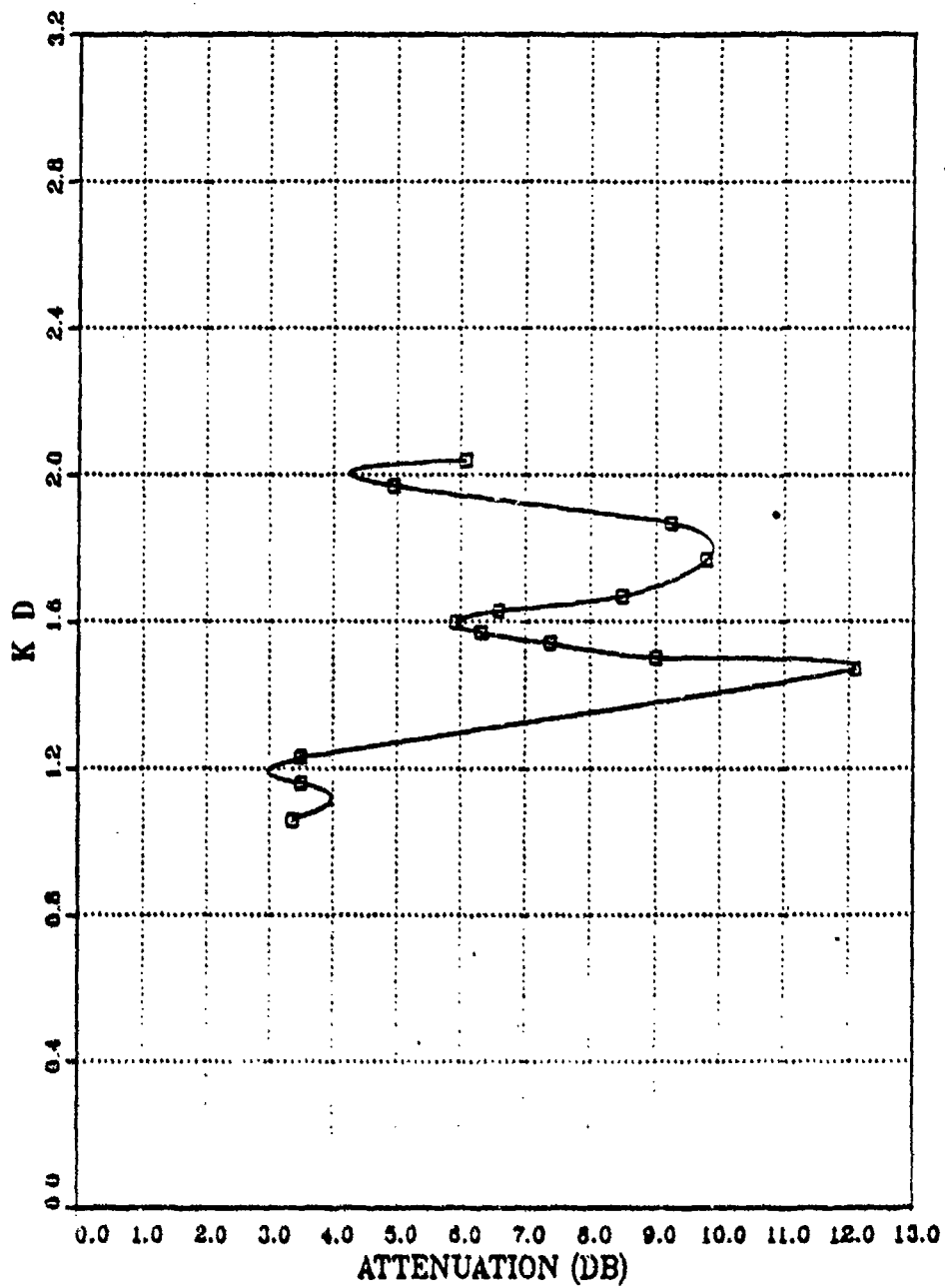


Figure 4.11 Attenuation of a Snyder Switched Parallel Array.  
Element Spacing =  $1/4$  Wavelength.

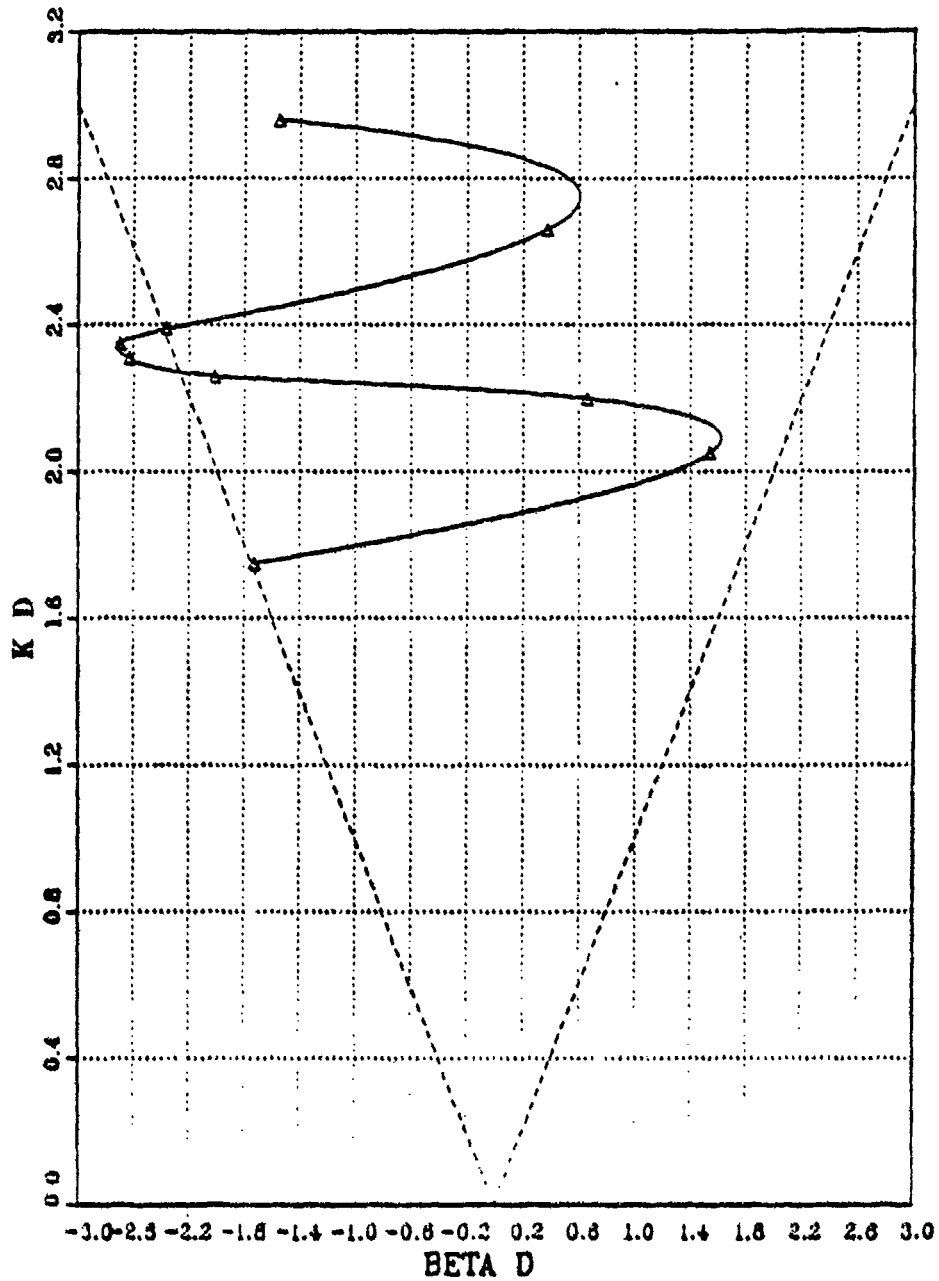


Figure 4.12  $k$ - $\beta$  Diagram for a Snyder Switched Parallel Array.  
Element Spacing =  $3/8$  Wavelength.

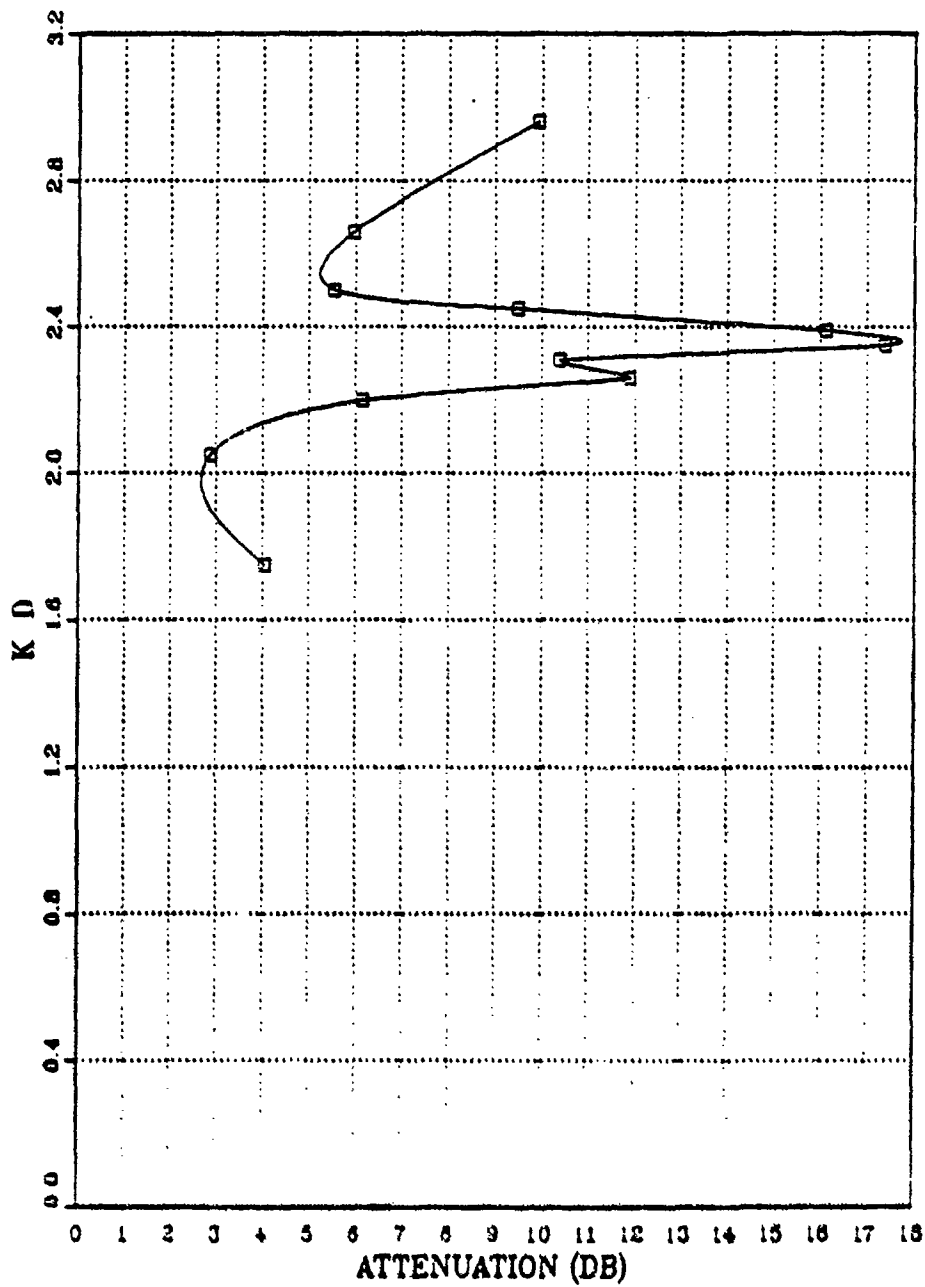


Figure 4.13 Attenuation of a Snyder Switched Parallel Array.  
Element Spacing =  $3/8$  Wavelength.

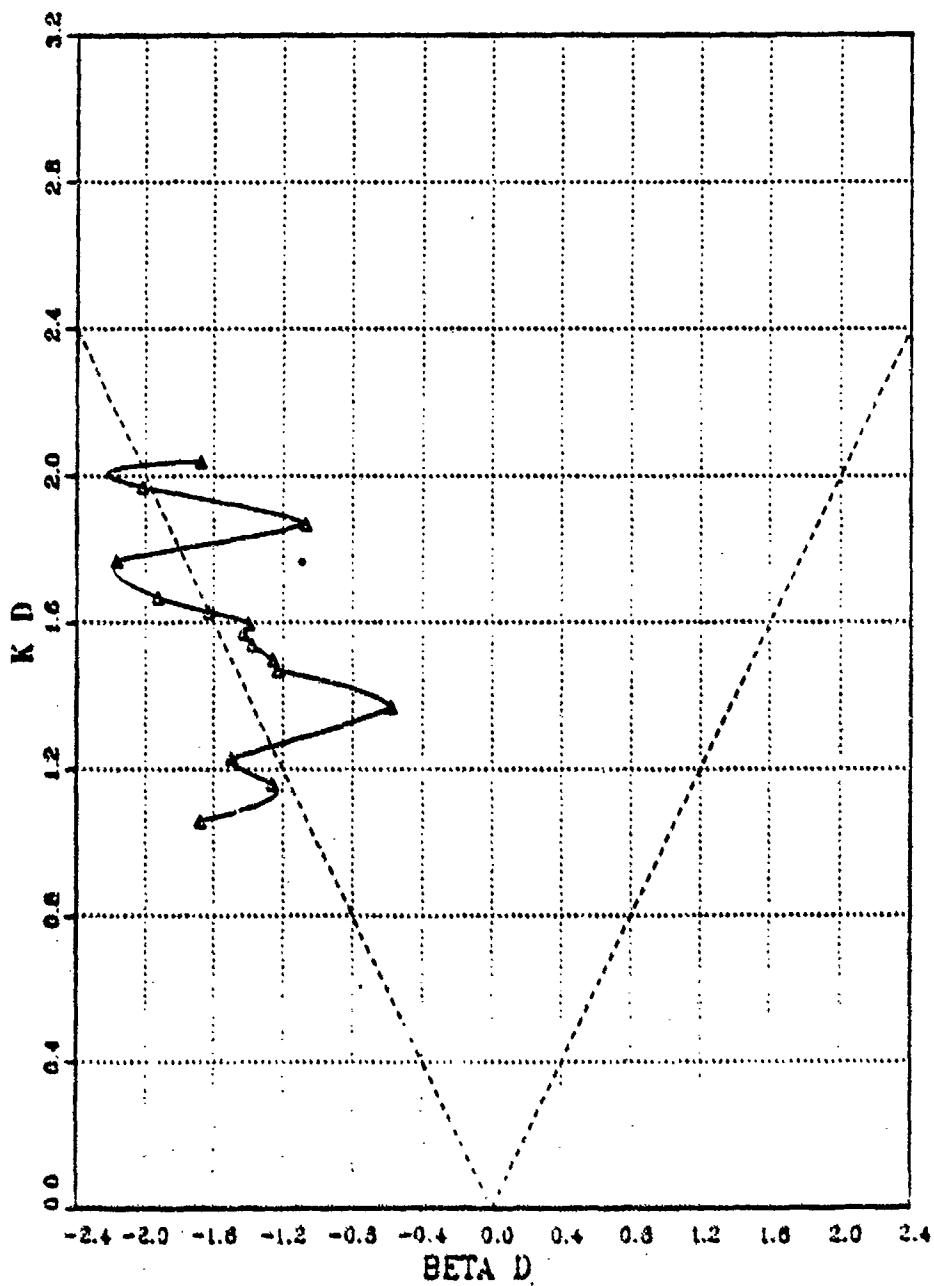


Figure 4.14  $k$ - $\beta$  Diagram for a Snyder Unswitched Parallel Array.  
Element Spacing =  $1/4$  Wavelength.

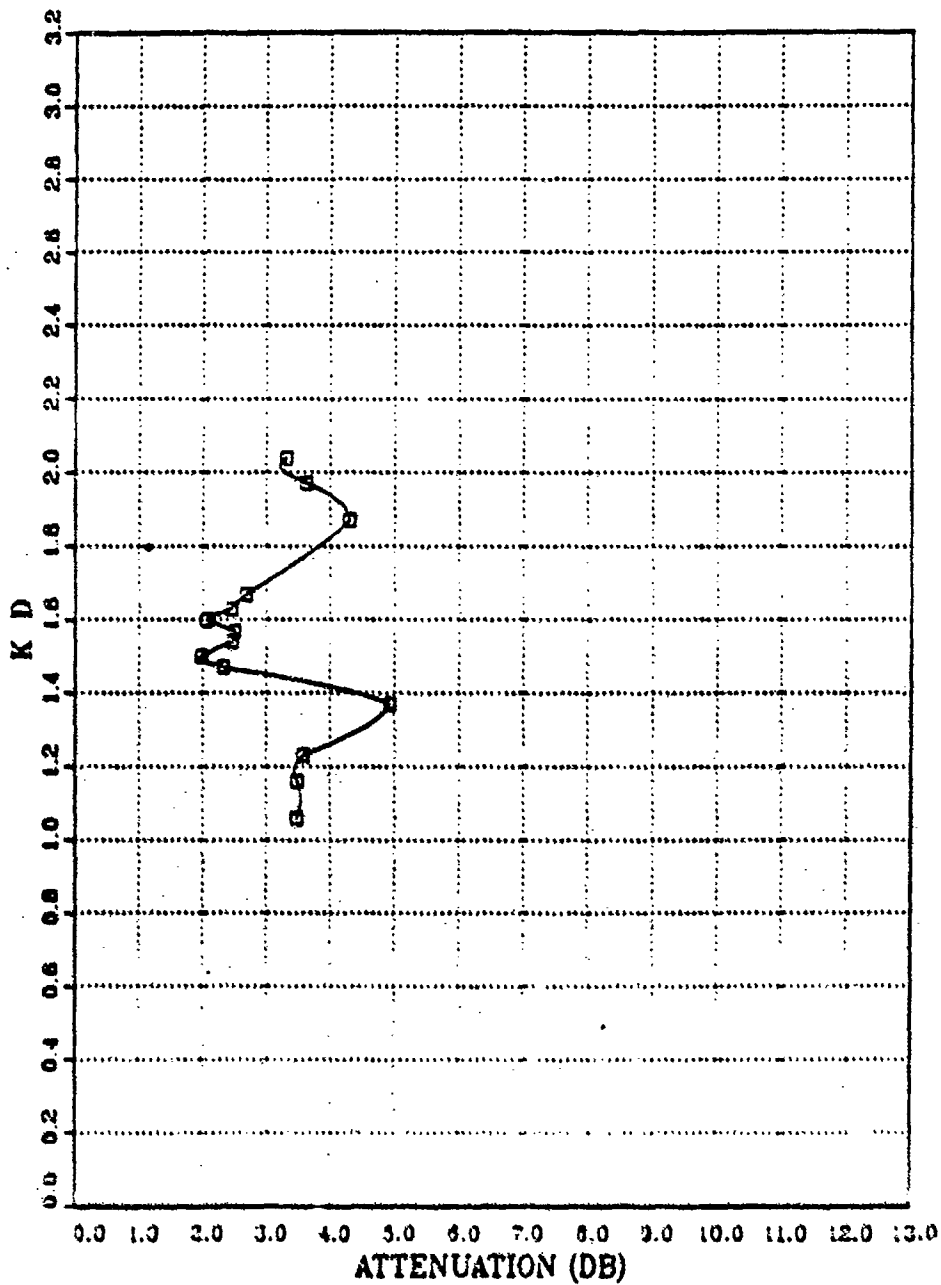


Figure 4.15 Attenuation of a Snyder Unswitched Parallel Array.  
 Element Spacing = 1/4 Wavelength.

there are no coaxial transmission line sections and the input impedance to each element is 73 ohms, the same as that used in the standard dipole in chapter two. The same values were used for the physical dimensions, element spacing, transmission feed lines, voltage excitation, near field measurements, and frequencies.

The resulting  $k$ - $\beta$  diagrams for the conventional array are Figures 4.16 and 4.17. These diagrams show very similar results as those for the  $3/8$  wavelength Snyder array (Figures 4.12 and 4.13). The  $R_b$  and  $R_f$  regions are about the same in both cases, as are the attenuation curves. The highest attenuation in both cases is about 17.5 decibels in the  $R_b$  region. The frequency bands of the  $R_b$  regions are almost identical so that there appears to be no bandwidth gain in the Snyder array. A direct comparison of the two arrays is presented as Figures 4.18 and 4.19.

A standard dipole array with  $1/2$  wavelength element spacing was also modeled with NEC, but the results were as poor as the  $1/2$  wavelength Snyder switched parallel array. The near field plots for the  $3/8$  and  $1/2$  wavelength standard dipole arrays are included as Appendix E.



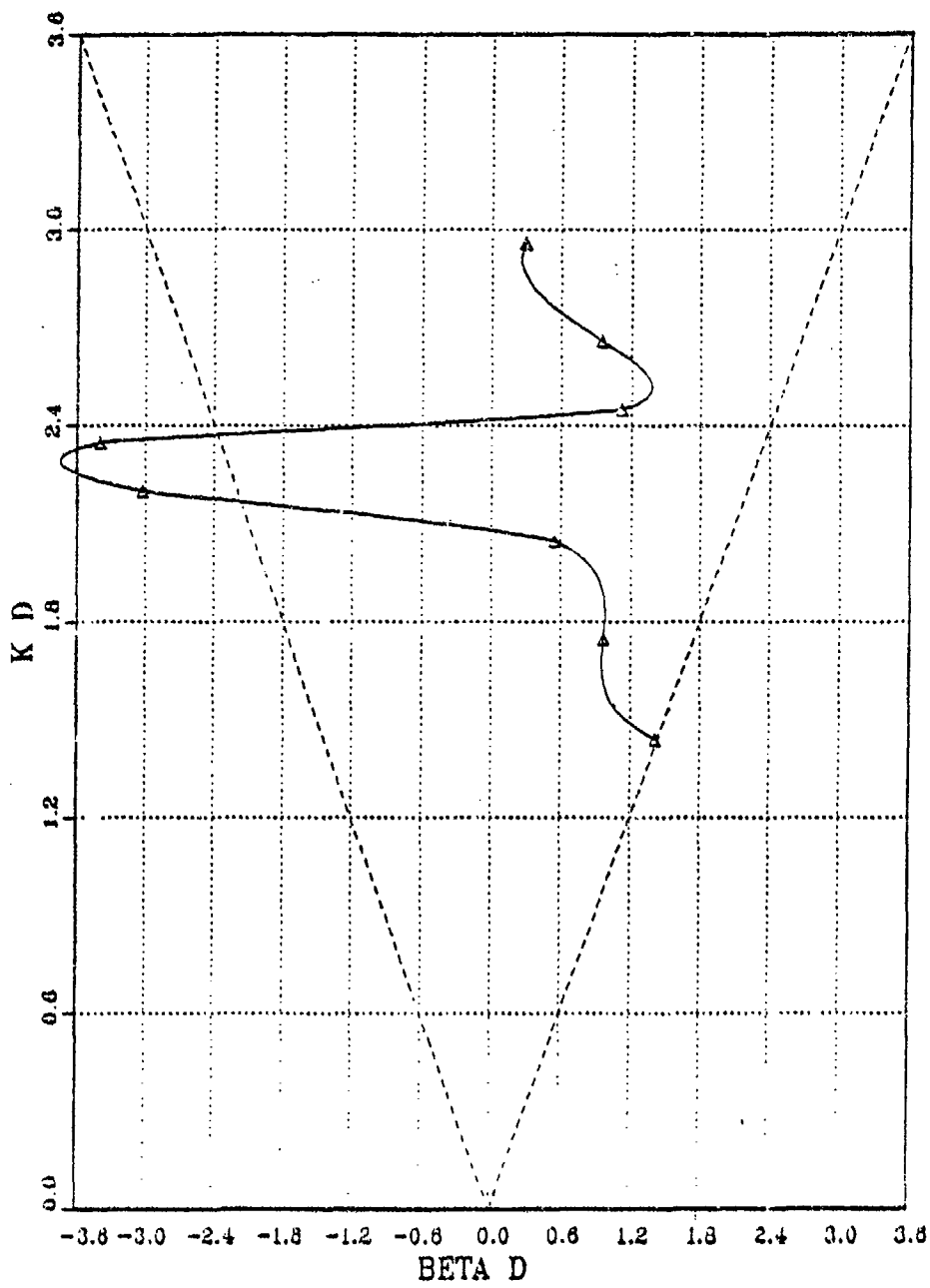


Figure 4.16  $k$ - $\beta$  Diagram for a Standard Switched Parallel Array.  
Element Spacing =  $3/8$  Wavelength.

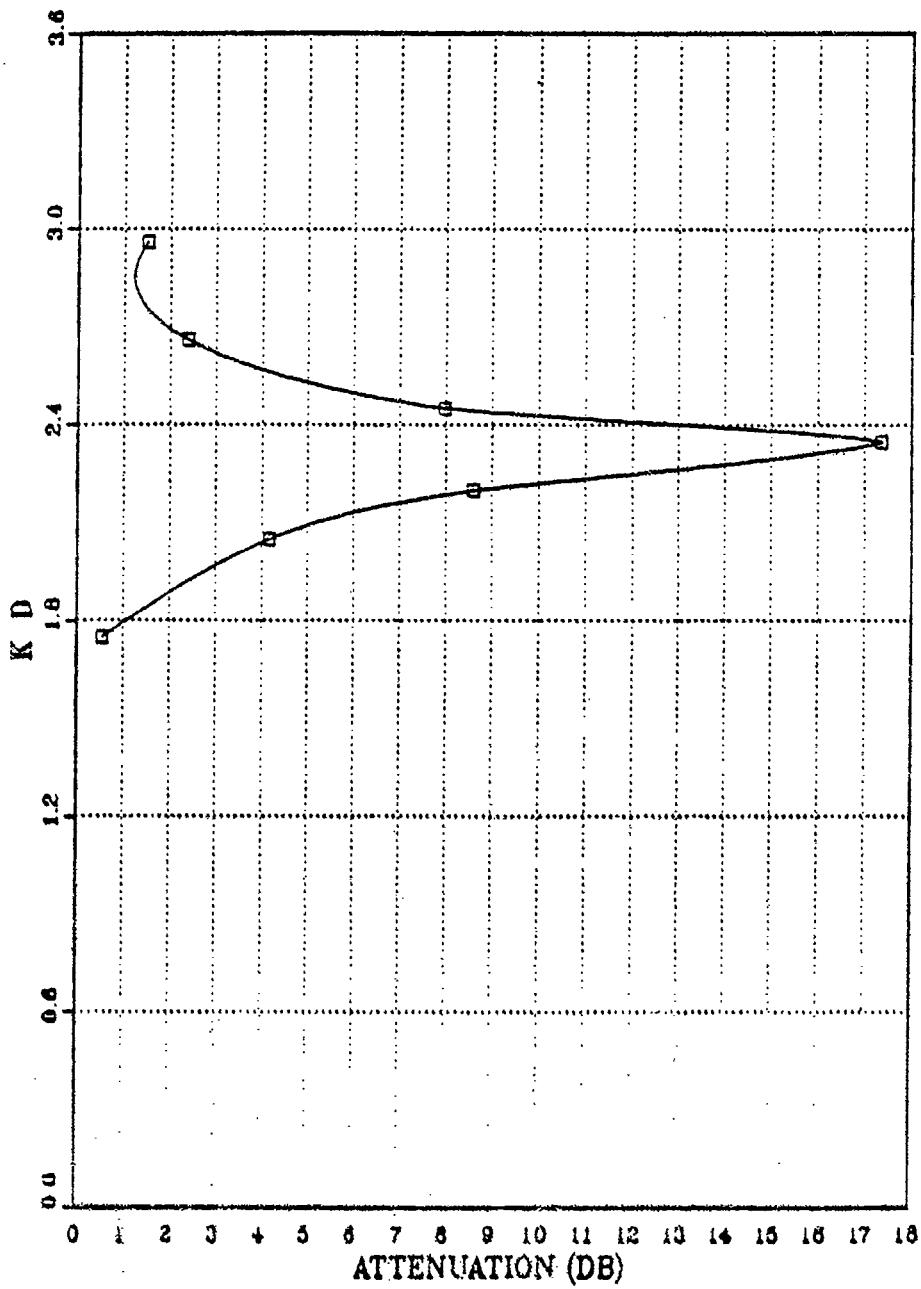


Figure 4.17 Attenuation of a Standard Switched Parallel Array.  
Element Spacing =  $3/8$  Wavelength.

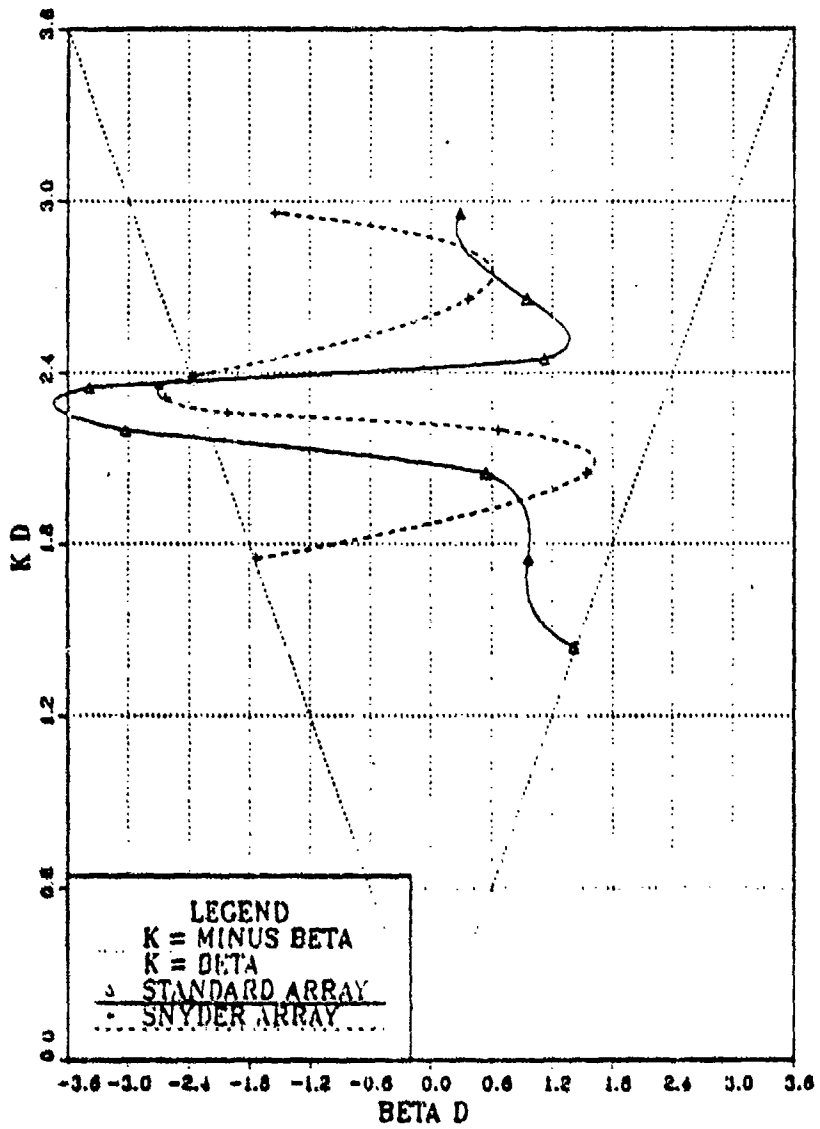


Figure 4.18  $k$ - $\beta$  Diagram Comparison.

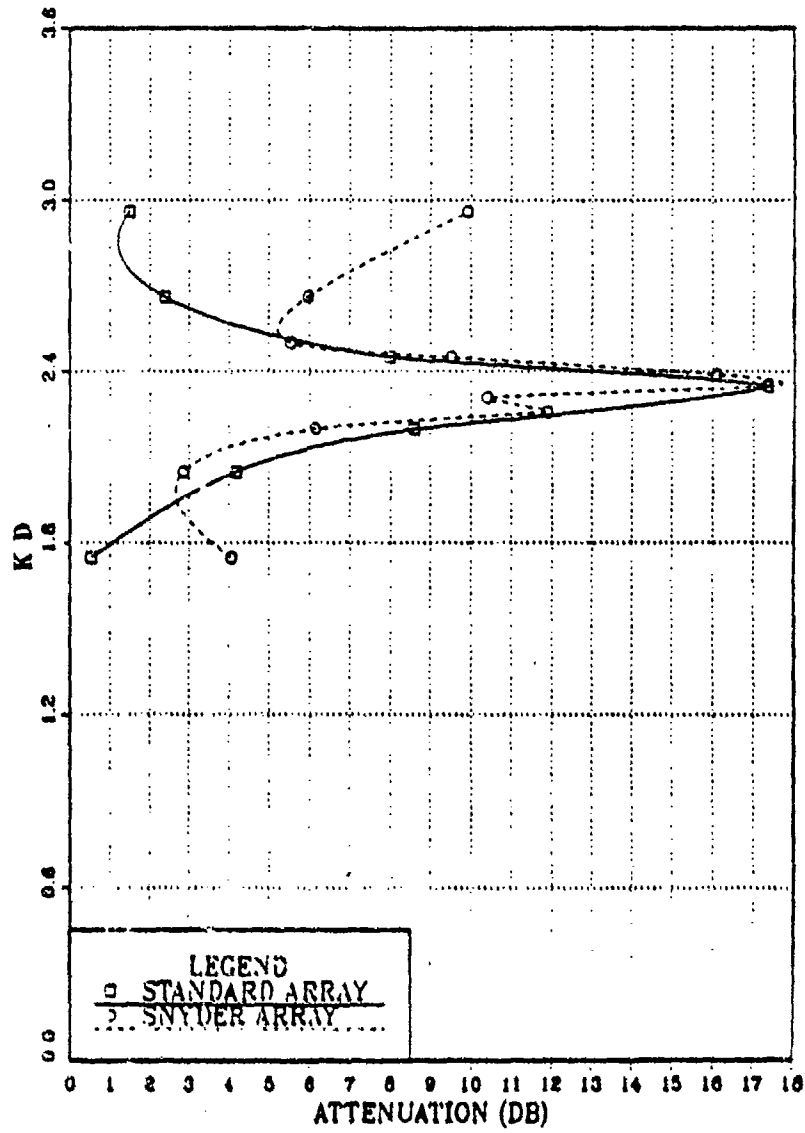


Figure 4.19 Attenuation Comparison.

## V. CONCLUSIONS AND RECOMMENDATIONS

This thesis examined the feasibility of designing a log-periodic dipole array with more operational bandwidth per element than the LPDAs currently in use. To accomplish this, a Snyder dipole made of coaxial transmission line was modeled using the Numerical Electromagnetics Code (NEC). It was then placed in a uniform array and different configurations were tried by varying the type of feed and the element spacing. The performance of each antenna was then based on the  $k$ - $\beta$  and attenuation diagrams created from the NEC output.

The first conclusion one can draw from the NEC results is that a Snyder dipole can be designed and built with an operational bandwidth greater than that of a standard dipole. This greater bandwidth will then allow a larger deviation in the operating frequency without serious degradation of the impedance match. Another advantage of the Snyder dipole is that it achieves the same bandwidth as a standard dipole of larger diameter, and therefore reduces the weight.

The second conclusion drawn from the research is that the NEC model for the Snyder dipole is accurate since the results are consistent with the designer's claims and other antenna models. Since nothing was found in the literature to reference on the use of coaxial transmission line elements in uniform arrays, it is assumed the NEC model for the array is also accurate. The  $k$ - $\beta$  and attenuation diagrams showed that backward radiation was produced at some frequency for every kind of feed and element spacing used, but the attenuation was often so low that no radiation from the antenna could occur. For the case where there was high attenuation, the bandwidth was no better than that of a standard array of the same element spacing. This leads to the final conclusion; the Snyder dipole does not improve the bandwidth of a conventional uniform array.

The results of the Snyder uniform array data are disappointing, but before completely disregarding the Snyder dipole as an LPDA element, it is recommended that the effort of this study be continued by modeling a uniform array over various grounds to see if there is any advantage in using the Snyder dipole in that situation. It is also recommended that a Snyder LPDA be modeled on NEC. This study showed that the Snyder uniform array performed no better than a standard uniform array, but the

characteristics of the mutual impedance of the Snyder LPDA elements may prove advantageous in a tapered array. Modeling a Snyder LPDA may require a new set of design nomograms based on input impedance since the nomograms currently used for standard LPDAs may not be applicable. If the same conclusions are reached as those from this research, the Snyder dipole array should be removed from consideration as a potentially successful LPDA.

It should be noted that even though the Snyder dipole failed as a uniform array, it did produce excellent results as a single dipole. The Snyder dipole should be considered for any use where an increased dipole bandwidth is desired or necessary, particularly if coaxial transmission cable can be used to maximize the performance.

# APPENDIX A

## NEC DATA SETS

```

CN
CN THE SNYDER DIPOLE (WITH DOUBLE RADIUS SEGMENTS,
CN COMPARED TO SNYDER'S DIMENSIONS)
CN
CN 3.560 - 4.234 MHZ
CN
CN HALF WAVE HIGH IN FREE SPACE
CN
CN L1 = 31.66'
CN D1 = .296"
CN L2 = 31.66'
CN D2 = .144"
CN Z0 = 25 OHMS (TWO 50 OHM LINES IN PARALLEL)
CN
CN ZNORM = 145 OHMS (BALUN LOAD)
CN
CN
CN
CN GN 1.5, -43.32,0.0, -31.66,0.0, .006 END PORTION/EQUAL LENGTH SEGS
UN 2.15, -31.66,0.0, 31.66,0.0, .0124 CENTER PORTION/EQUAL LENGTH SEGS
CN 1.5, 31.66,0.0, 43.32,0.0, .006 OTHER END
CN 0.0, 0.0,0.0, 0.0,131.5, 001.003 RAISE UP TO HALF WAVE
CN 90.1, 0.0,0.0, 0.0,1, .0001 T.L. SHORT CIRCUIT WIRE
CN 0.0, 0.0, //, 2000,0.0, 090.090 MOVE IT WAY OUT
CN 1 PT TO METERS
CN 0
CN PT -1.1,1.1 SUPPRESS CURRENT PRINTOUT
TL 2.0,90.1, 25.0,19.30, 0.0,1E6,1E6 T.L. STUB
EX 0.2,0.01, 1.0,145 FEED CENTER/ASK FOR IMPEDANCE TABLE
PR 1.30,0.0, 3.560,1.004 30 PREGS/MULTIPLICATIVE STEPPING
CN
CN
CN

```

```

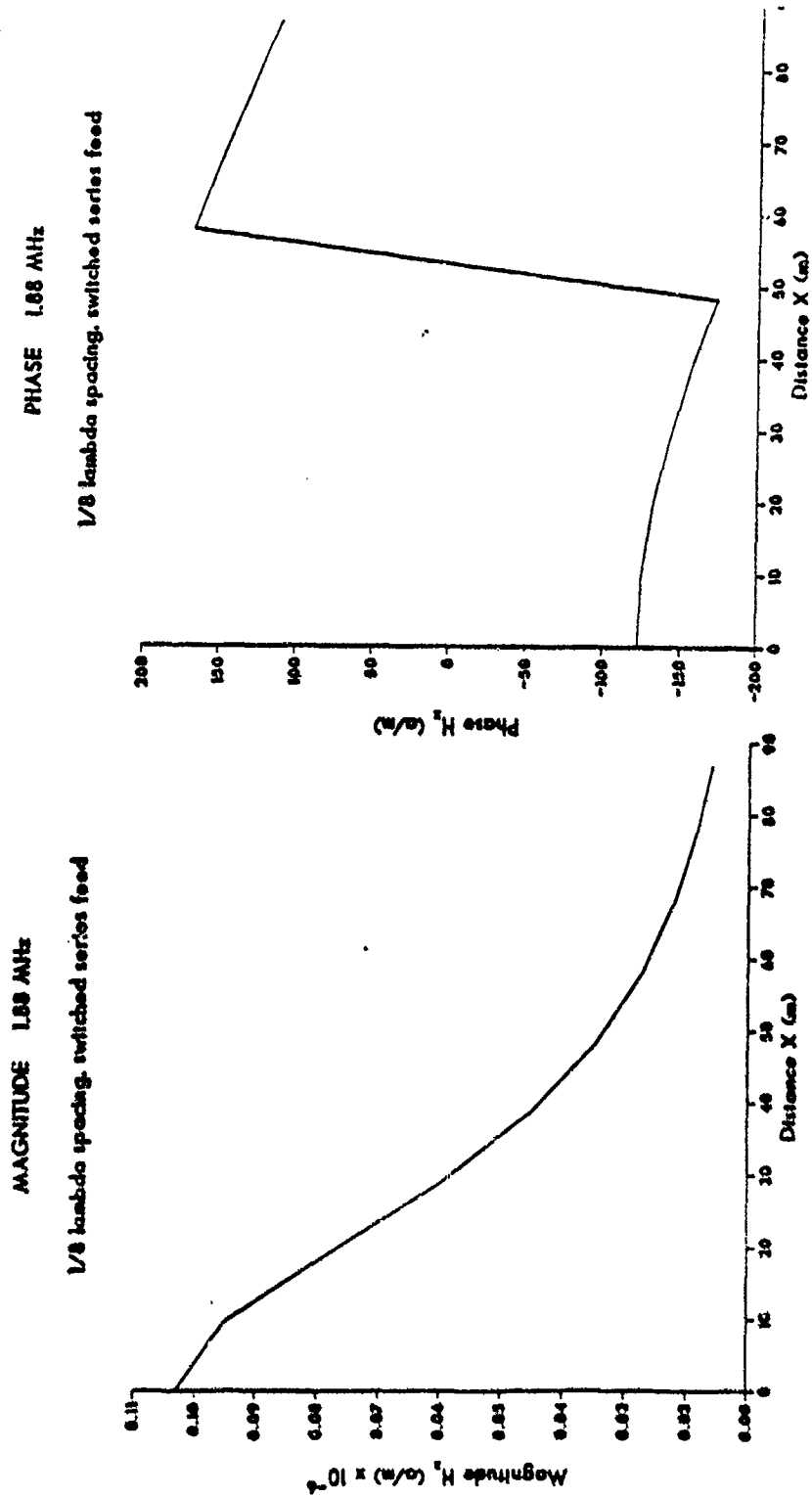
CM
CM      UNIFORM SHYDER DIPOLE ARRAY
CM      (SWITCHED SERIES FEED)
CM
CM      DIPOLE:  LENGTH= 1/4 LAMBDA AT FREQ= 3.38 MHZ
CM                SEGMENT LENGTHS= 31.66 FT
CM                THIN DIAMETER= 0.144" = 0.00183 METER RADIUS
CM                THICK DIAMETER= 0.296" = 0.00376 METER RADIUS
CM
CM      10 ELEMENT ARRAY
CM      ELEMENT SPACING = 1/8 WAVELENGTH (28.95 METERS)
CM
CM      Z0= 25 OHMS (THO 50 OHM LINES IN PARALLEL, OR
CM          12.5 BESIDE 12.5 IN PARALLEL)
CM      Z-NORM = 145 OHMS (BALUN LOAD)
CM      Z-FEED LINES = 300 OHMS
CM
CE
GM 10.5, 0.,-19.30,0, 0.,-9.65,0, 0.00183  FIRST THIN SEGMENT
GM 20.16, 0.,-9.65,0, 0.,-9.65,0, 0.00376  MIDDLE THICK SEGMENTS
GM 30.5, 0.,-9.65,0, 0.,19.30,0, 0.00183  OTHER THIN SEGMENT
GM 1.9, 0.0,0, 28.95,0,0, 010.030  9 MORE, 1/8 LAMBDA APART
GM 40.1, 0.0,0, 0.0,1, 0.0001  TL SHORT CKT STUB & FEED LINES
GM 1.21, 0.0,0, 28.95,0,0, 040.040  19 MORE TL SLUUS = 2 FEEDS
GM 0.0, 0.0,0, 1000,0,0, 340.061  MOVE TL STUBS & FEED LINES OUT
GM 0.0, 0.0,0, 0.0,38.6, 010.061  RAISE ARRAY LAMBDA/2 HIGH
GE 3
TL 20.8,40.1,12.5,19.30,0,0,1E6,1E6  TL STUBS (2 PER ELEMENT)
TL 20.9,41.1,12.5,19.30,0,0,1E6,1E6
TL 21.8,42.1,12.5,19.30,0,0,1E6,1E6
TL 21.9,43.1,12.5,19.30,0,0,1E6,1E6
TL 22.8,44.1,12.5,19.30,0,0,1E6,1E6
TL 22.9,45.1,12.5,19.30,0,0,1E6,1E6
TL 23.8,46.1,12.5,19.30,0,0,1E6,1E6
TL 23.9,47.1,12.5,19.30,0,0,1E6,1E6
TL 24.8,48.1,12.5,19.30,0,0,1E6,1E6
TL 24.9,49.1,12.5,19.30,0,0,1E6,1E6
TL 25.8,50.1,12.5,19.30,0,0,1E6,1E6
TL 25.9,51.1,12.5,19.30,0,0,1E6,1E6
TL 26.8,52.1,12.5,19.30,0,0,1E6,1E6
TL 26.9,53.1,12.5,19.30,0,0,1E6,1E6
TL 27.8,54.1,12.5,19.30,0,0,1E6,1E6
TL 27.9,55.1,12.5,19.30,0,0,1E6,1E6
TL 28.8,56.1,12.5,19.30,0,0,1E6,1E6
TL 28.9,57.1,12.5,19.30,0,0,1E6,1E6
TL 29.8,58.1,12.5,19.30,0,0,1E6,1E6
TL 29.9,59.1,12.5,19.30,0,0,1E6,1E6
TL 60.1,20.8,300,19.30,0,0,0,0  TL STUBS COMPLETE
TL 20.9,21.8,300, 0,0,0,0  FEED LINE TO THE ARRAY
TL 21.9,22.0,300, 0,0,0,0  START SWITCHED SERIES FEED
TL 22.9,23.8,300, 0,0,0,0  STRAIGHT LINE METHOD USED
TL 23.9,24.8,300, 0,0,0,0  FOR BLANK T.L. LENGTH
TL 24.9,25.8,300, 0,0,0,0
TL 25.9,26.8,300, 0,0,0,0
TL 26.9,27.8,300, 0,0,0,0
TL 27.9,28.8,300, 0,0,0,0
TL 28.9,29.8,300, 0,0,0,0
TL 29.9,61.1,300,19.30,0,0,0.0033,0  FEED LINES END @ MATCHD IMPONCE
EX 0.60,1.01,1.0,145  EXCITE ARRAY/ASK FOR IMP TABLE
FR 0.1,0.0,3.88,0  1 FREQUENCY
PL 2.2,1,1  STORE NEAR FIELD X-COMPONENT
NM 0,10,1,1,0,0,0,8,28.95,0,0  NEAR FIELD DATA, 0.8 METER UP
XQ
EN

```



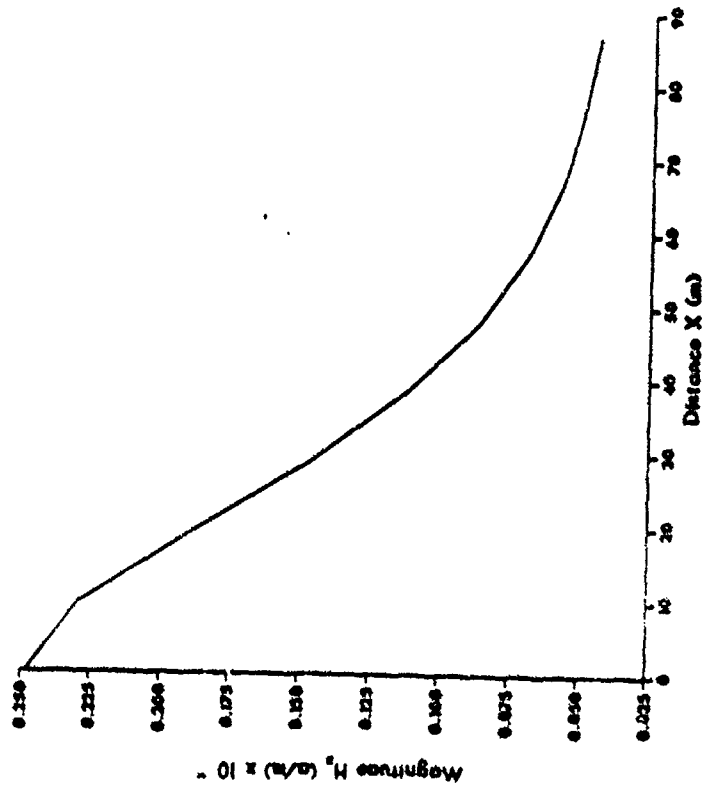
# APPENDIX B

## NEAR-MAGNETIC FIELD PLOTS FOR SNYDER SWITCHED SERIES ARRAYS



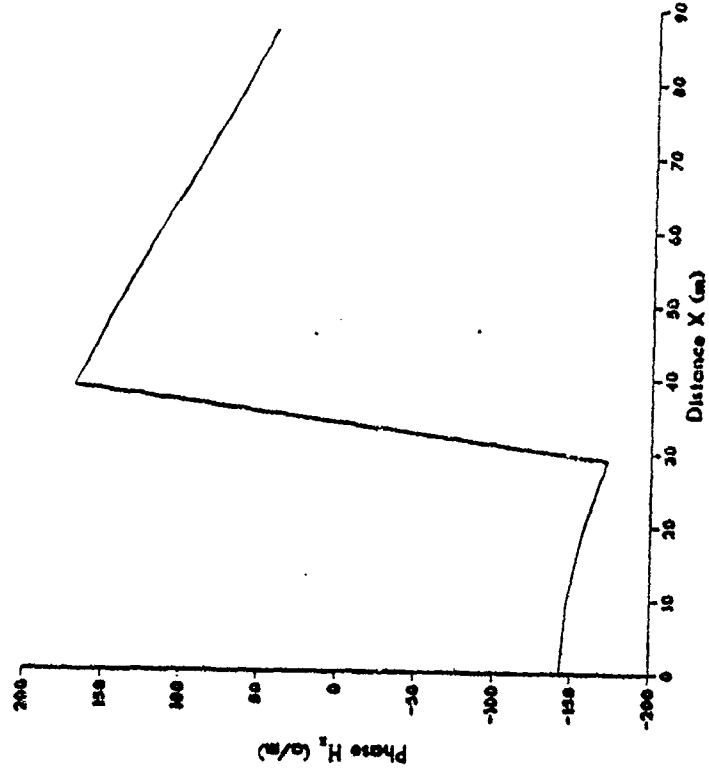
**MAGNITUDE 2.38 MHz**

1/8 lambda spacing, switched series feed



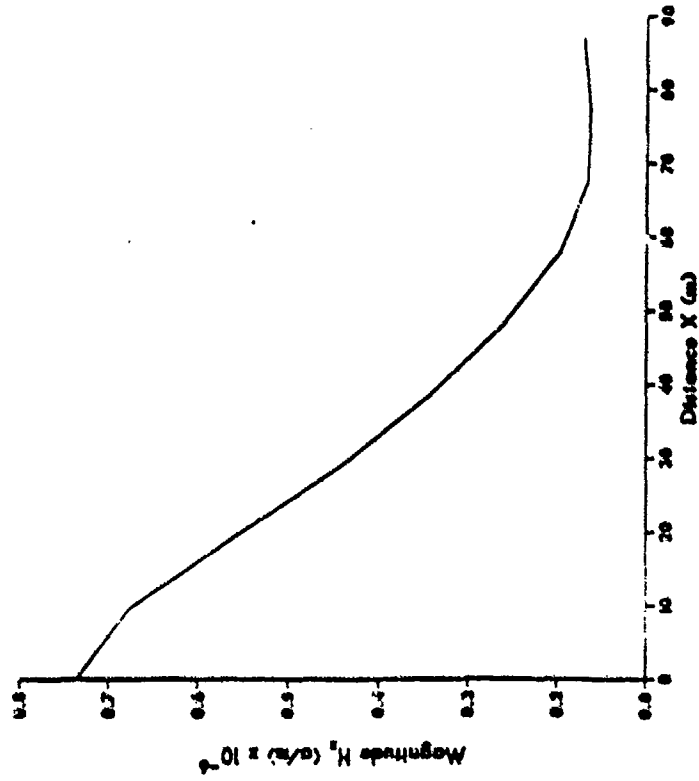
**PHASE 2.38 MHz**

1/8 lambda spacing, switched series feed



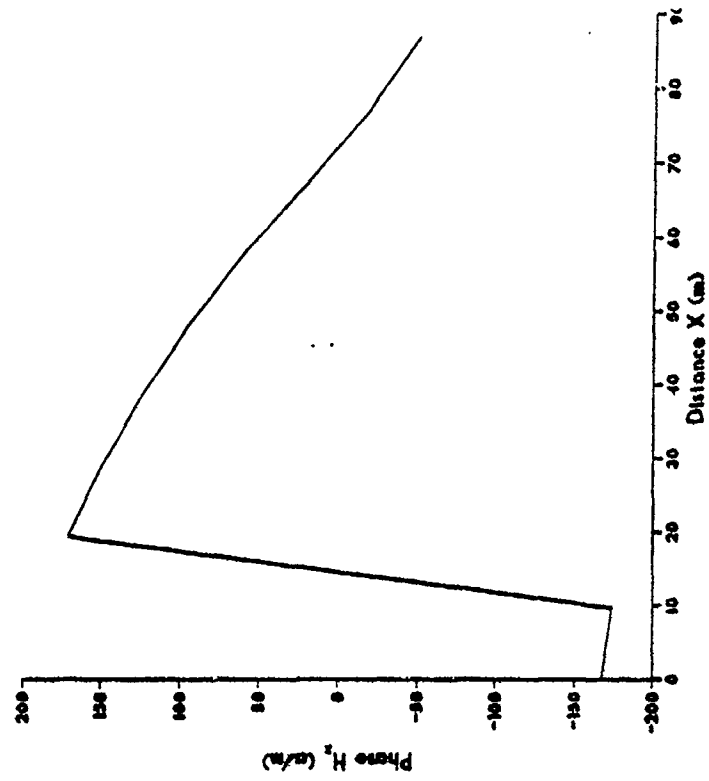
**MAGNITUDE 2.88 MHz**

1/8 lambda spacing, switched series feed



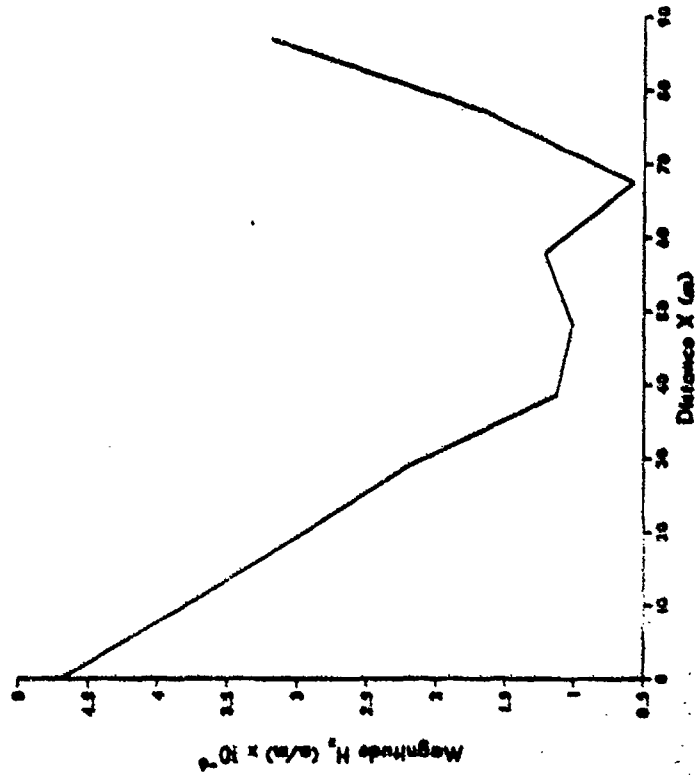
**PHASE 2.88 MHz**

1/8 lambda spacing, switched series feed



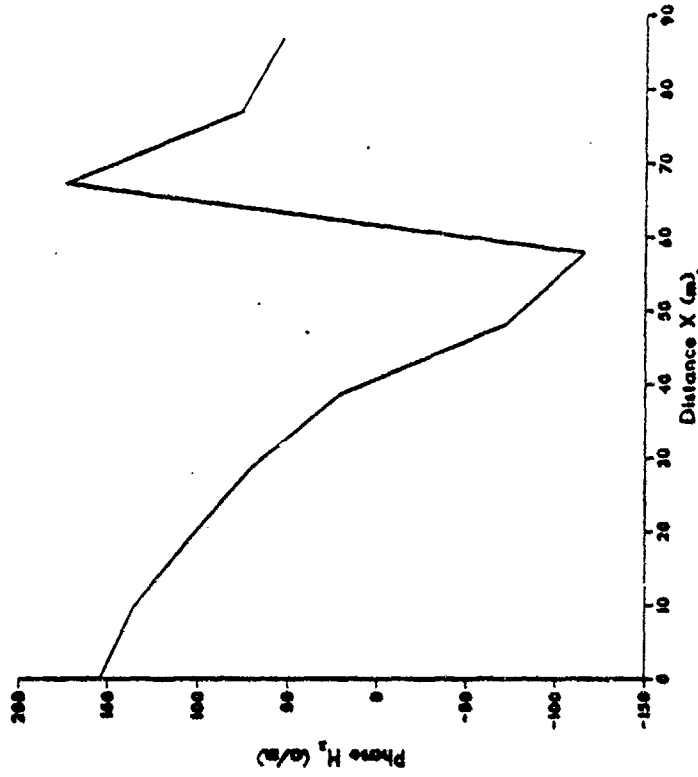
MAGNITUDE 2.38 MHz

1/8 lambda spacing, switched series feed



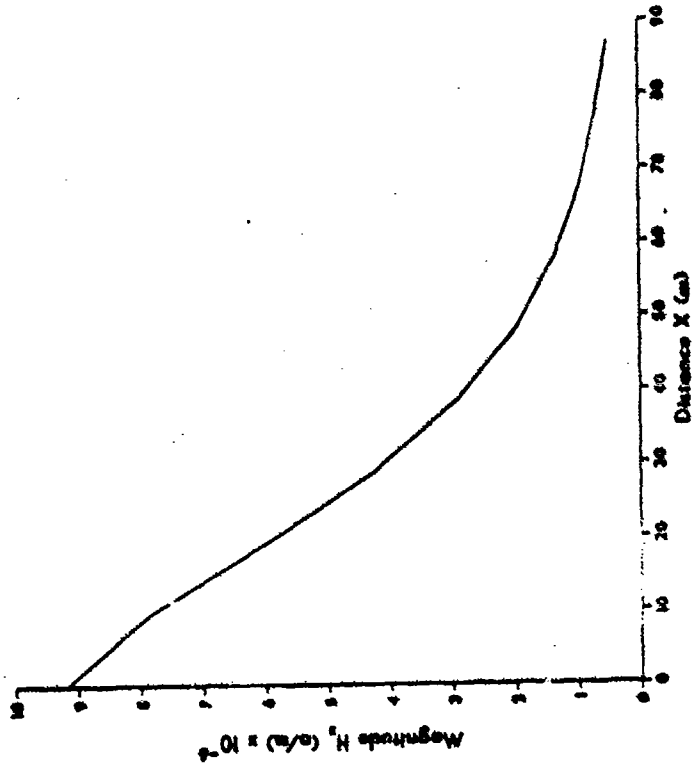
PHASE 3.36 MHz

1/8 lambda spacing, switched series feed



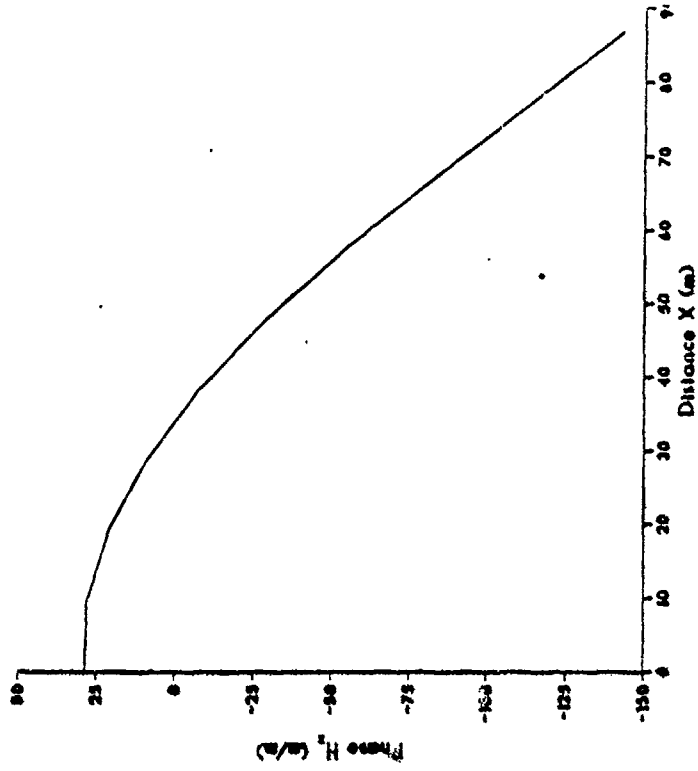
MAGNITUDE 3.63 MHz

1/8 lambda spacing, switched series feed

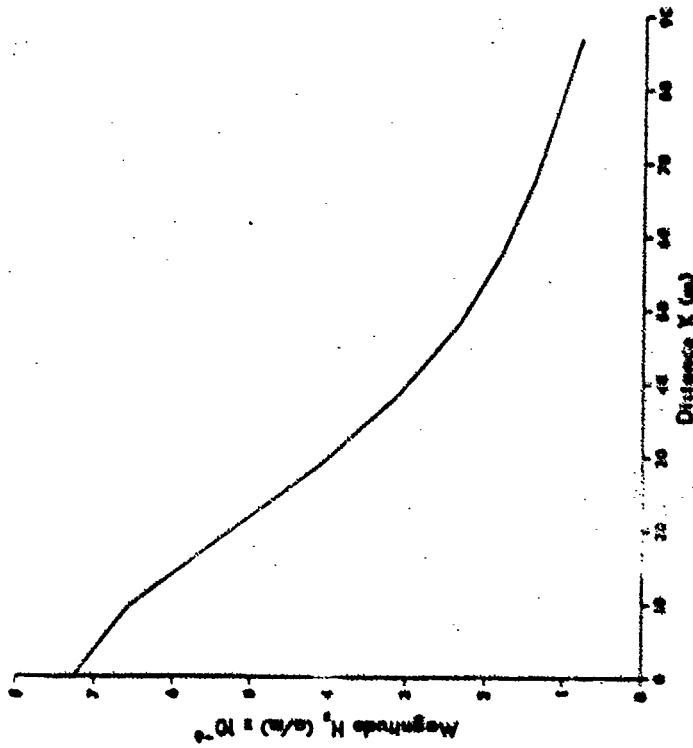


PHASE 3.63 MHz

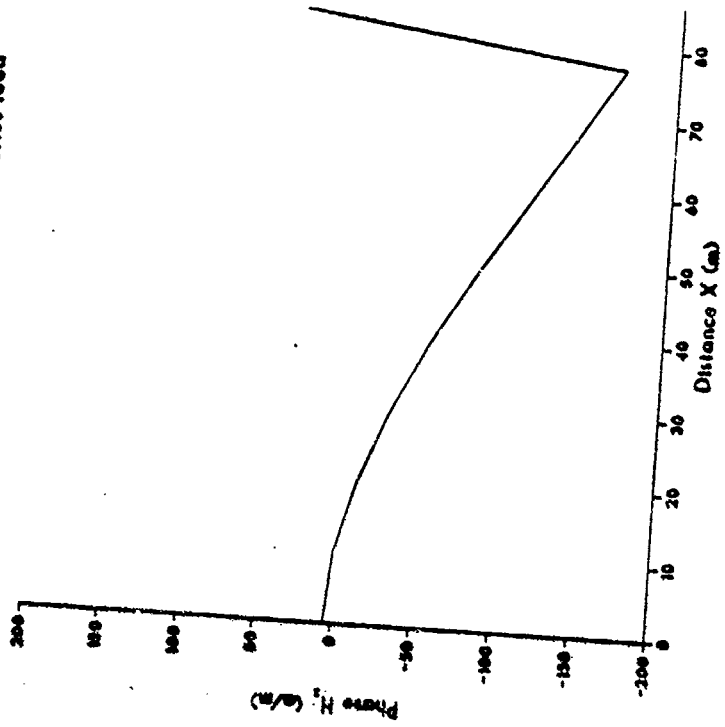
1/8 lambda spacing, switched series feed



**MAGNITUDE 3.72 MHz**  
 1/8 lambda spacing, switched series feed

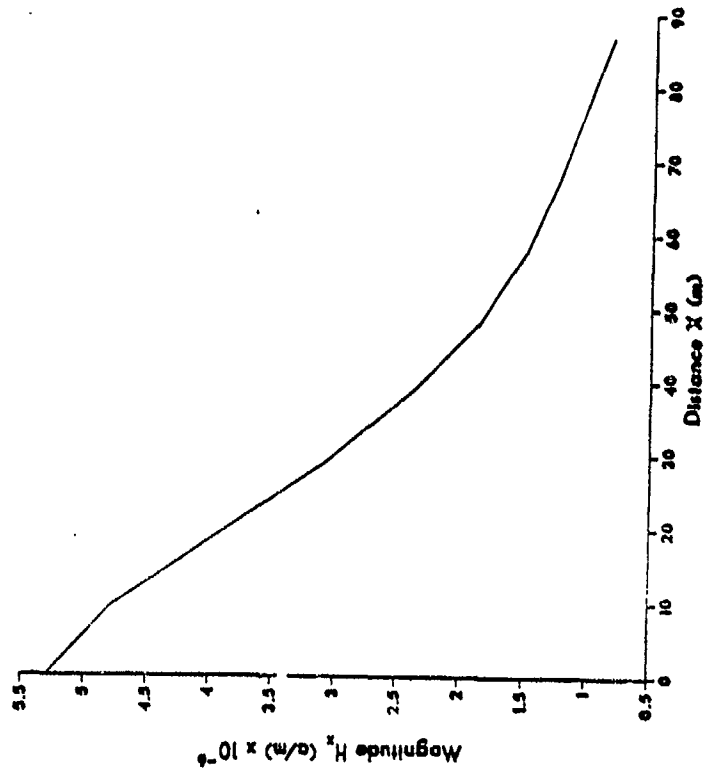


**PHASE 3.72 MHz**  
 1/8 lambda spacing, switched series feed



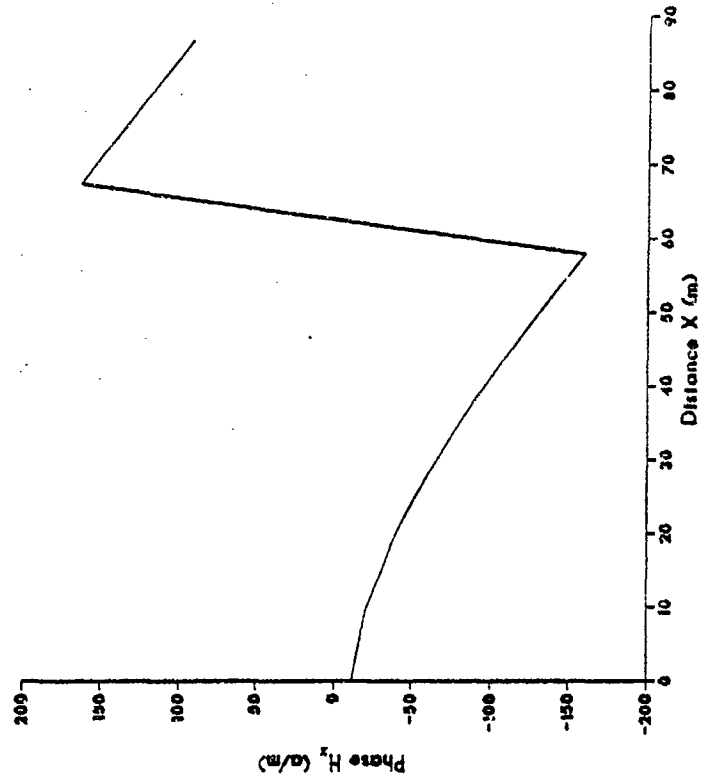
**MAGNITUDE 3.81 MHz**

1/8 lambda spacing, switched series feed



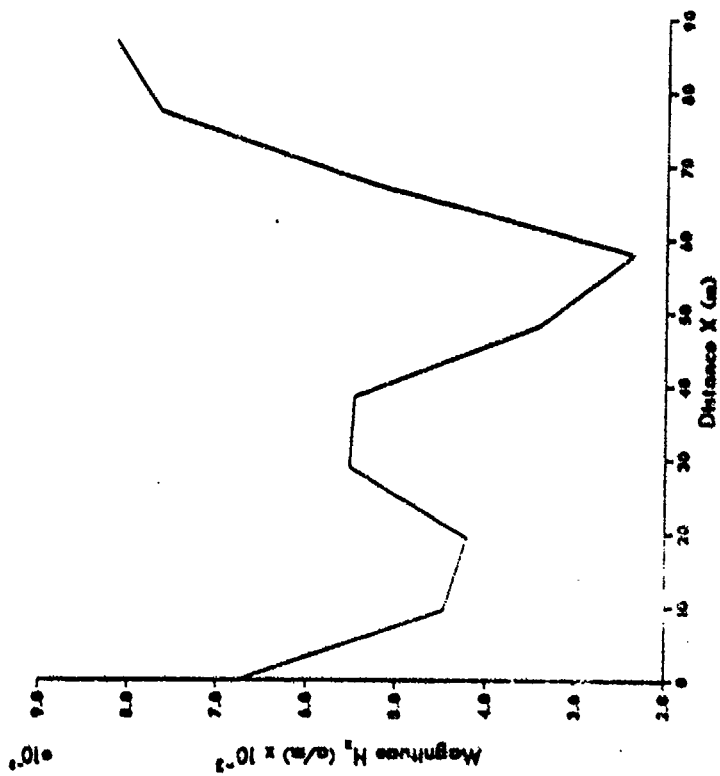
**PHASE 3.81 MHz**

1/8 lambda spacing, switched series feed



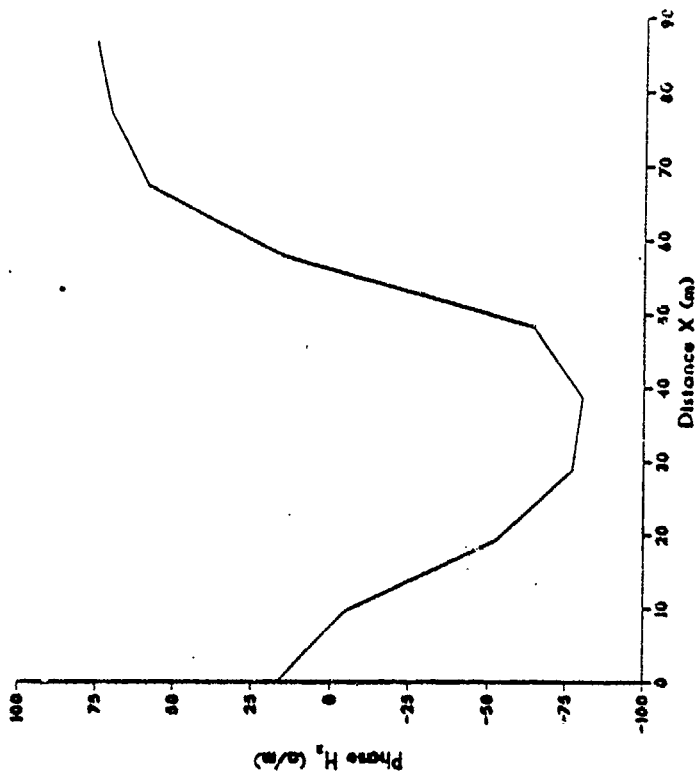
MAGNITUDE 3.88 MHz

1/8 lambda spacing, switched series feed



PHASE 3.88 MHz

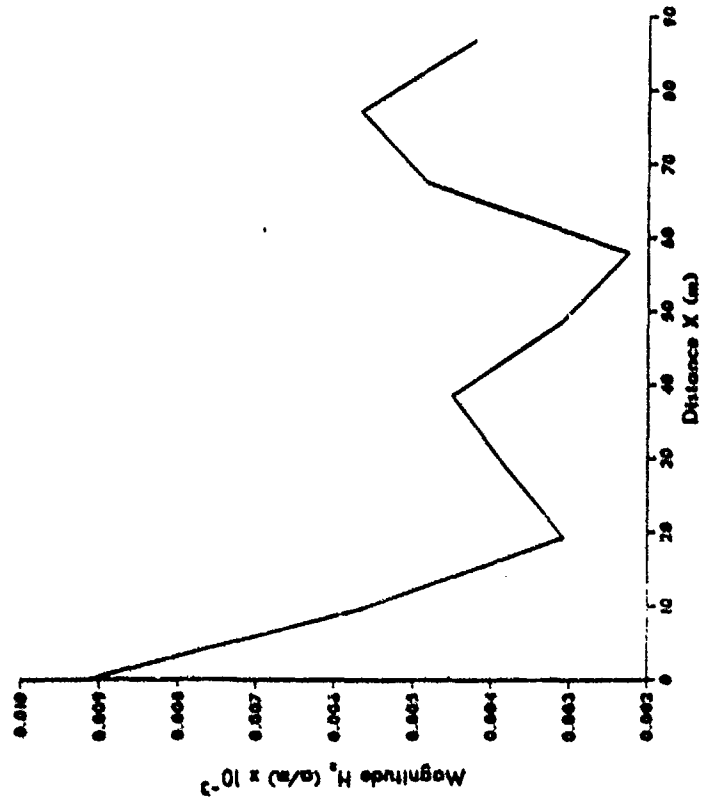
1/8 lambda spacing, switched series feed





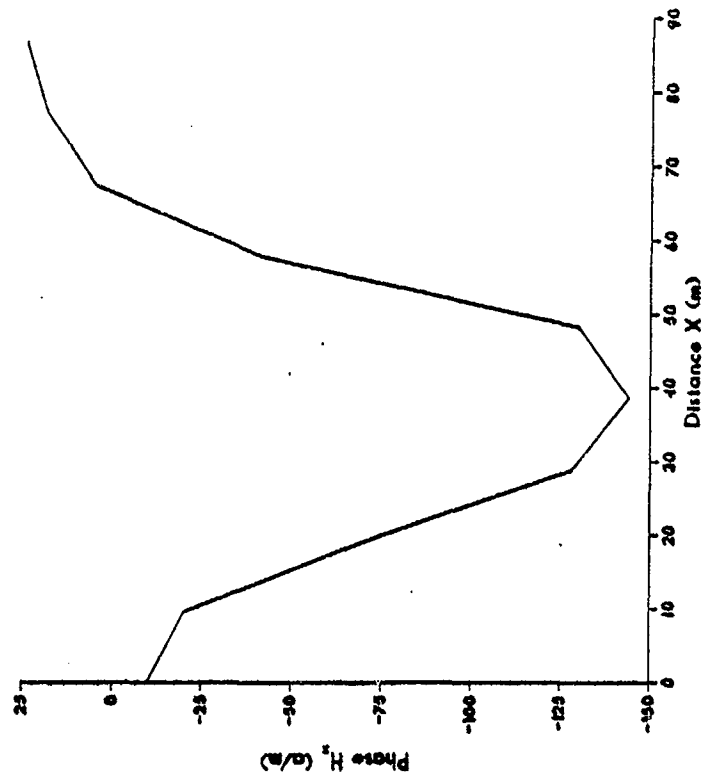
MAGNITUDE 3.95 MHz

1/8 lambda spacing, switched series feed



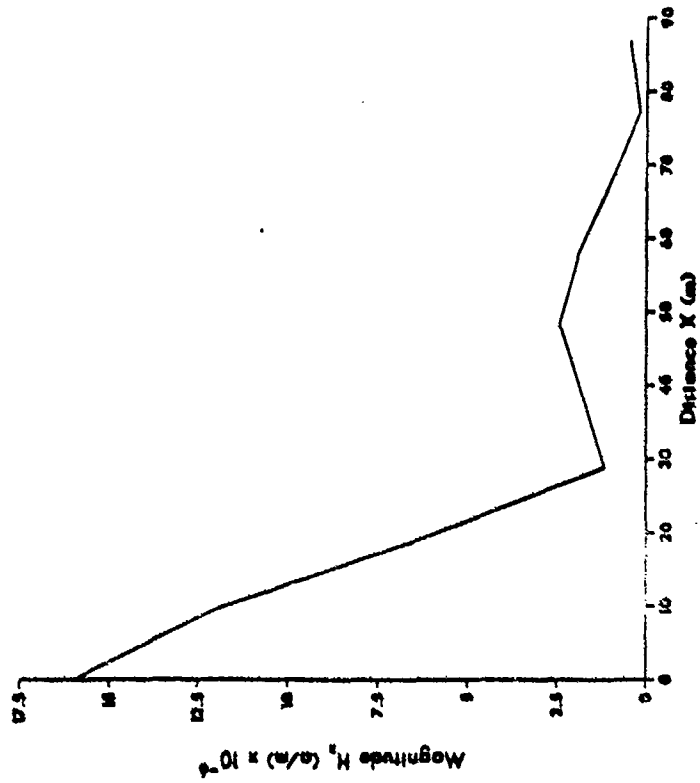
PHASE 3.95 MHz

1/8 lambda spacing, switched series feed



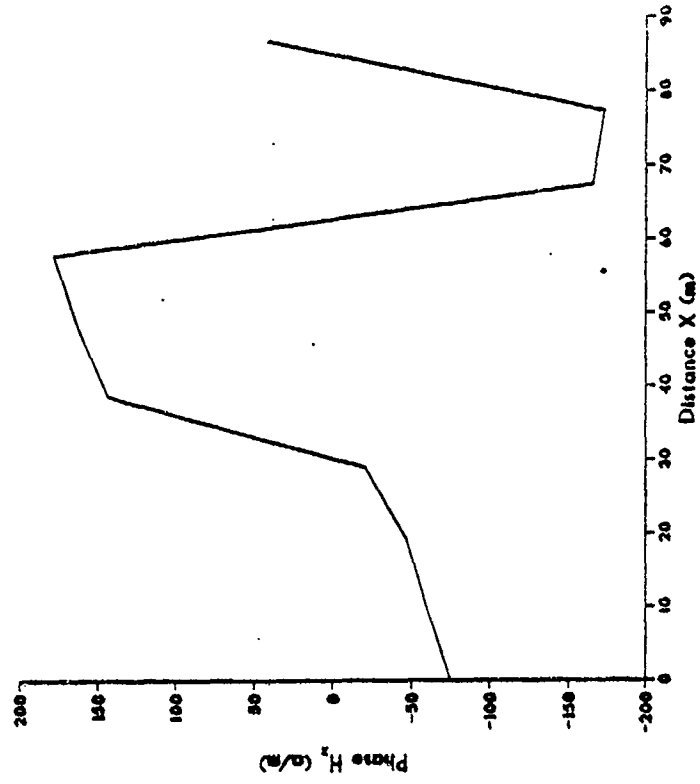
MAGNITUDE 4.04 MHz

1/8 lambda spacing, switched series feed



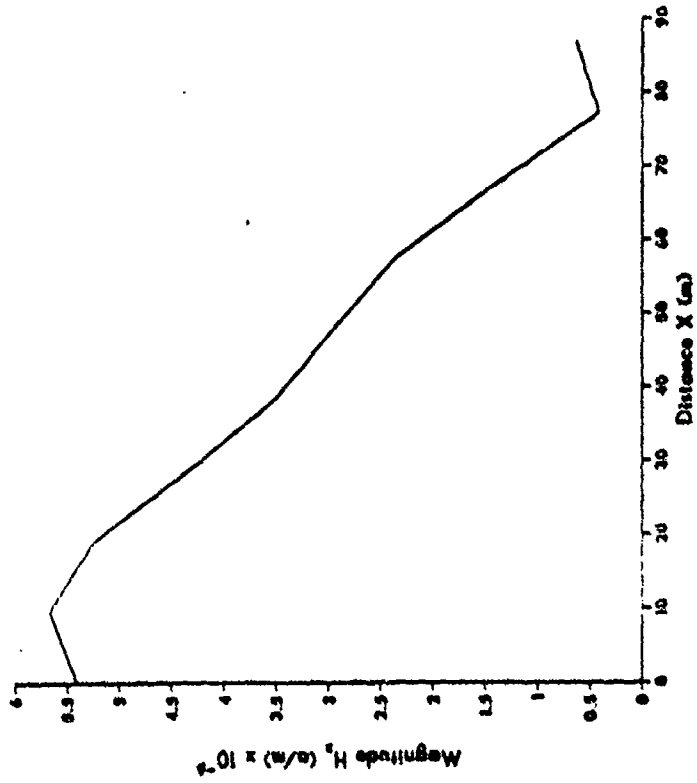
PHASE 4.04 MHz

1/8 lambda spacing, switched series feed



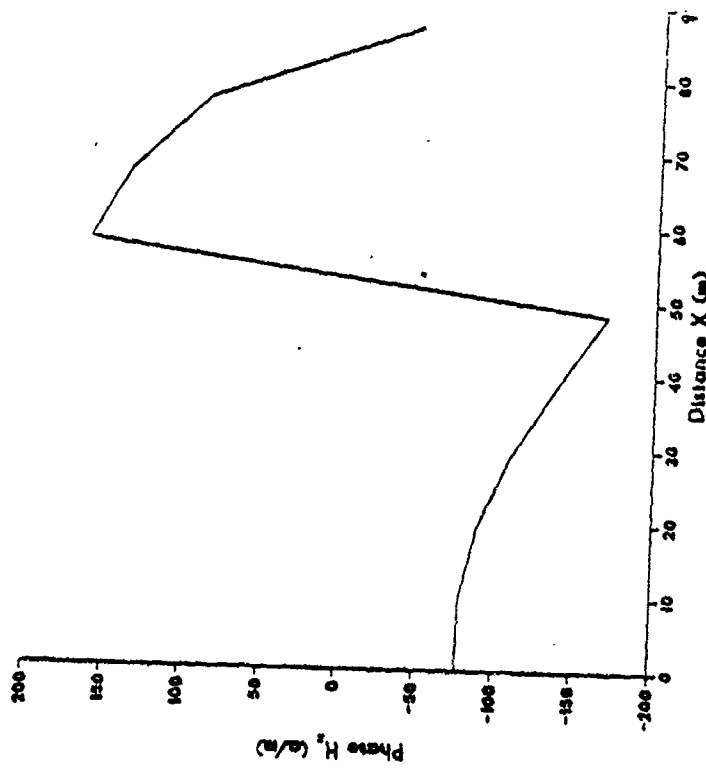
MAGNITUDE 4.13 MHz

1/8 lambda spacing, switched series feed



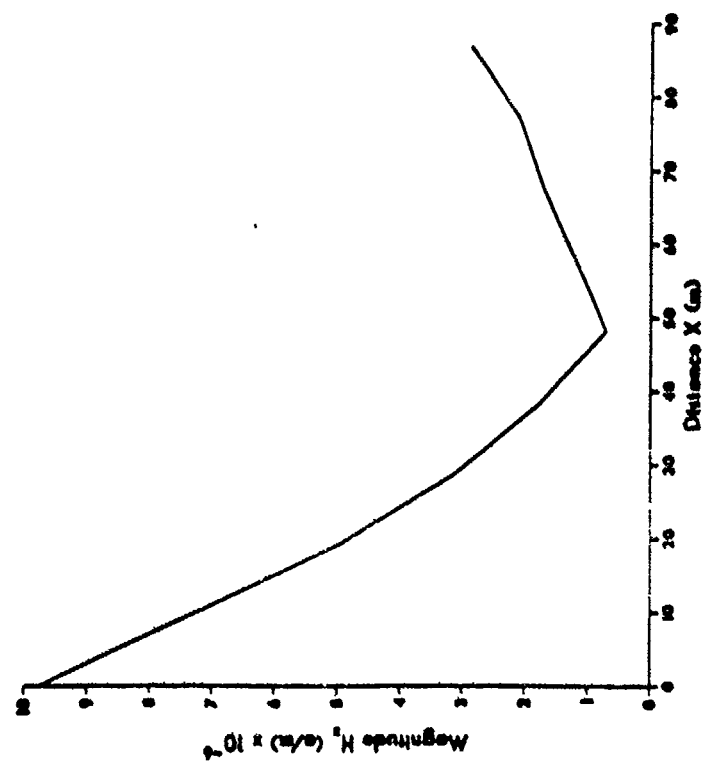
PHASE 4.13 MHz

1/8 lambda spacing, switched series feed



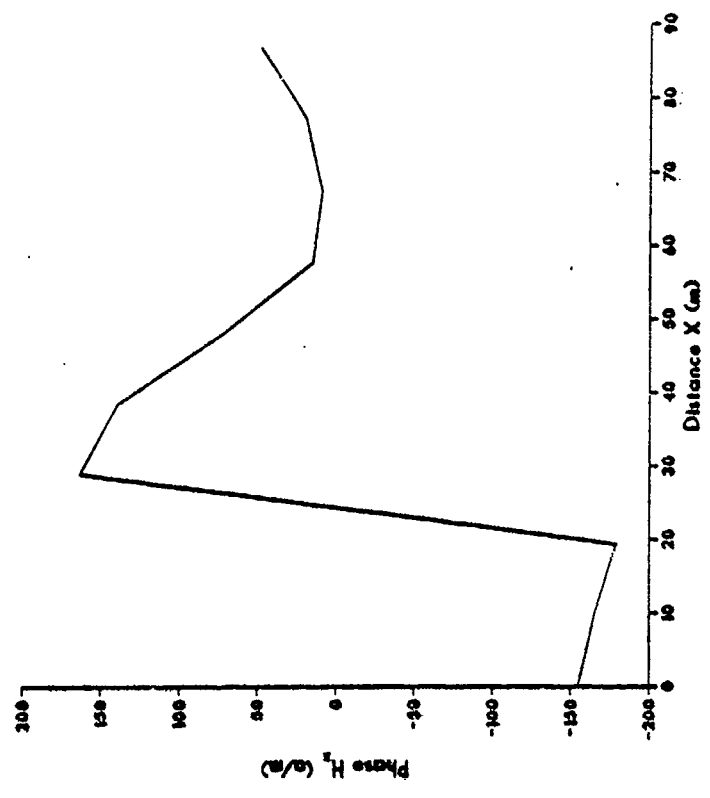
MAGNITUDE 4.38 MHz

1/8 lambda spacing, switched series feed



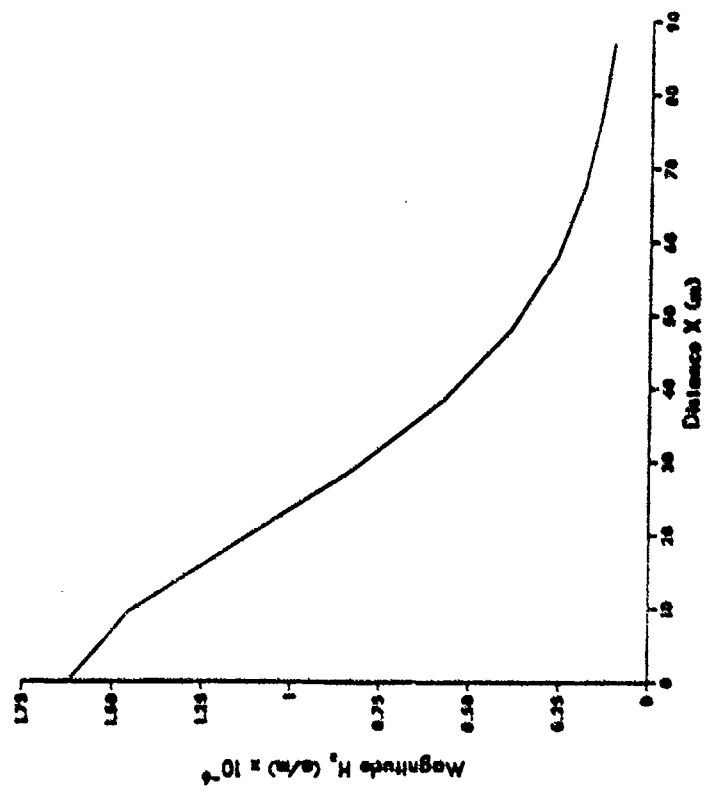
PHASE 4.38 MHz

1/8 lambda spacing, switched series feed



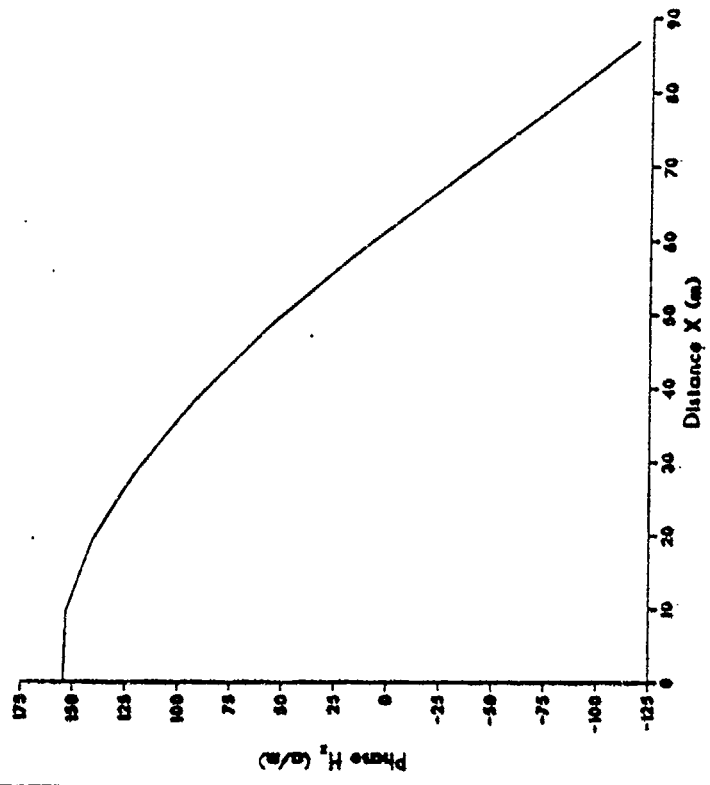
**MAGNITUDE 4.88 MHz**

1/8 lambda spacing, switched series feed



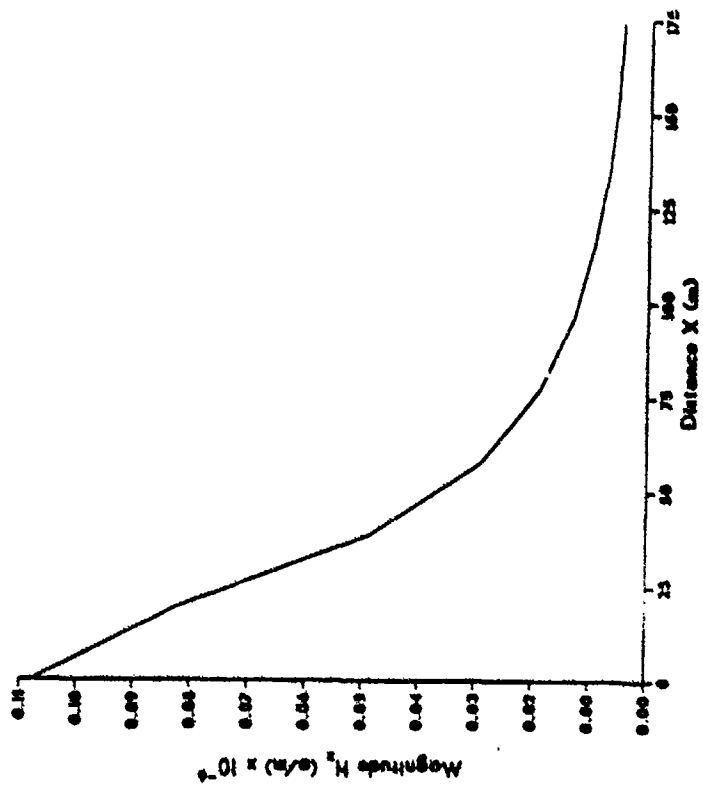
**PHASE 4.88 MHz**

1/8 lambda spacing, switched series feed



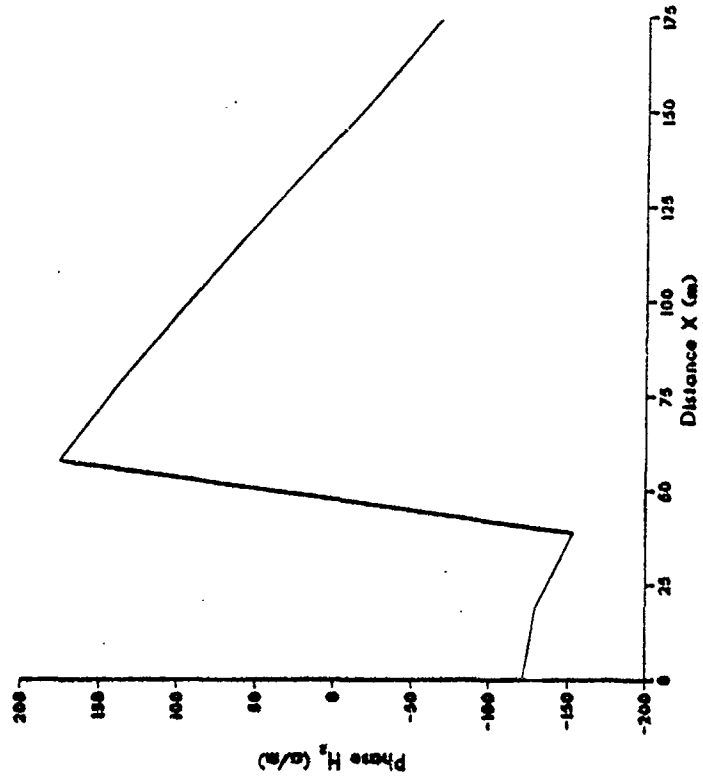
**MAGNITUDE 1.88 MHz**

1/4 lambda spacing, switched series feed



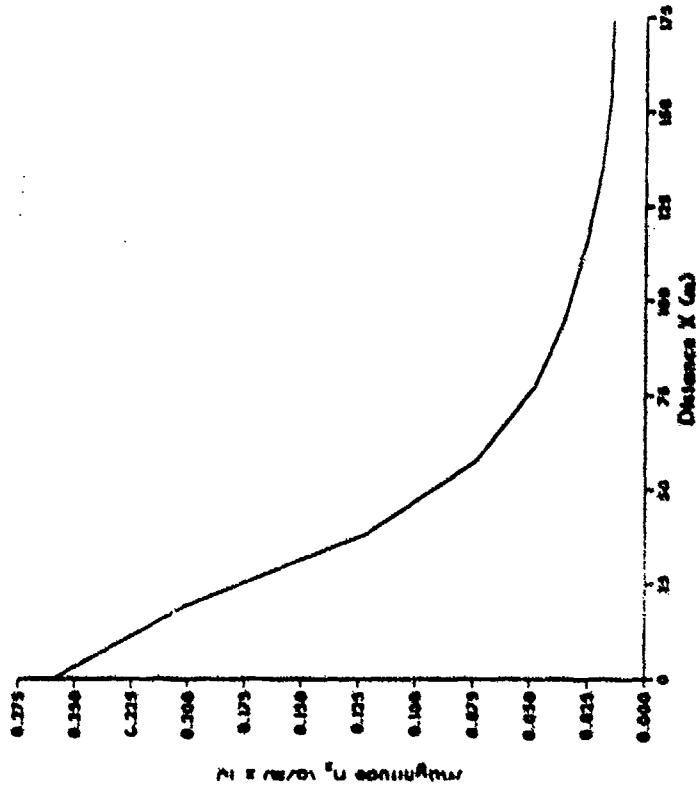
**PHASE 1.88 MHz**

1/4 lambda spacing, switched series feed



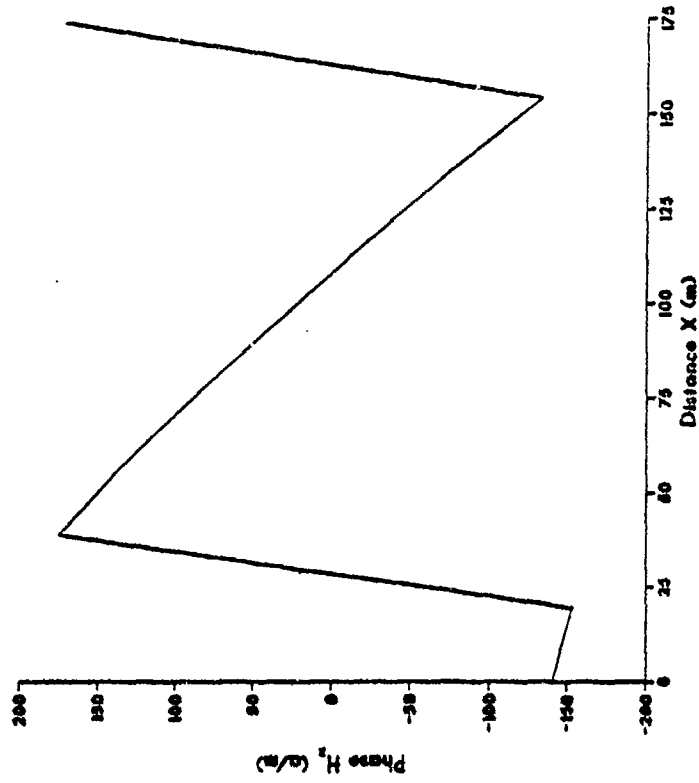
MAGNITUDE 2.38 MHz

1/4 lambda spacing, switched series feed



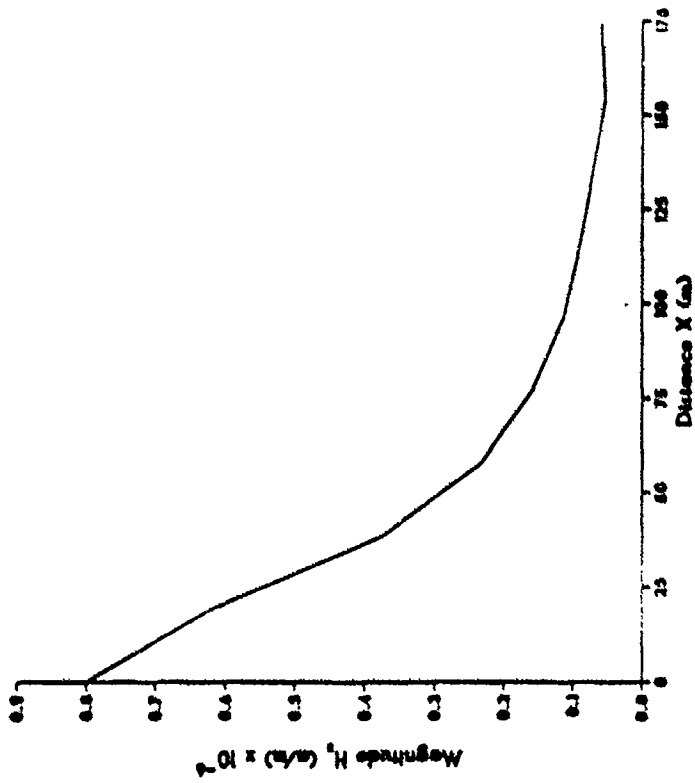
PHASE 2.38 MHz

1/4 lambda spacing, switched series feed



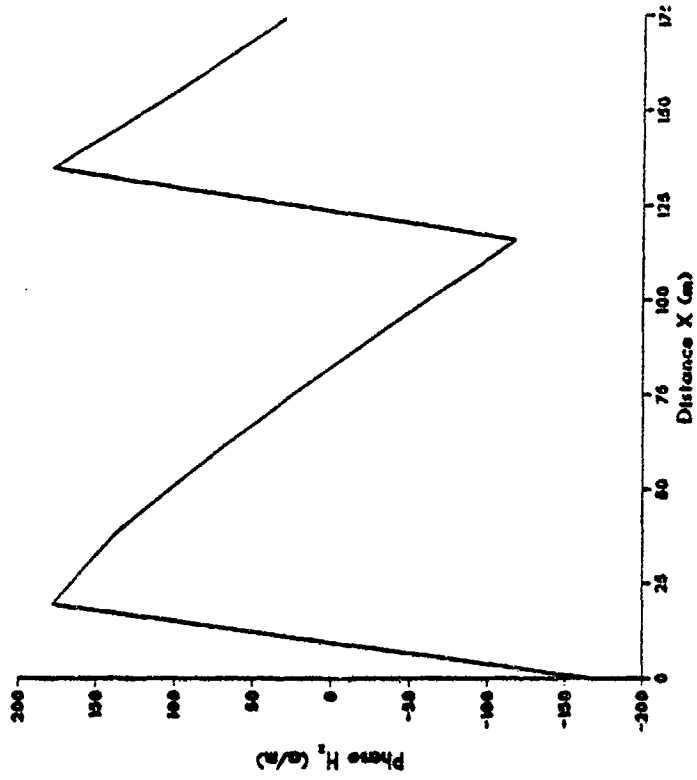
MAGNITUDE 2.88 MHz

1/4 lambda spacing, switched series feed



PHASE 2.88 MHz

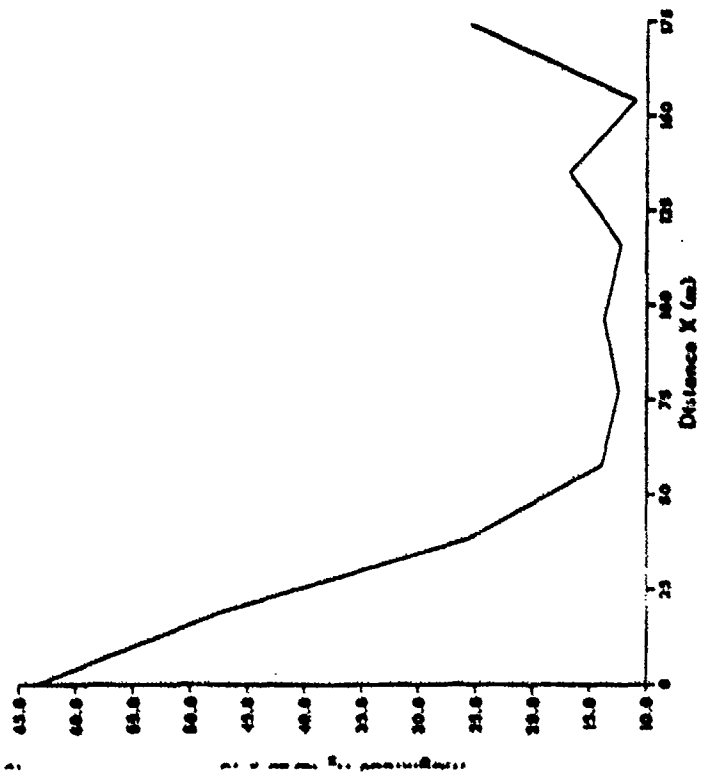
1/4 lambda spacing, switched series feed





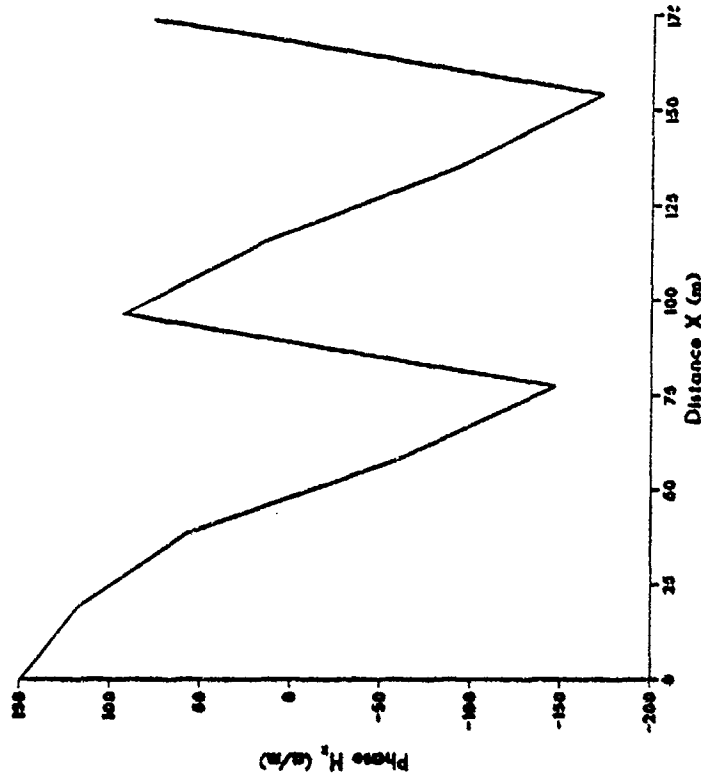
MAGNITUDE 3.38 MHz

1/4 lambda spacing, switched series feed



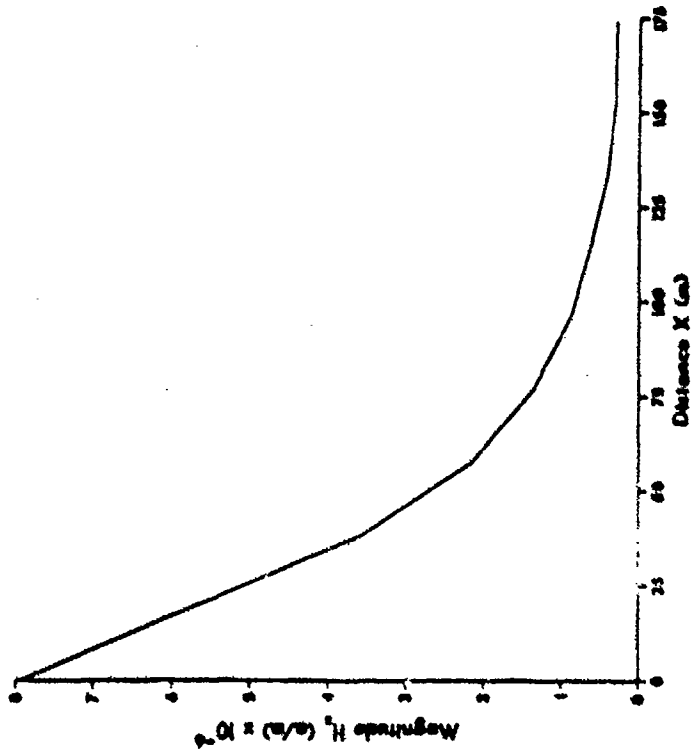
PHASE 3.38 MHz

1/4 lambda spacing, switched series feed



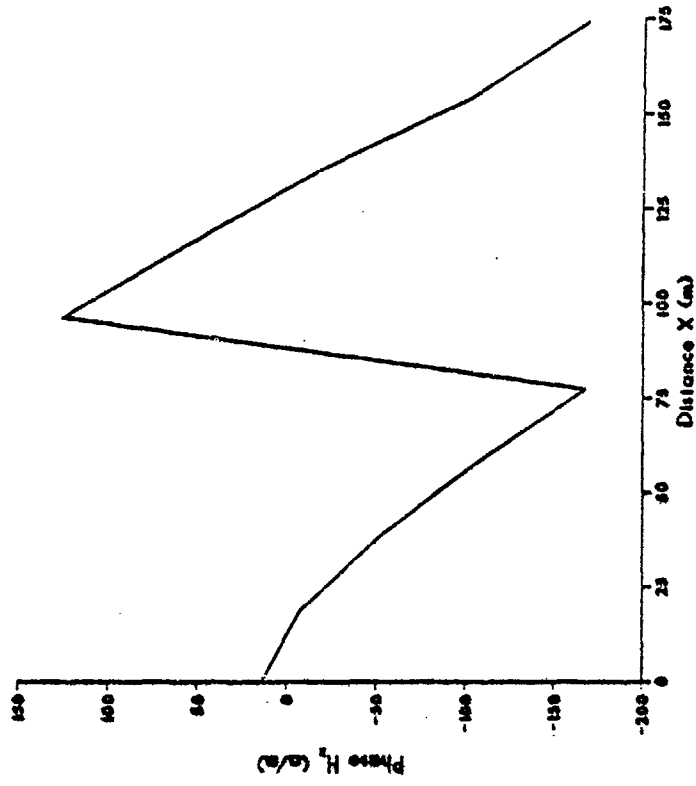
**MAGNITUDE 3.63 MHz**

1/4 lambda spacing, switched series feed



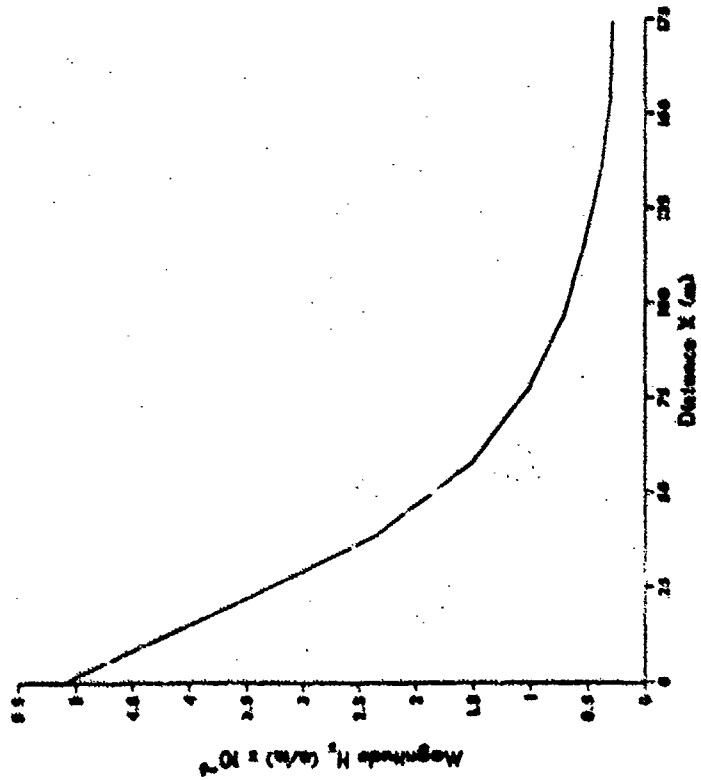
**PHASE 3.63 MHz**

1/4 lambda spacing, switched series feed



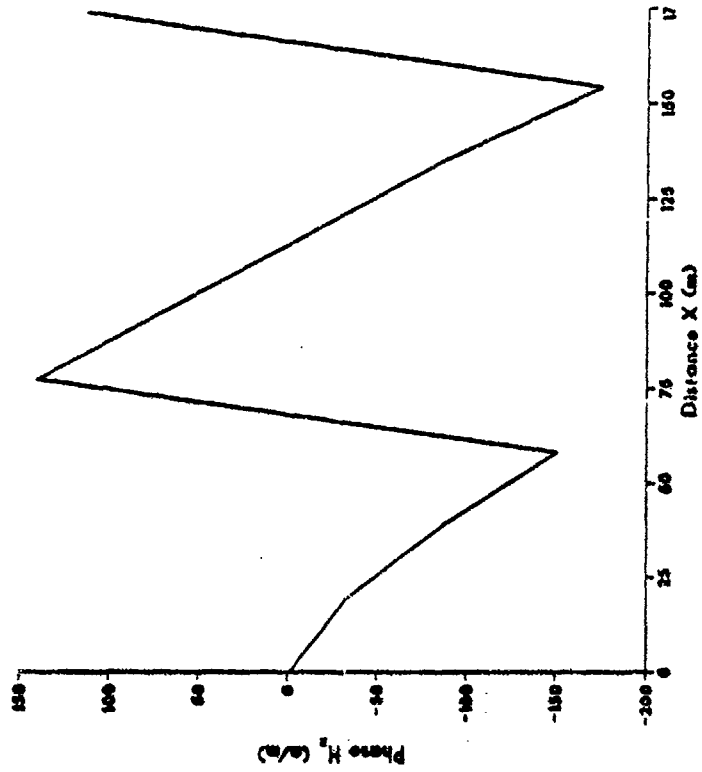
**MAGNITUDE 3.72 MHz**

1/4 lambda spacing, switched series feed



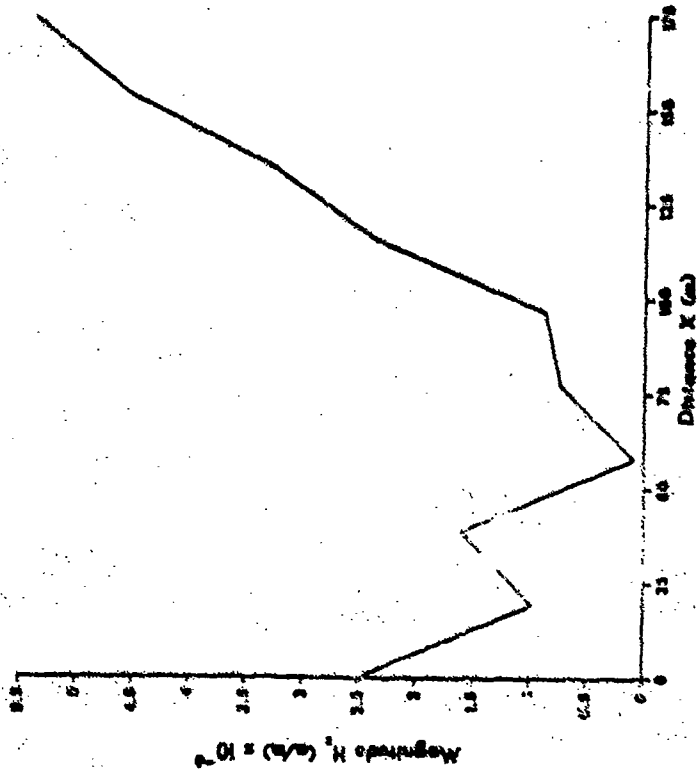
**PHASE 3.72 MHz**

1/4 lambda spacing, switched series feed



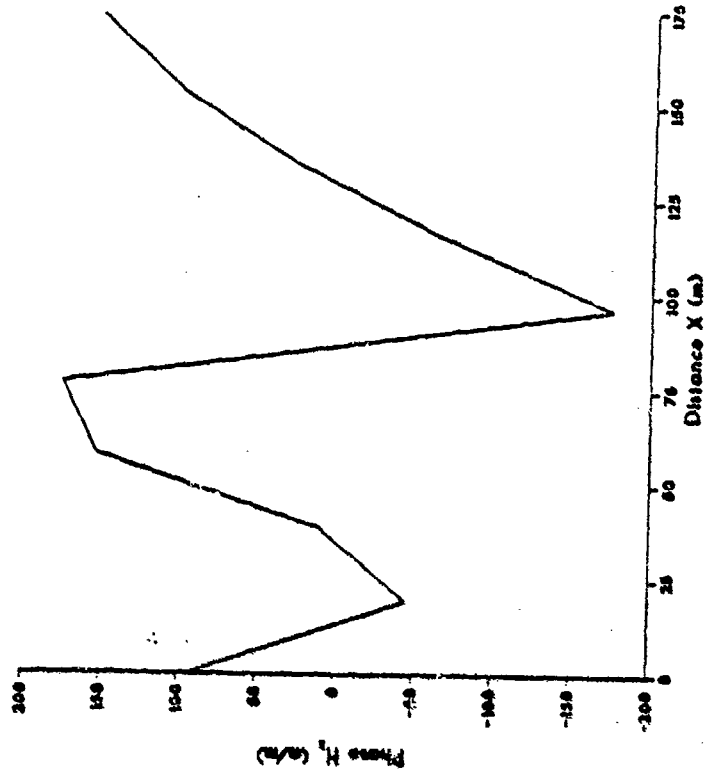
MAGNITUDE 2.81 MHz

1/4 lambda spacing, switched series feed



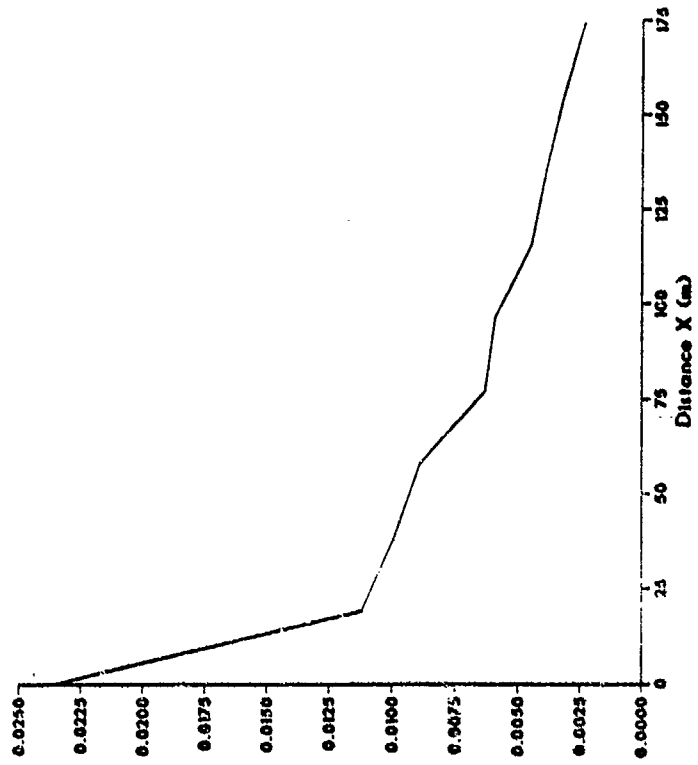
PHASE 3.81 MHz

1/4 lambda spacing, switched series feed



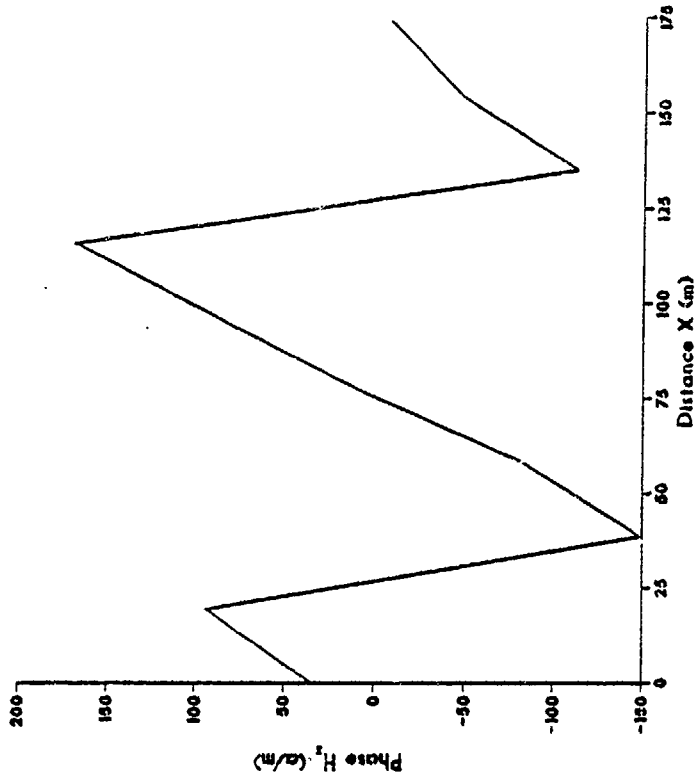
MAGNITUDE 3.88 MHz

1/4 lambda spacing, switched series feed



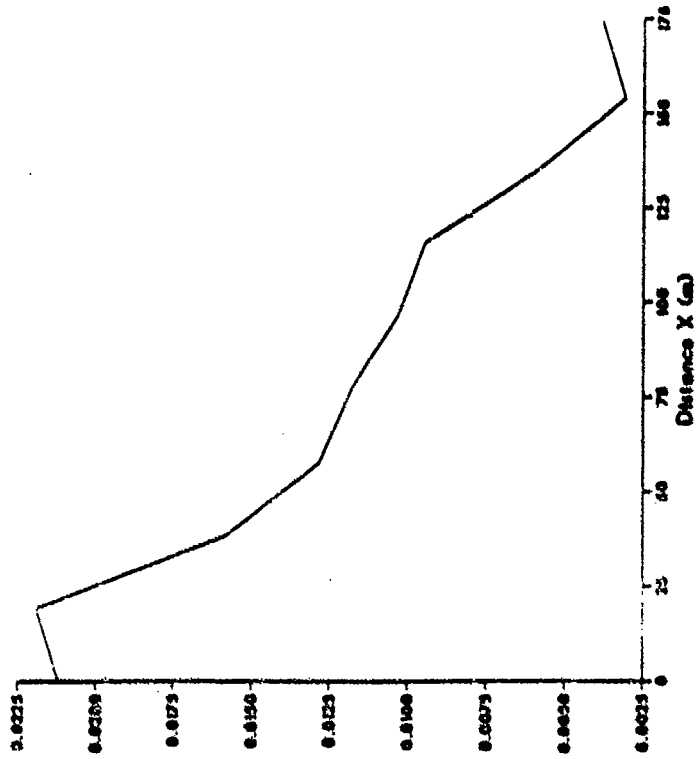
PHASE 3.88 MHz

1/4 lambda spacing, switched series feed



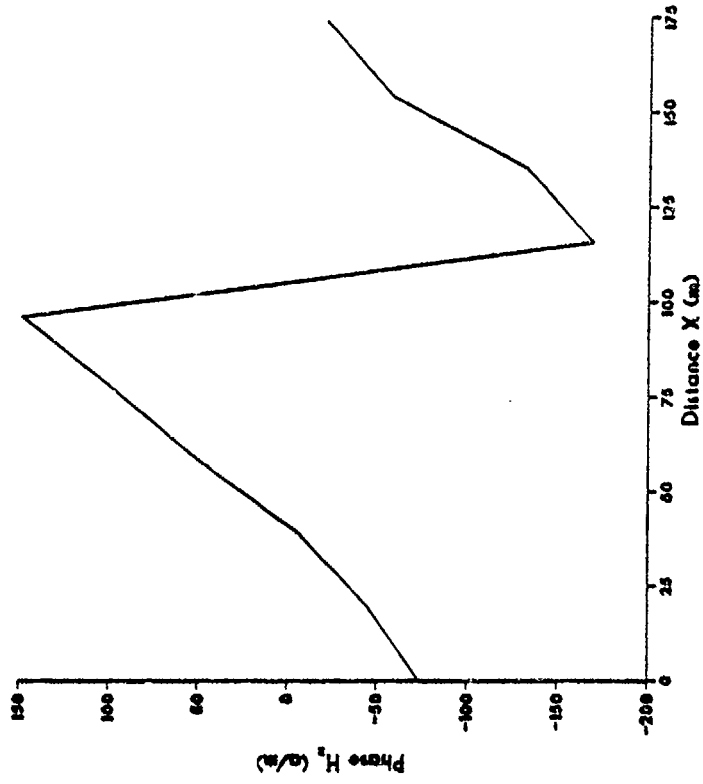
MAGNITUDE 3.95 MHz

1/4 lambda spacing, switched series feed



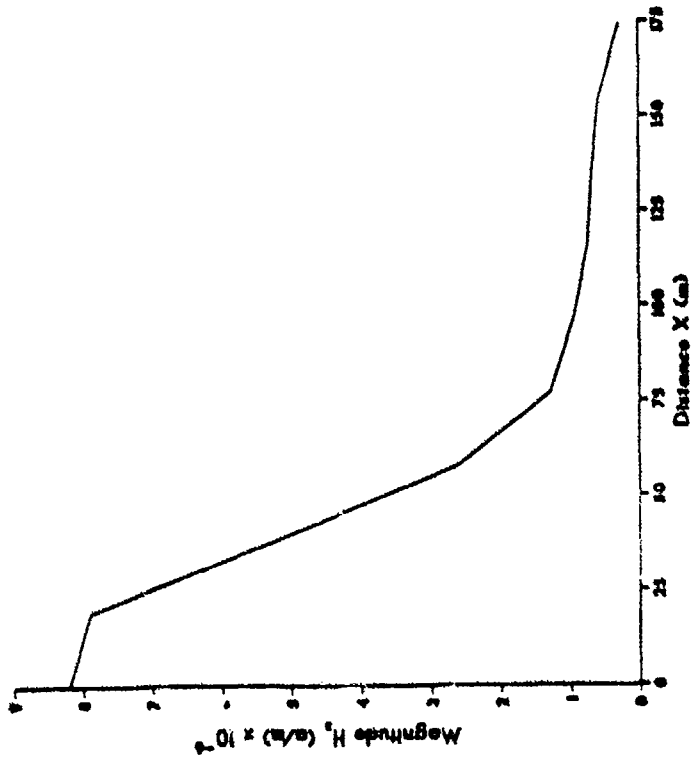
PHASE 3.95 MHz

1/4 lambda spacing, switched series feed



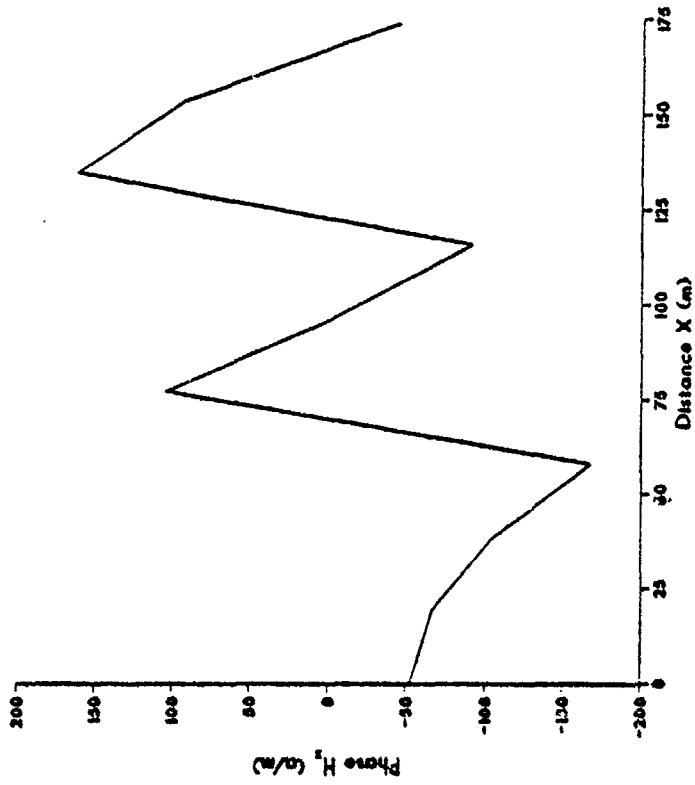
MAGNITUDE 4.04 MHz

1/4 lambda spacing, switched series feed



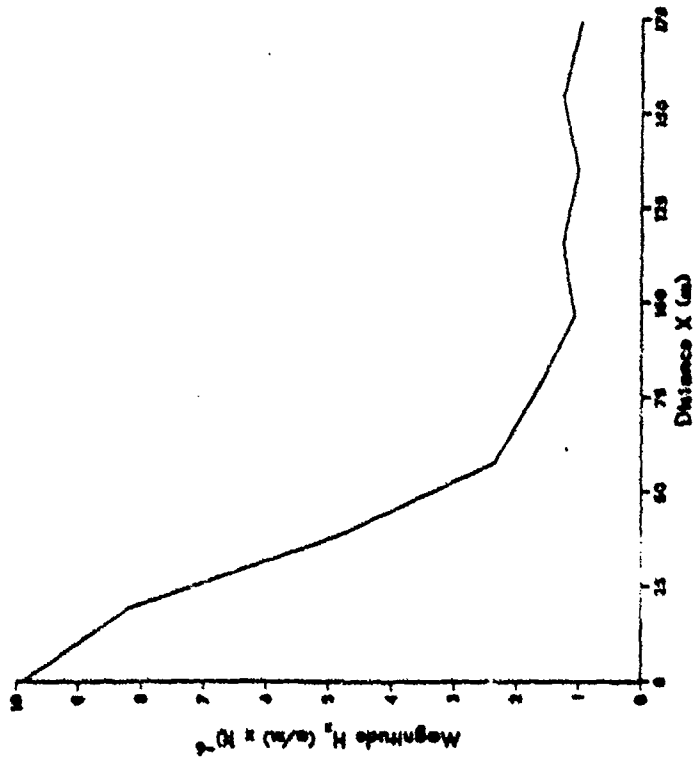
PHASE 4.04 MHz

1/4 lambda spacing, switched series feed



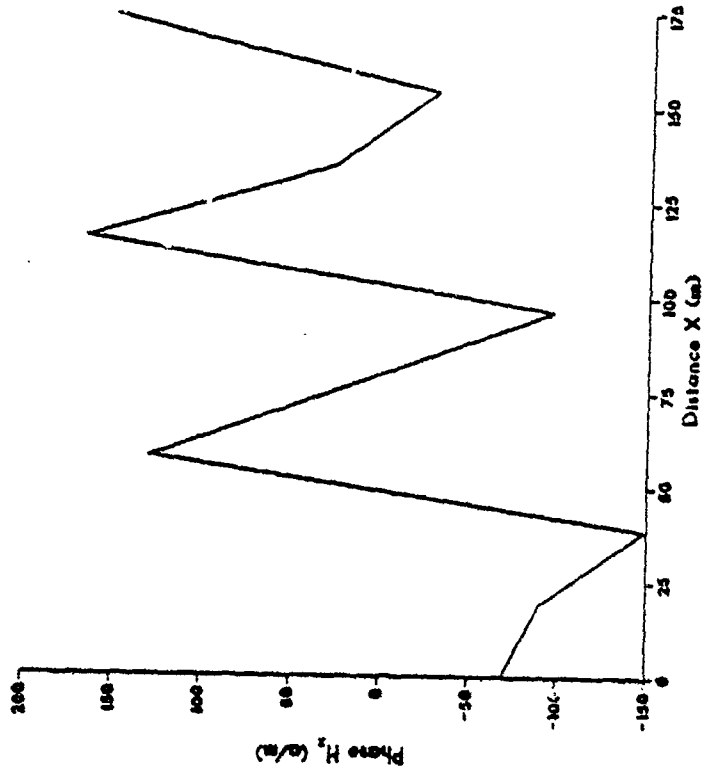
**MAGNITUDE 4.13 MHz**

*1/4 lambda spacing, switched series feed*



**PHASE 4.13 MHz**

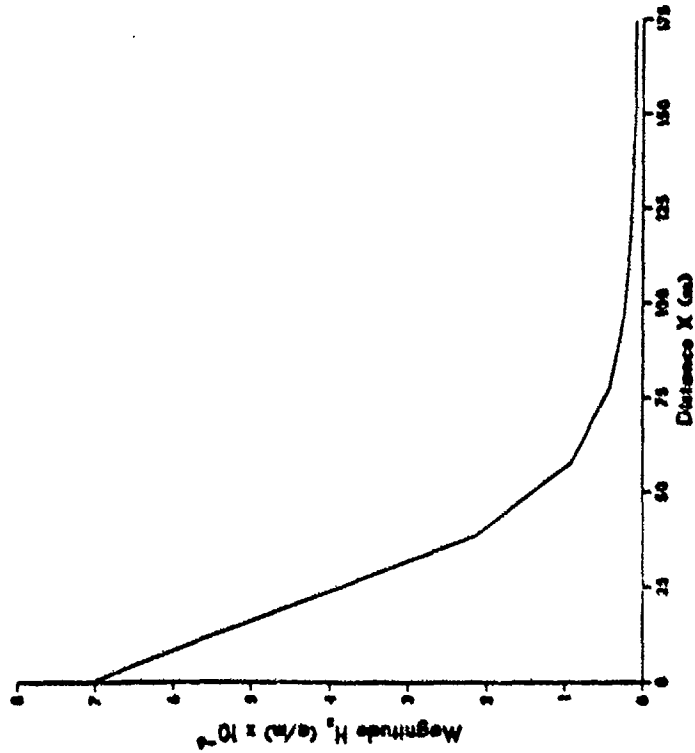
*1/4 lambda spacing, switched series feed*





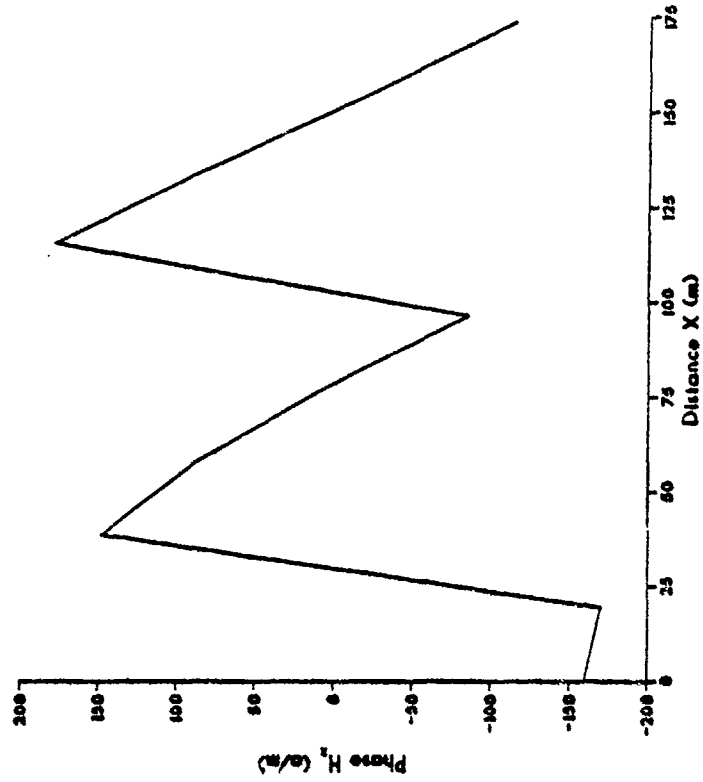
**MAGNITUDE 4.38 MHz**

1/4 lambda spacing, switched series feed



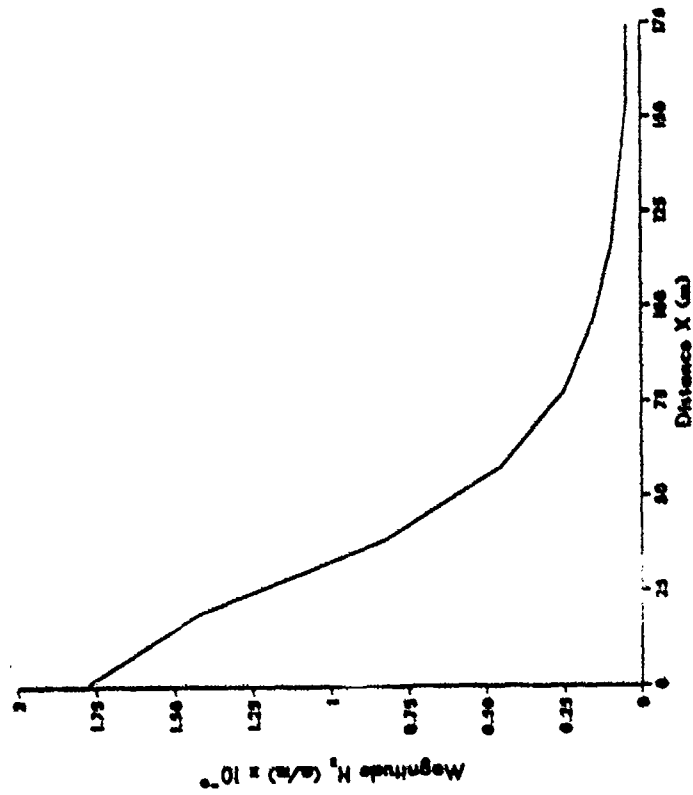
**PHASE 4.38 MHz**

1/4 lambda spacing, switched series feed



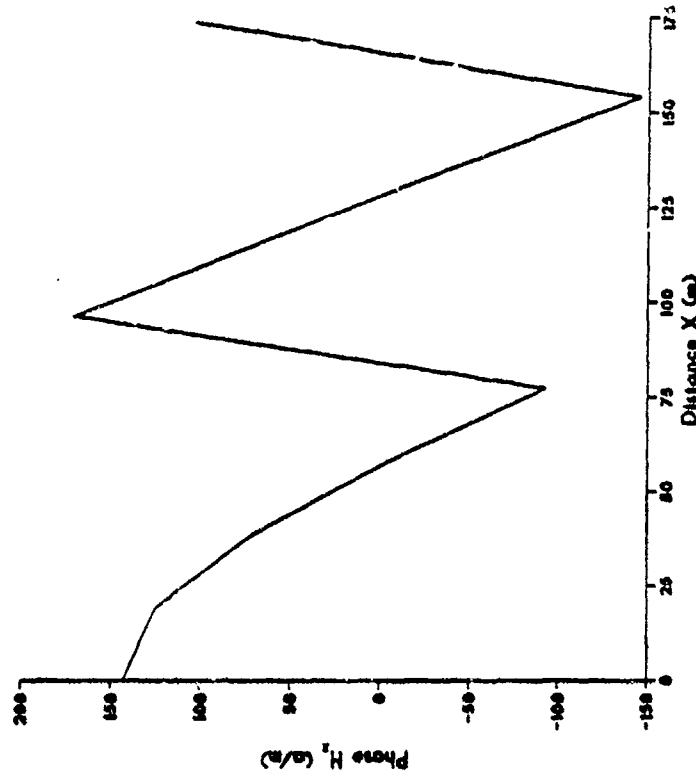
**MAGNITUDE 4.88 MHz**

1/4 lambda spacing, switched series feed



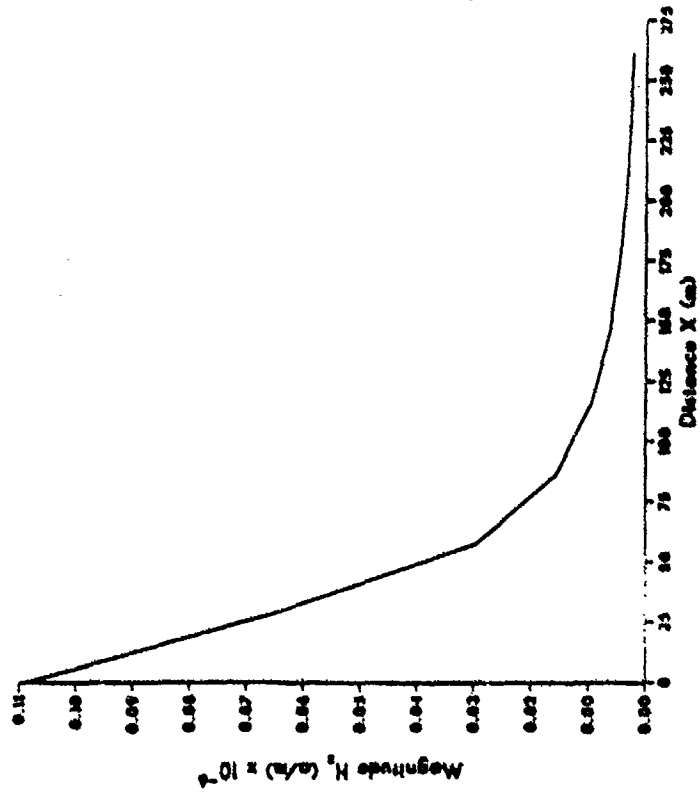
**PHASE 4.88 MHz**

1/4 lambda spacing, switched series feed



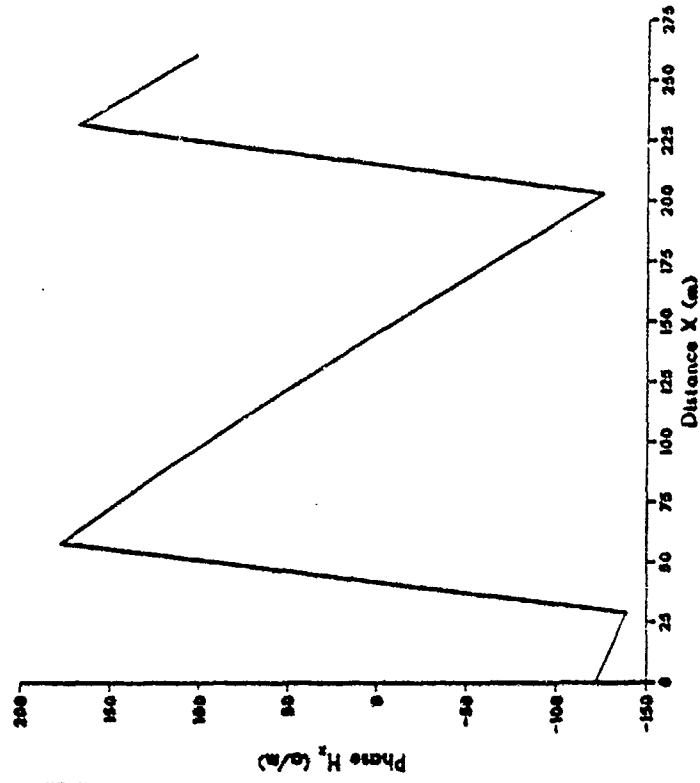
MAGNITUDE 1.88 MHz

3/8 lambda spacing, switched series feed



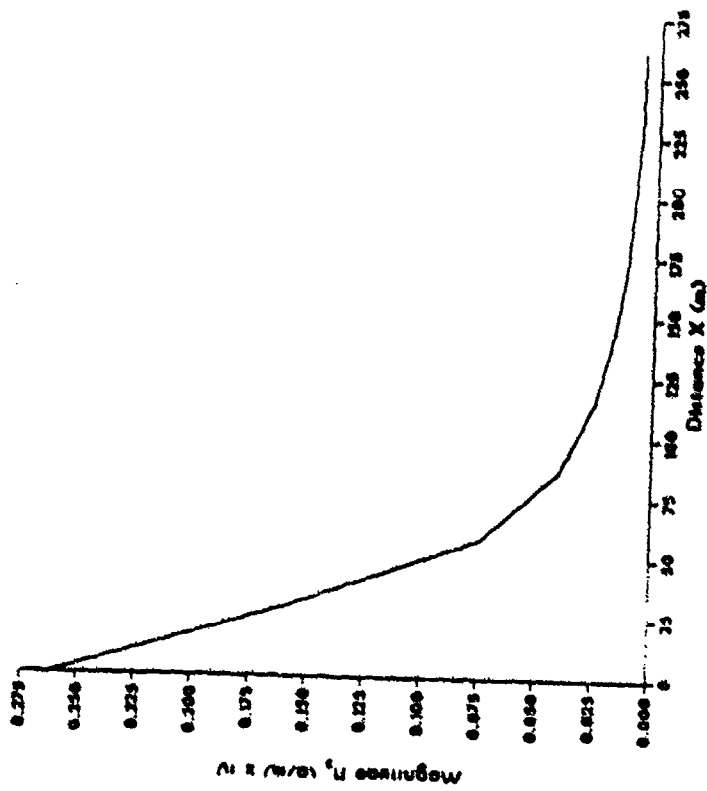
PHASE 1.88 MHz

3/8 lambda spacing, switched series feed



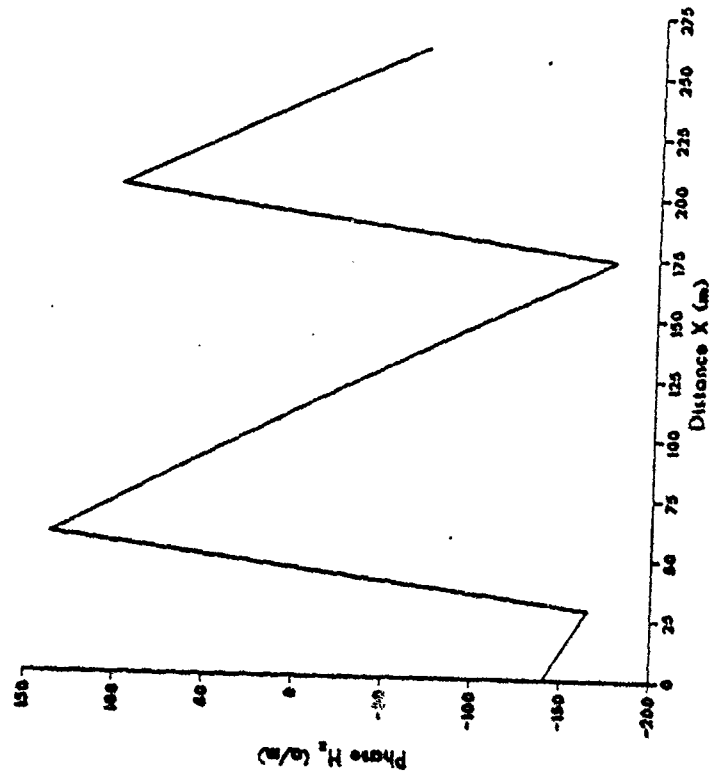
**MAGNITUDE 2.38 MHz**

3/8 lambda spacing, switched series feed



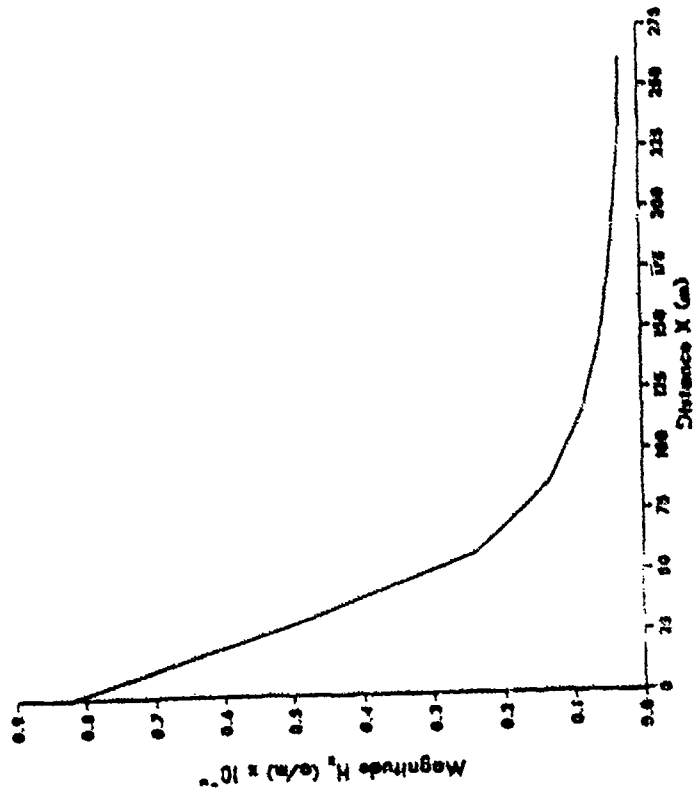
**PHASE 2.38 MHz**

3/8 lambda spacing, switched series feed



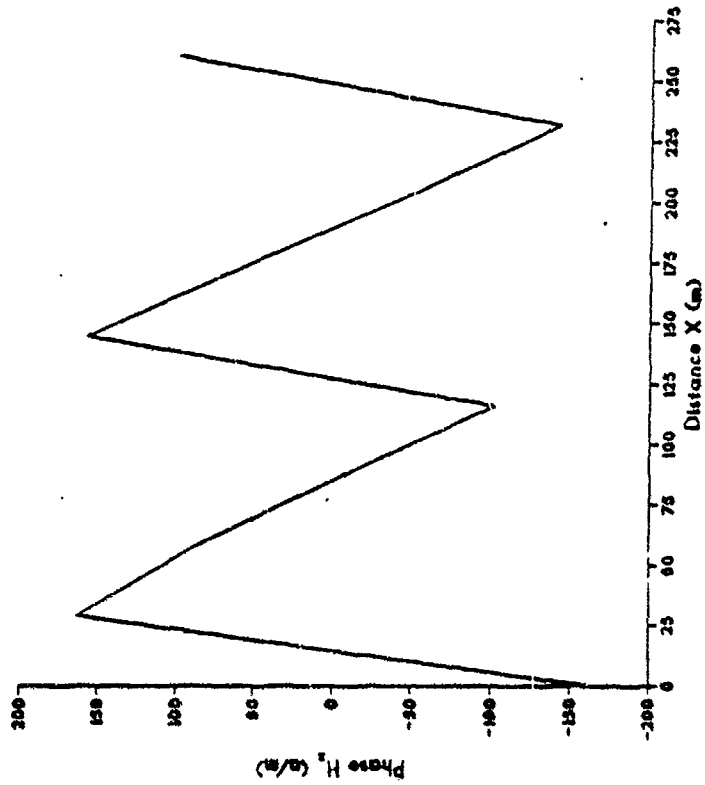
**MAGNITUDE 2.88 MHz**

3/8 lambda spacing, switched series feed



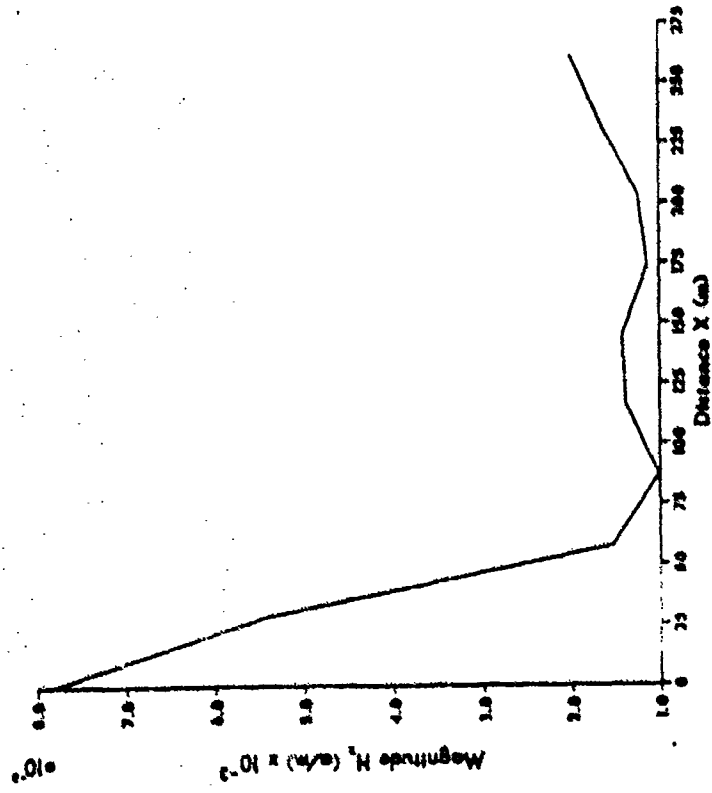
**PHASE 2.88 MHz**

3/8 lambda spacing, switched series feed



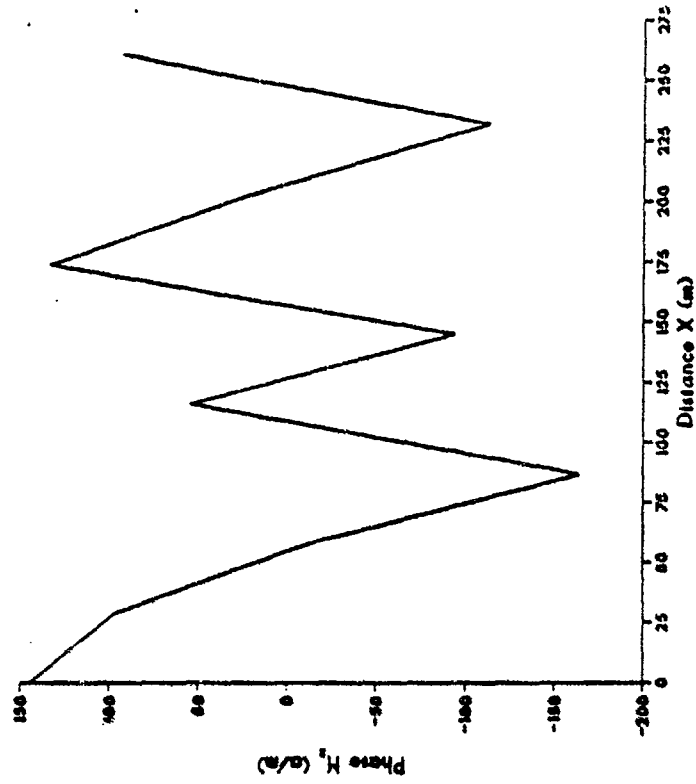
MAGNITUDE 3.35 MHz

3/8 lambda spacing, switched series feed



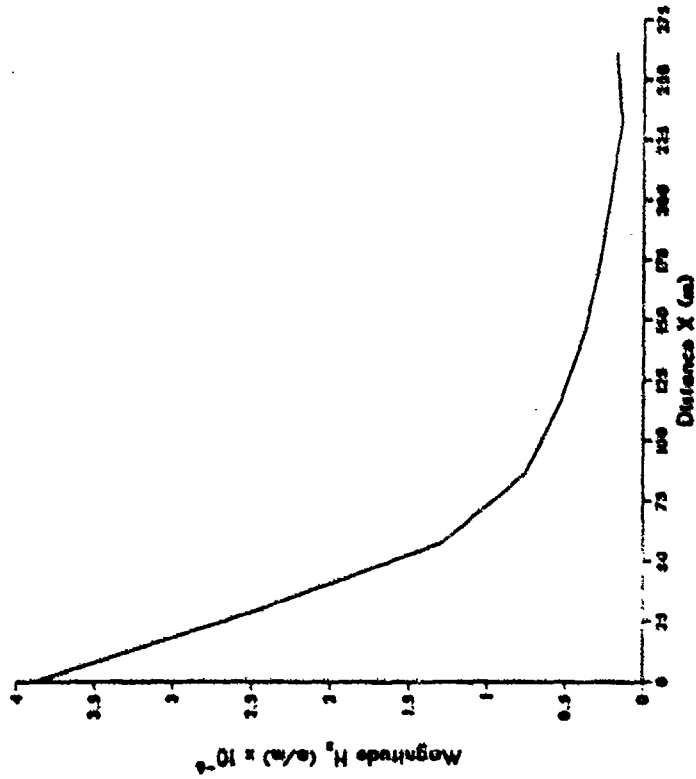
PHASE 3.35 MHz

3/8 lambda spacing, switched series feed



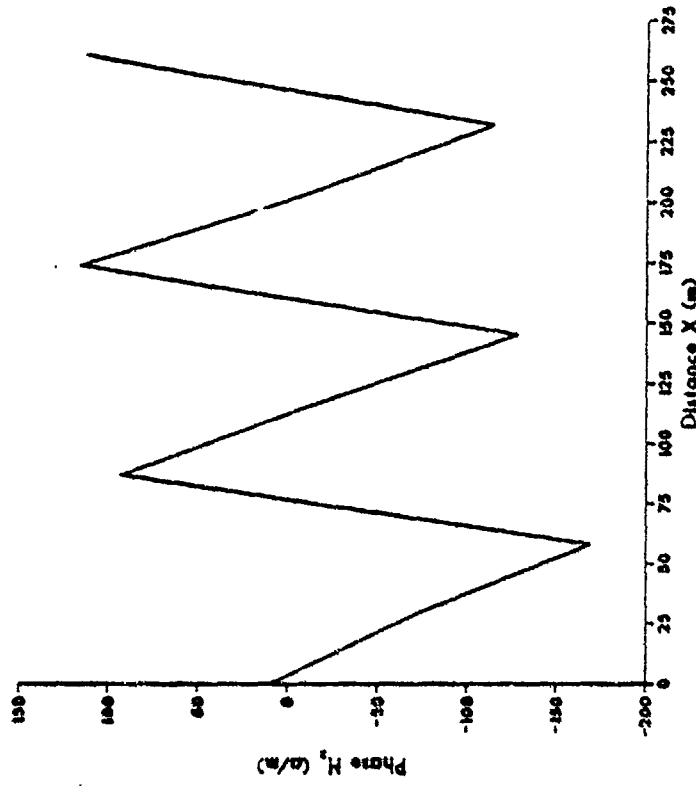
MAGNITUDE 3.63 MHz

3/8 lambda spacing, switched series feed



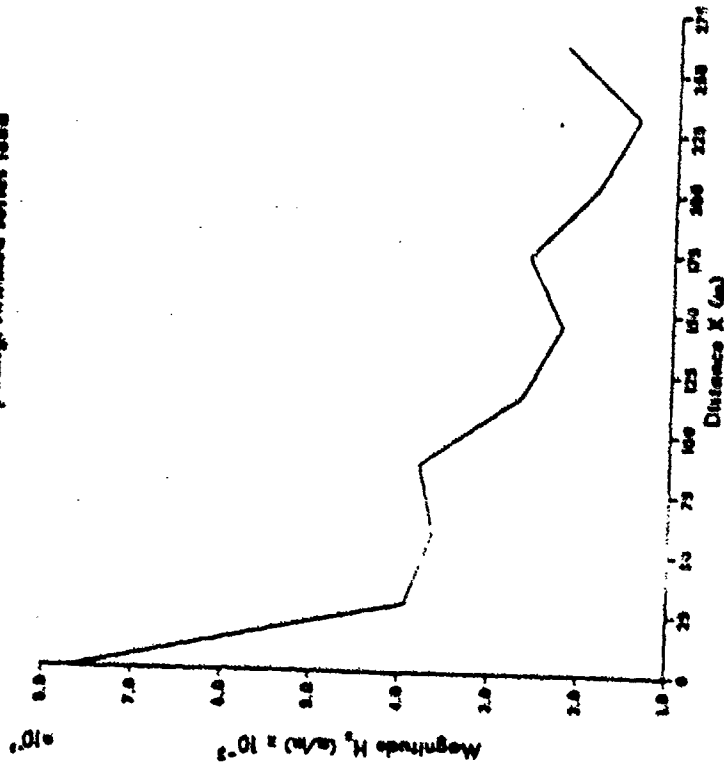
PHASE 3.63 MHz

3/8 lambda spacing, switched series feed



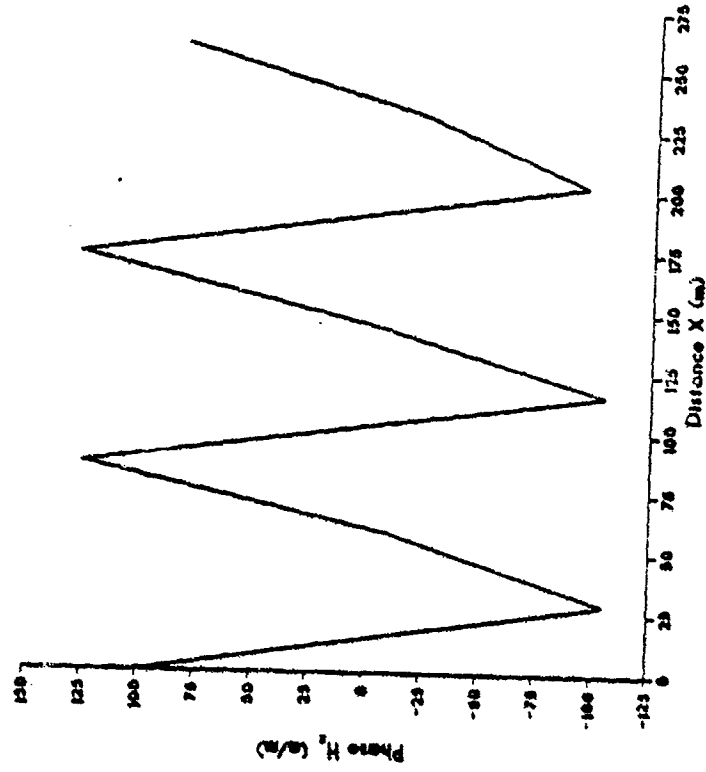
MAGNITUDE 3.72 MHz

3/8 lambda spacing, switched series feed



PHASE 3.72 MHz

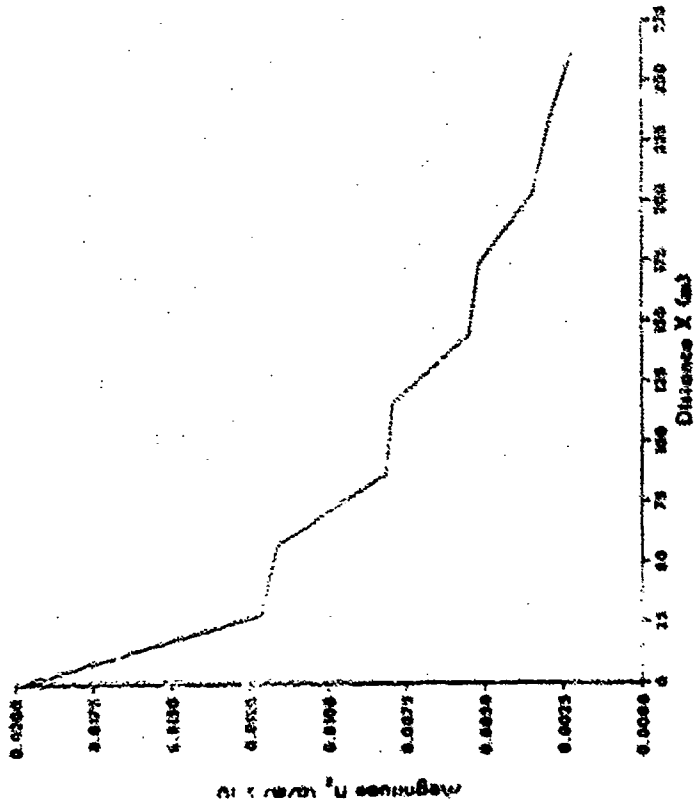
3/8 lambda spacing, switched series feed





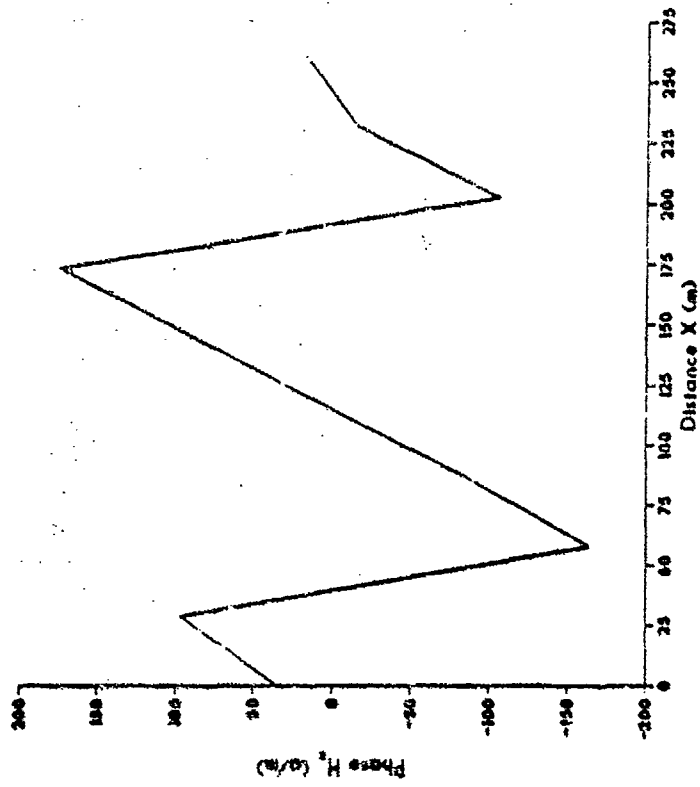
**MAGNITUDE 3.81 MHz**

3/8 lambda spacing, switched series feed



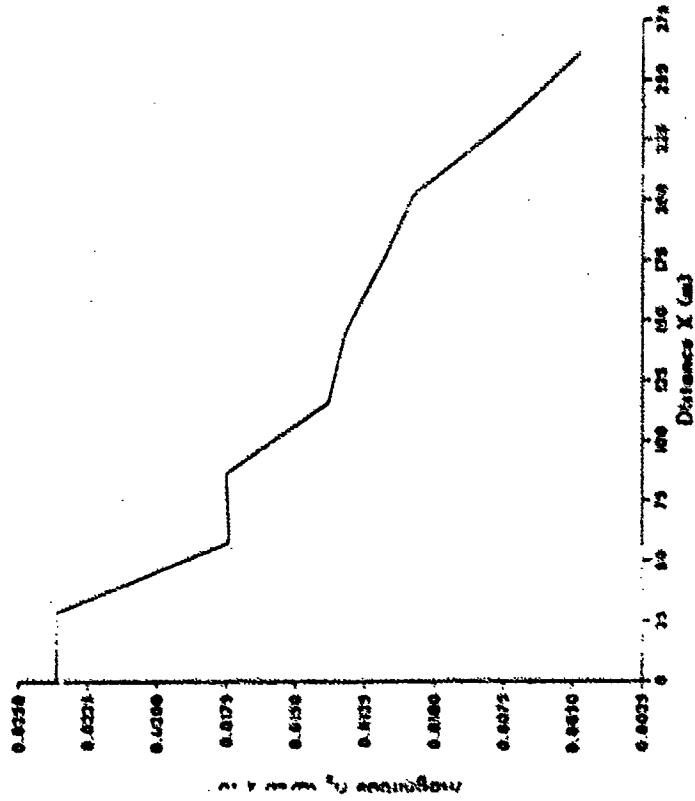
**PHASE 3.81 MHz**

3/8 lambda spacing, switched series feed



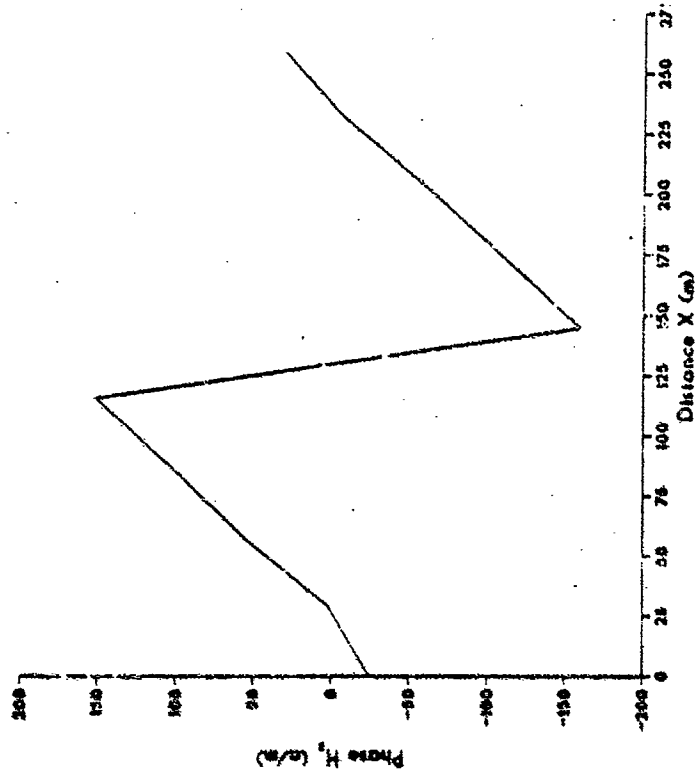
MAGNITUDE 3.88 MHz

3/8 lambda spacing, switched series feed



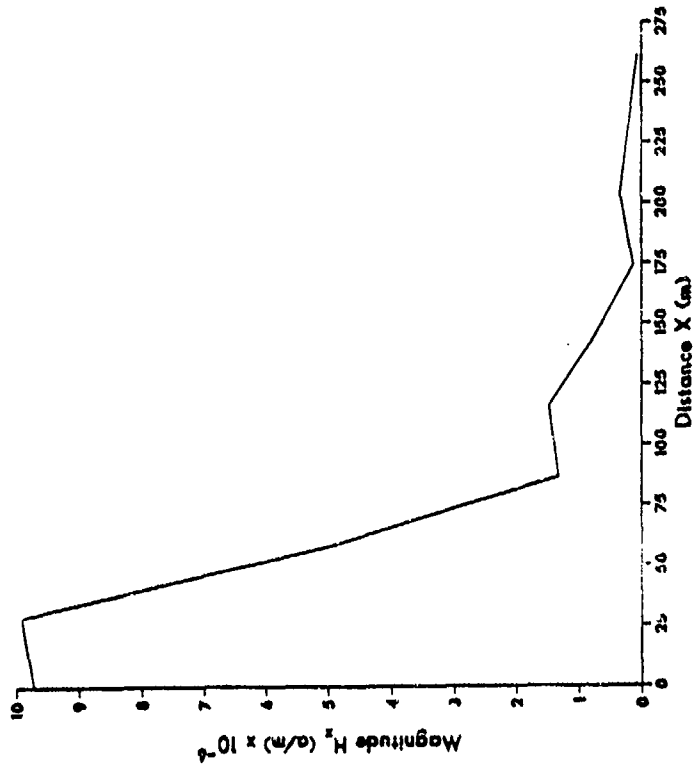
PHASE 3.88 MHz

3/8 lambda spacing, switched series feed



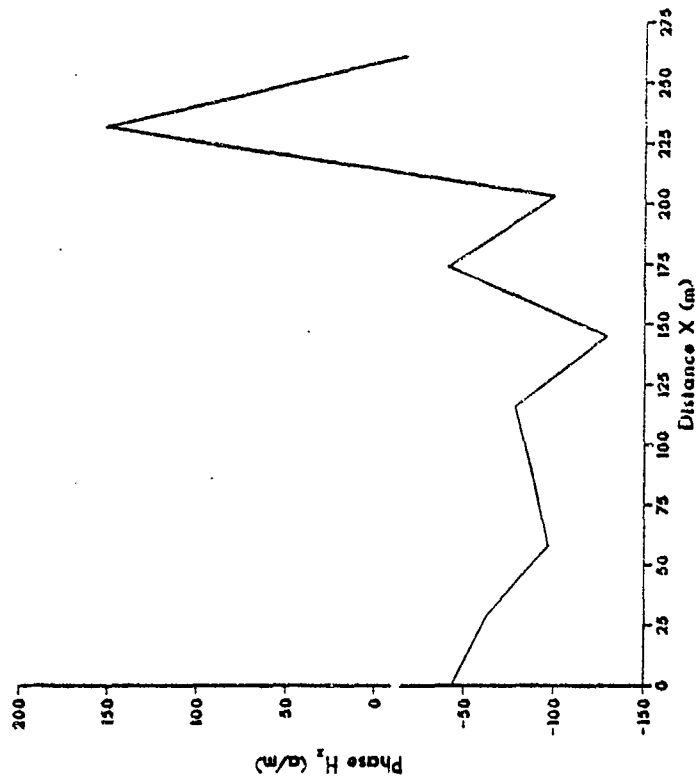
MAGNITUDE 3.95 MHz

3/8 lambda spacing, switched series feed



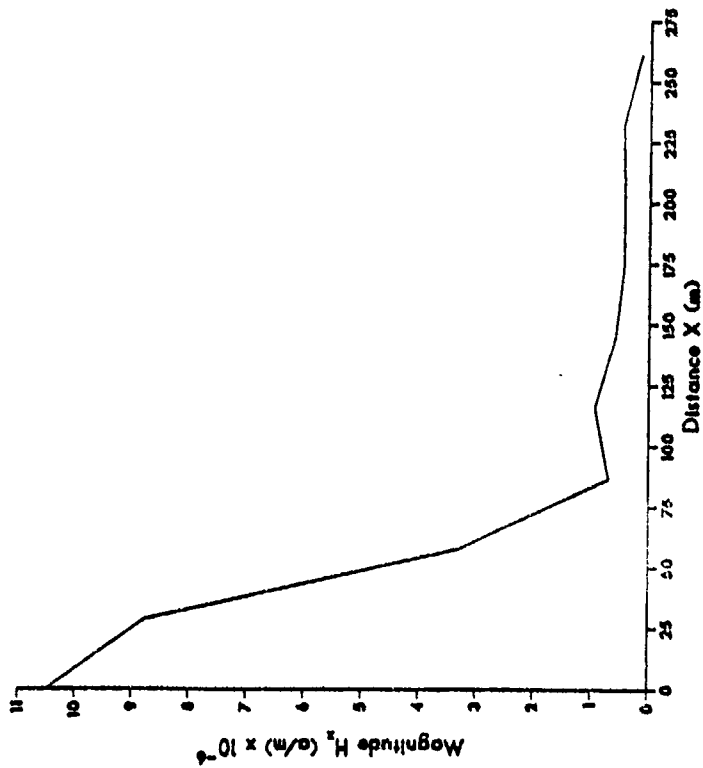
PHASE 3.95 MHz

3/8 lambda spacing, switched series feed



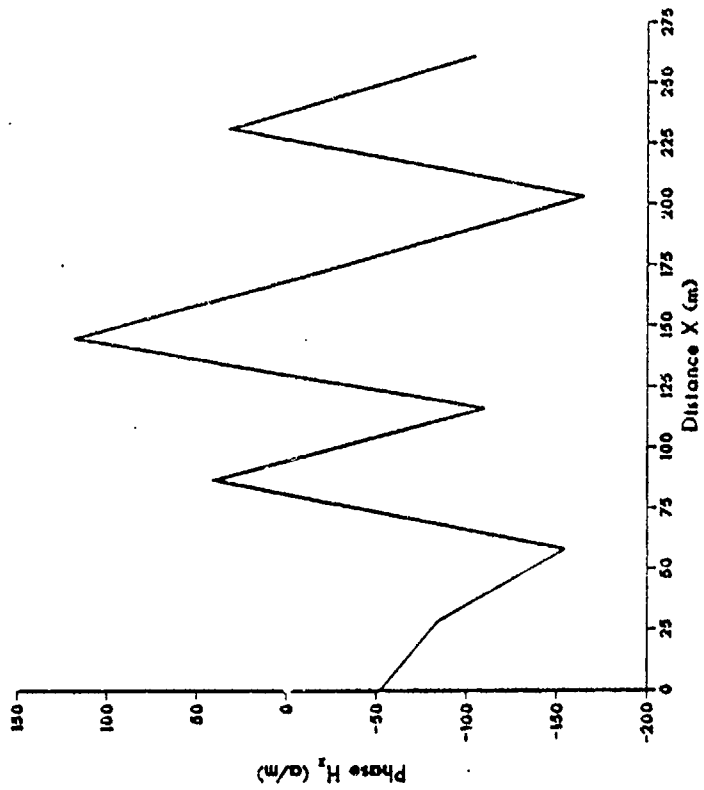
MAGNITUDE 4.04 MHz

3/8 lambda spacing, switched series feed



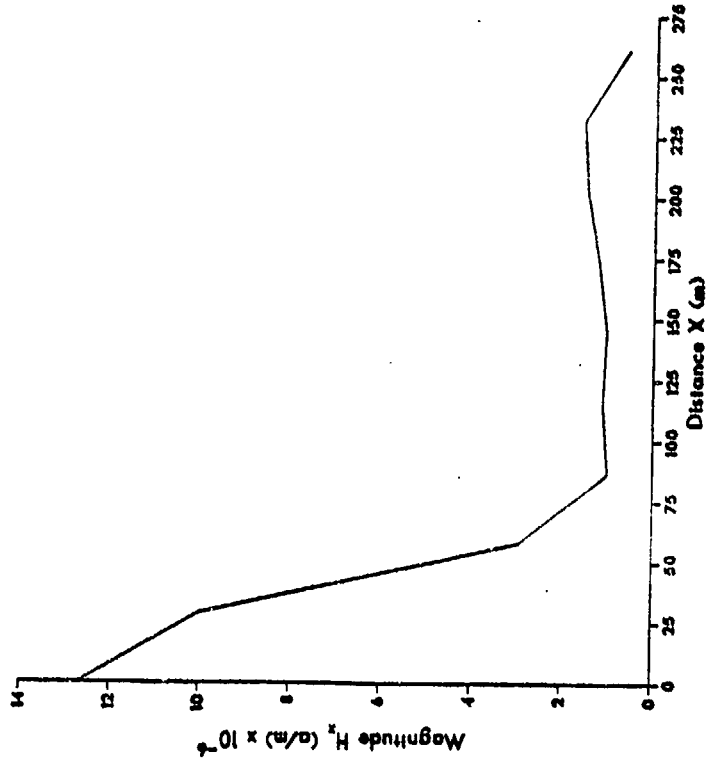
PHASE 4.04 MHz

3/8 lambda spacing, switched series feed



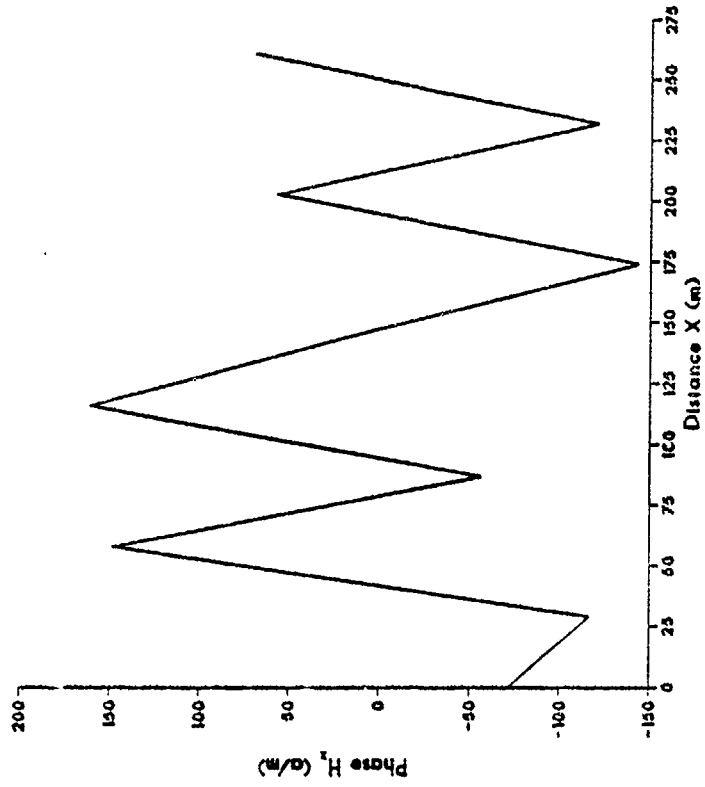
MAGNITUDE 4.13 MHz

3/8 lambda spacing, switched series feed



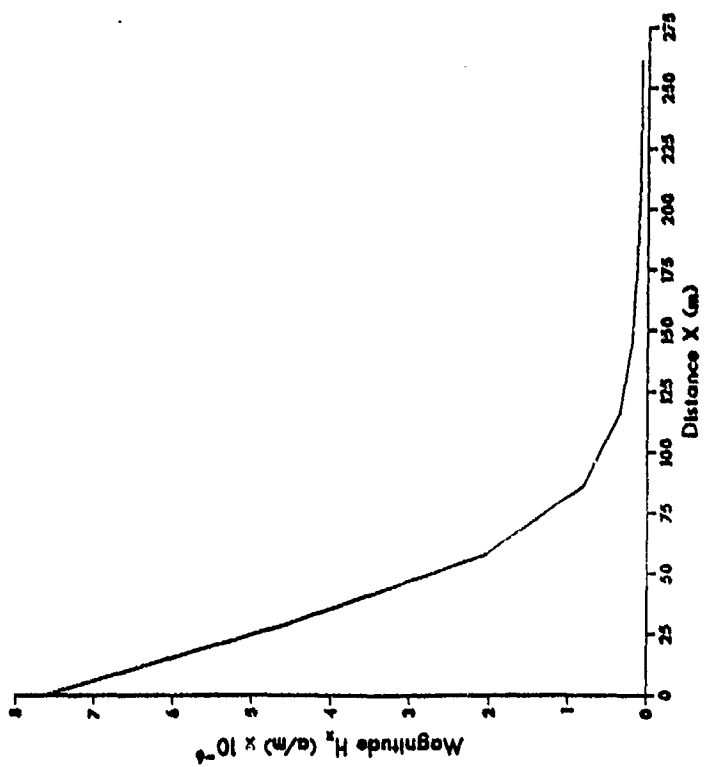
PHASE 4.13 MHz

3/8 lambda spacing, switched series feed



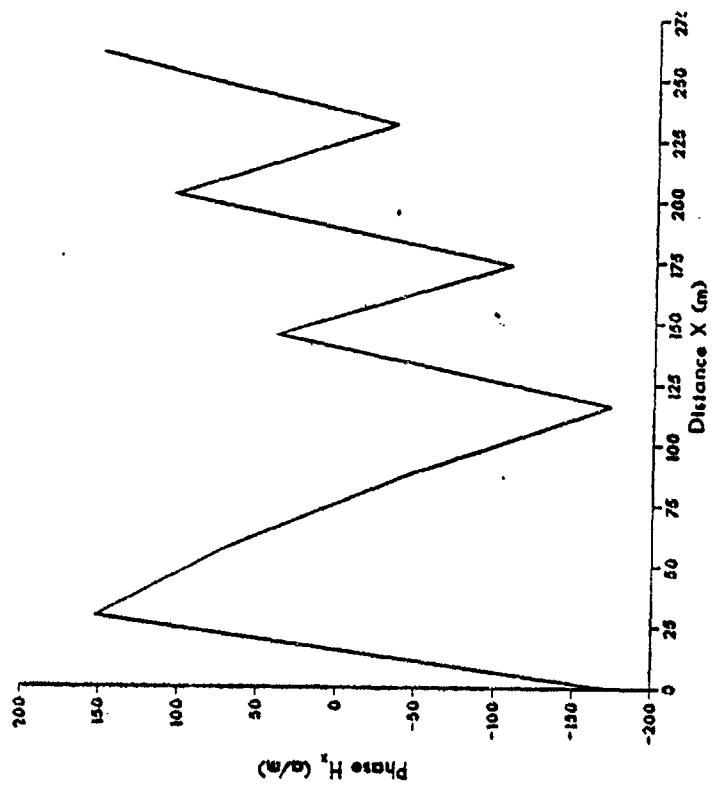
MAGNITUDE 4.38 MHz

3/8 lambda spacing, switched series feed



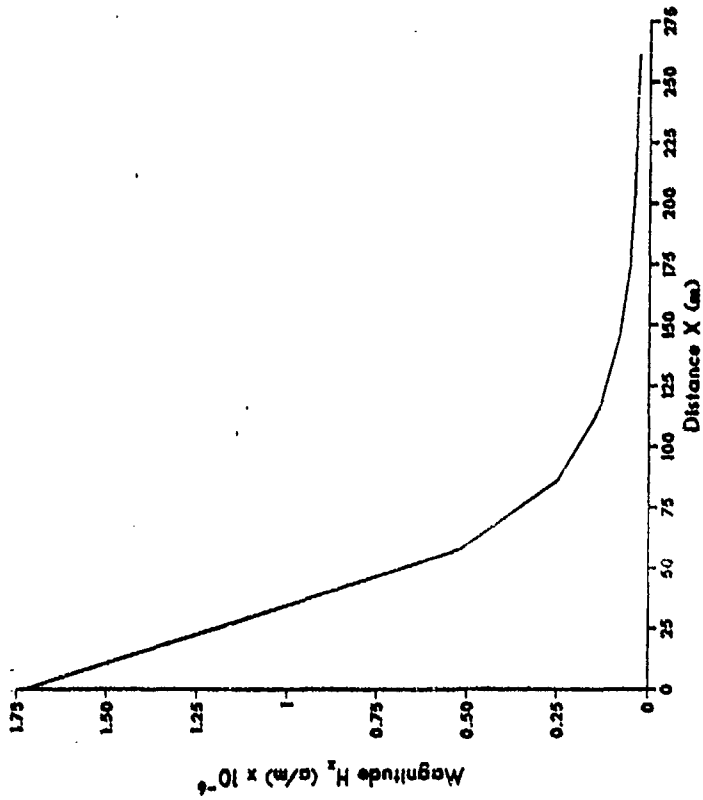
PHASE 4.38 MHz

3/8 lambda spacing, switched series feed



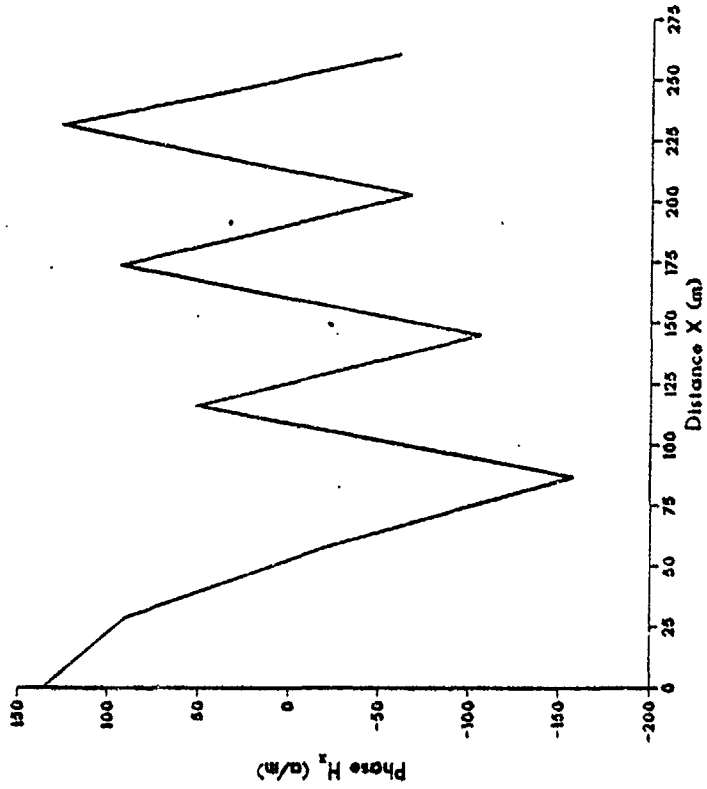
MAGNITUDE 4.86 MHz

3/8 lambda spacing, switched series feed



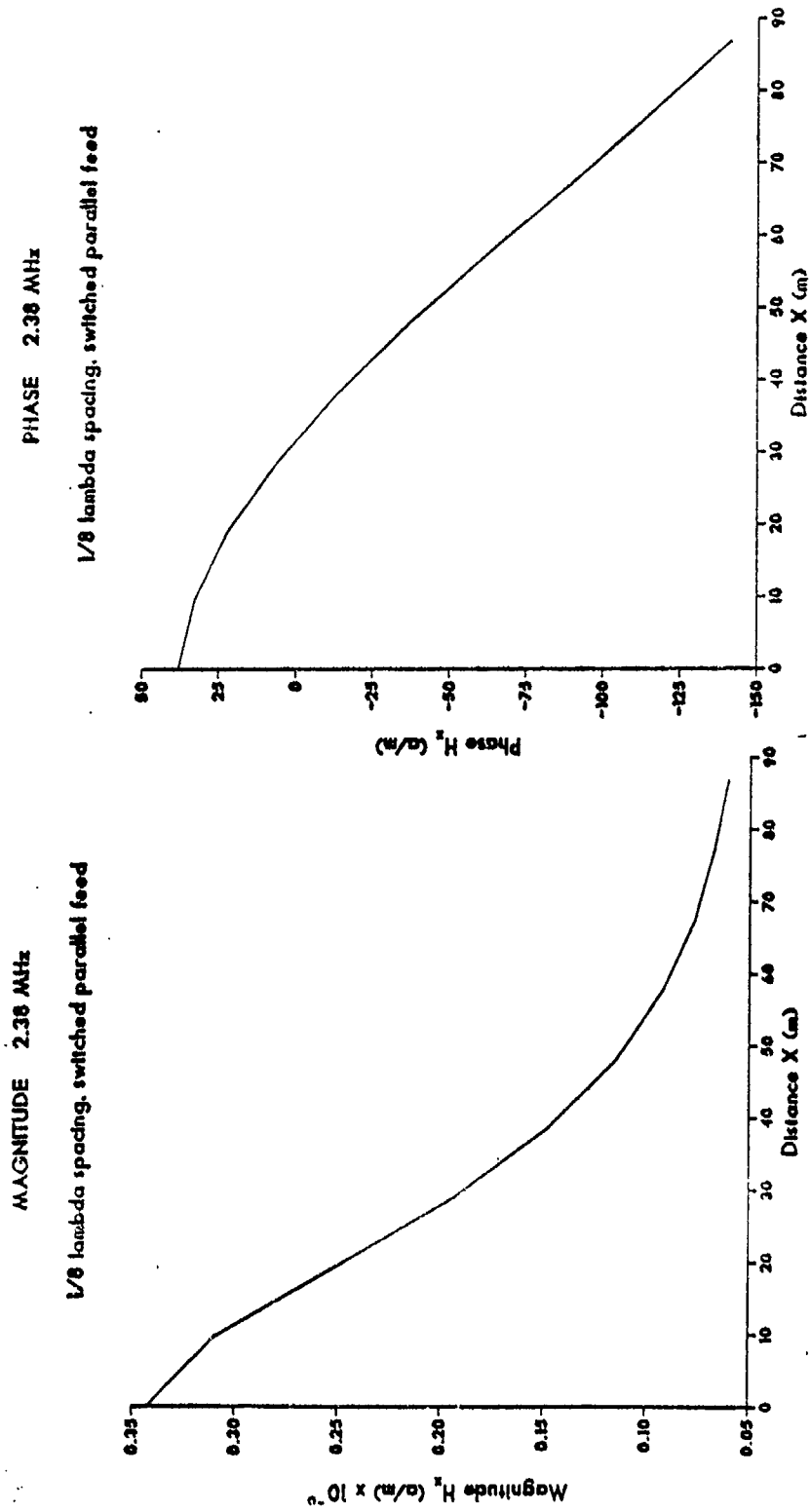
PHASE 4.86 MHz

3/8 lambda spacing, switched series feed



# APPENDIX C

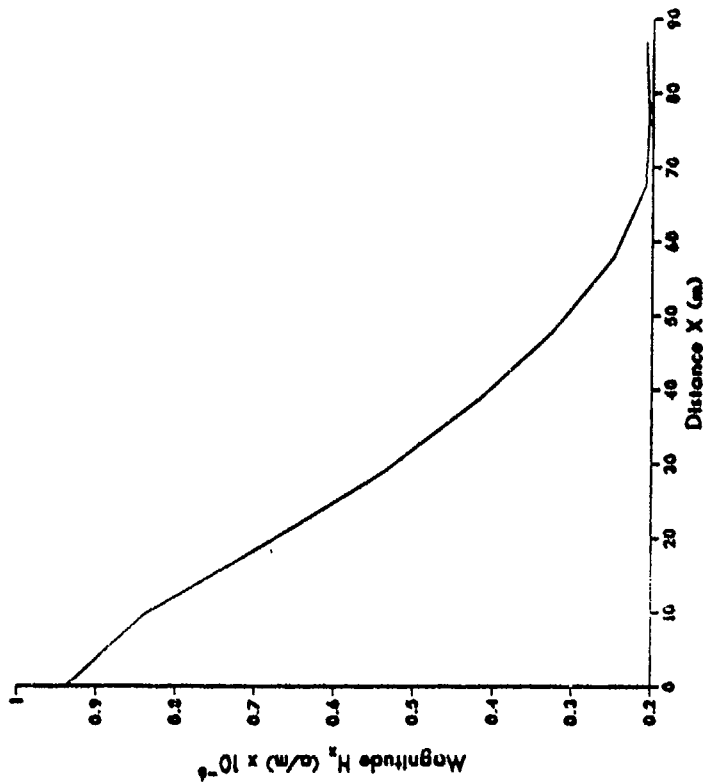
## NEAR-MAGNETIC FIELD PLOTS FOR SNYDER SWITCHED PARALLEL ARRAYS





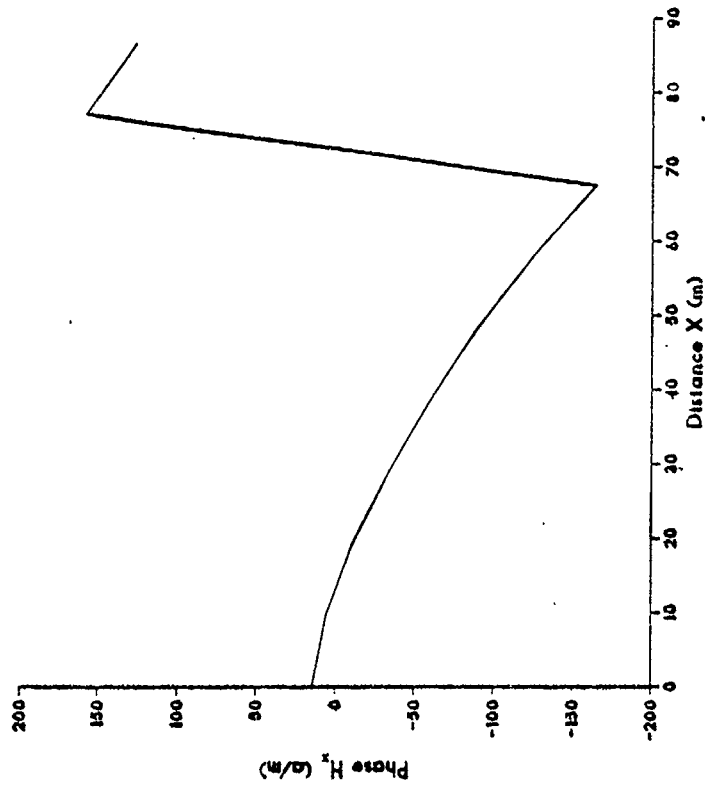
MAGNITUDE 2.88 MHz

1/8 lambda spacing, switched parallel feed



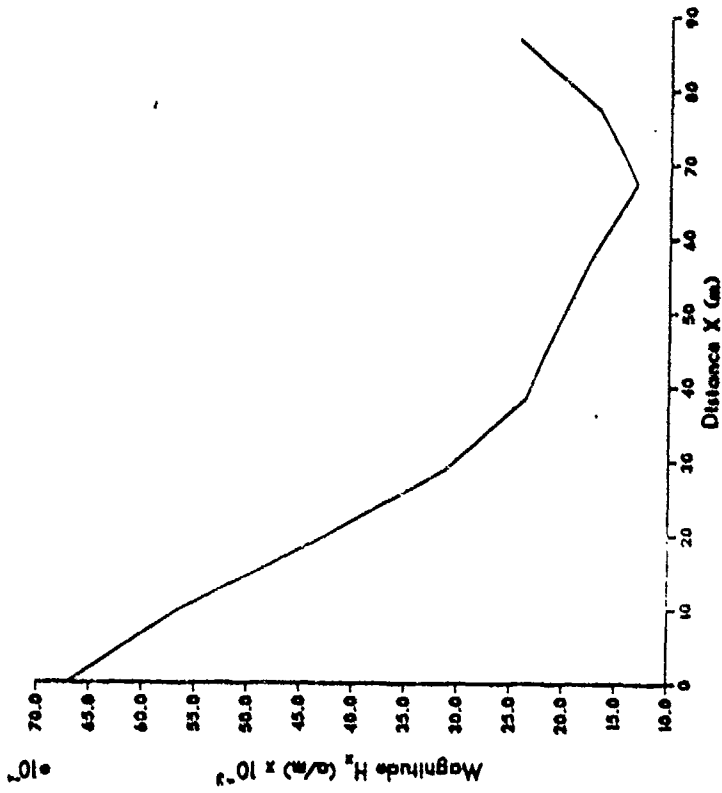
PHASE 2.88 MHz

1/8 lambda spacing, switched parallel feed



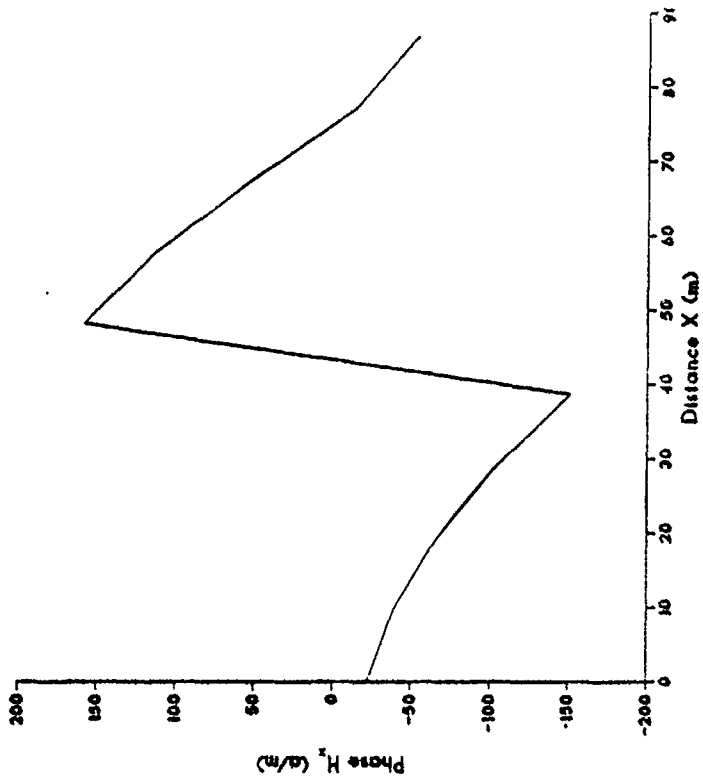
MAGNITUDE 3.38 MHz

1/8 lambda spacing, switched parallel feed



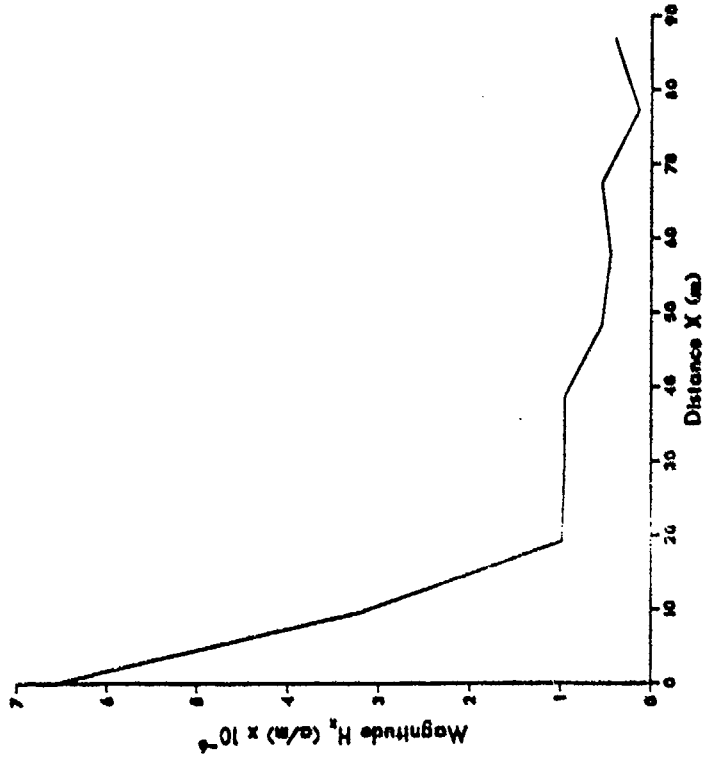
PHASE 3.38 MHz

1/8 lambda spacing, switched parallel feed



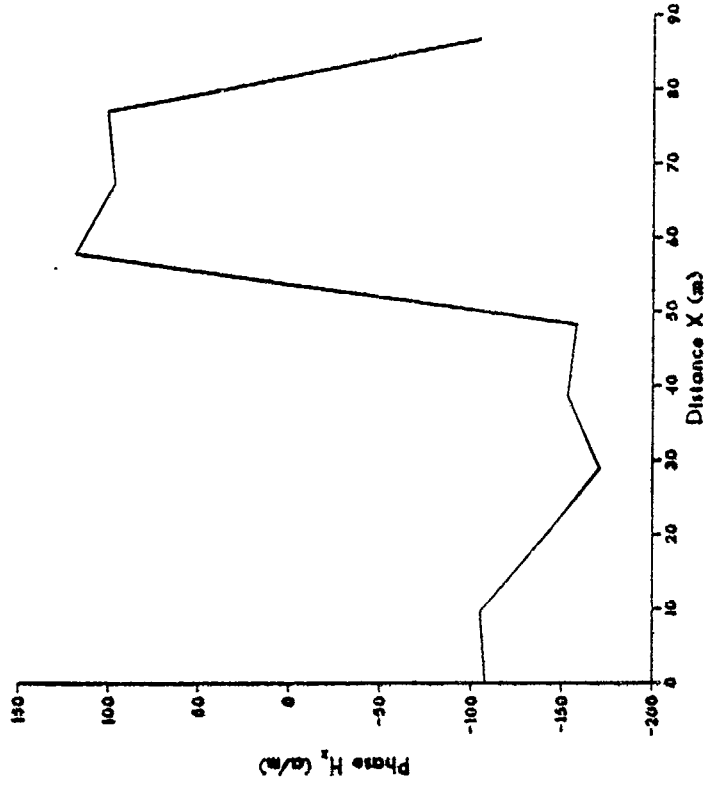
MAGNITUDE 3.63 MHz

1/8 lambda spacing, switched parallel feed



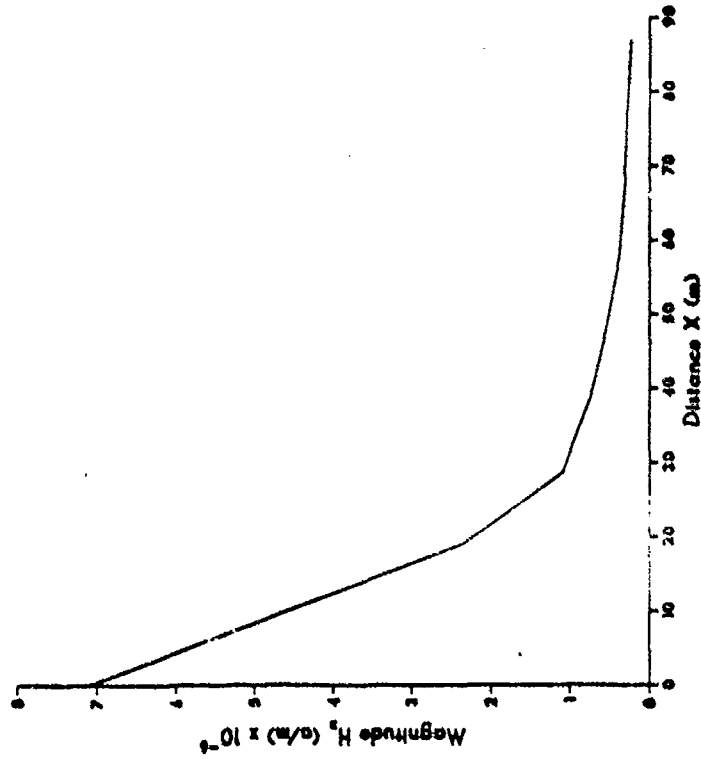
PHASE 3.63 MHz

1/8 lambda spacing, switched parallel feed



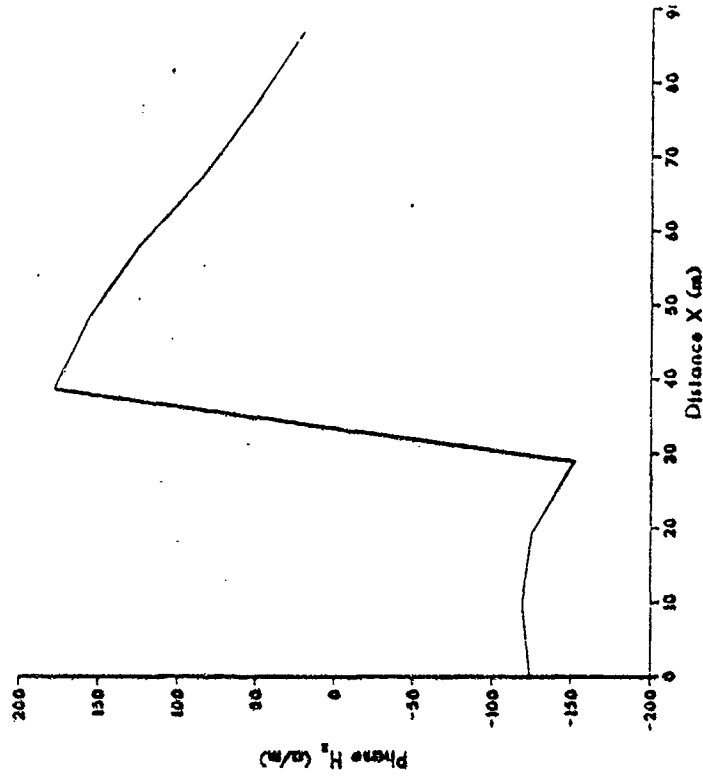
MAGNITUDE 3.72 MHz

1/8 lambda spacing, switched parallel feed



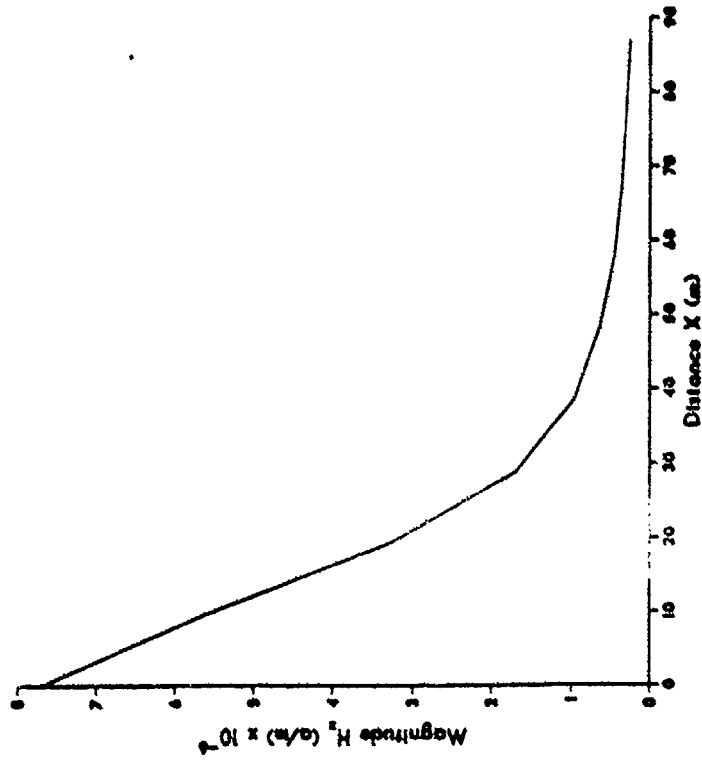
PHASE 3.72 MHz

1/8 lambda spacing, switched parallel feed



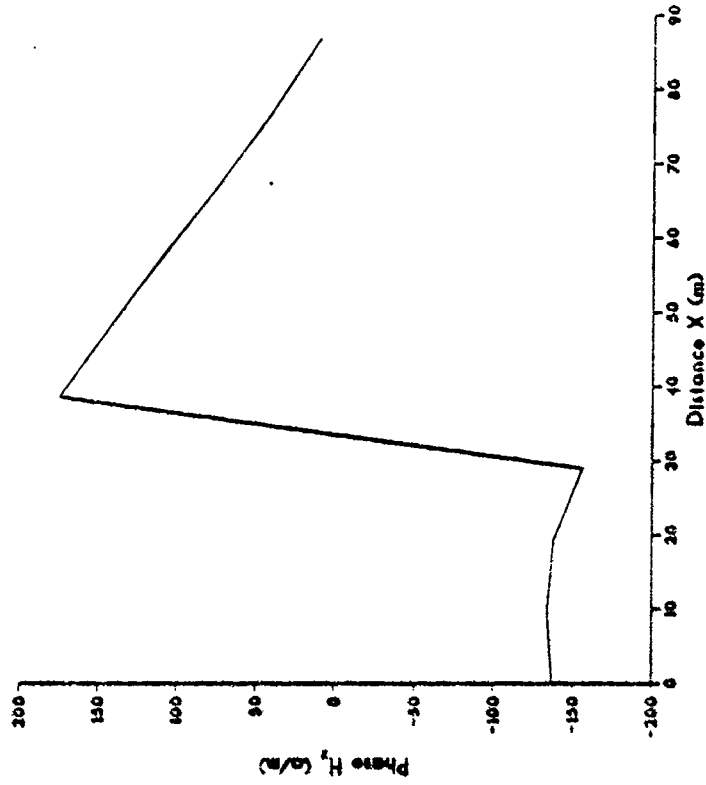
MAGNITUDE 3.81 MHz

1/8 lambda spacing, switched parallel feed



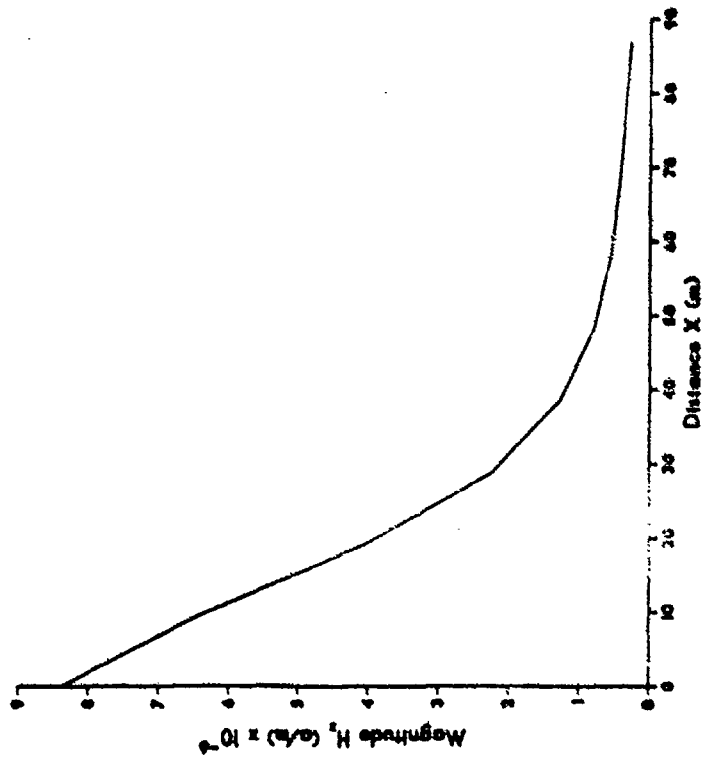
PHASE 3.81 MHz

1/8 lambda spacing, switched parallel feed



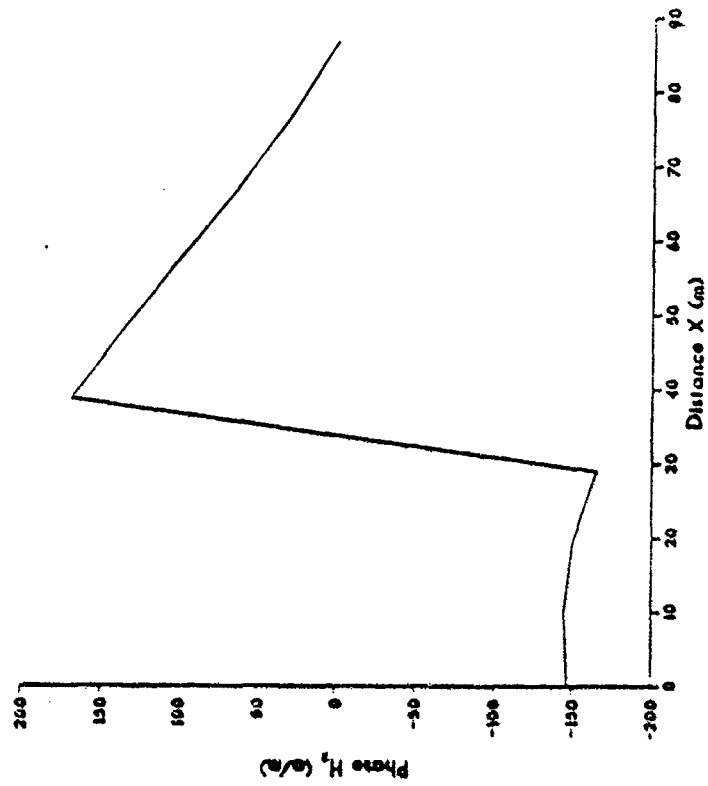
**MAGNITUDE 3.88 MHz**

1/8 lambda spacing, switched parallel feed



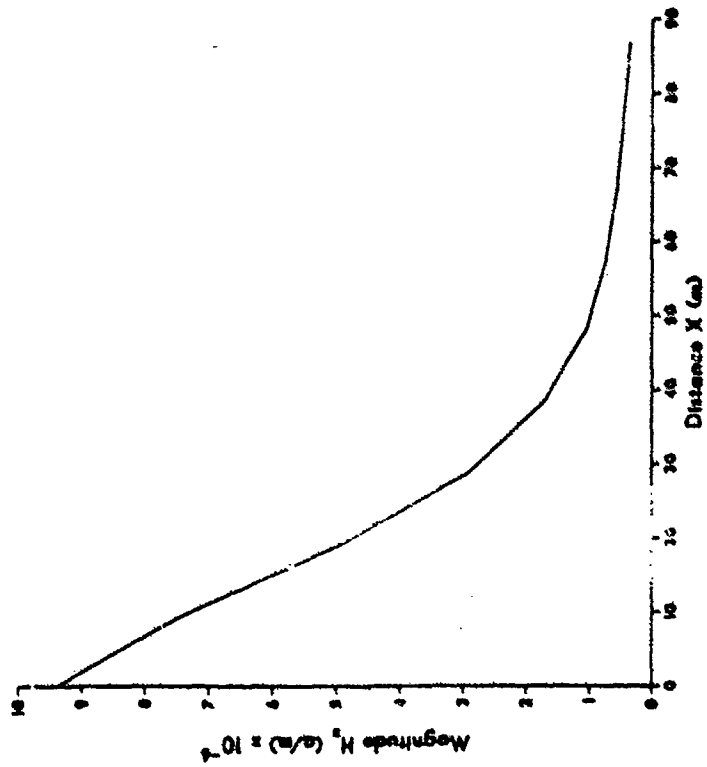
**PHASE 3.88 MHz**

1/8 lambda spacing, switched parallel feed



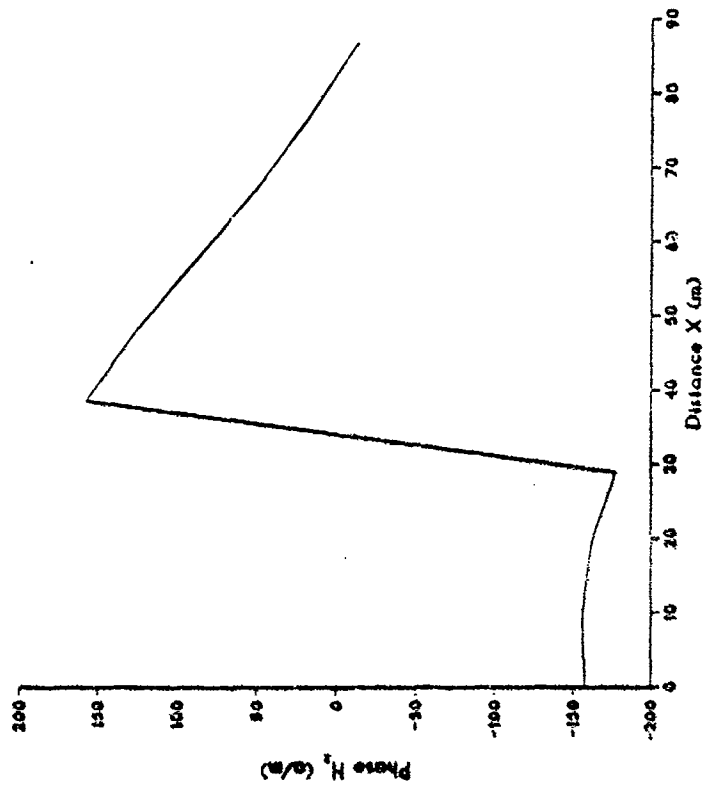
MAGNITUDE 3.95 MHz

1/8 lambda spacing, switched parallel feed



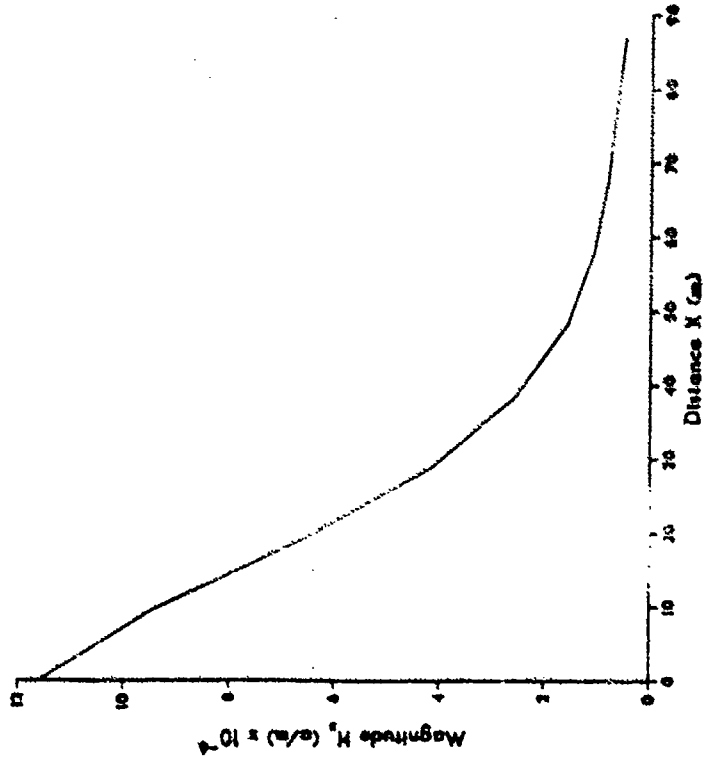
PHASE 3.95 MHz

1/8 lambda spacing, switched parallel feed



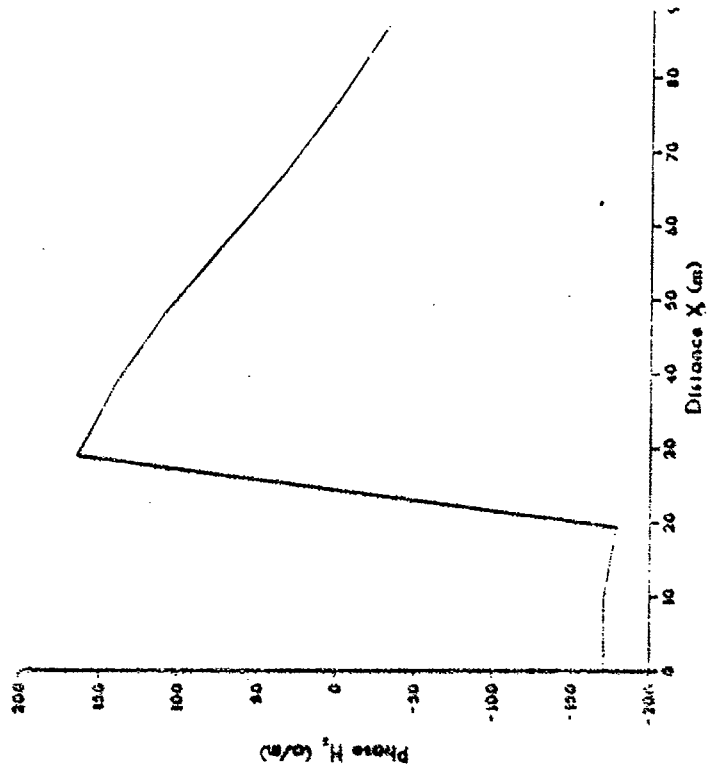
**MAGNITUDE 4.04 MHz**

**1/8 lambda spacing, switched parallel feed**



**PHASE 4.04 MHz**

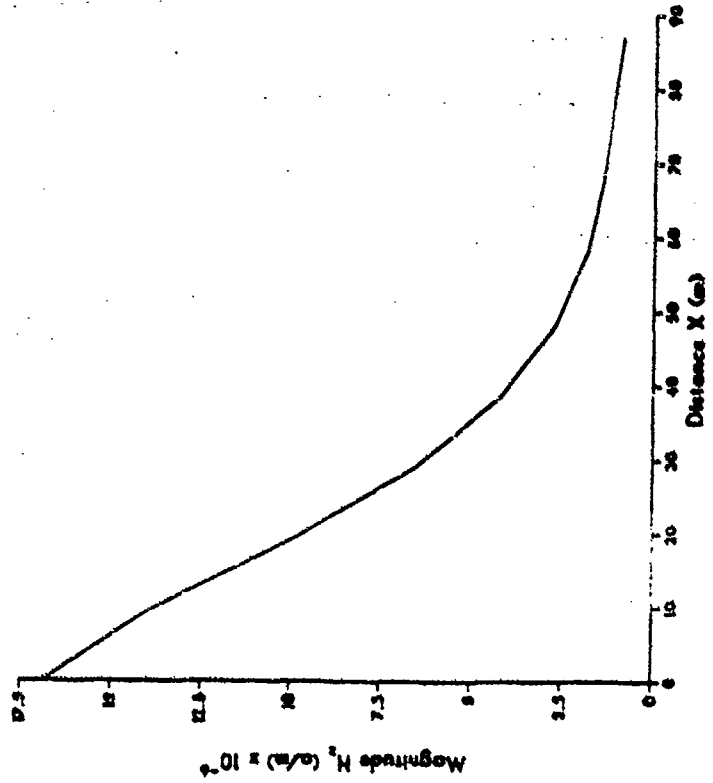
**1/8 lambda spacing, switched parallel feed**





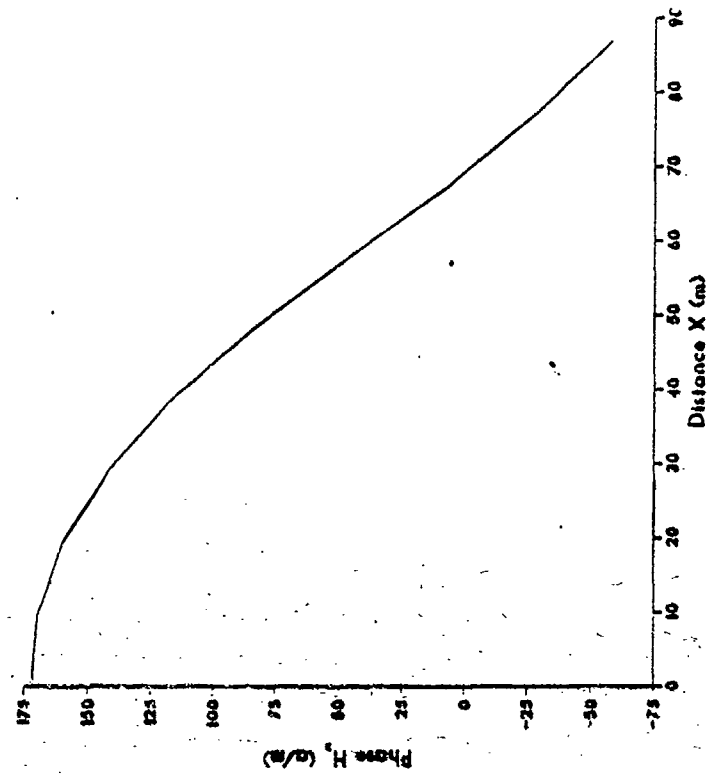
MAGNITUDE 4.13 MHz

1/8 lambda spacing, switched parallel feed



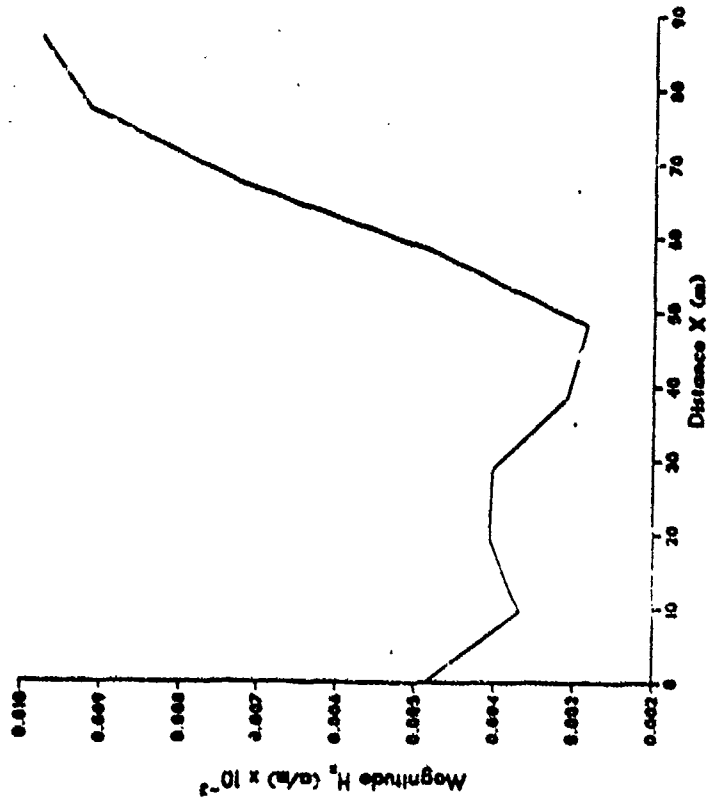
PHASE 4.13 MHz

1/8 lambda spacing, switched parallel feed



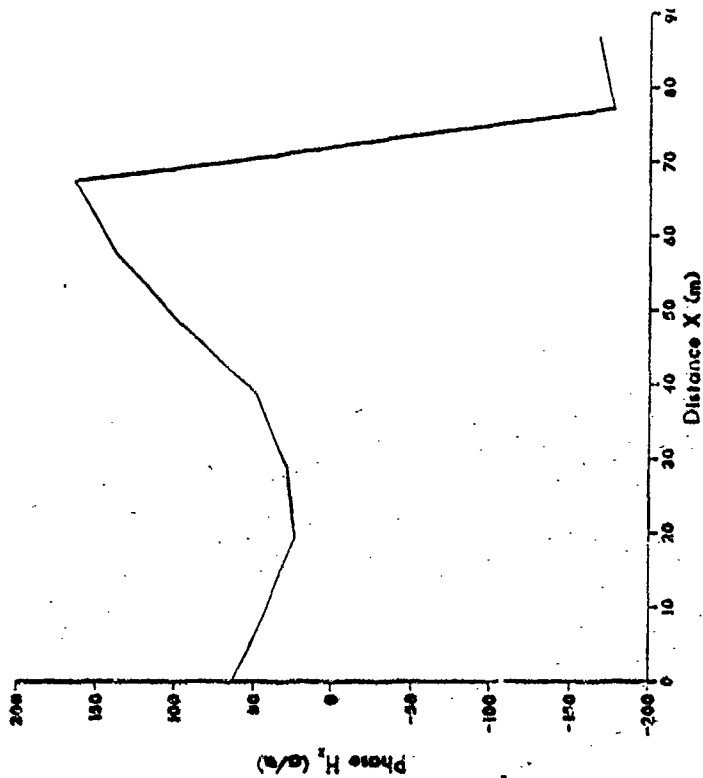
**MAGNITUDE 4.38 MHz**

1/8 lambda spacing, switched parallel feed



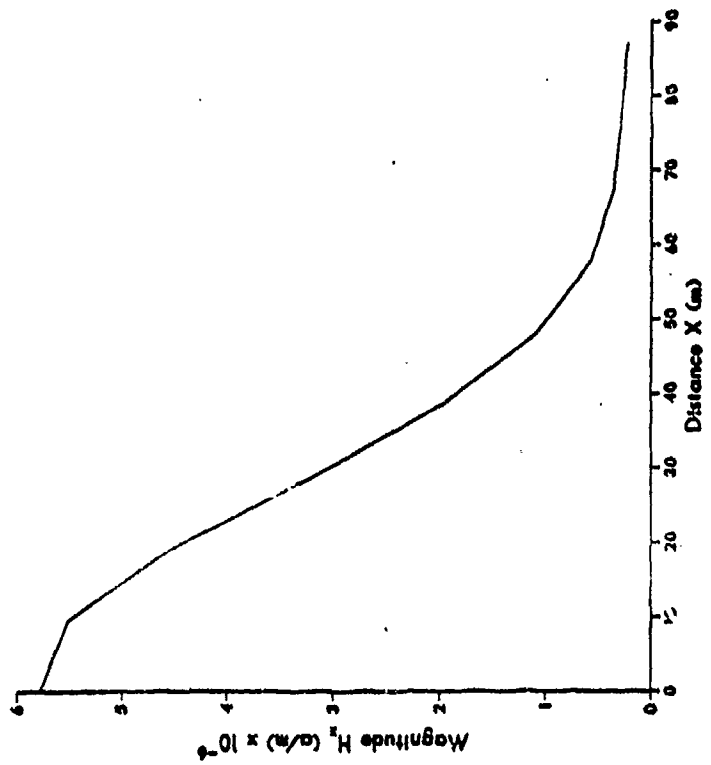
**PHASE 4.38 MHz**

1/8 lambda spacing, switched parallel feed



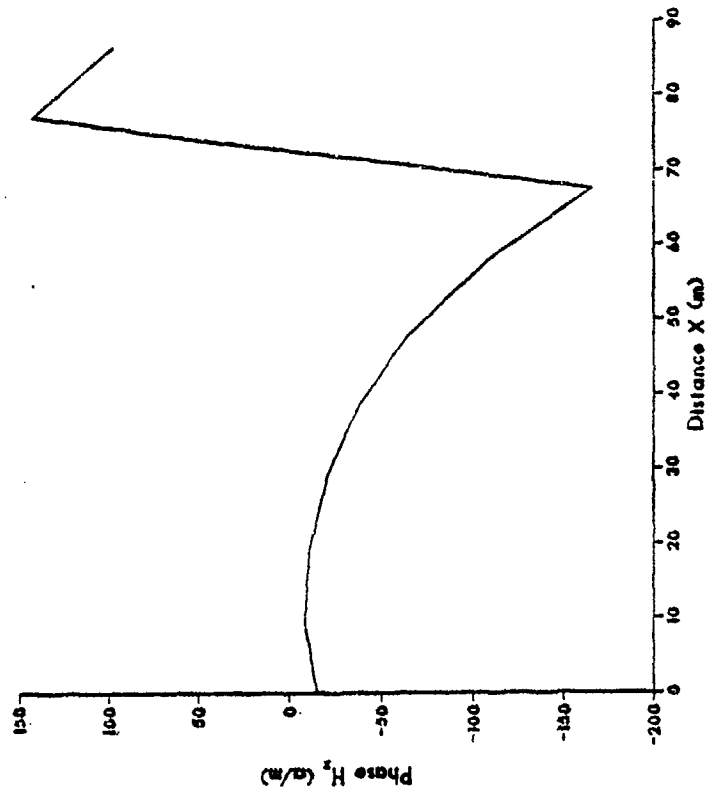
**MAGNITUDE 4.86 MHz**

1/8 lambda spacing, switched parallel feed

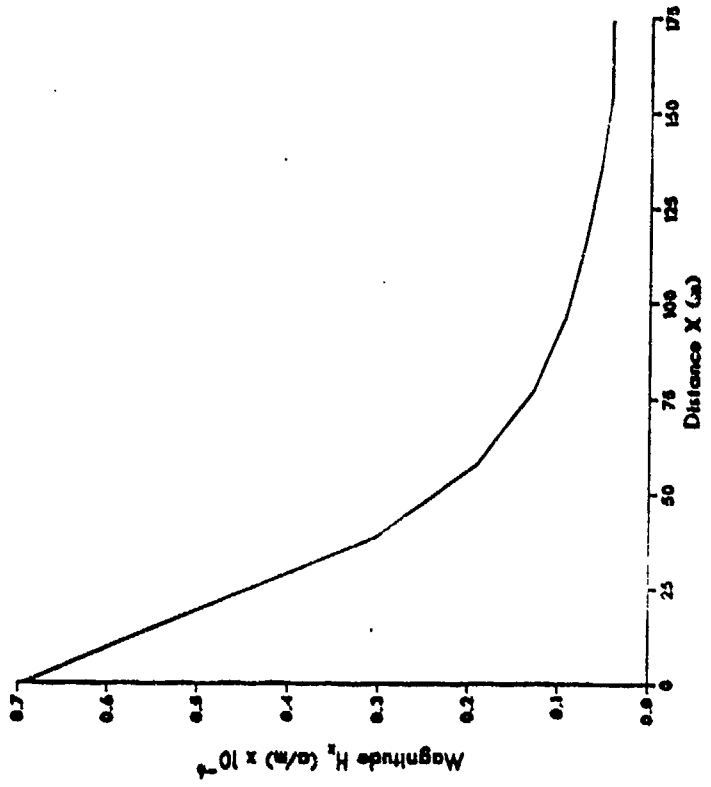


**PHASE 4.86 MHz**

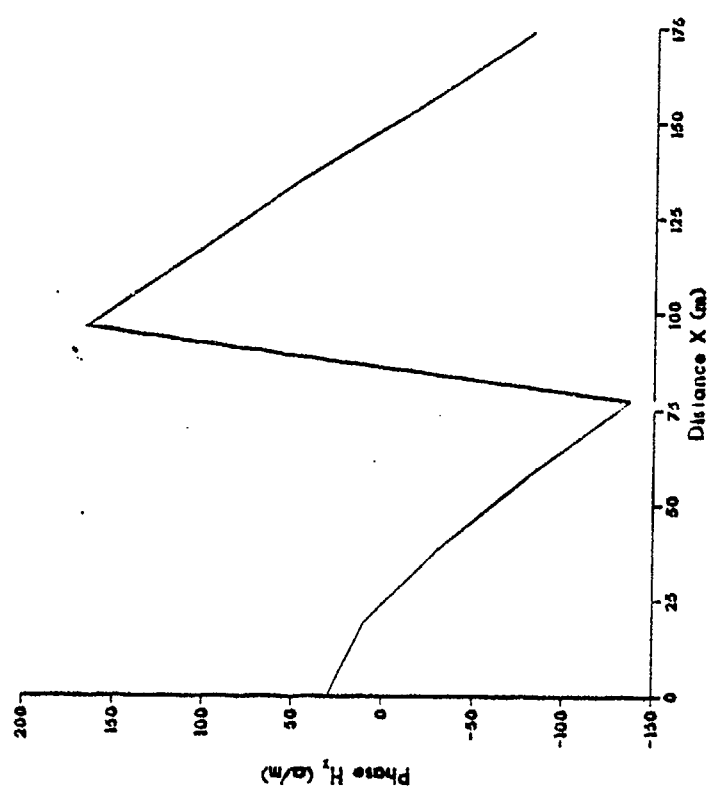
1/8 lambda spacing, switched parallel feed



**MAGNITUDE 2.63 MHz**  
 1/4 lambda spacing, switched parallel feed

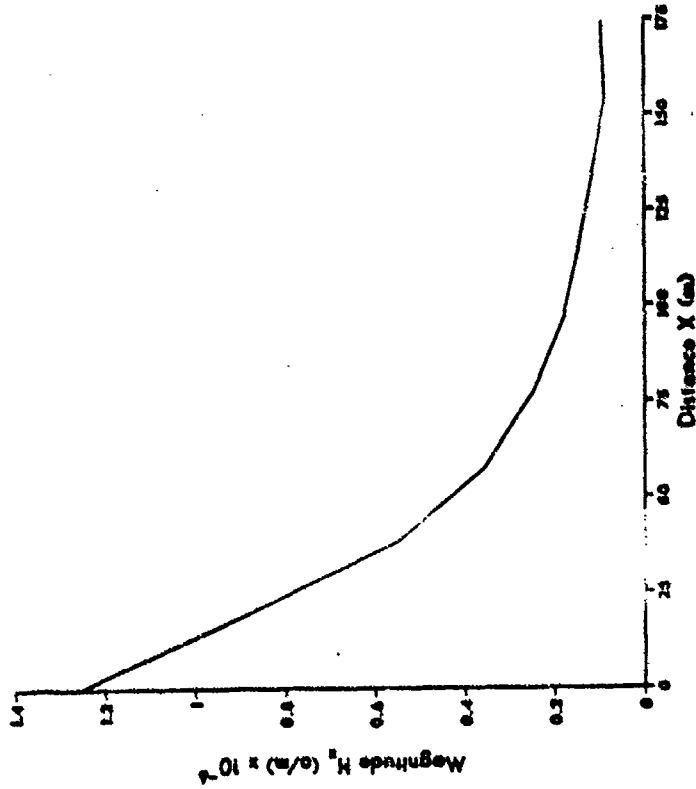


**PHASE 2.63 MHz**  
 1/4 lambda spacing, switched parallel feed



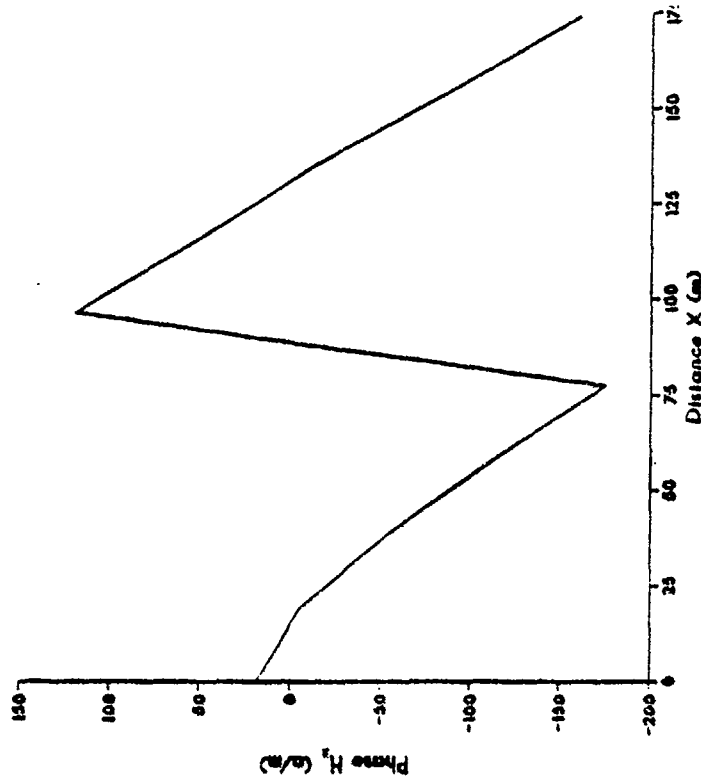
MAGNITUDE 2.88 MHz

1/4 lambda spacing, switched parallel feed



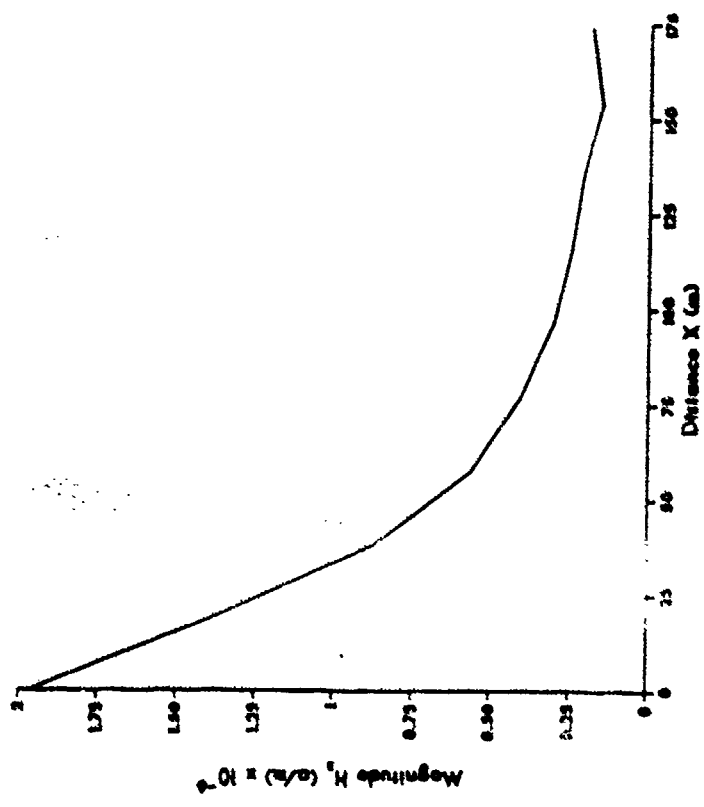
PHASE 2.88 MHz

1/4 lambda spacing, switched parallel feed



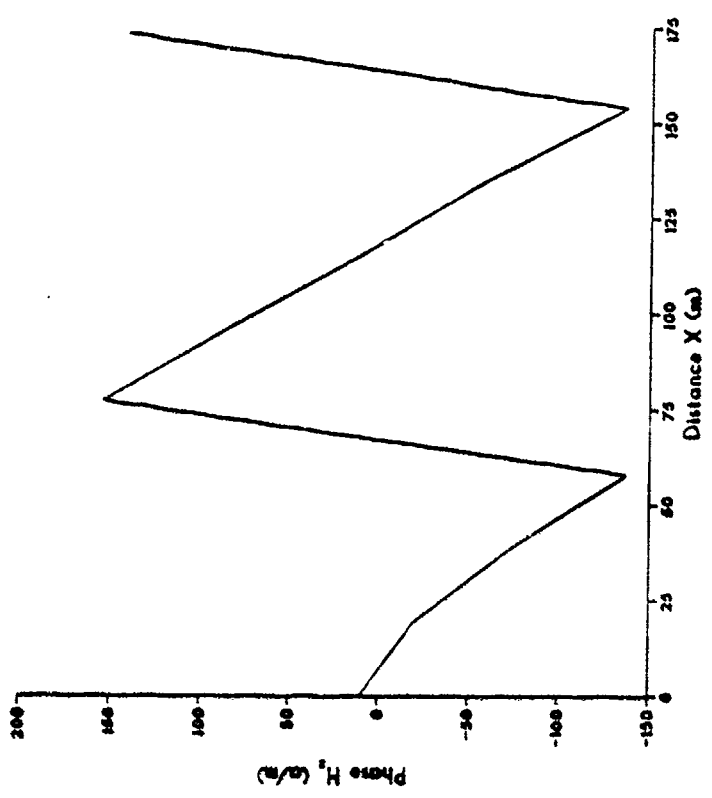
MAGNITUDE 3.04 MHz

1/4 lambda spacing, switched parallel feed



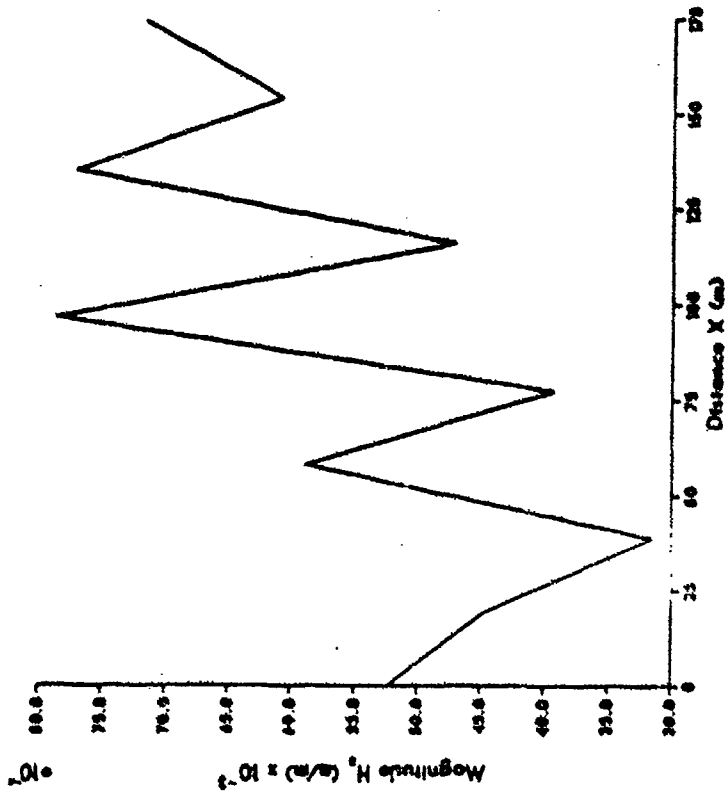
PHASE 3.04 MHz

1/4 lambda spacing, switched parallel feed



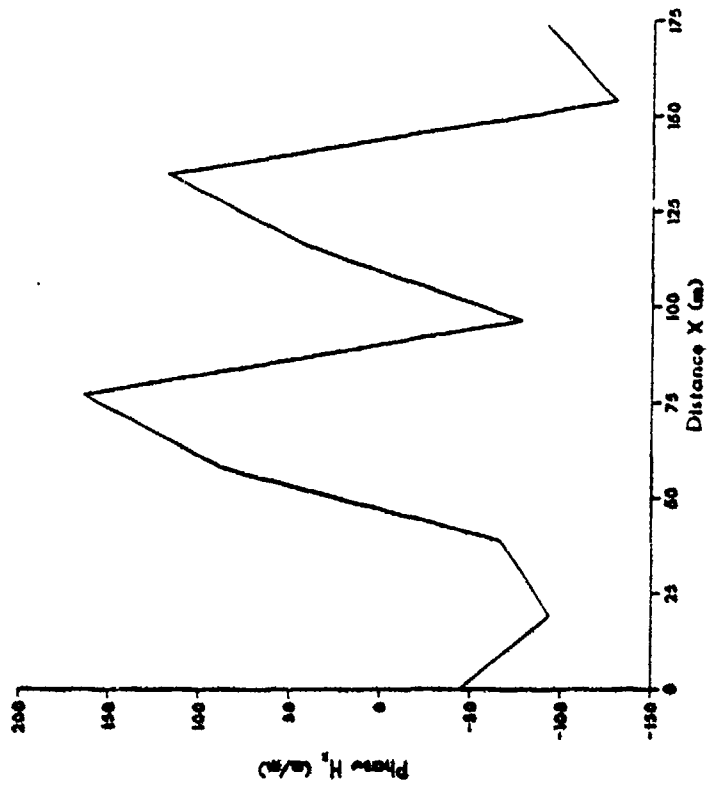
MAGNITUDE 3.38 MHz

1/4 lambda spacing, switched parallel feed



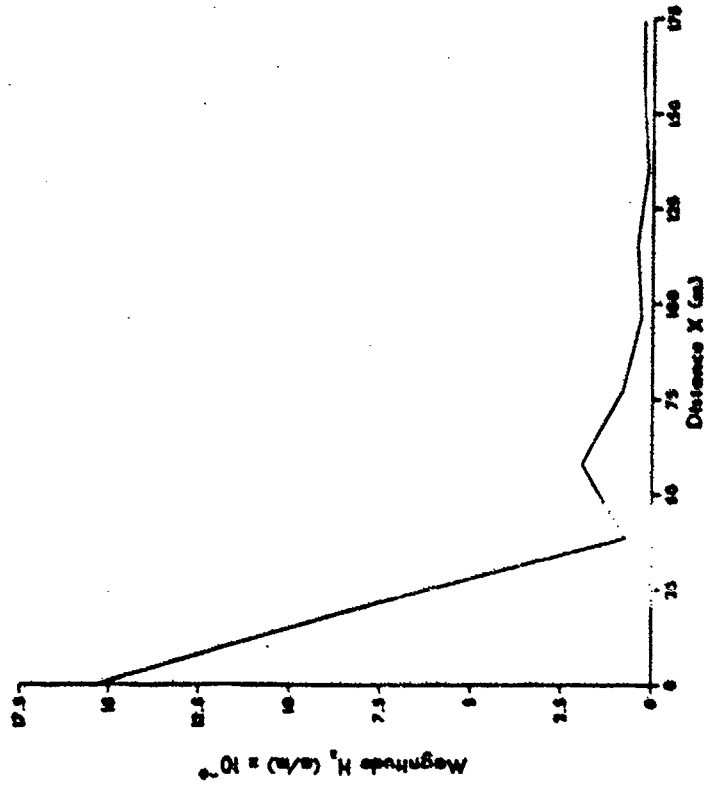
PHASE 3.38 MHz

1/4 lambda spacing, switched parallel feed



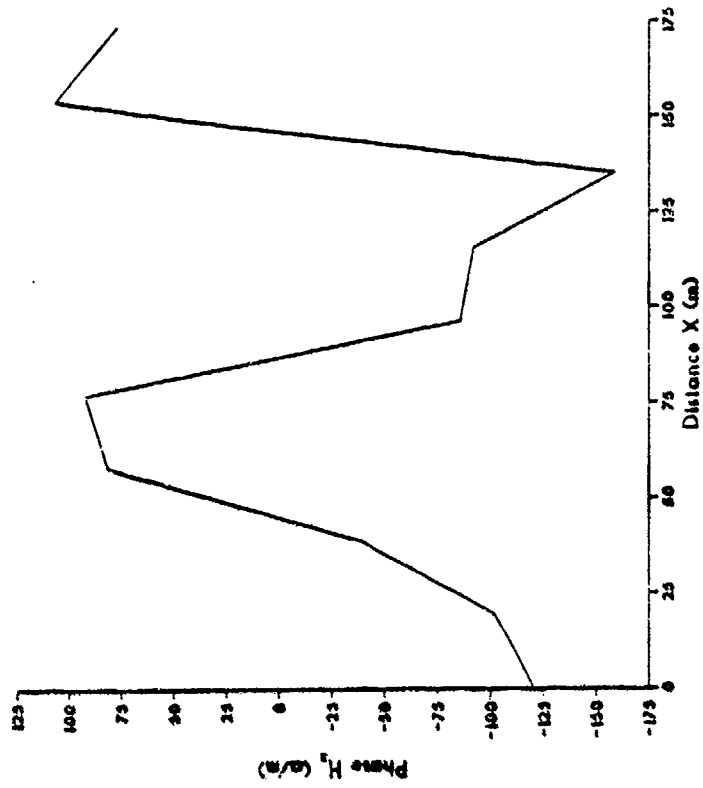
**MAGNITUDE 3.63 MHz**

*1/4 lambda spacing, switched parallel feed*



**PHASE 3.63 MHz**

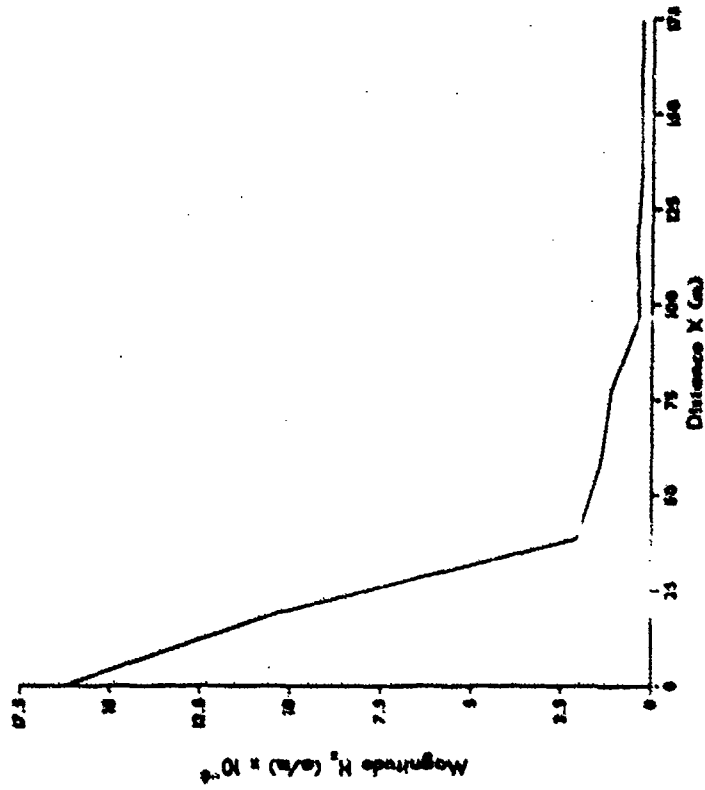
*1/4 lambda spacing, switched parallel feed*





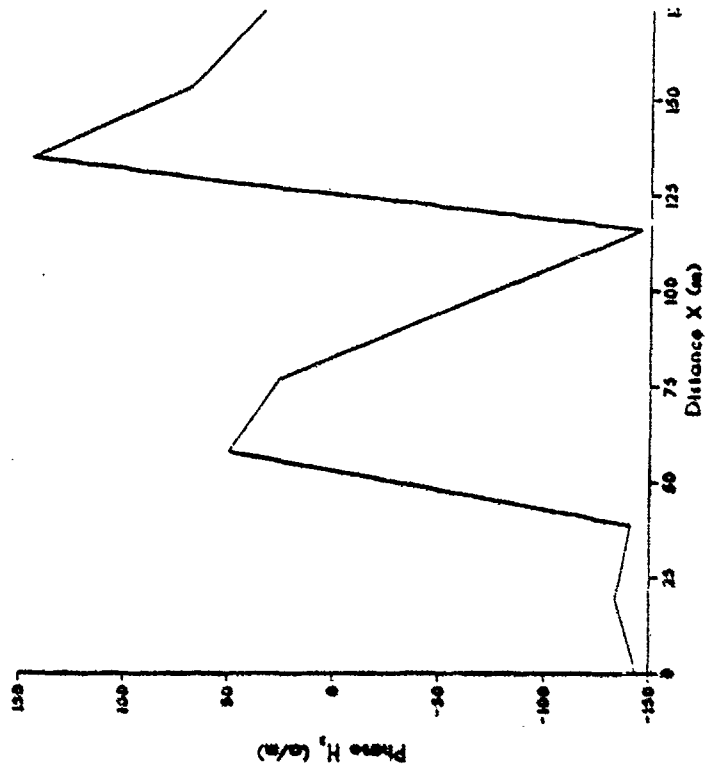
MAGNITUDE 3.72 MHz

1/4 lambda spacing, switched parallel feed



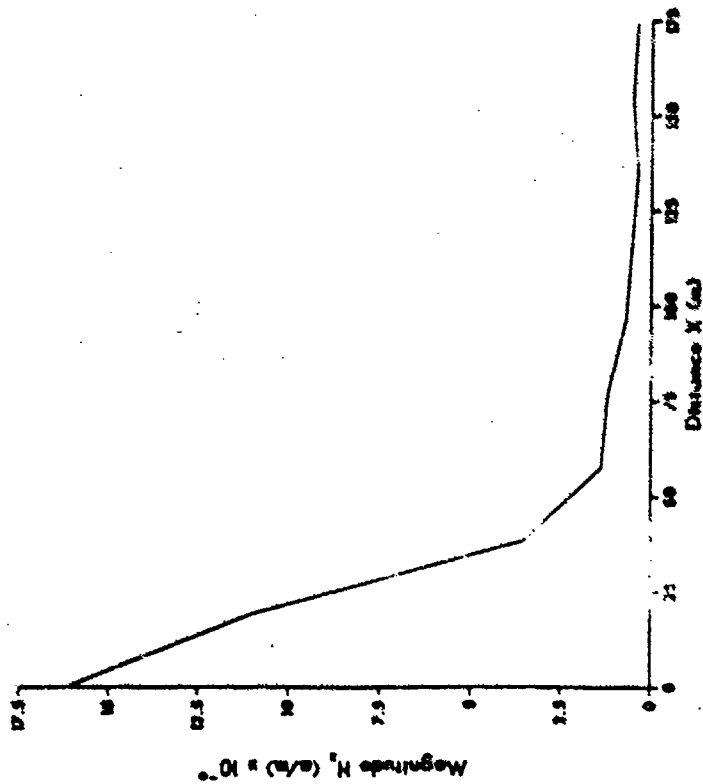
PHASE 3.72 MHz

1/4 lambda spacing, switched parallel feed



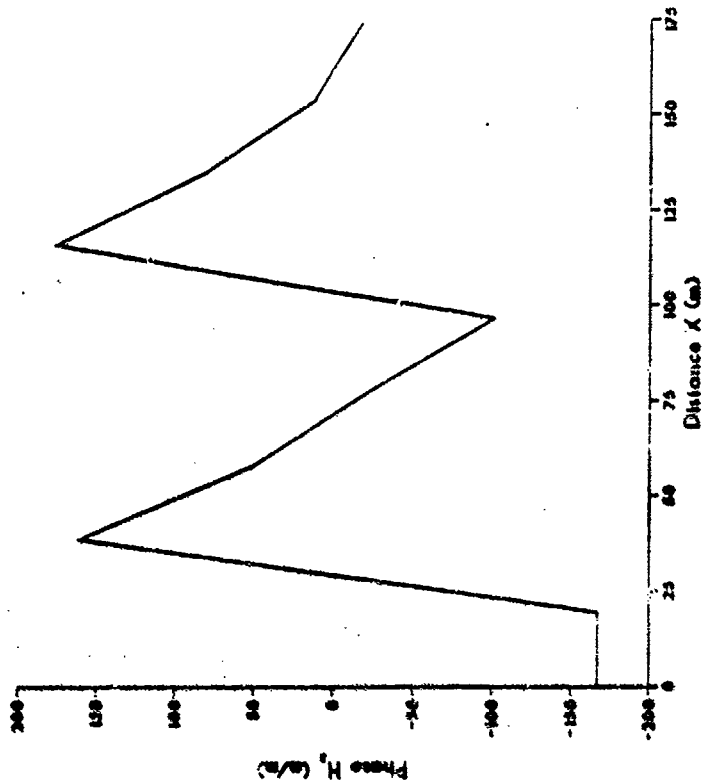
MAGNITUDE 3.81 MHz

1/4 lambda spacing, switched parallel feed



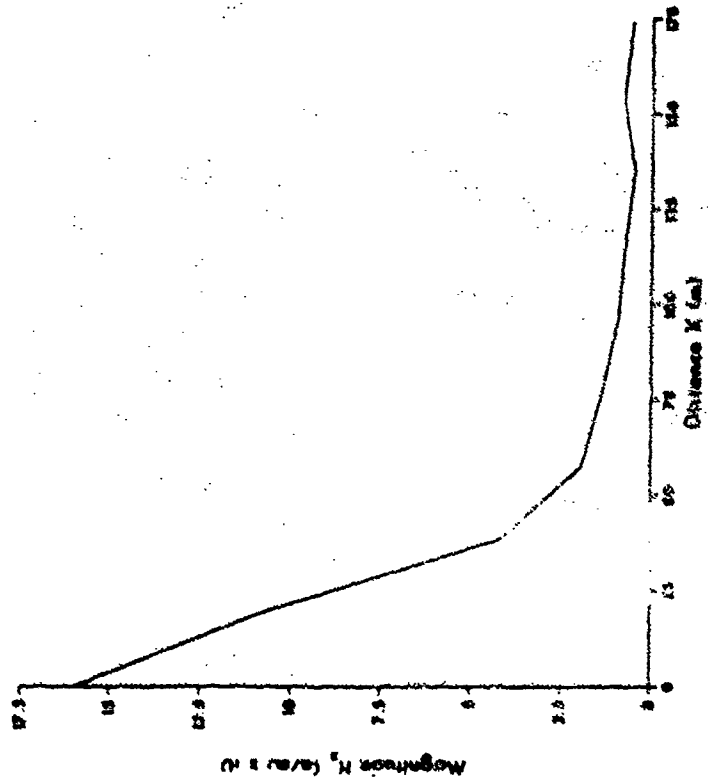
PHASE 3.81 MHz

1/4 lambda spacing, switched parallel feed



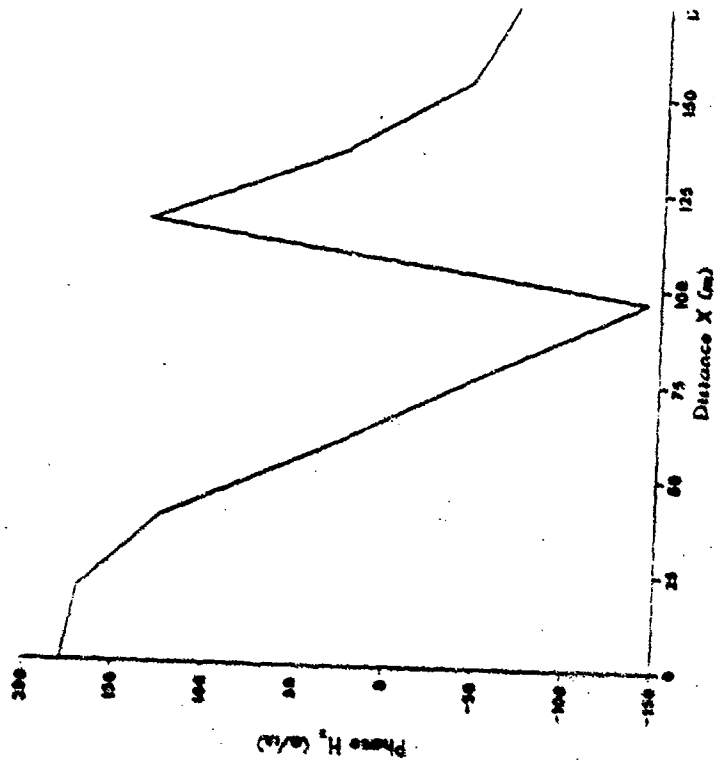
MAGNITUDE 3.88 MHz

1/4 lambda spacing, switched parallel feed



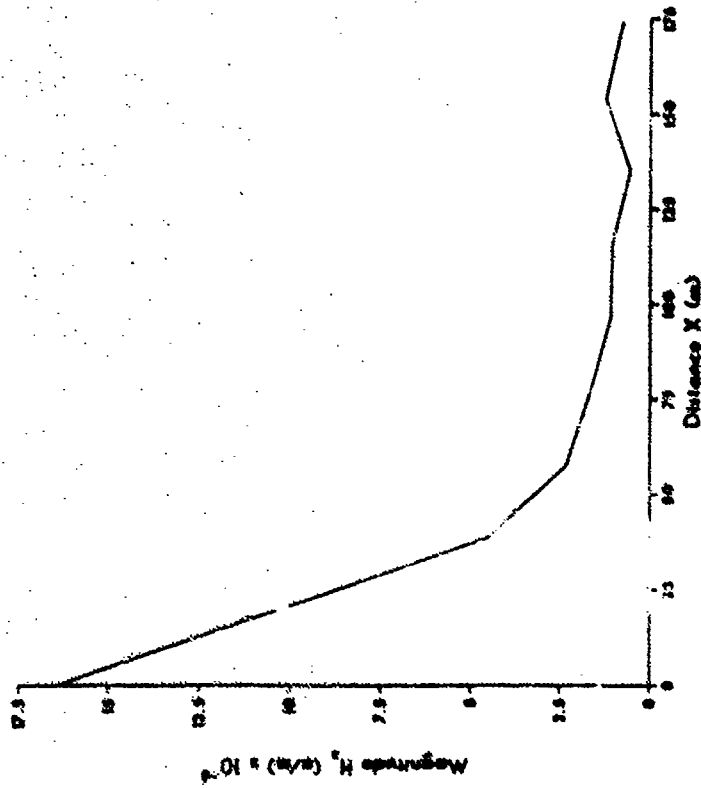
PHASE 3.88 MHz

1/4 lambda spacing, switched parallel feed



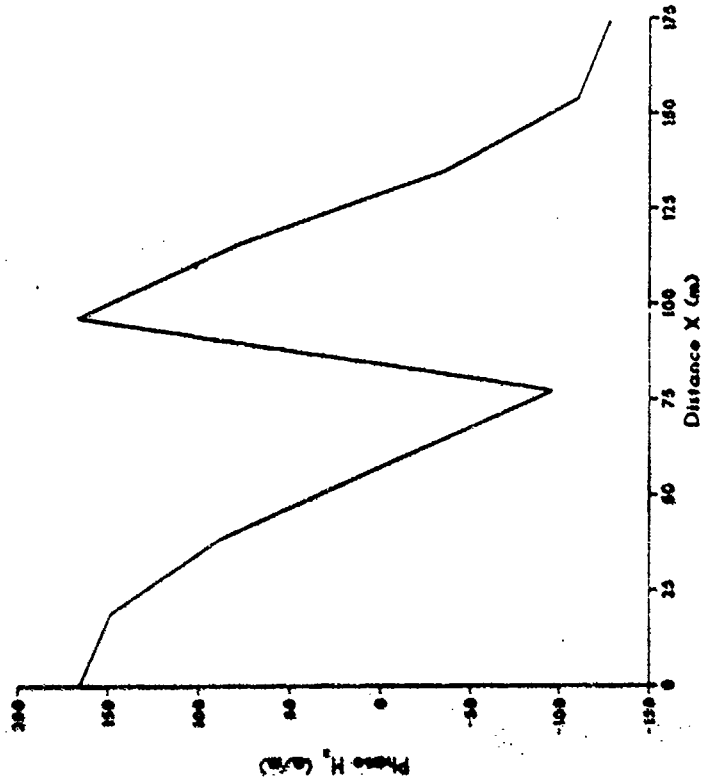
MAGNITUDE 3.95 MHz

1/4 lambda spacing, switched parallel feed



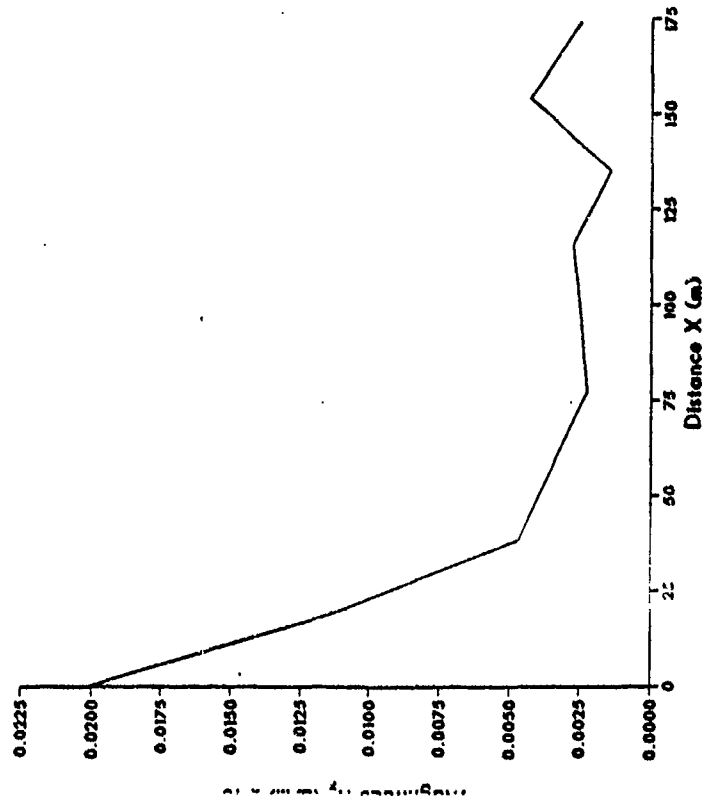
PHASE 3.95 MHz

1/4 lambda spacing, switched parallel feed



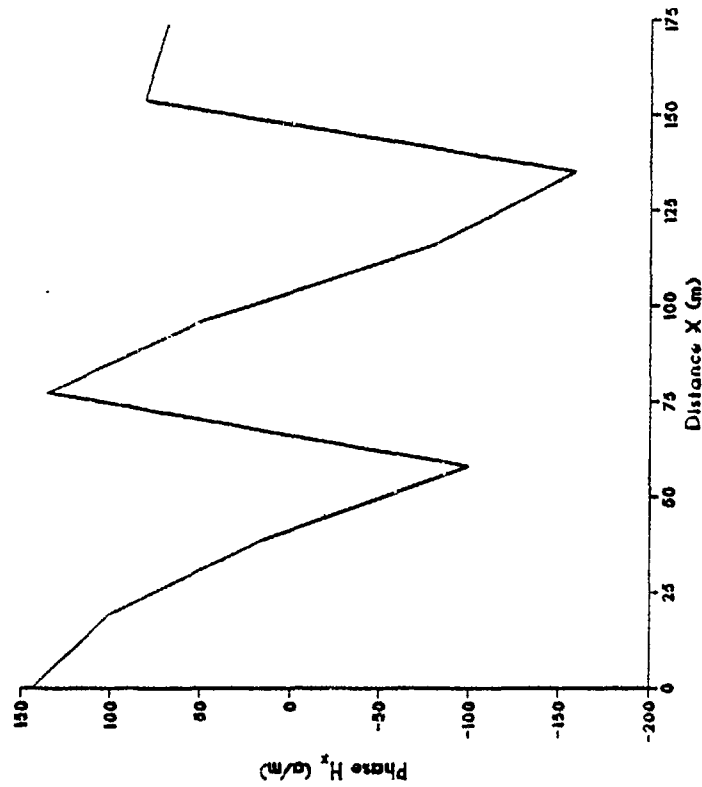
MAGNITUDE 4.04 MHz

1/4 lambda spacing, switched parallel feed



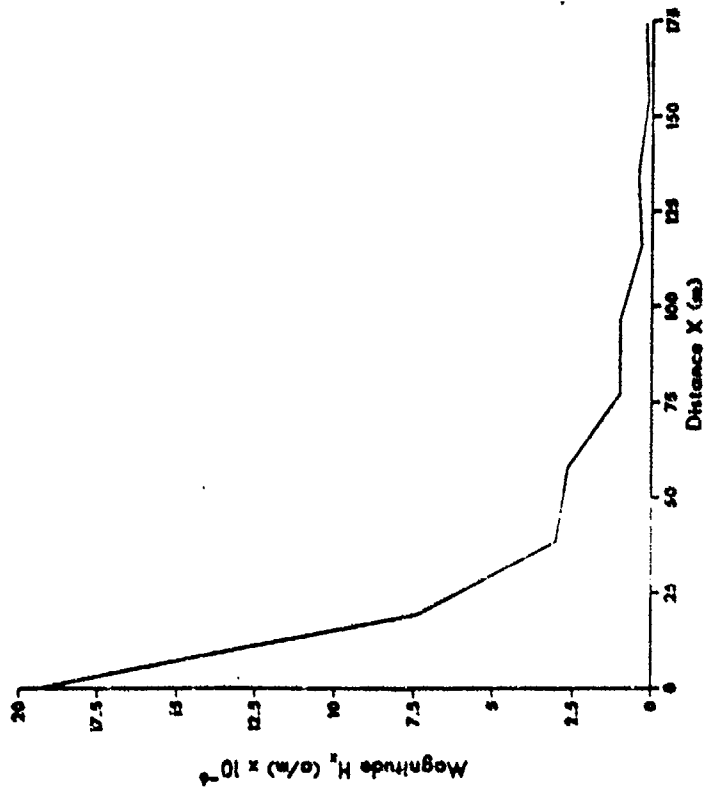
PHASE 4.04 MHz

1/4 lambda spacing, switched parallel feed



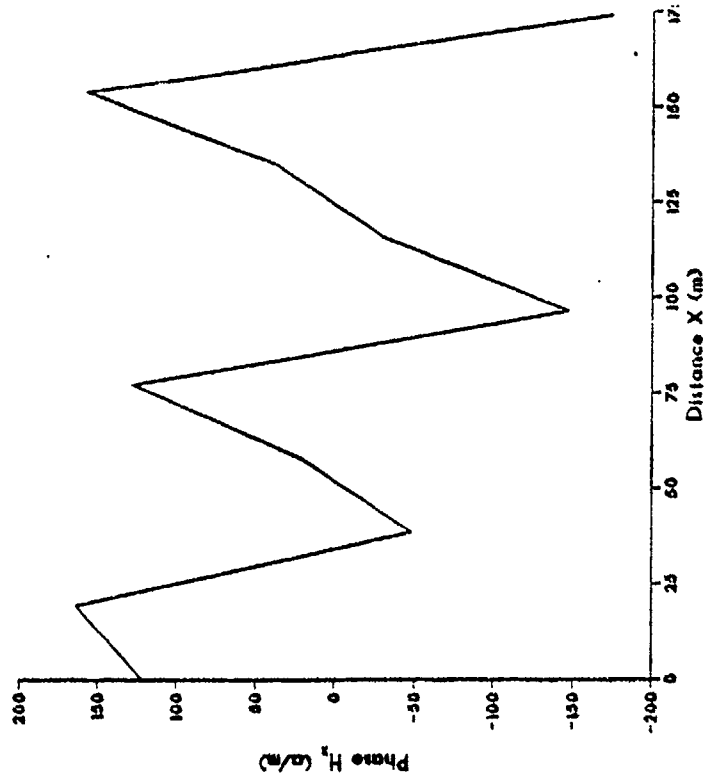
**MAGNITUDE 4.13 MHz**

1/4 lambda spacing, switched parallel feed



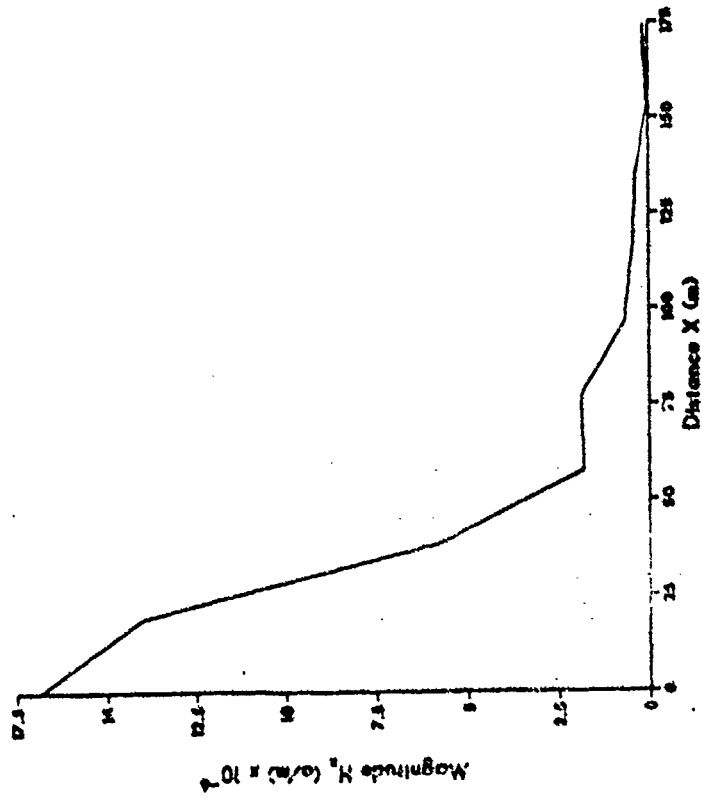
**PHASE 4.13 MHz**

1/4 lambda spacing, switched parallel feed



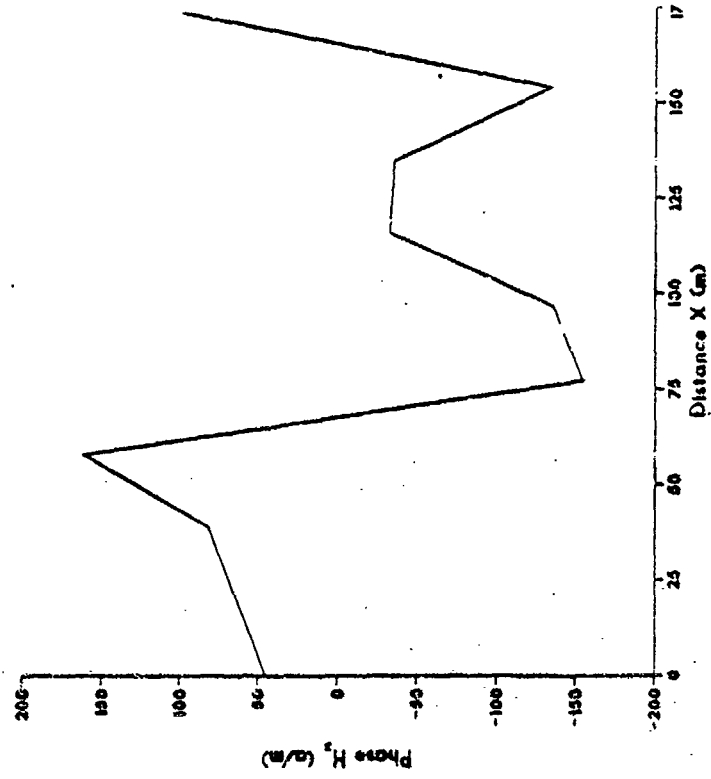
MAGNITUDE 4.38 MHz

1/4 lambda spacing, switched parallel feed



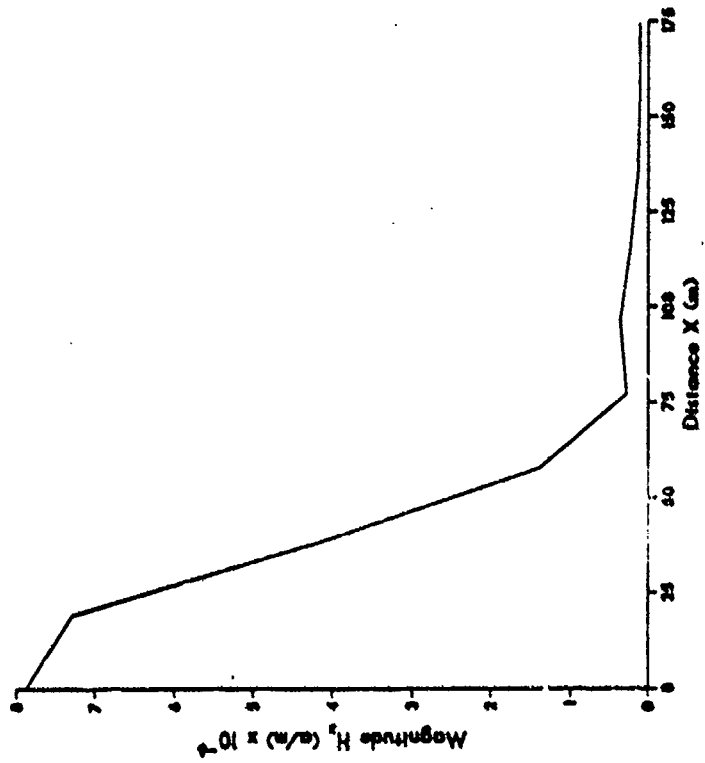
PHASE 4.38 MHz

1/4 lambda spacing, switched parallel feed



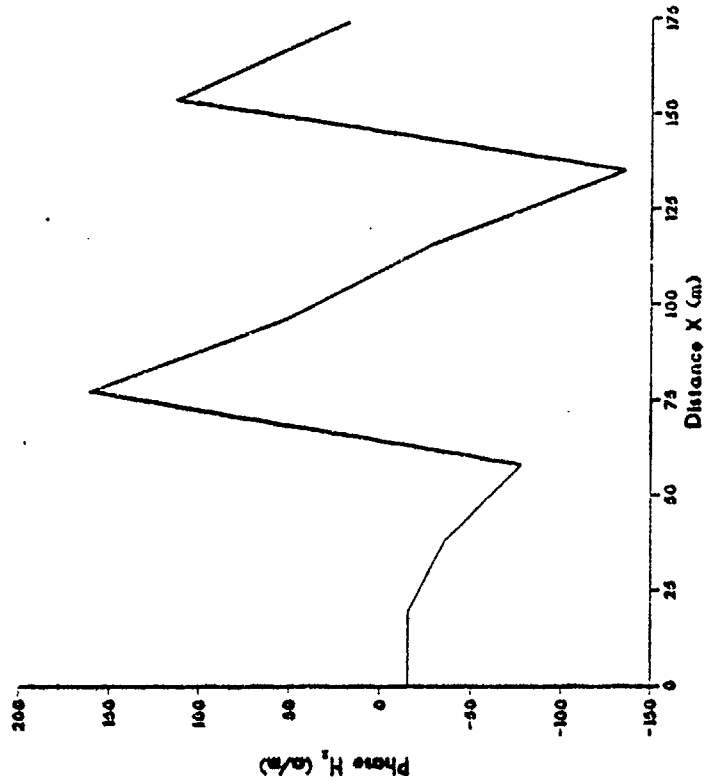
MAGNITUDE 4.63 MHz

1/4 lambda spacing, switched parallel feed



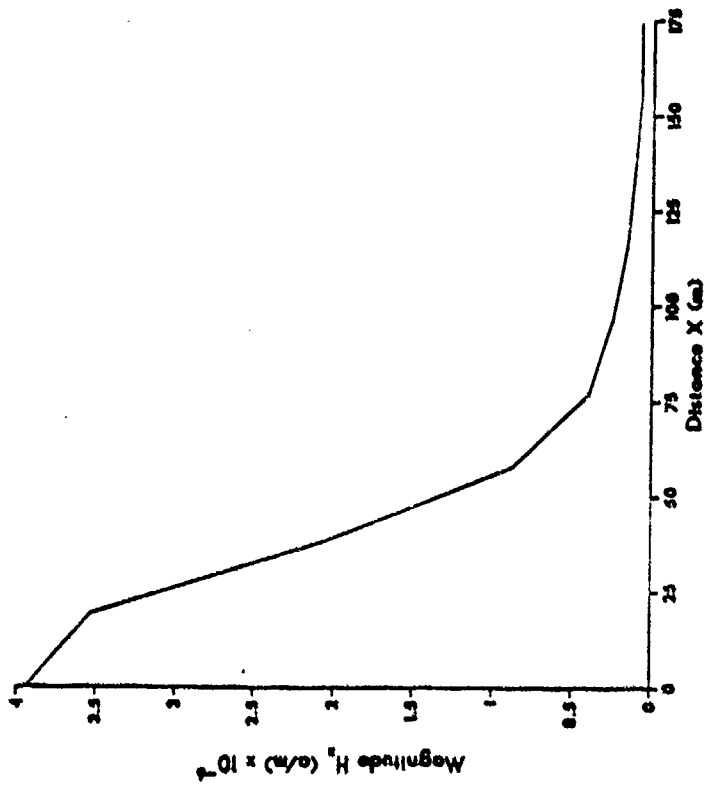
PHASE 4.63 MHz

1/4 lambda spacing, switched parallel feed

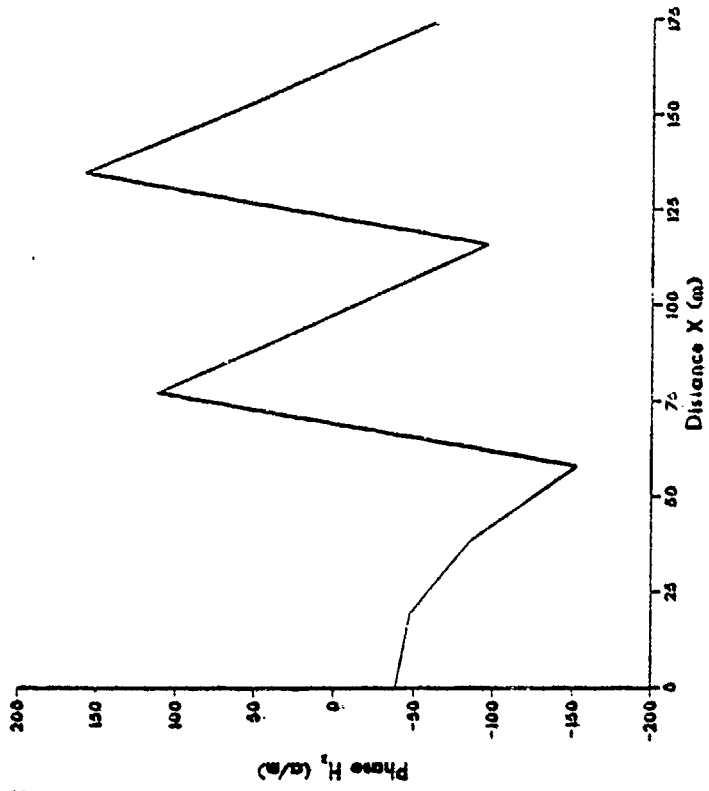




**MAGNITUDE 4.88 MHz**  
**1/4 lambda spacing, switched parallel feed**

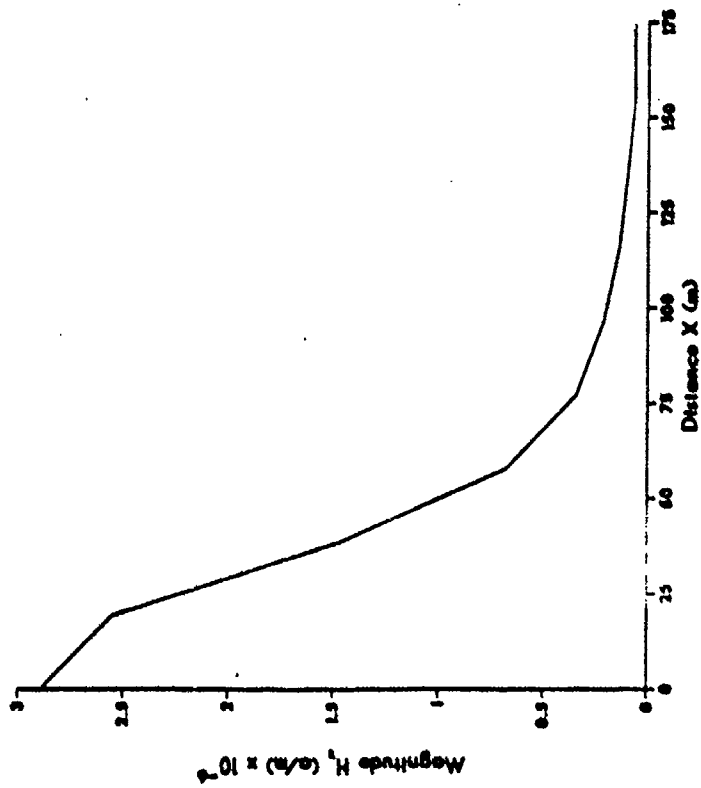


**PHASE 4.88 MHz**  
**1/4 lambda spacing, switched parallel feed**



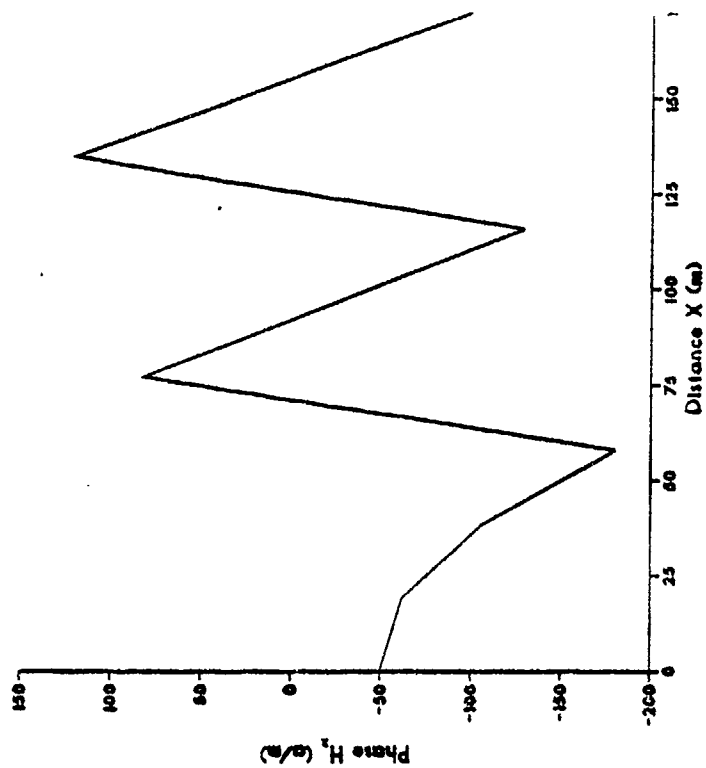
MAGNITUDE 5.04 MHz

1/4 lambda spacing, switched parallel feed



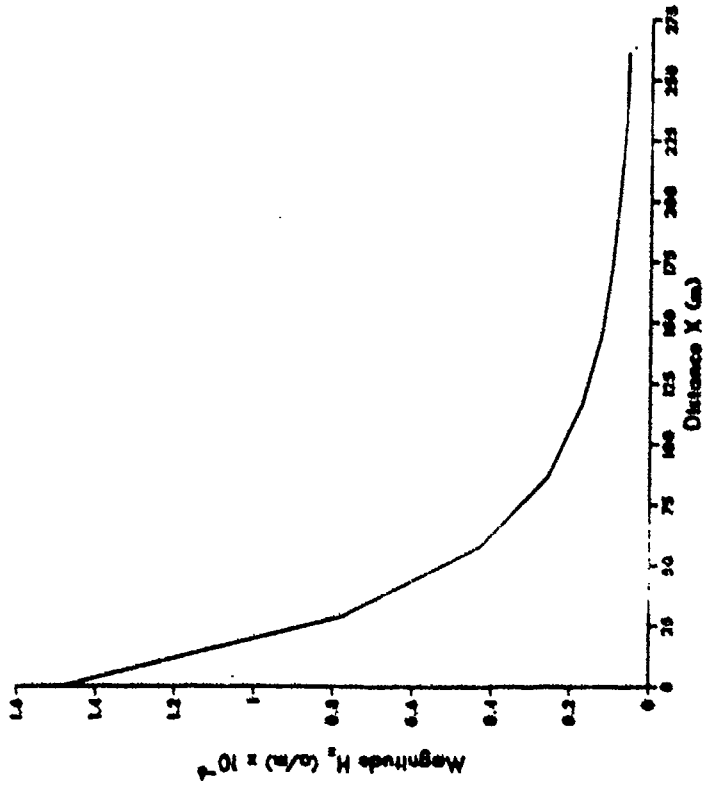
PHASE 5.04 MHz

1/4 lambda spacing, switched parallel feed



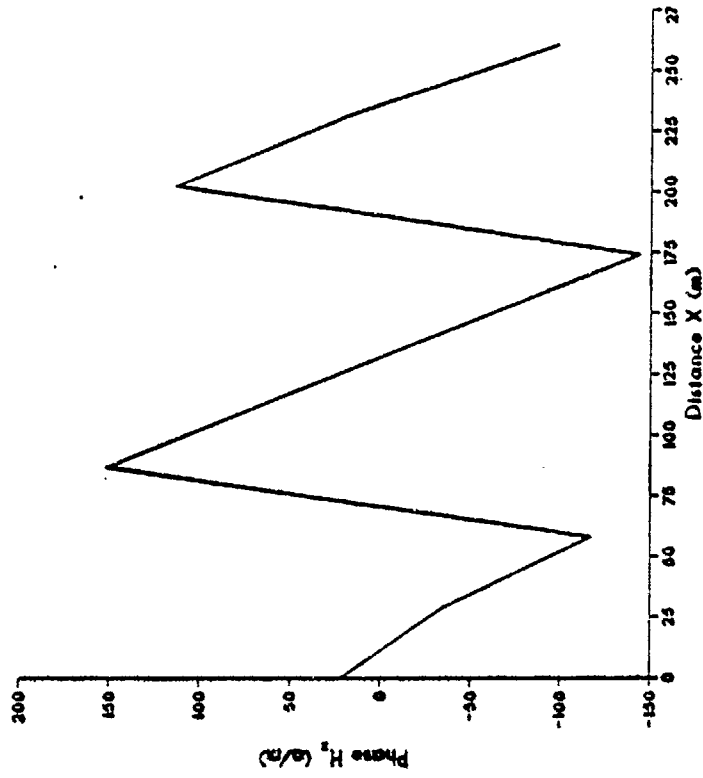
**MAGNITUDE 2.88 MHz**

3/8 lambda spacing, switched parallel feed



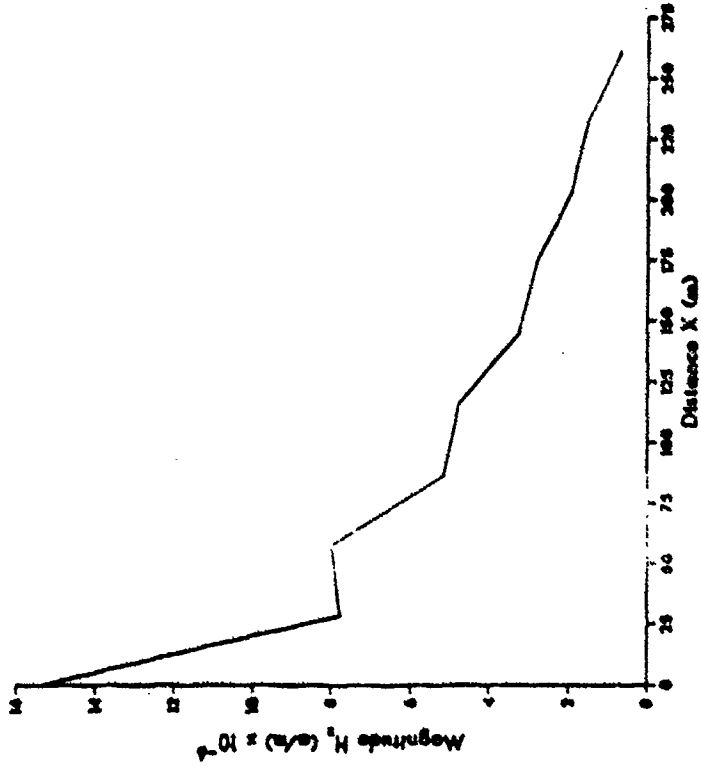
**PHASE 2.88 MHz**

3/8 lambda spacing, switched parallel feed



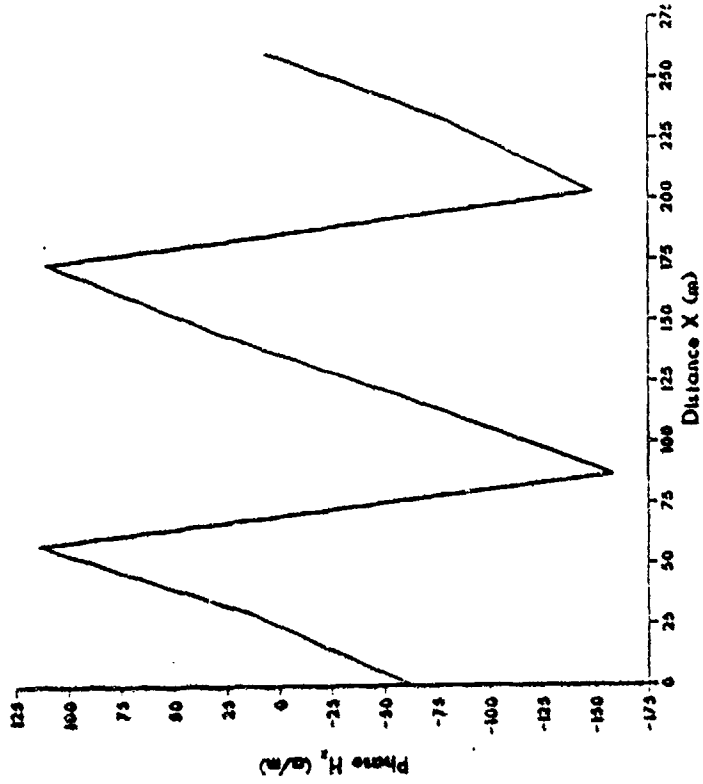
MAGNITUDE 3.38 MHz

3/8 lambda spacing, switched parallel feed



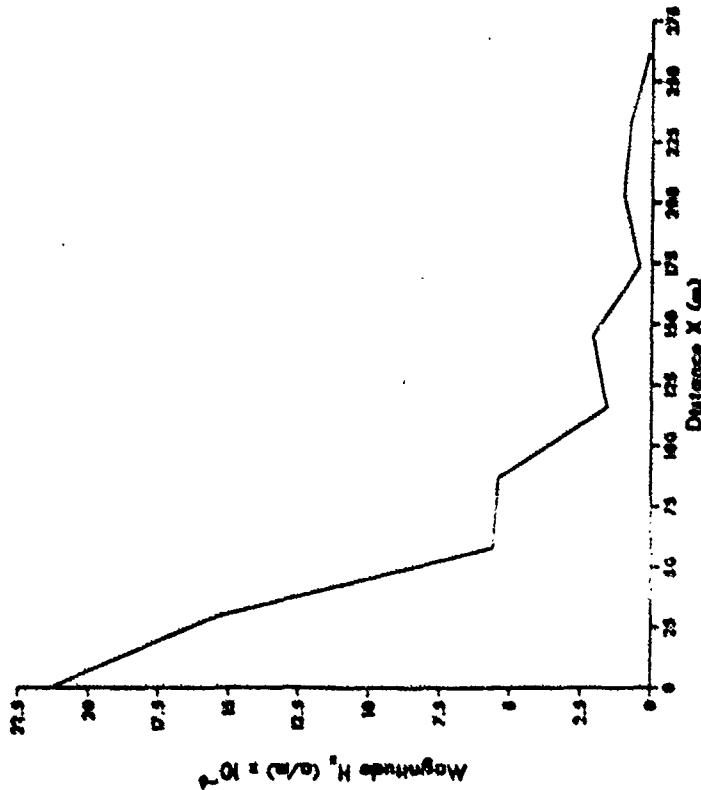
PHASE 3.38 MHz

3/8 lambda spacing, switched parallel feed



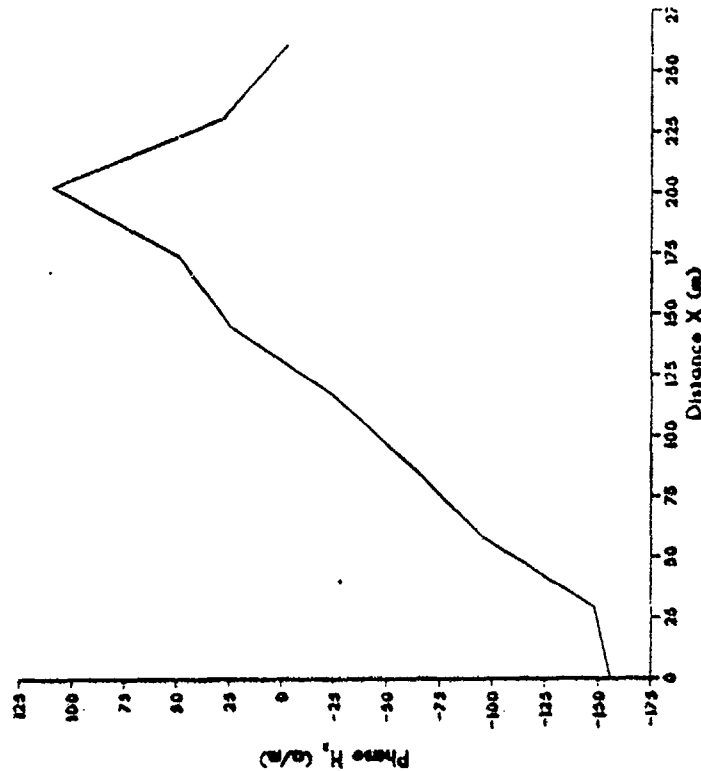
MAGNITUDE 3.63 MHz

3/8 lambda spacing, switched parallel feed



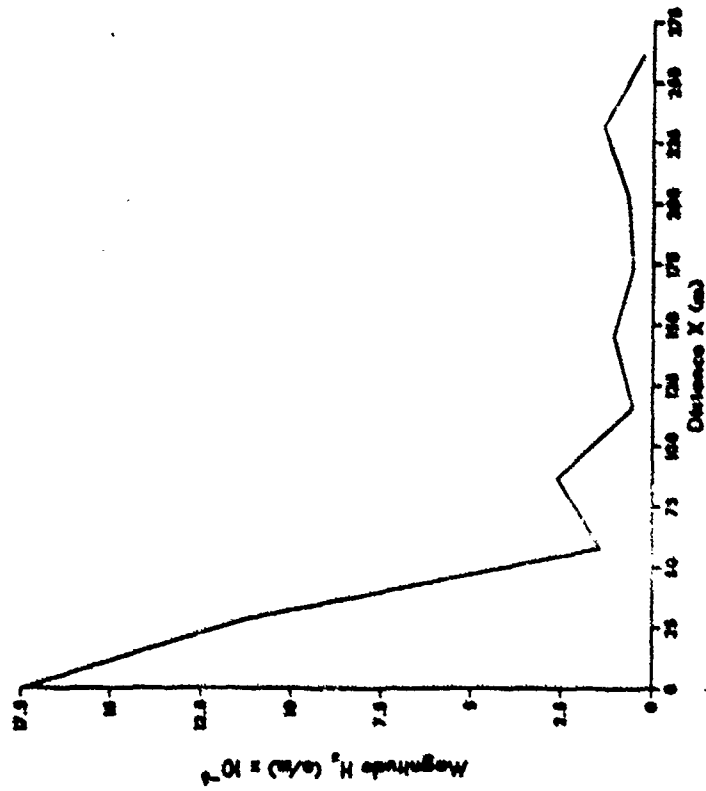
PHASE 3.63 MHz

3/8 lambda spacing, switched parallel feed



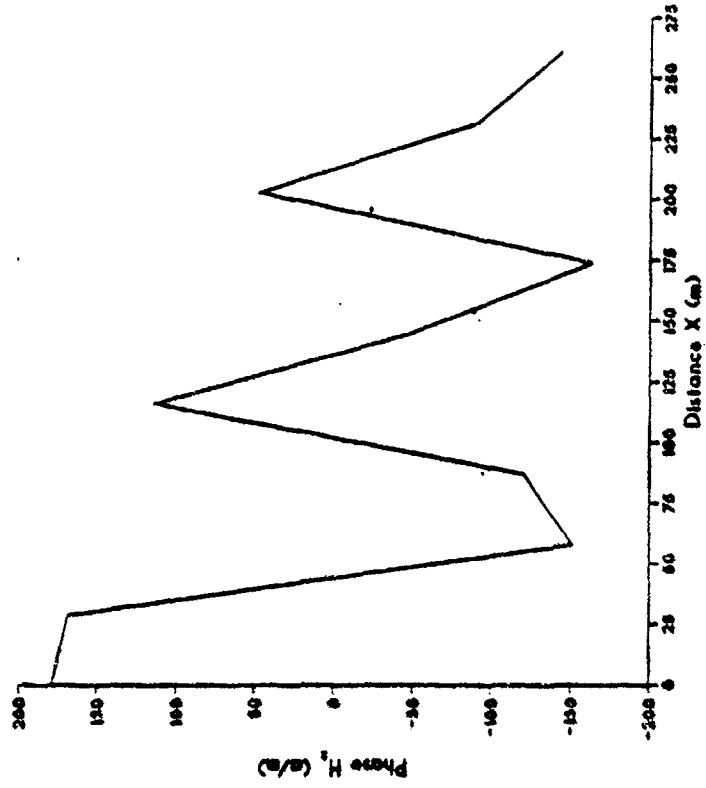
**MAGNITUDE 3.72 MHz**

**3/8 lambda spacing, switched parallel feed**



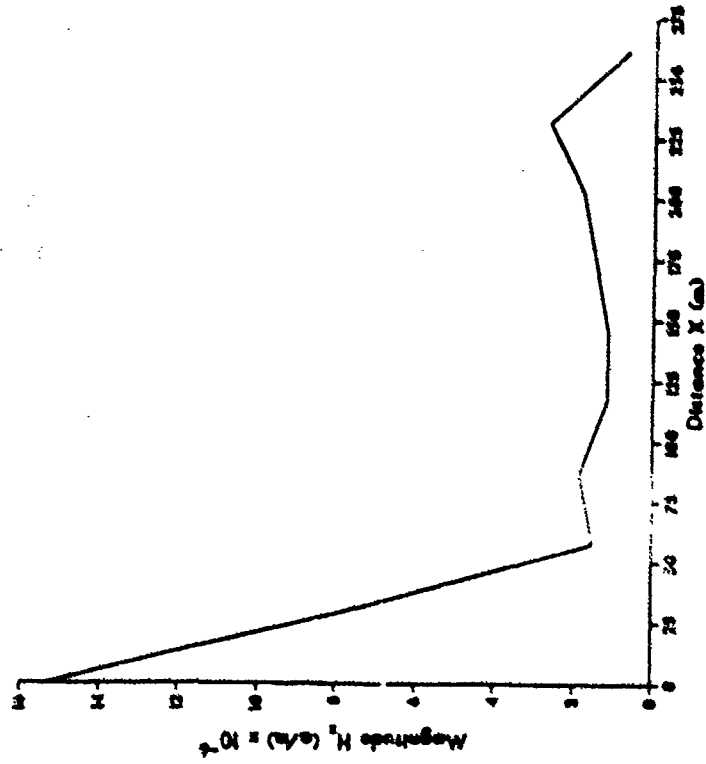
**PHASE 3.72 MHz**

**3/8 lambda spacing, switched parallel feed**



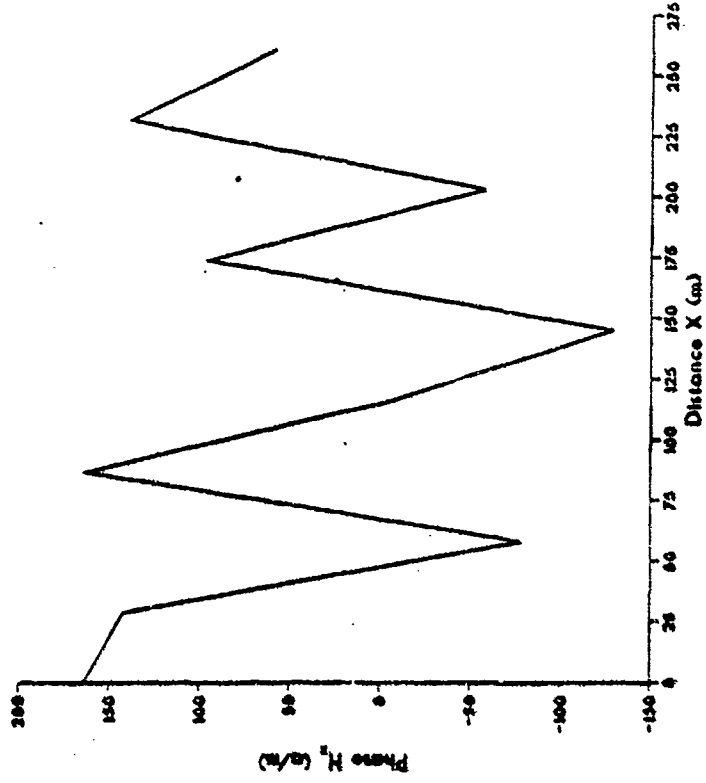
**MAGNITUDE 3.61 MHz**

3/8 lambda spacing, switched parallel feed



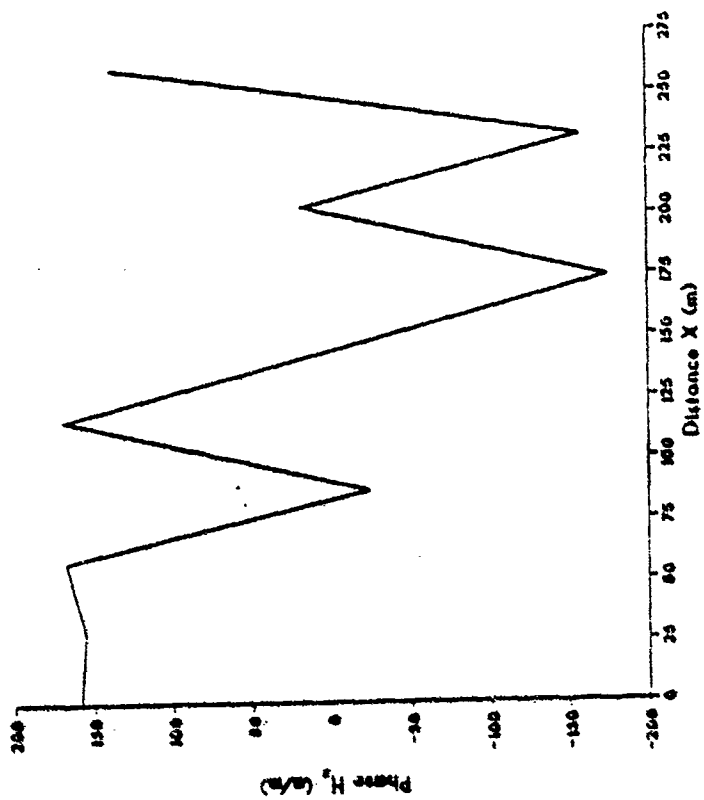
**PHASE 3.61 MHz**

3/8 lambda spacing, switched parallel feed



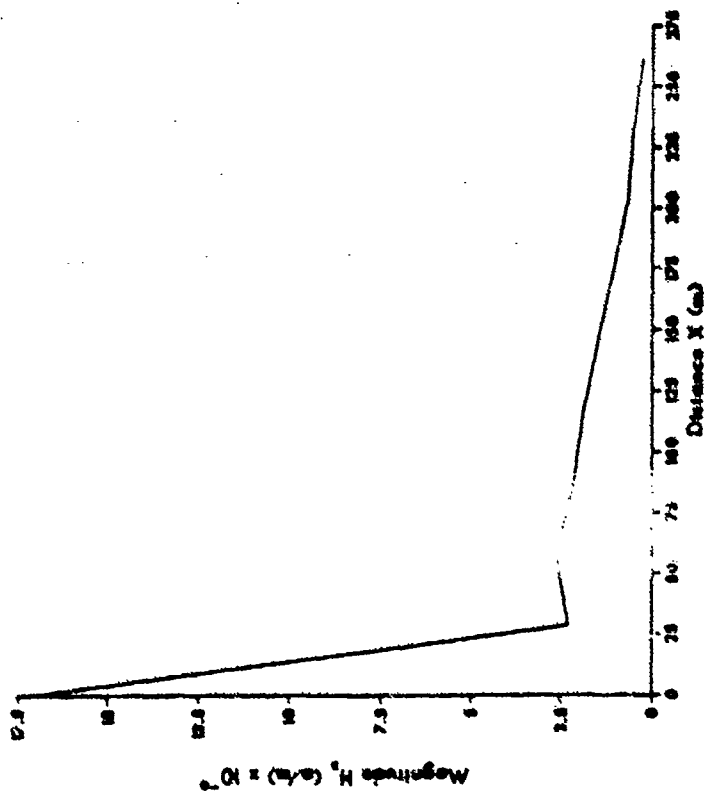
PHASE 3.88 MHz

3/8 lambda spacing, switched parallel feed



MAGNITUDE 3.88 MHz

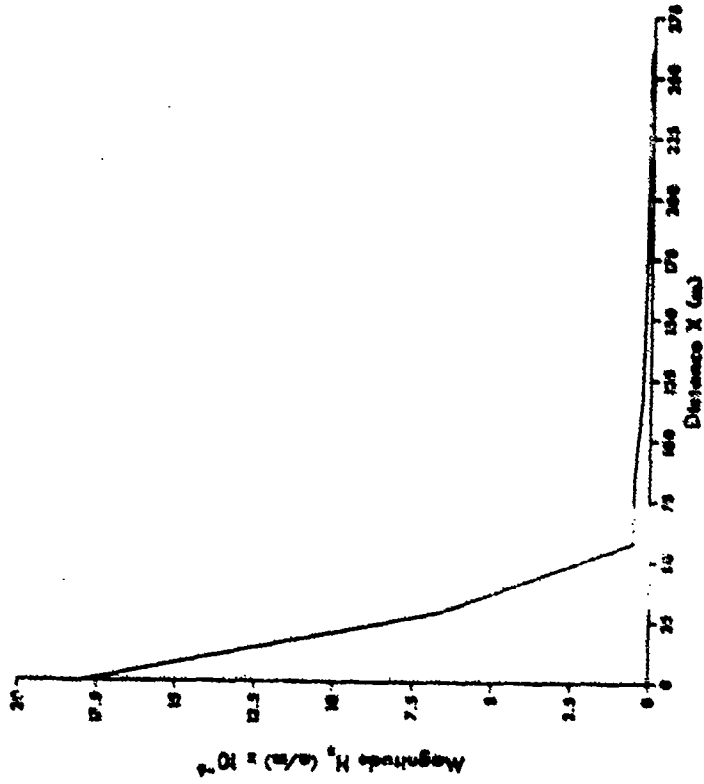
3/8 lambda spacing, switched parallel feed





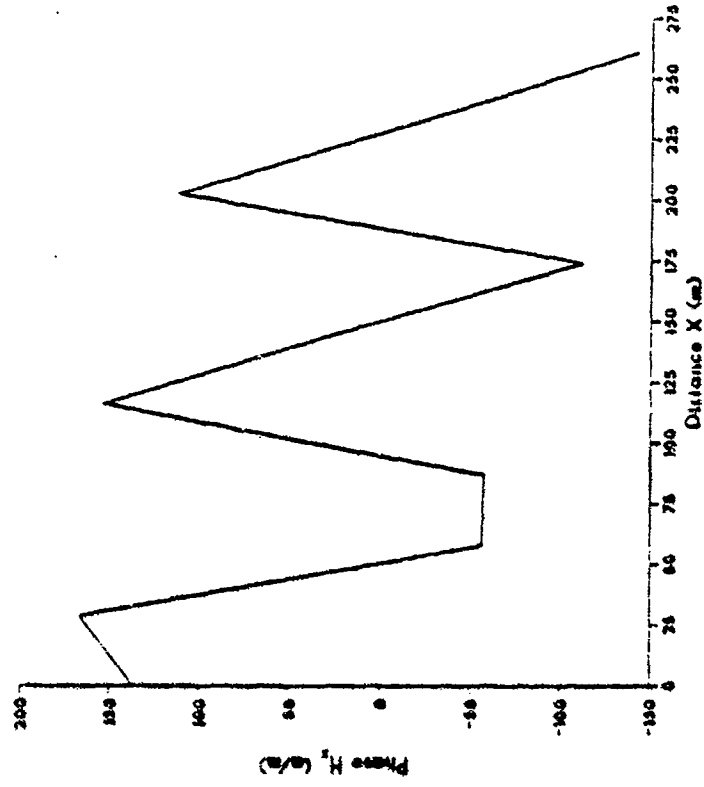
MAGNITUDE 3.95 MHz

3/8 lambda spacing, switched parallel feed

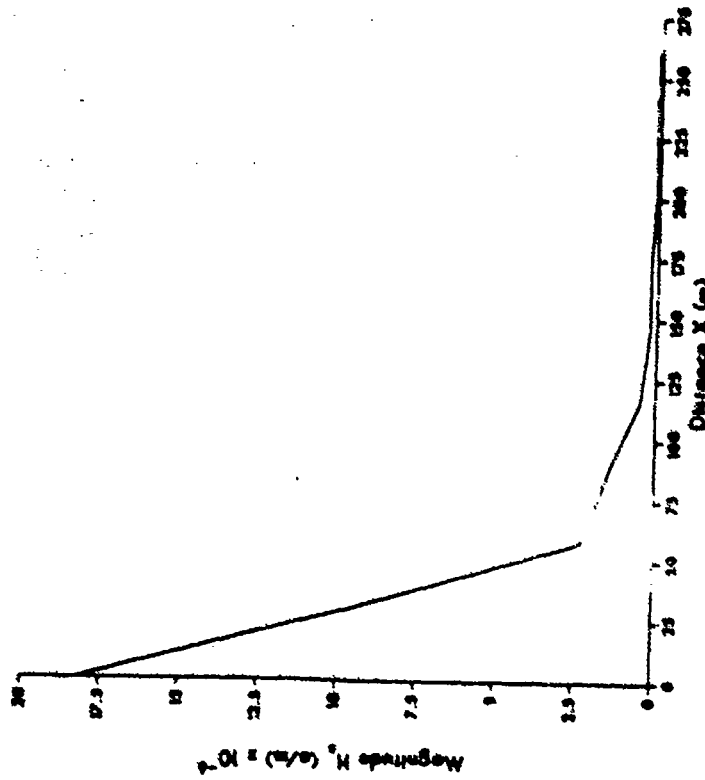


PHASE 3.95 MHz

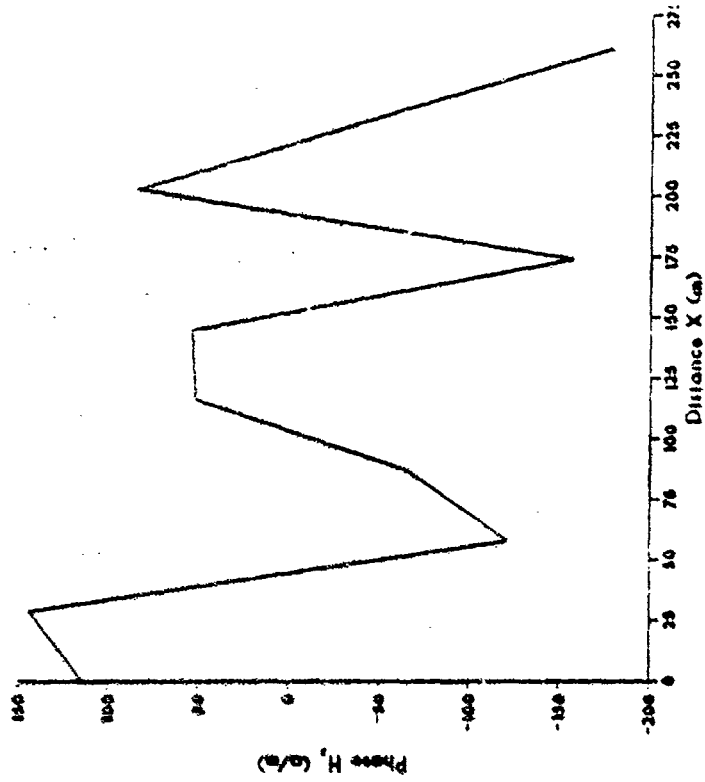
3/8 lambda spacing, switched parallel feed



MAGNITUDE 4.04 MHz  
 3/8 lambda spacing, switched parallel feed

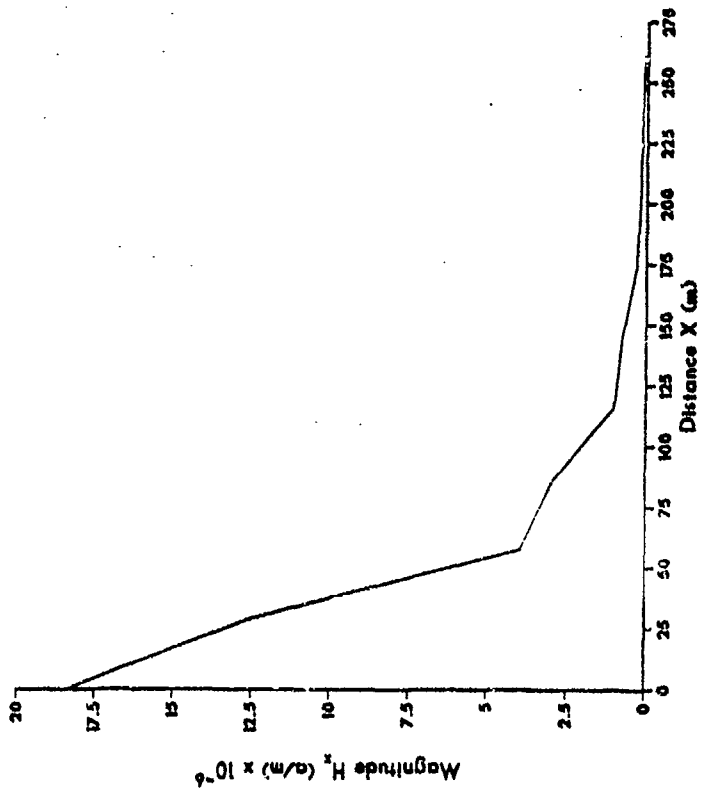


PHASE 4.04 MHz  
 3/8 lambda spacing, switched parallel feed



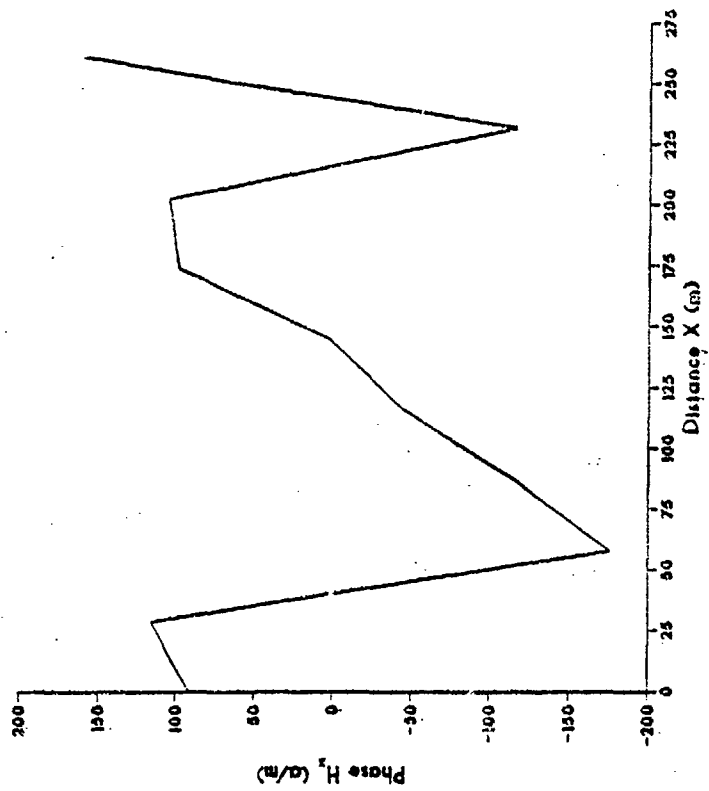
**MAGNITUDE 4.13 MHz**

3/8 lambda spacing, switched paraboloid feed

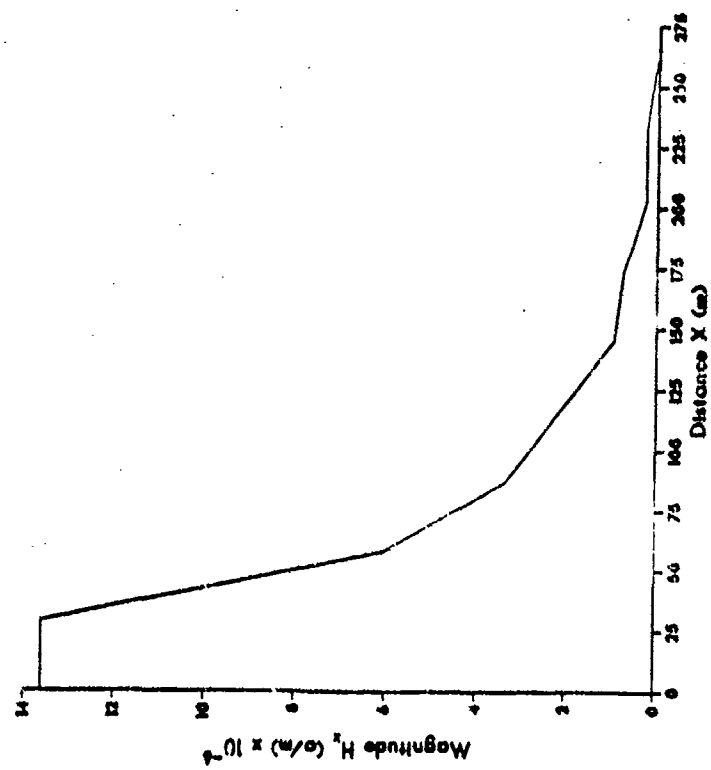


**PHASE 4.13 MHz**

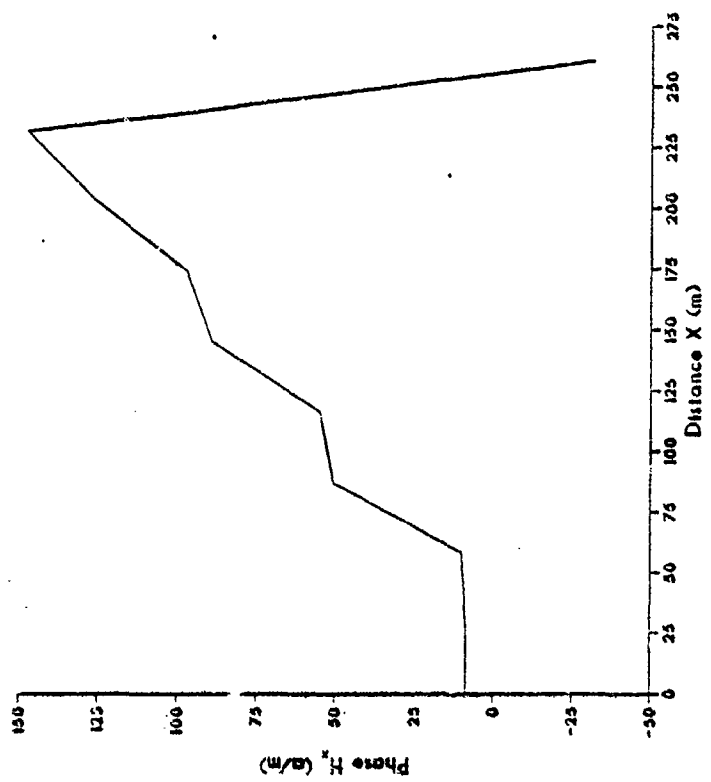
3/8 lambda spacing, switched parallel feed



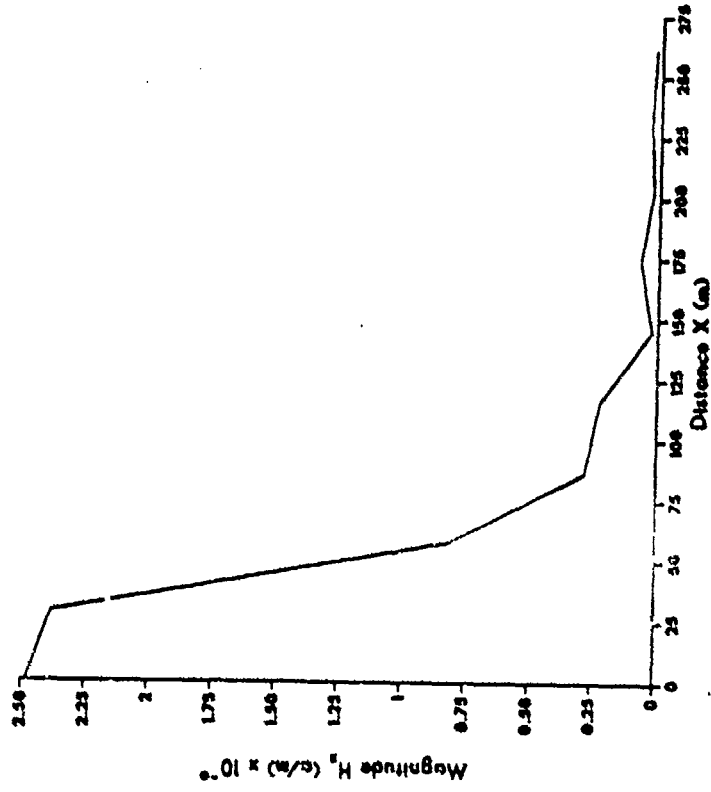
**MAGNITUDE 4.38 MHz**  
 3/8 lambda spacing, switched parallel feed



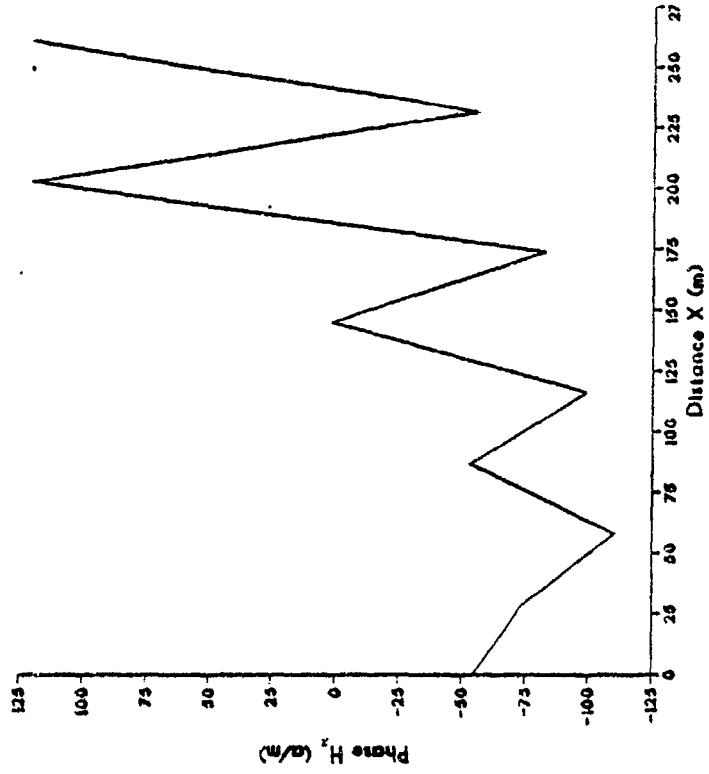
**PHASE 4.38 MHz**  
 3/8 lambda spacing, switched parallel feed



**MAGNITUDE 4.86 MHz**  
 3/8 lambda spacing, switched parallel feed

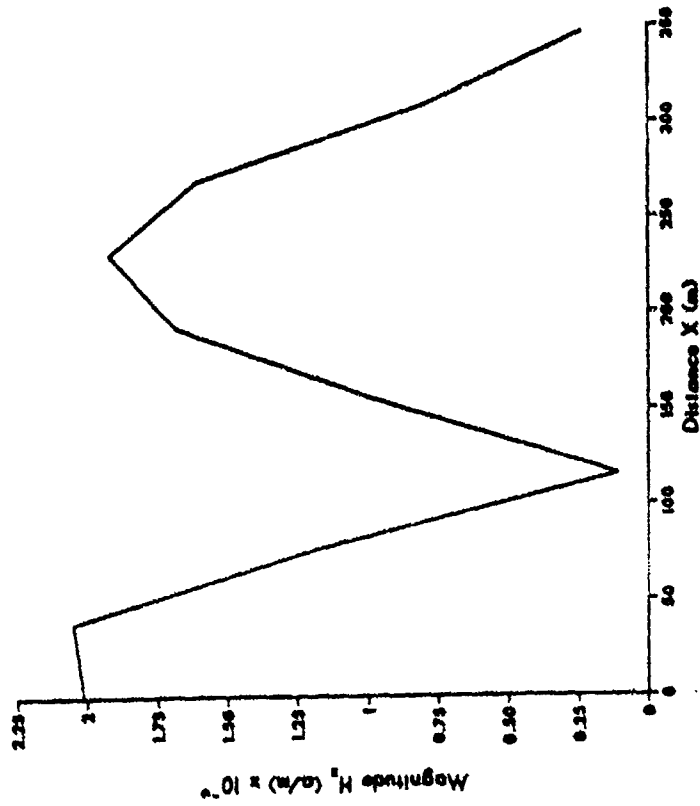


**PHASE 4.86 MHz**  
 3/8 lambda spacing, switched parallel feed



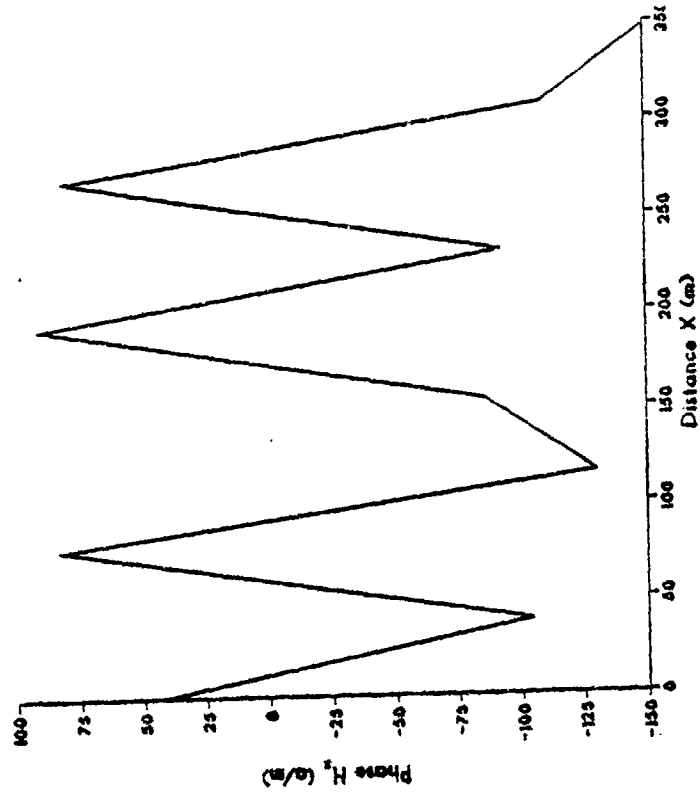
MAGNITUDE 2.88 MHz

1/2 lambda spacing, switched parallel feed



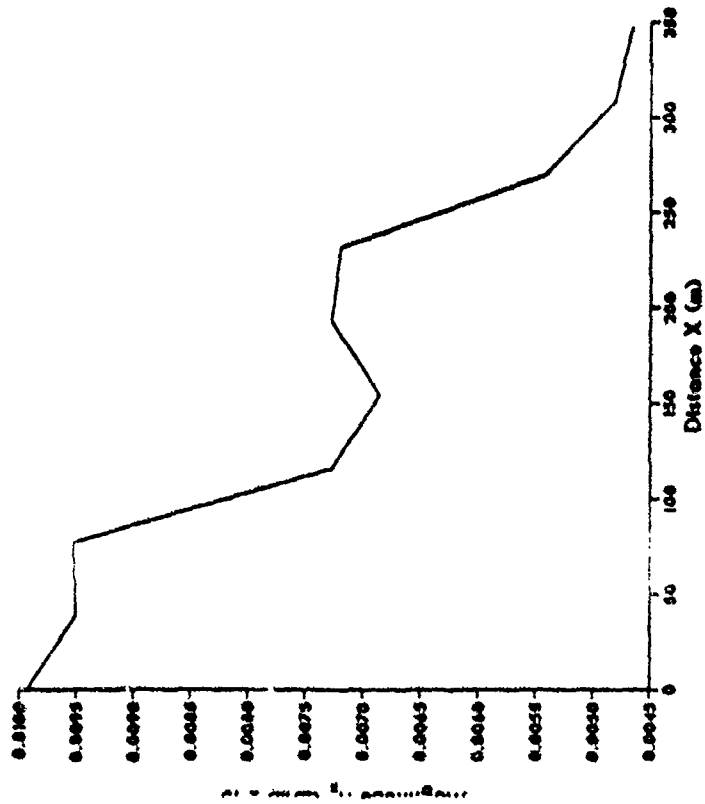
PHASE 2.88 MHz

1/2 lambda spacing, switched parallel feed



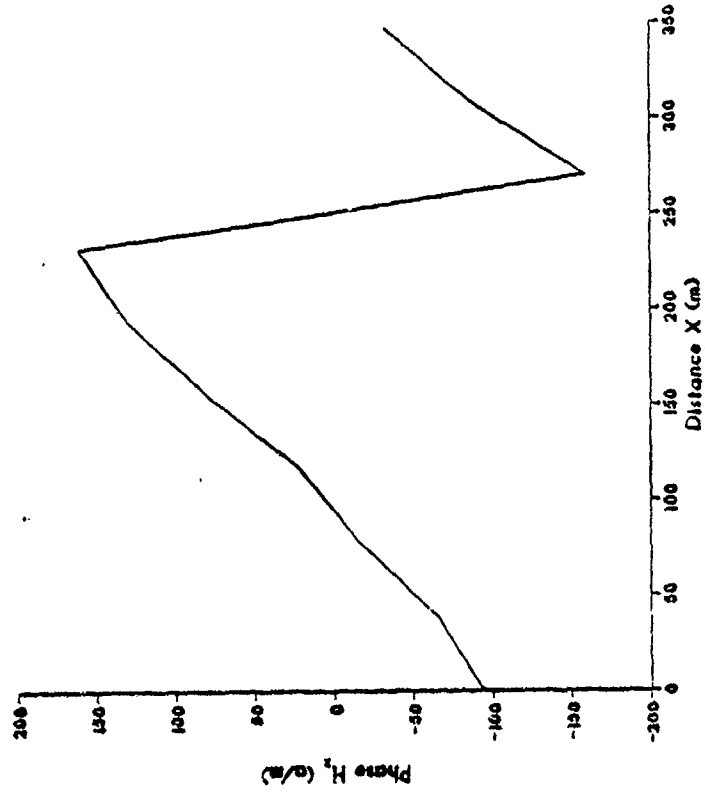
MAGNITUDE 3.38 MHz

1/2 lambda spacing, switched parallel feed



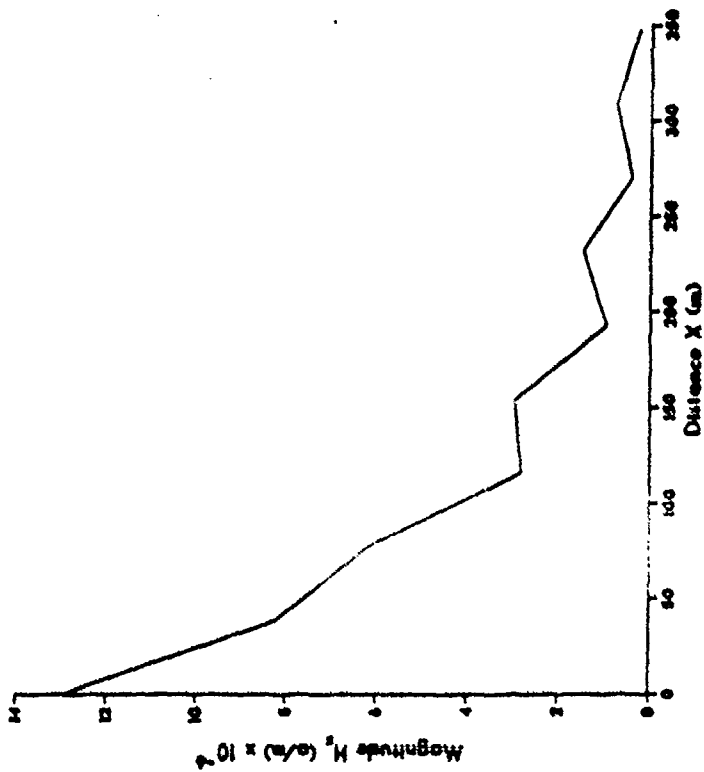
PHASE 3.38 MHz

1/2 lambda spacing, switched parallel feed



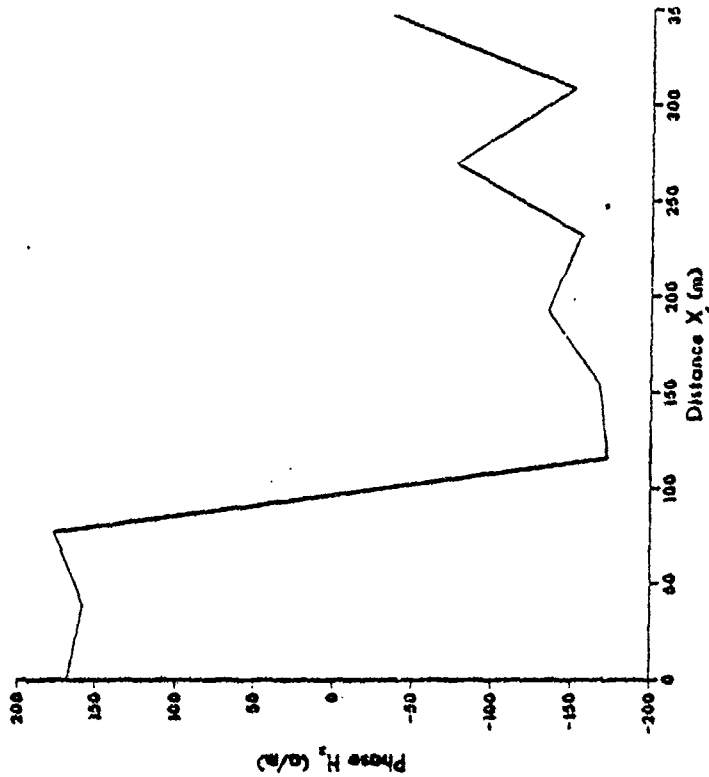
MAGNITUDE 3.63 MHz

1/2 lambda spacing, switched parallel feed



PHASE 3.63 MHz

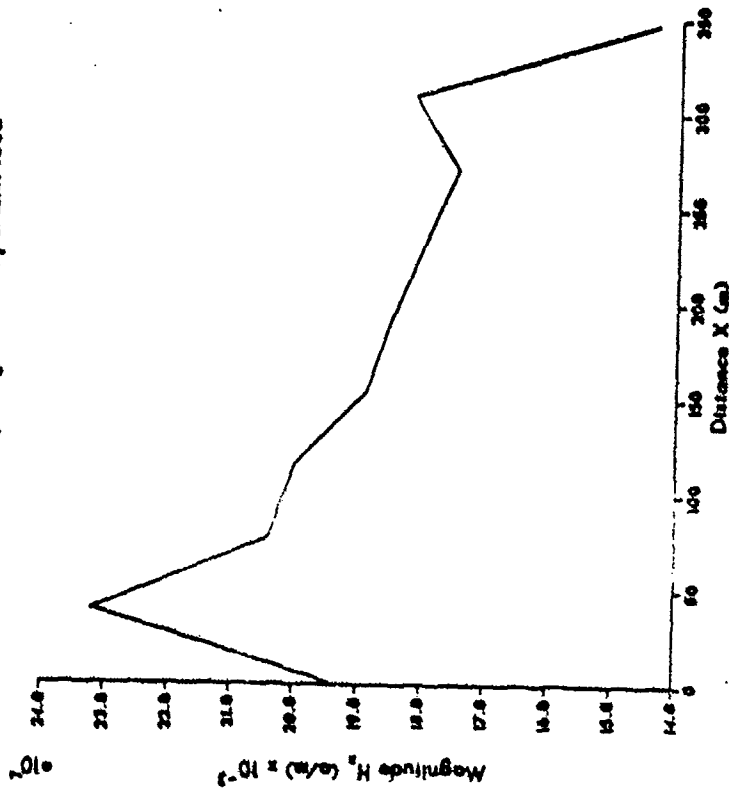
1/2 lambda spacing, switched parallel feed





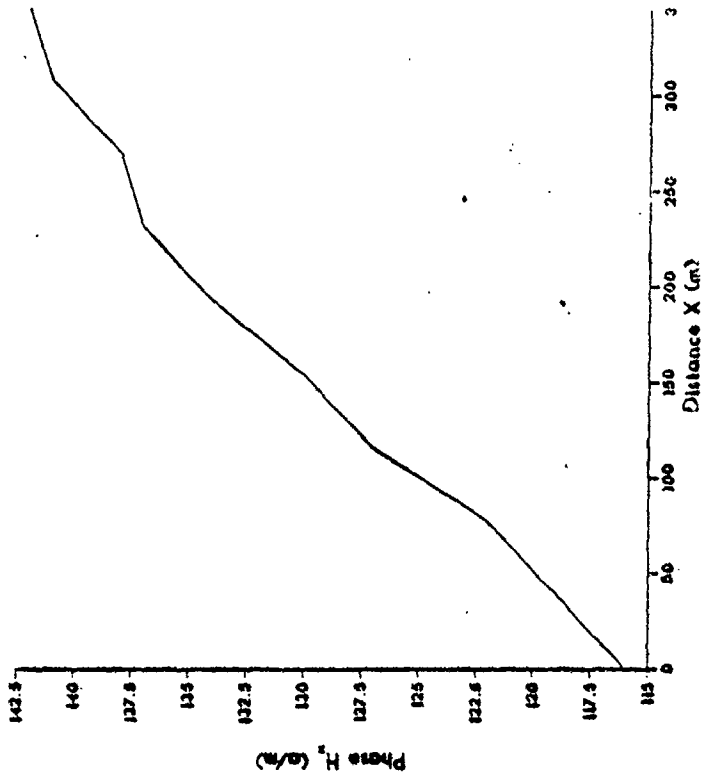
MAGNITUDE 3.88 MHz

1/2 lambda spacing, switched parallel feed



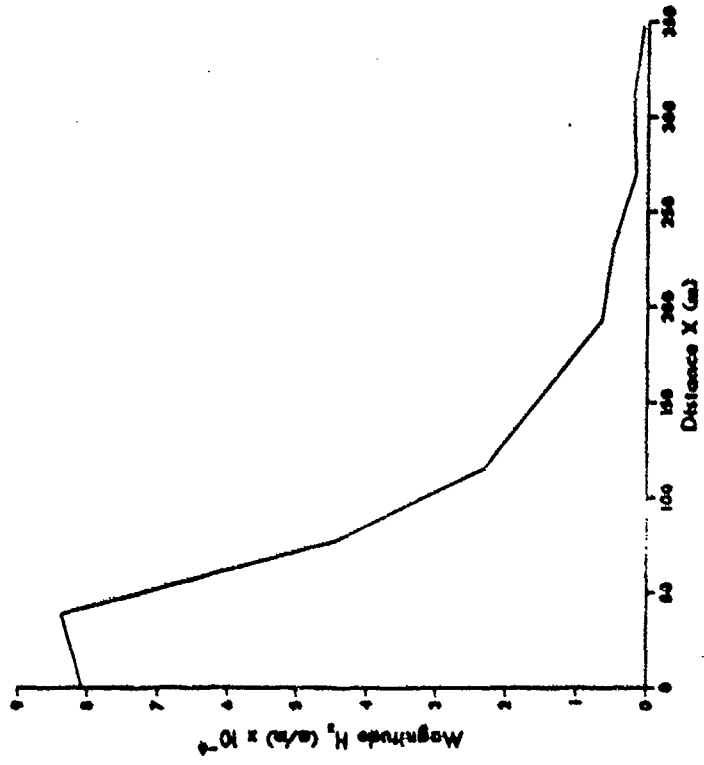
PHASE 3.88 MHz

1/2 lambda spacing, switched parallel feed



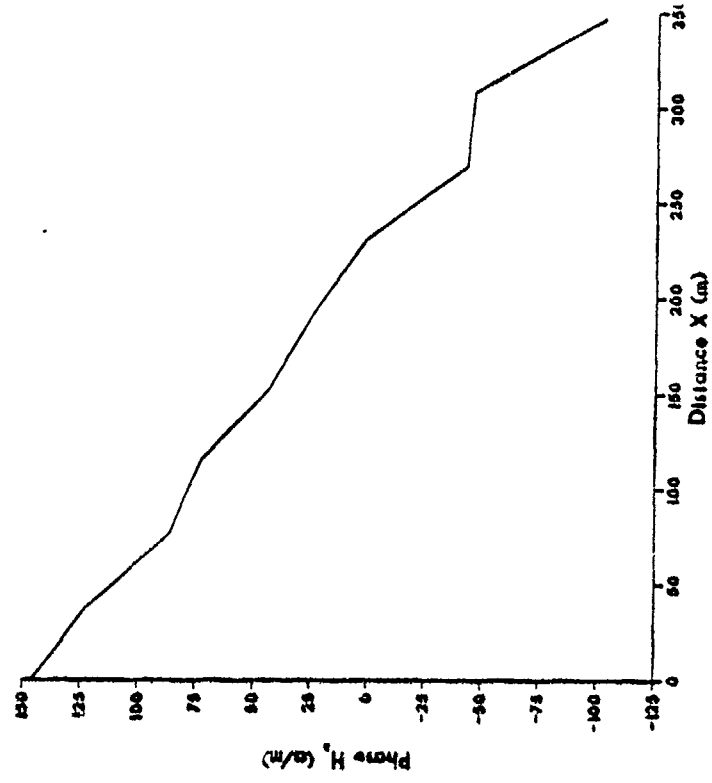
**MAGNITUDE 4.04 MHz**

**1/2 lambda spacing, switched parallel feed**



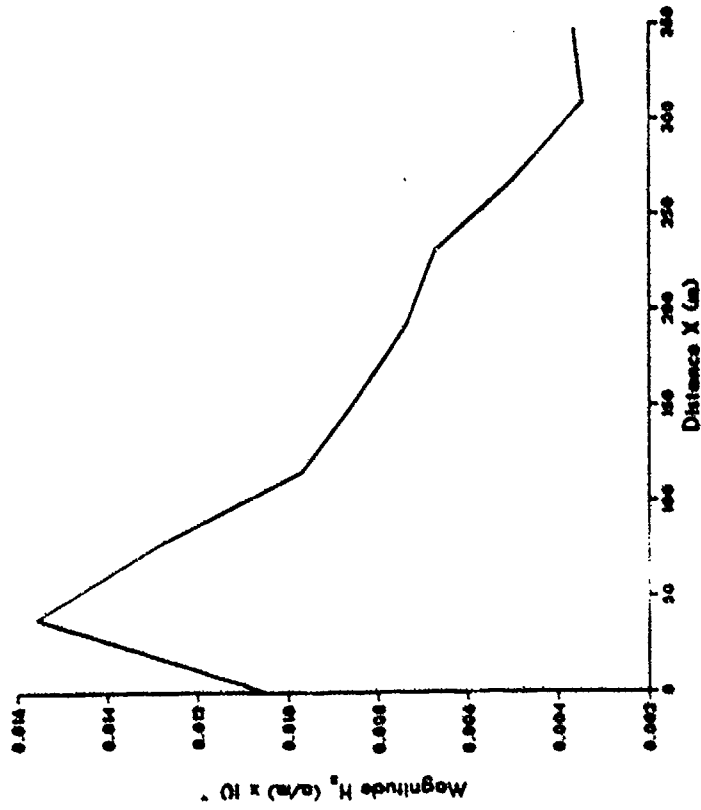
**PHASE 4.04 MHz**

**1/2 lambda spacing, switched parallel feed**



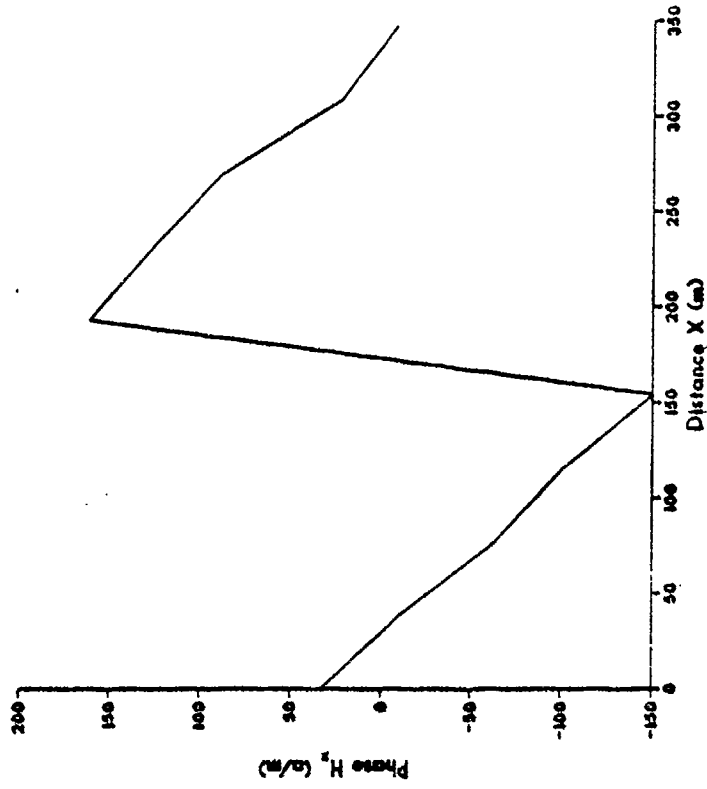
MAGNITUDE 4.38 MHz

1/2 lambda spacing, switched parallel feed

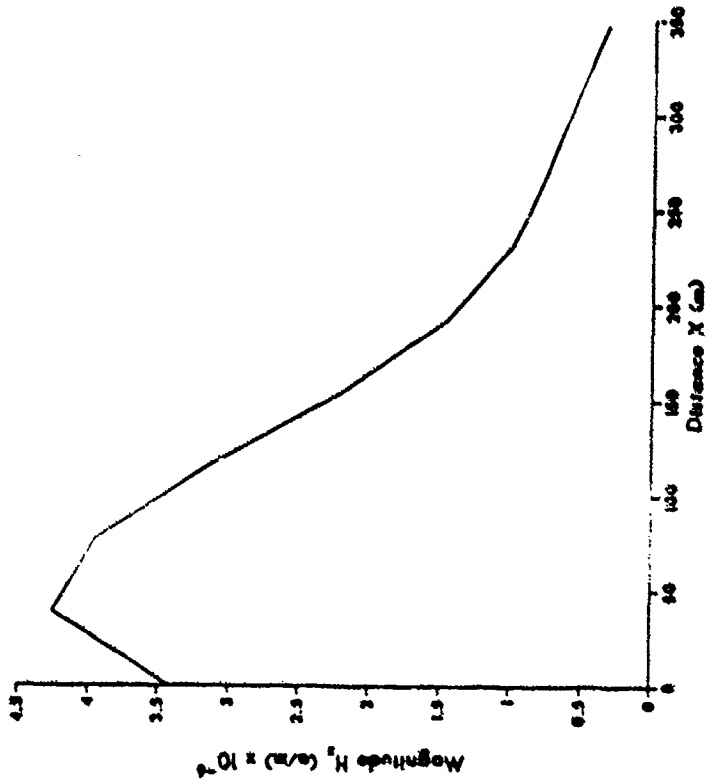


PHASE 4.38 MHz

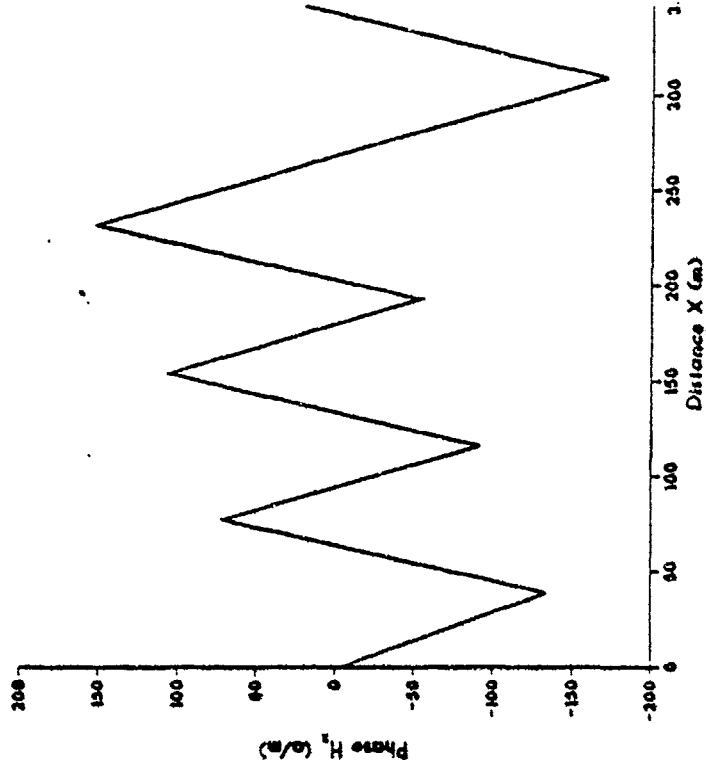
1/2 lambda spacing, switched parallel feed



**MAGNITUDE 4.88 MHz**  
 1/2 lambda spacing, switched parallel feed



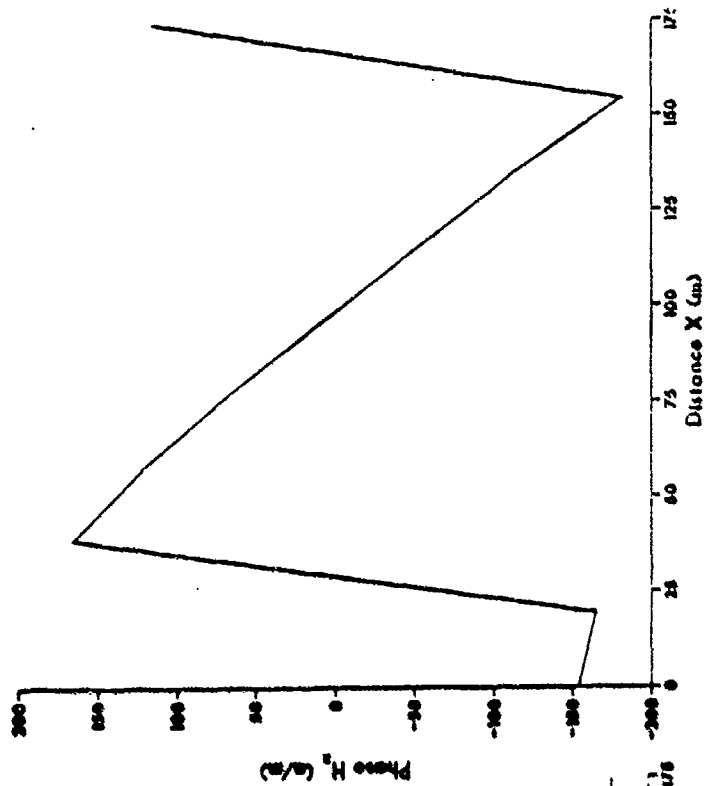
**PHASE 4.88 MHz**  
 1/2 lambda spacing, switched parallel feed



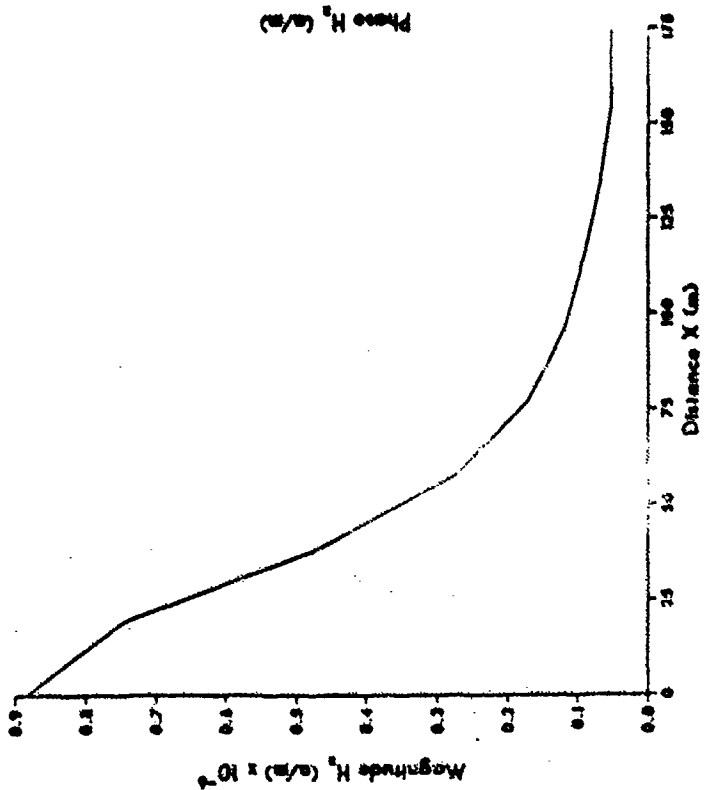
# APPENDIX D

## NEAR-MAGNETIC FIELD PLOTS FOR SNYDER UNSWITCHED PARALLEL ARRAY

PHASE 2.63 MHz  
1/4 lambda spacing, unswitched parallel feed

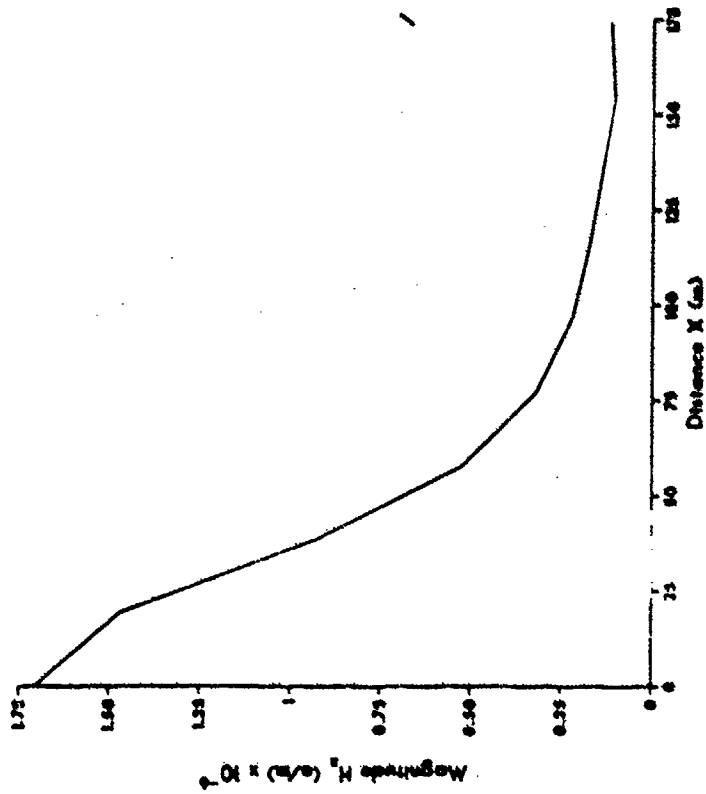


MAGNITUDE 2.63 MHz  
1/4 lambda spacing, unswitched parallel feed



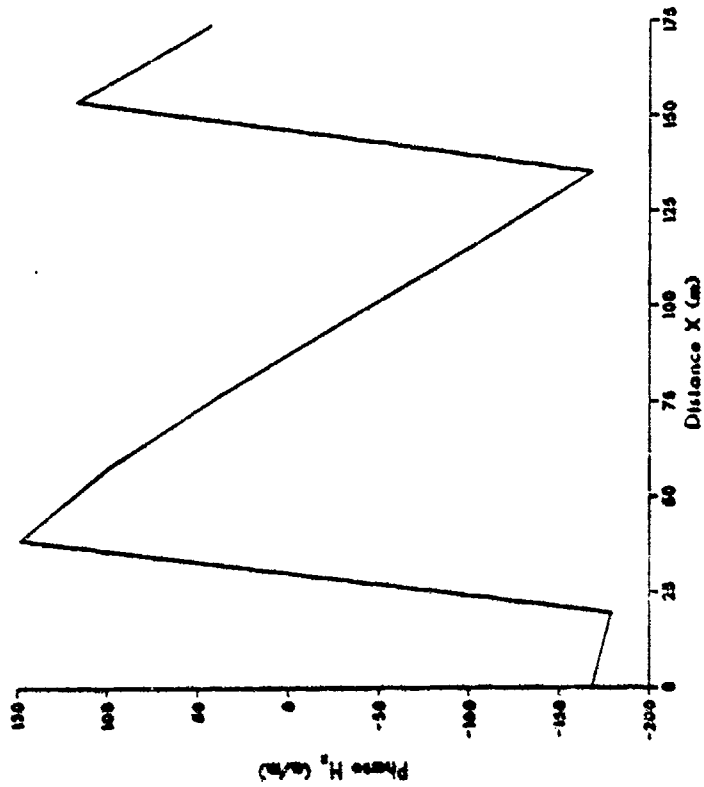
MAGNITUDE 2.88 MHz

1/4 lambda spacing, unswitched parallel feed



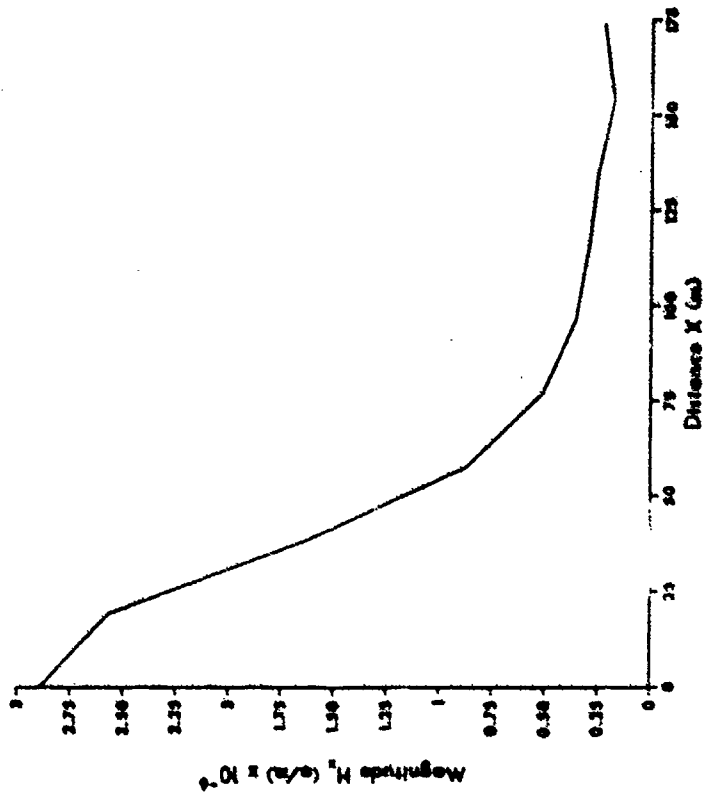
PHASE 2.88 MHz

1/4 lambda spacing, unswitched parallel feed



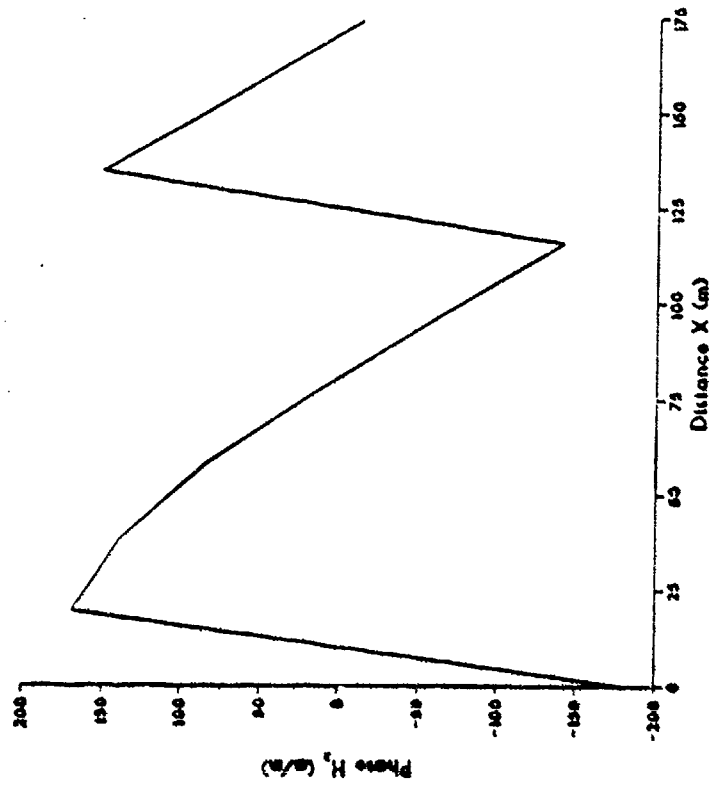
MAGNITUDE 3.04 MHz

1/4 lambda spacing, unswitched parallel feed



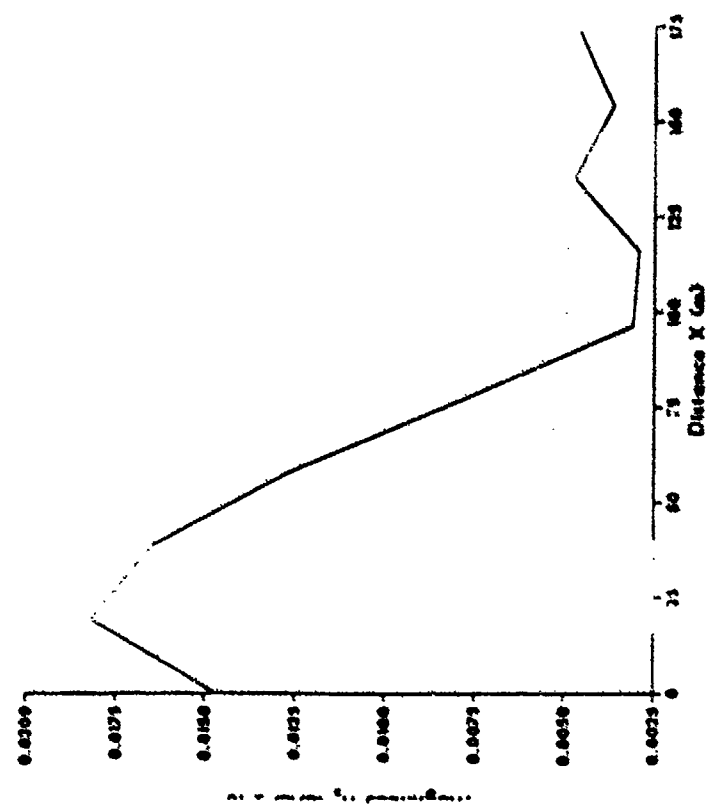
PHASE 3.04 MHz

1/4 lambda spacing, unswitched parallel feed



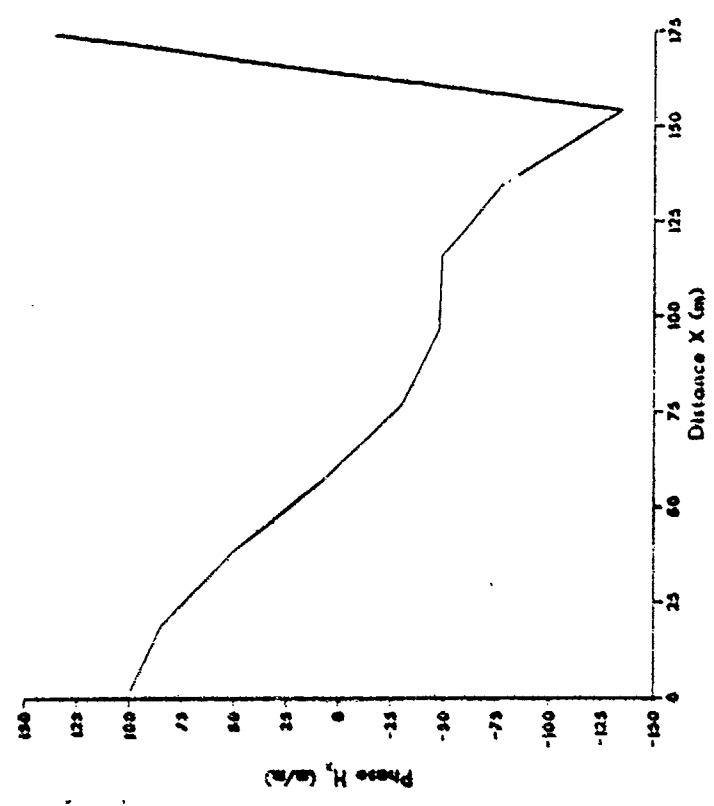
MAGNITUDE 3.38 MHz

1/4 lambda spacing, unswitched parallel feed



PHASE 3.38 MHz

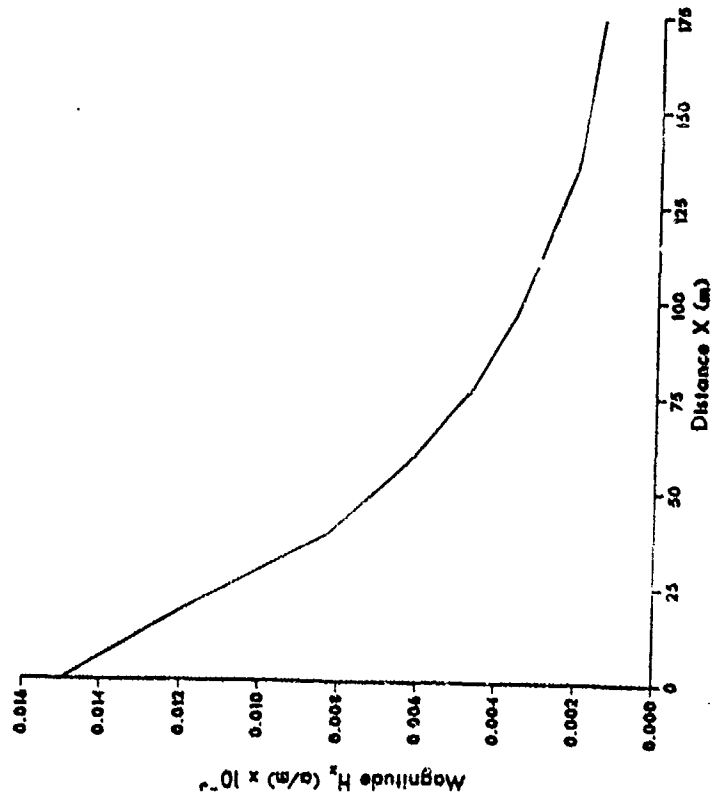
1/4 lambda spacing, unswitched parallel feed





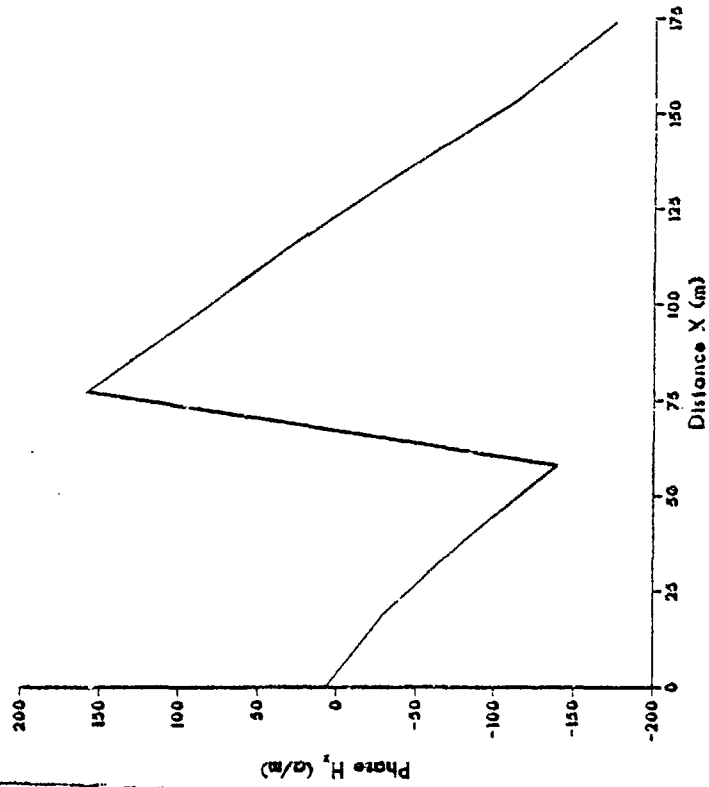
**MAGNITUDE 3.63 MHz**

1/4 lambda spacing, unswitched parallel feed



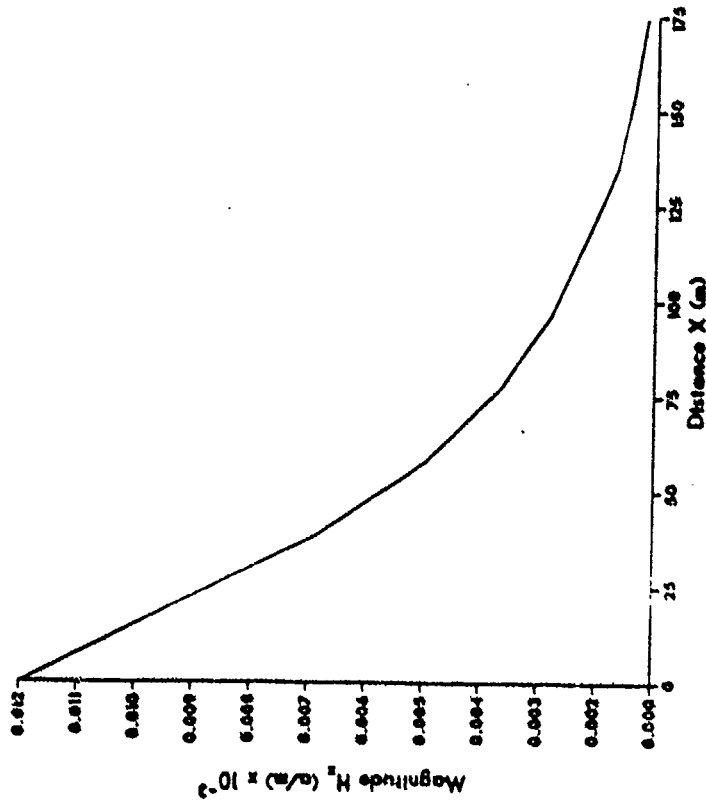
**PHASE 3.63 MHz**

1/4 lambda spacing, unswitched parallel feed



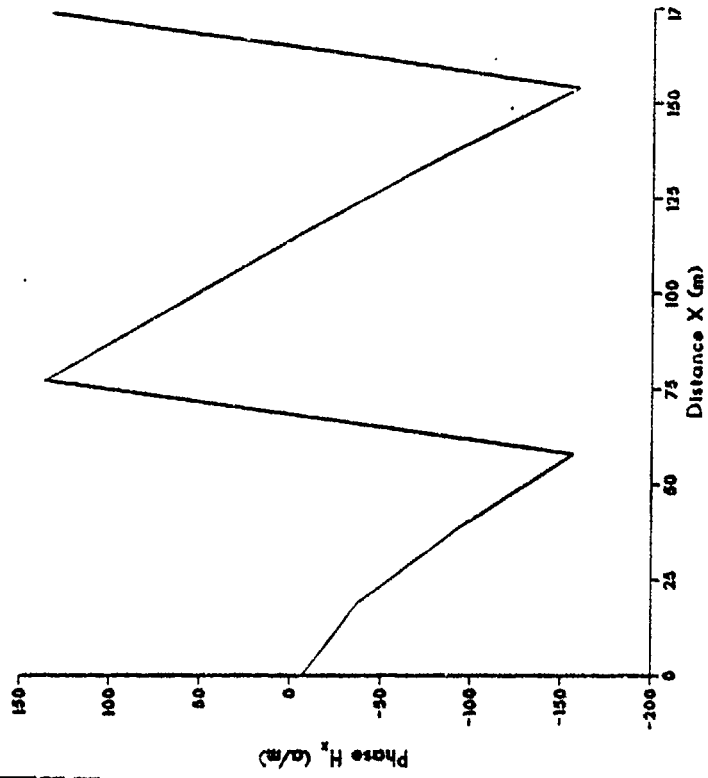
MAGNITUDE 3.72 MHz

1/4 lambda spacing, unswitched parallel feed



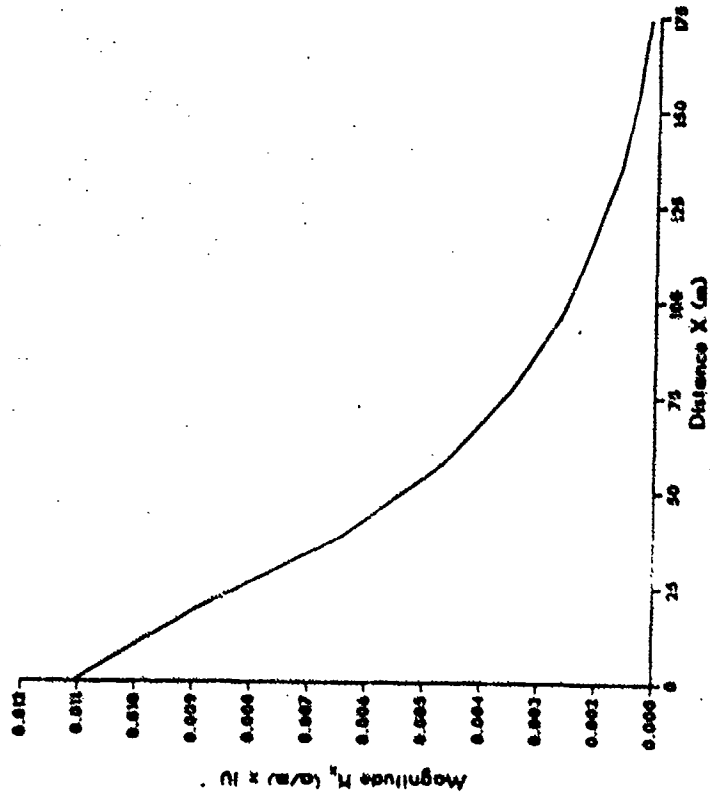
PHASE 3.72 MHz

1/4 lambda spacing, unswitched parallel feed



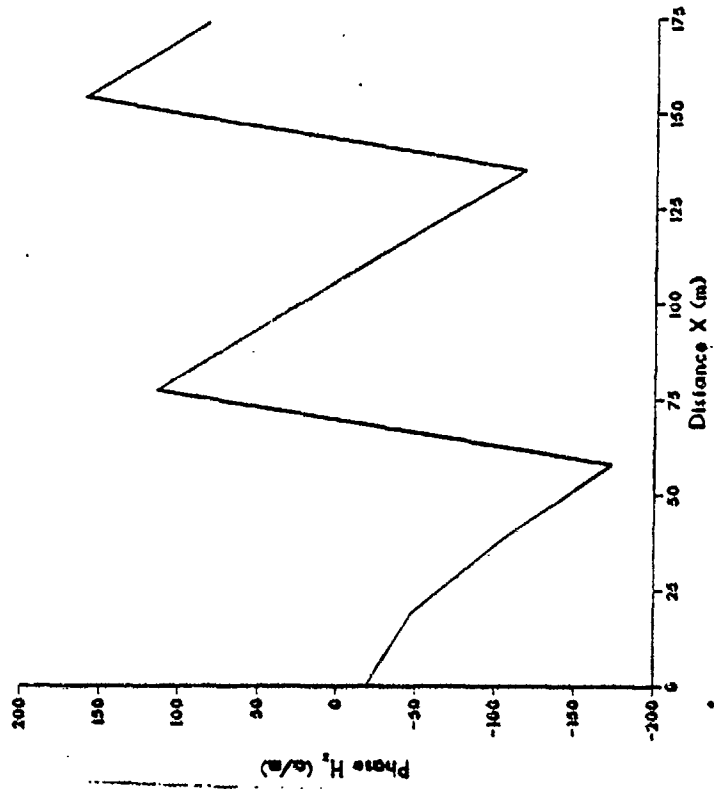
**MAGNITUDE 3.81 MHz**

1/4 lambda spacing, unswitched parallel feed



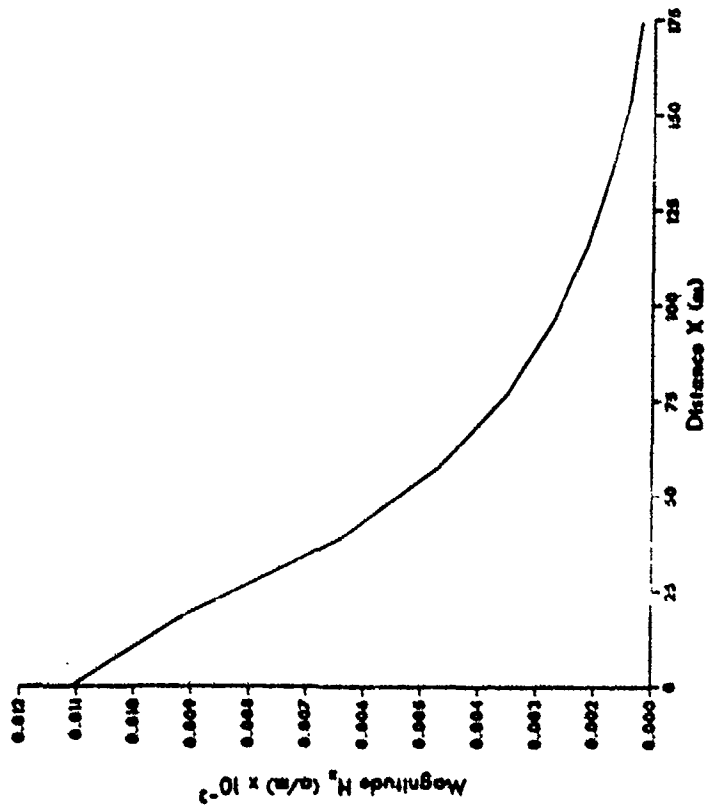
**PHASE 3.81 MHz**

1/4 lambda spacing, unswitched parallel feed



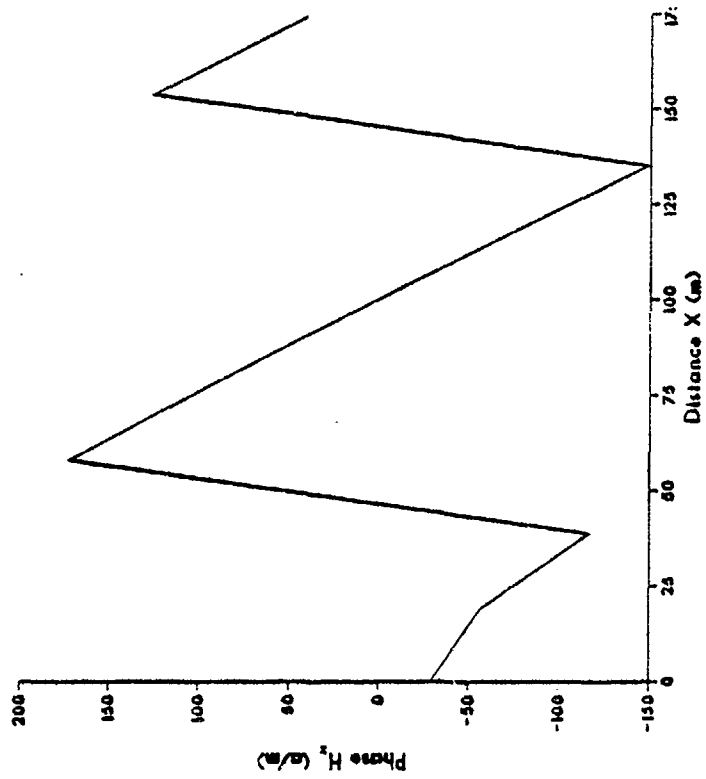
MAGNITUDE 3.88 MHz

1/4 lambda spacing, unswitched parallel feed



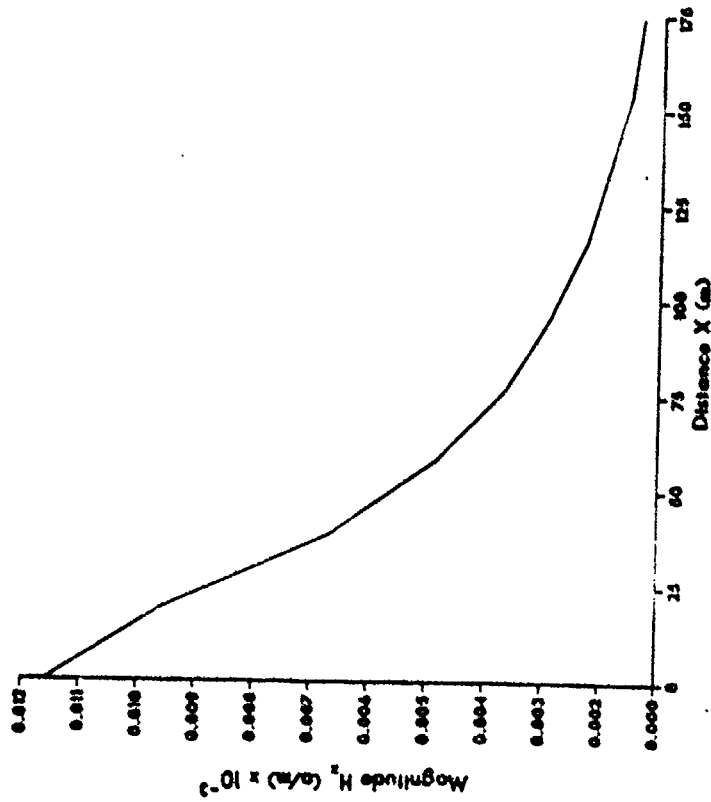
PHASE 3.88 MHz

1/4 lambda spacing, unswitched parallel feed



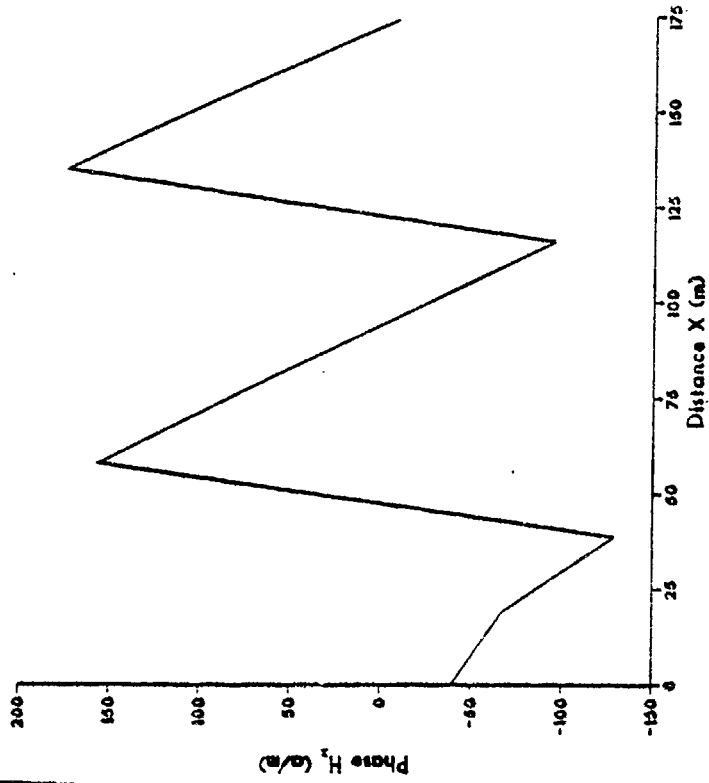
**MAGNITUDE 3.95 MHz**

**1/4 lambda spacing, unswitched parallel feed**



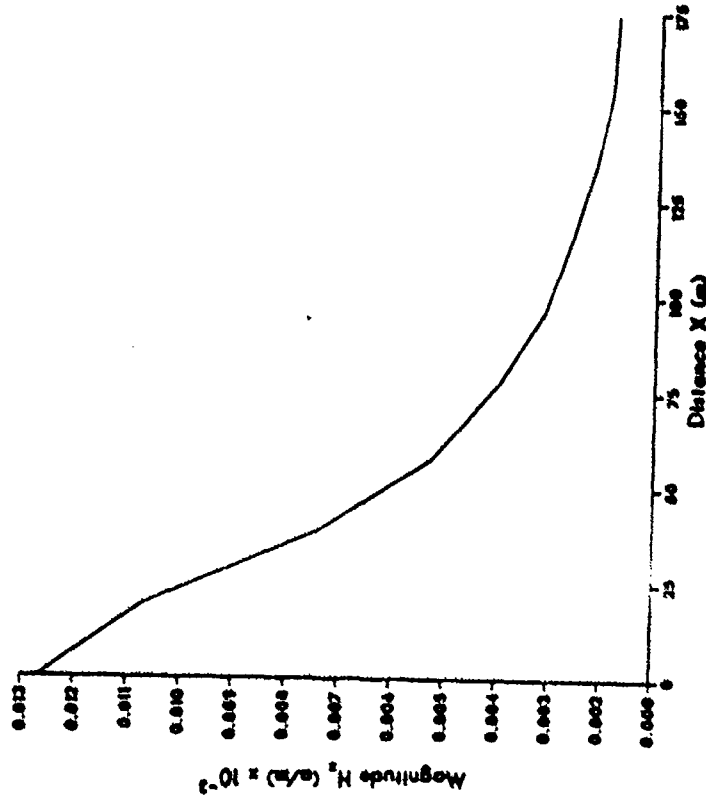
**PHASE 3.95 MHz**

**1/4 lambda spacing, unswitched parallel feed**



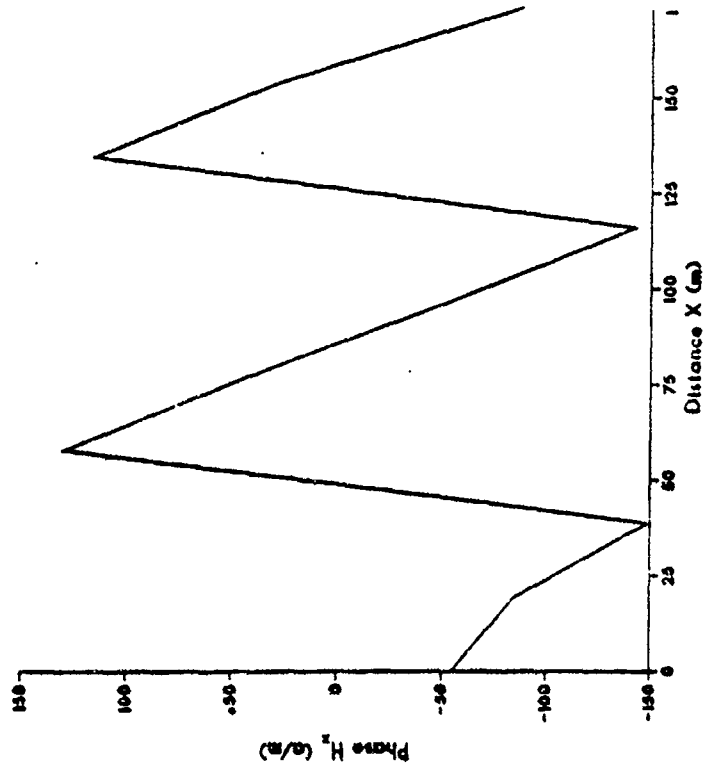
MAGNITUDE 4.04 MHz

1/4 lambda spacing, unswitched parallel feed



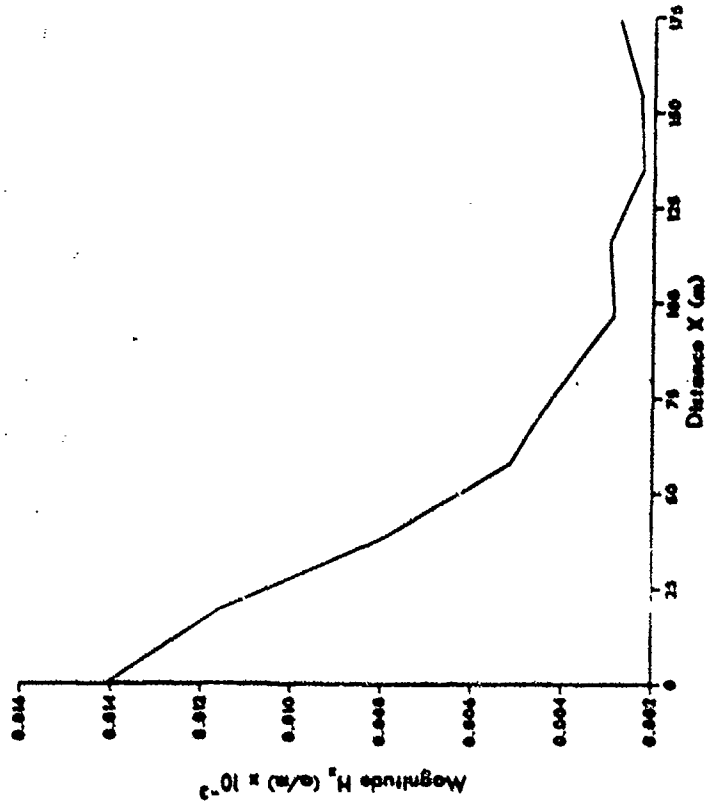
PHASE 4.04 MHz

1/4 lambda spacing, unswitched parallel feed



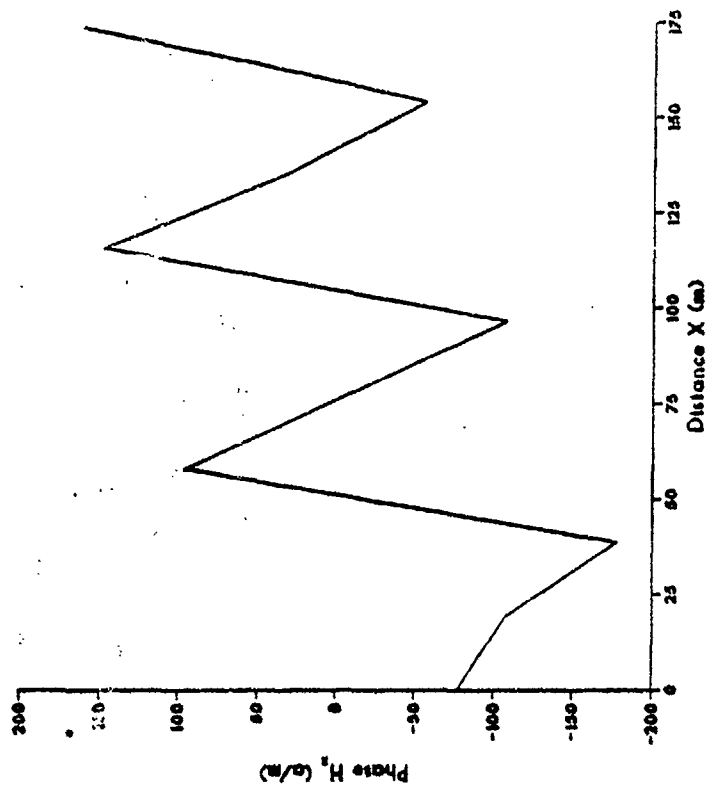
**MAGNITUDE 4.13 MHz**

*1/4 lambda spacing, unswitched parallel feed*



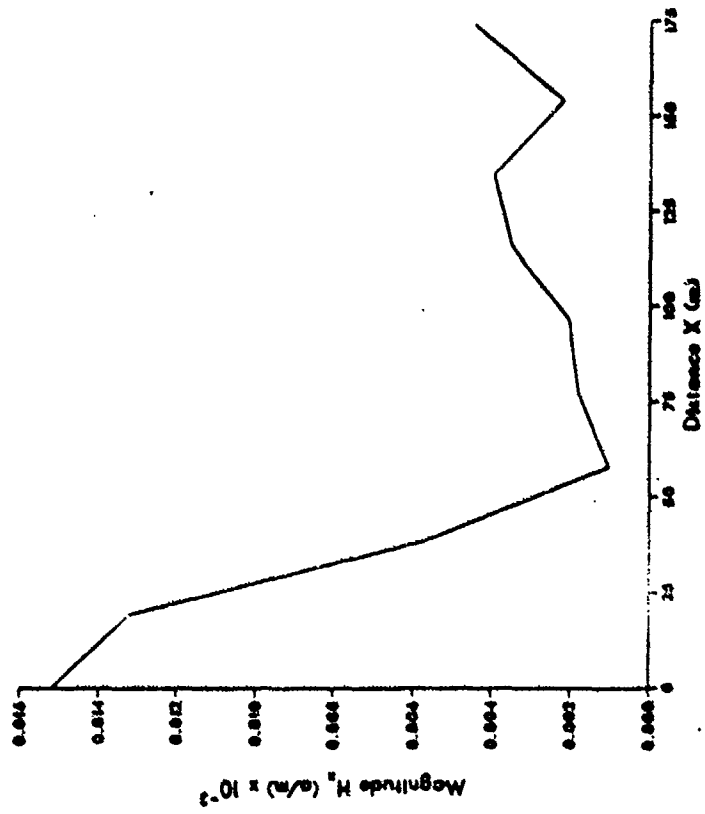
**PHASE 4.13 MHz**

*1/4 lambda spacing, unswitched parallel feed*



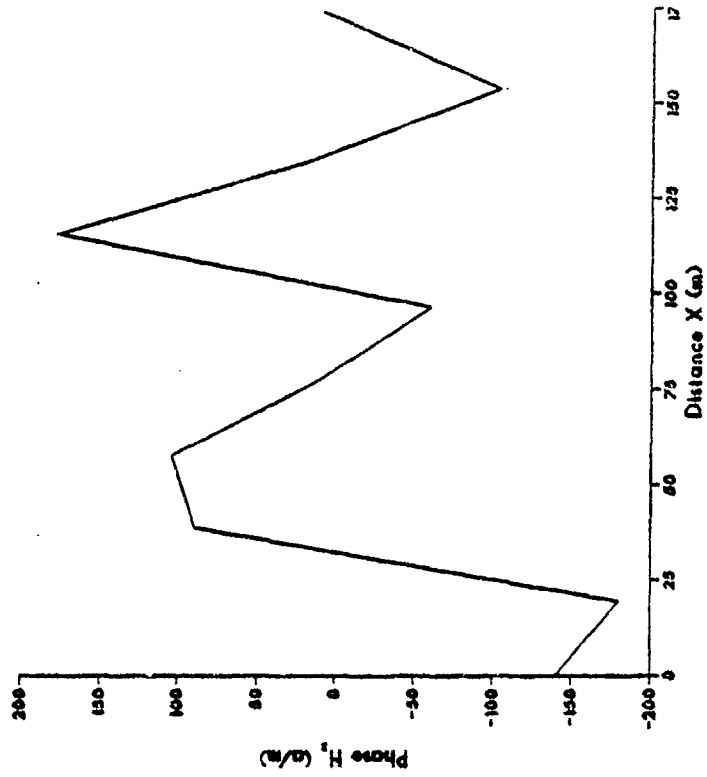
MAGNITUDE 4.38 MHz

1/4 lambda spacing, unswitched parallel feed



PHASE 4.38 MHz

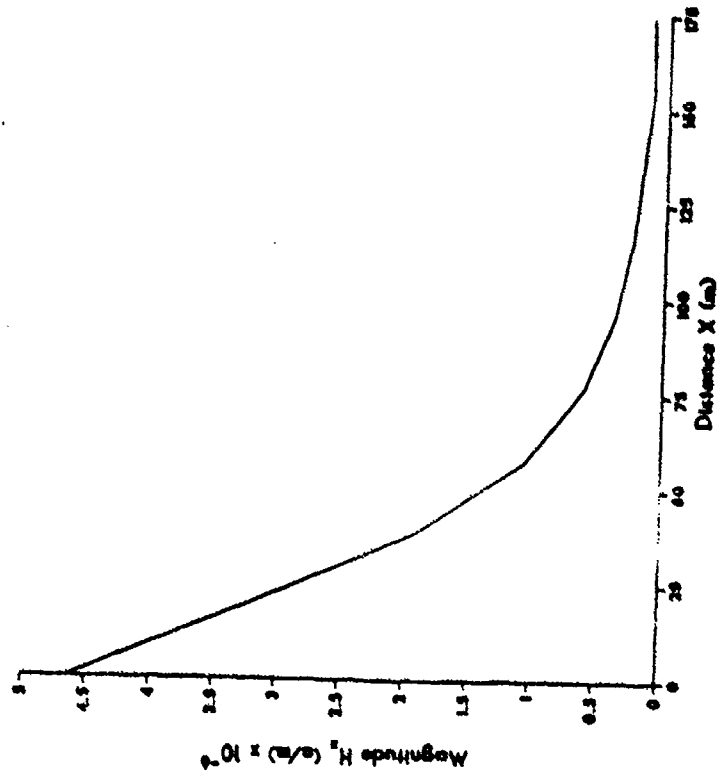
1/4 lambda spacing, unswitched parallel feed





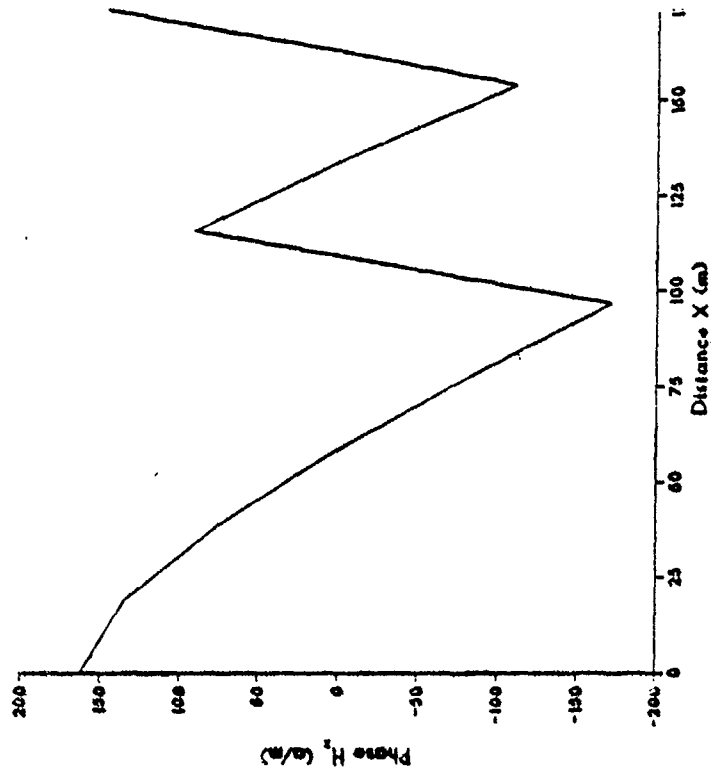
MAGNITUDE 4.63 MHz

1/4 lambda spacing, unswitched parallel feed



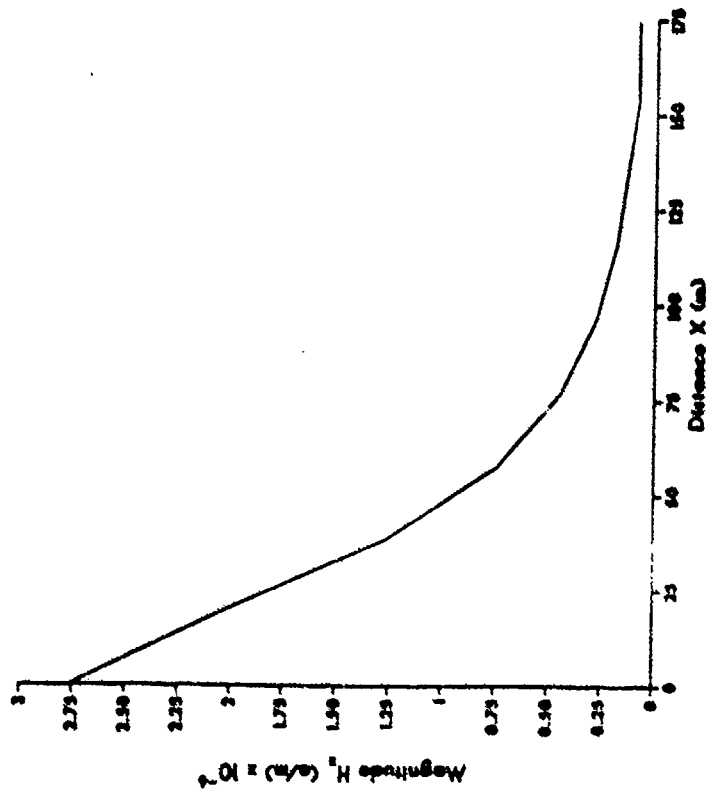
PHASE 4.63 MHz

1/4 lambda spacing, unswitched parallel feed



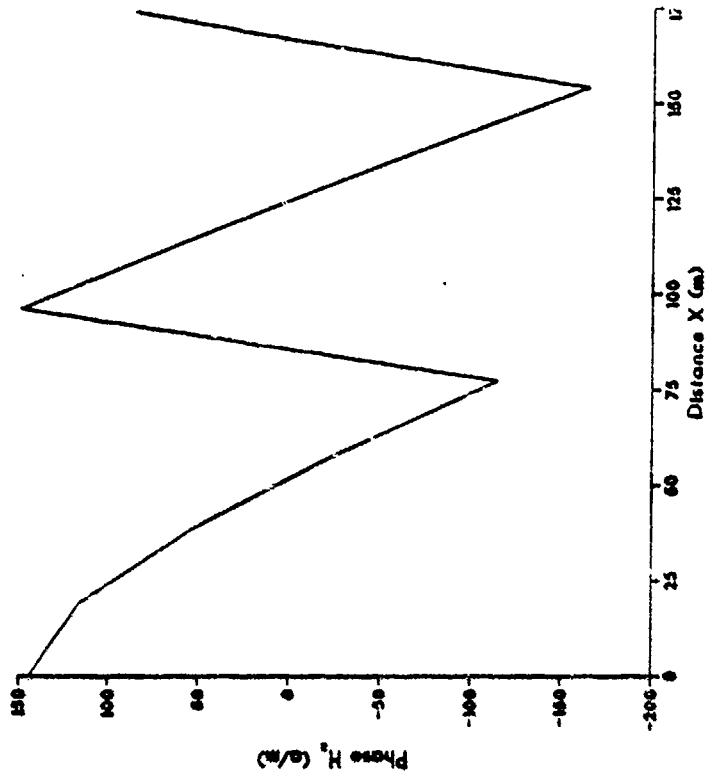
**MAGNITUDE 4.88 MHz**

1/4 lambda spacing, unswitched parallel feed



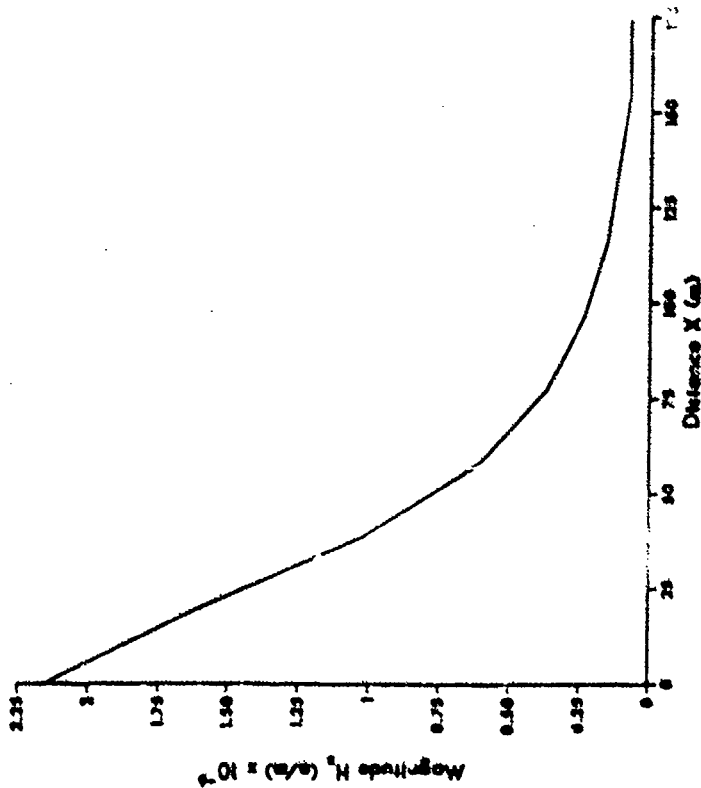
**PHASE 4.88 MHz**

1/4 lambda spacing, unswitched parallel feed



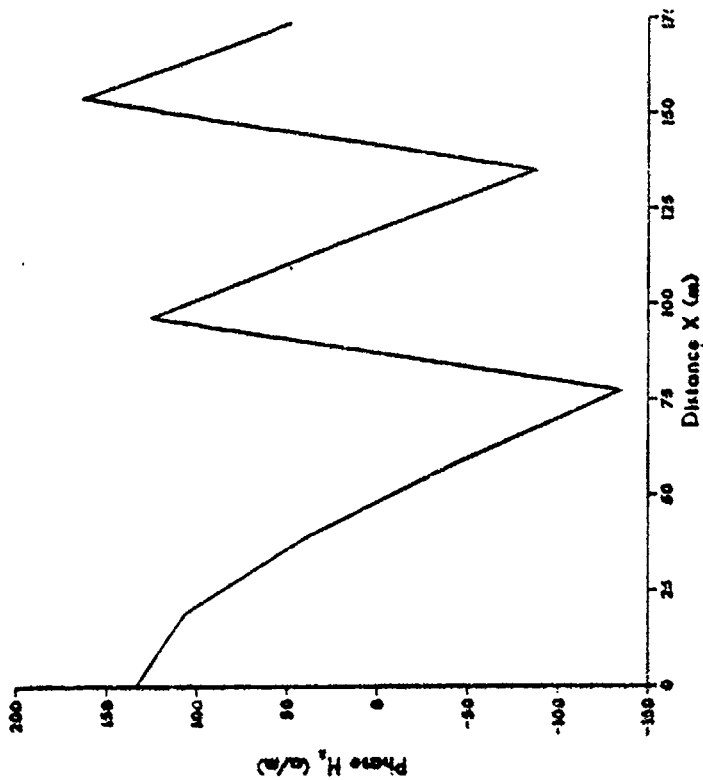
**MAGNITUDE 5.04 MHz**

1/4 lambda spacing, unswitched parallel feed



**PHASE 5.04 MHz**

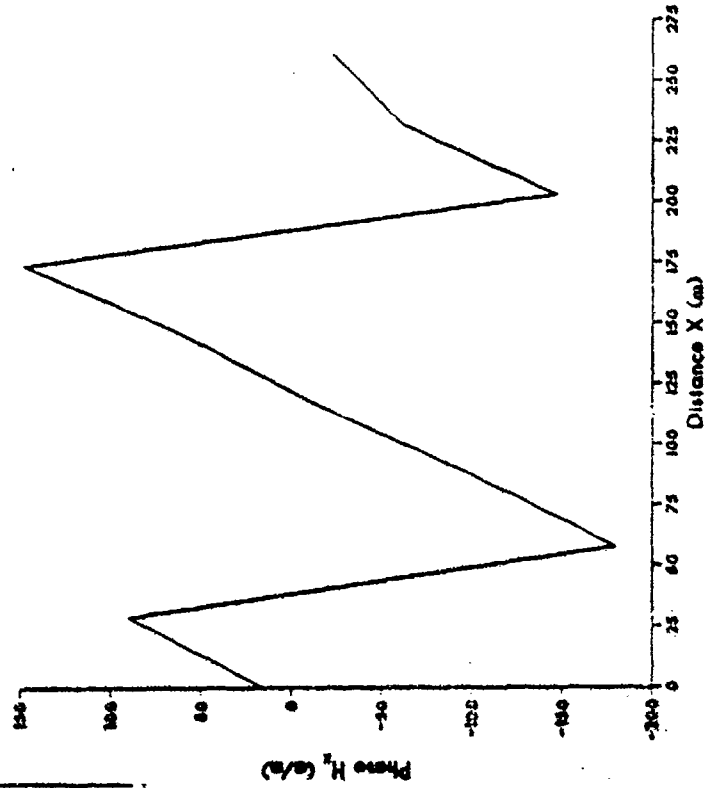
1/4 lambda spacing, unswitched parallel feed



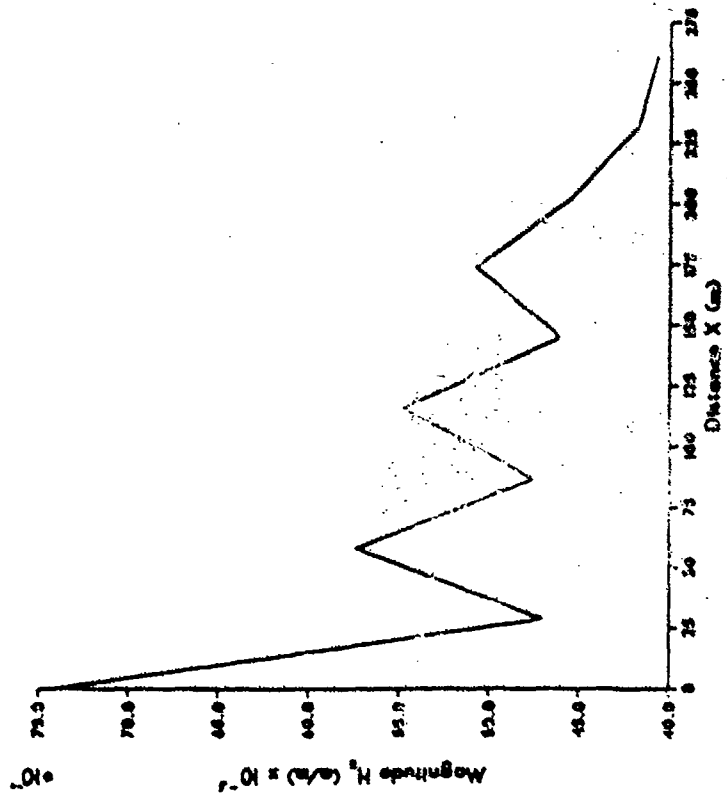
# APPENDIX E

## NEAR-MAGNETIC FIELD PLOTS FOR STANDARD ELEMENT ARRAYS

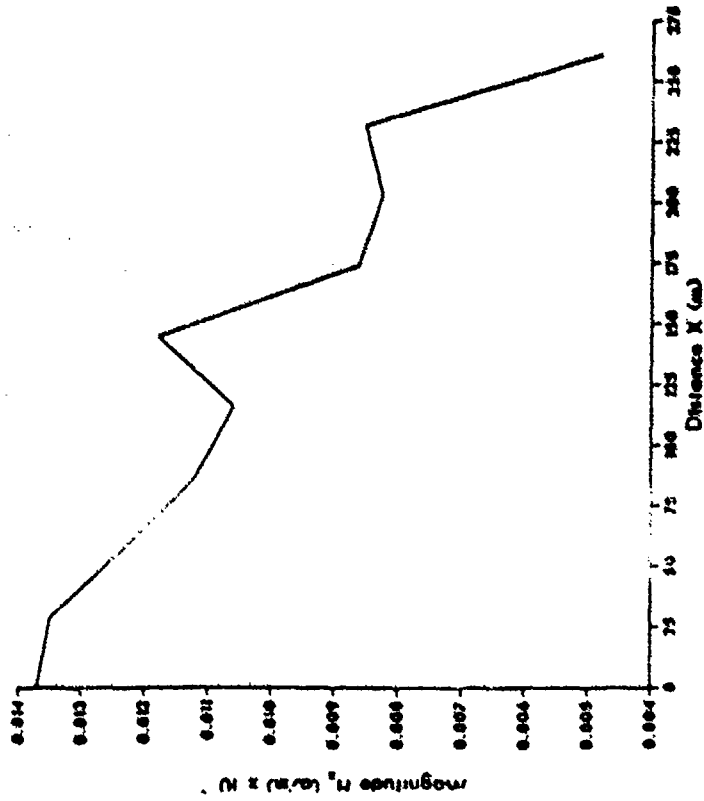
Standard Dipole Array - PHASE 2.38 MHz  
 3/8 lambda spacing, switched parallel feed



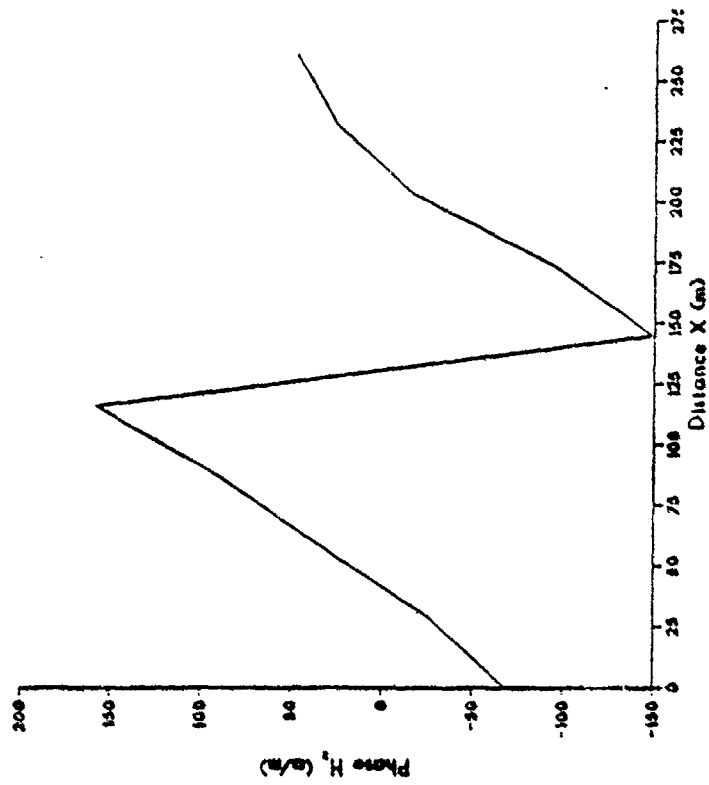
Standard Dipole Array - MAGNITUDE 2.38 MHz  
 3/8 lambda spacing, switched parallel feed



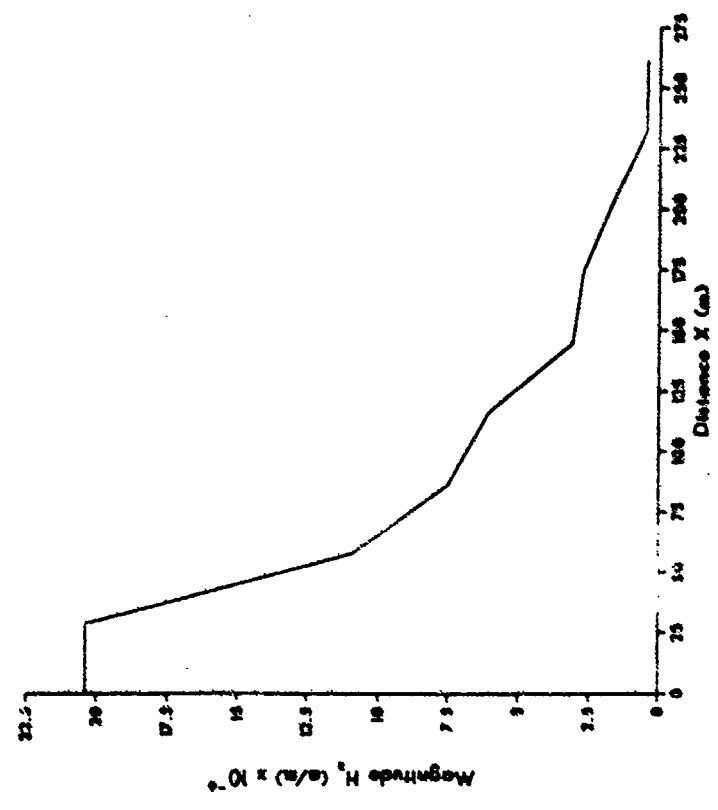
Standard Dipole Array - MAGNITUDE 2.88 MHz  
 3/8 lambda spacing, switched parallel feed



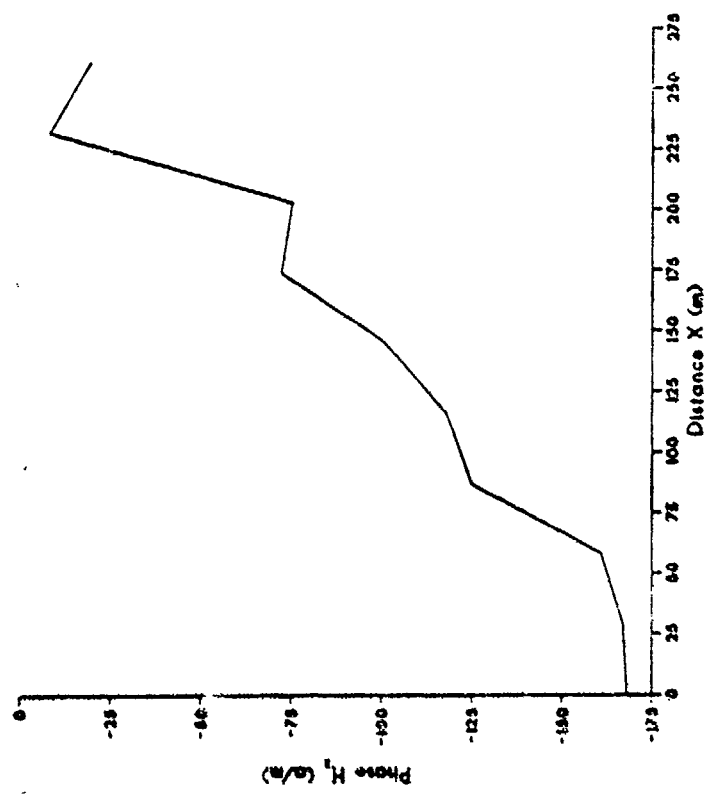
Standard Dipole Array - PHASE 2.88 MHz  
 3/8 lambda spacing, switched parallel feed



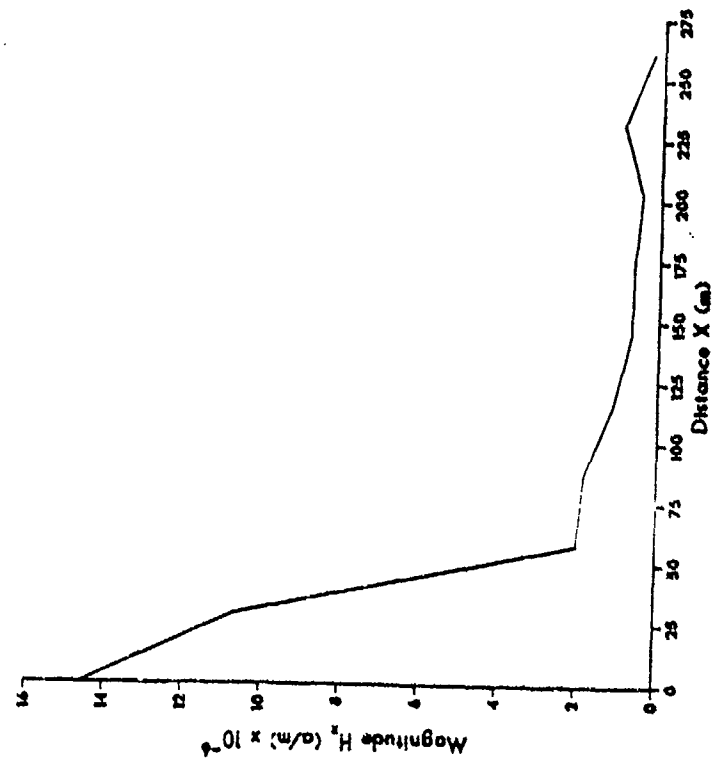
Standard Dipole Array - MAGNITUDE 3.36 MHz  
 3/8 lambda spacing, switched parallel feed



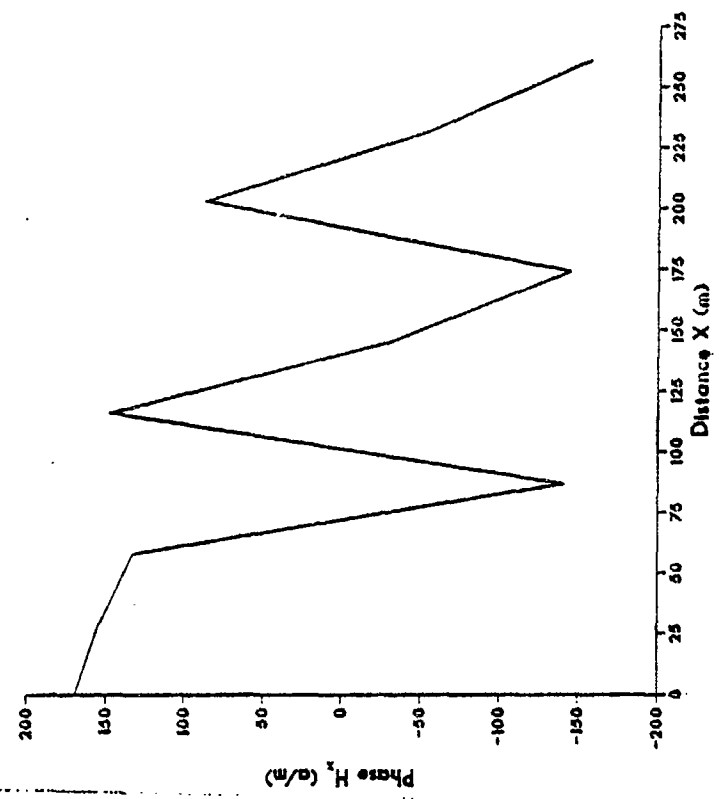
Standard Dipole Array - PHASE 3.36 MHz  
 3/8 lambda spacing, switched parallel feed



Standard Dipole Array - MAGNITUDE 3.63 MHz  
 3/8 lambda spacing, switched parallel feed

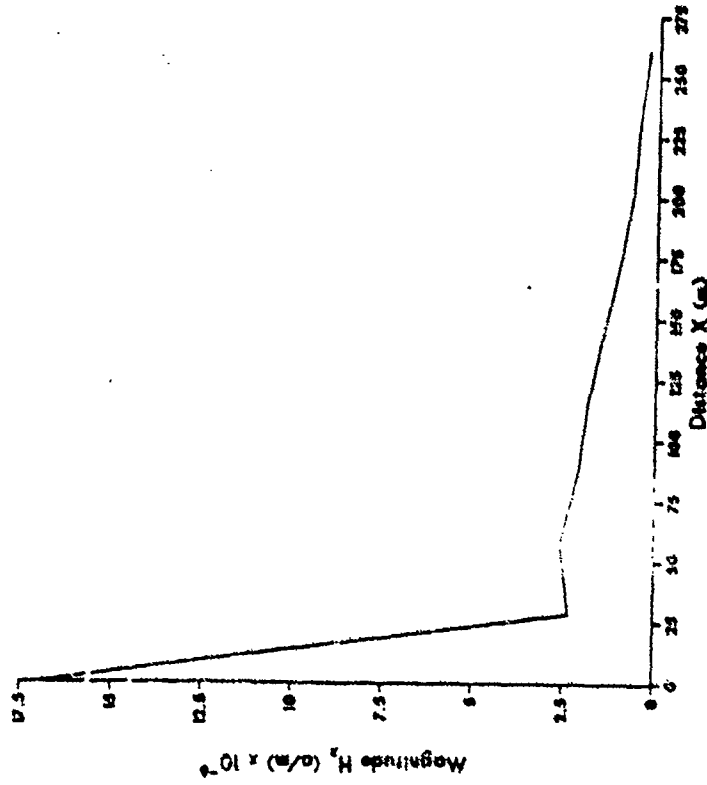


Standard Dipole Array - PHASE 3.63 MHz  
 3/8 lambda spacing, switched parallel feed



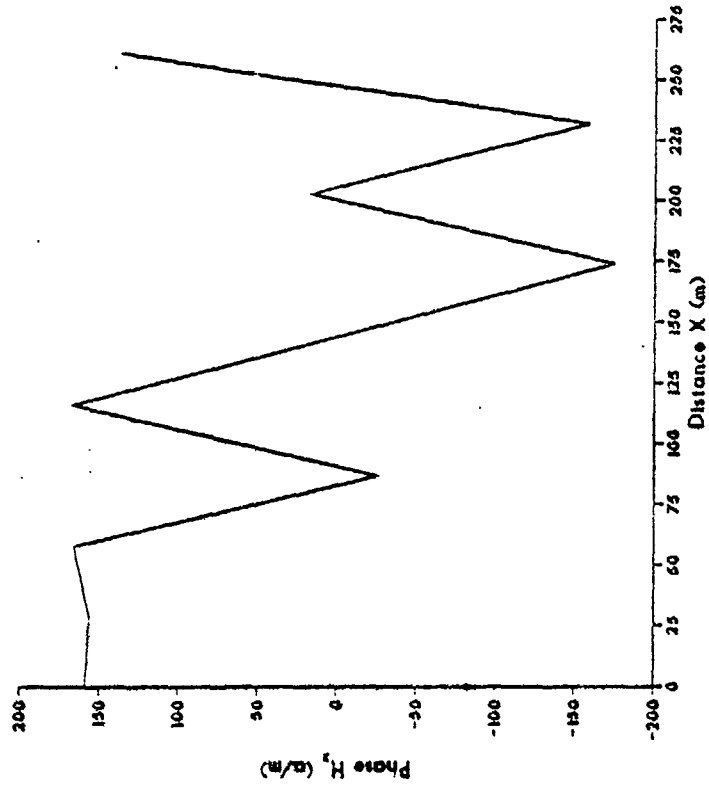
Standard Dipole Array - MAGNITUDE 3.88 MHz

3/8 lambda spacing, switched parallel feed



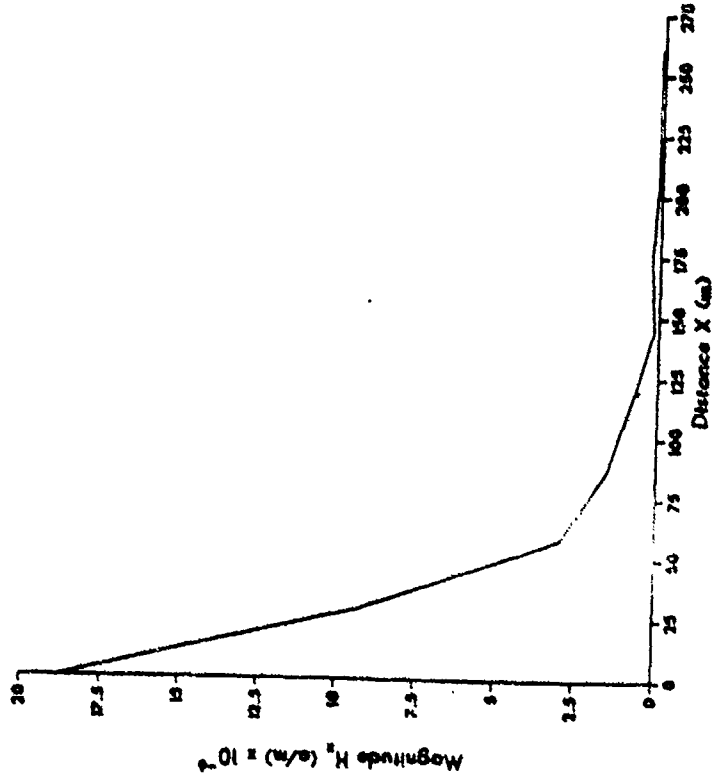
Standard Dipole Array - PHASE 3.88 MHz

3/8 lambda spacing, switched parallel feed

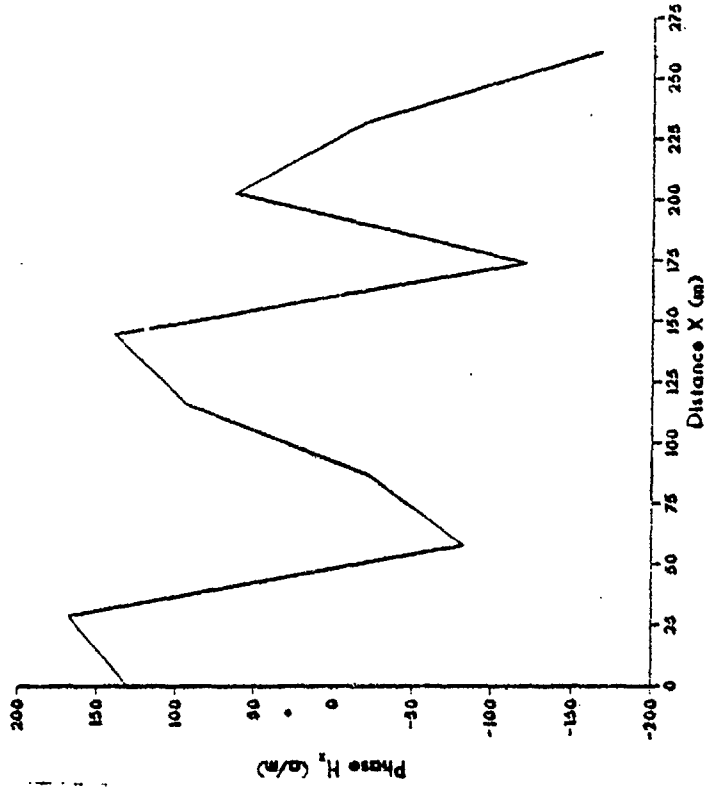




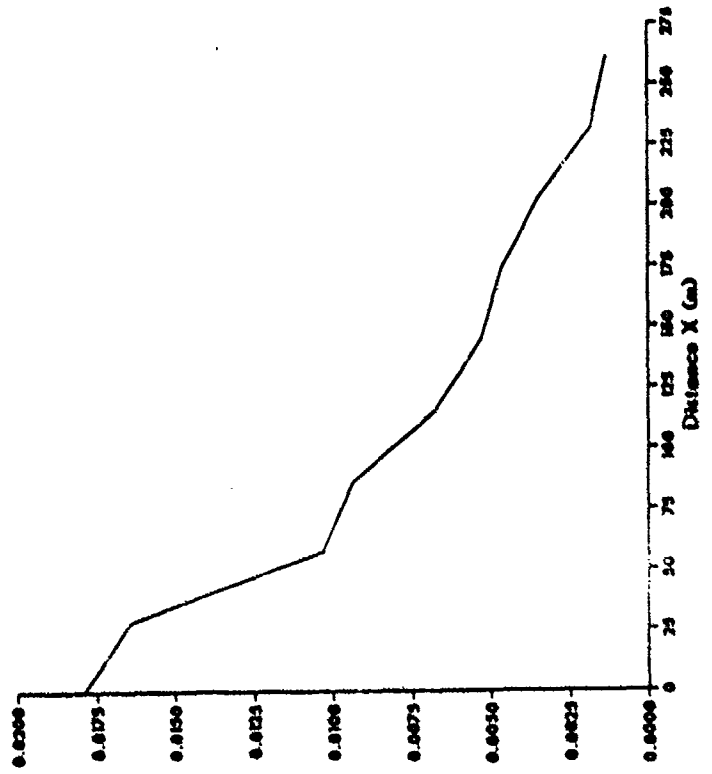
Standard Dipole Array - MAGNITUDE 4.04 MHz  
 3/8 lambda spacing, switched parallel feed



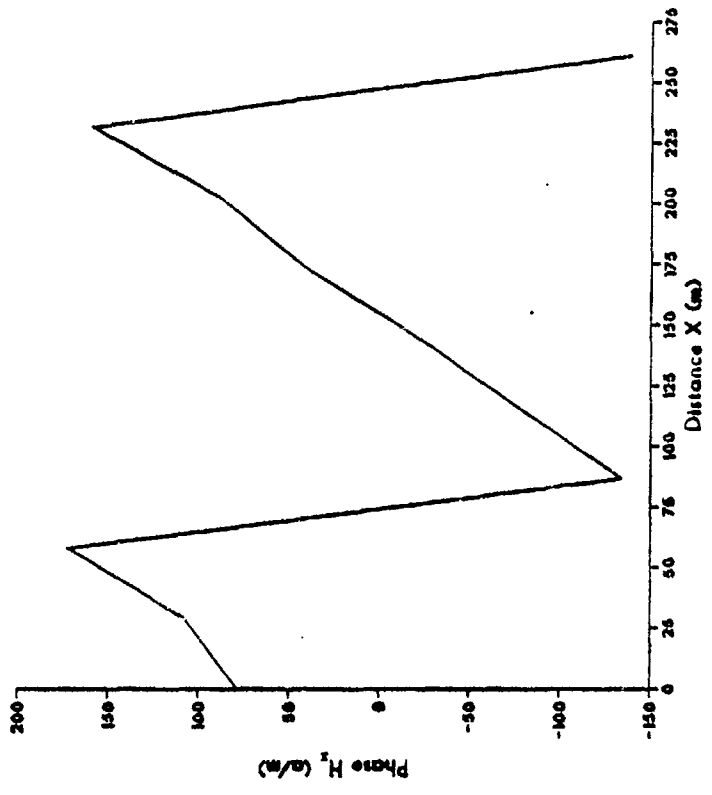
Standard Dipole Array - PHASE 4.04 MHz  
 3/8 lambda spacing, switched parallel feed



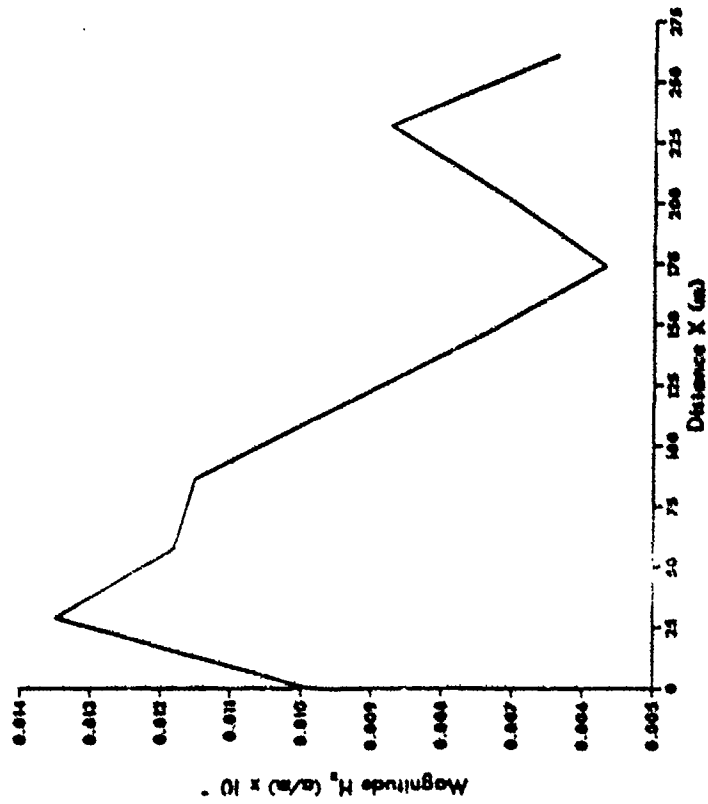
Standard Dipole Array - MAGNITUDE 4.38 MHz  
 3/8 lambda spacing, switched parallel feed



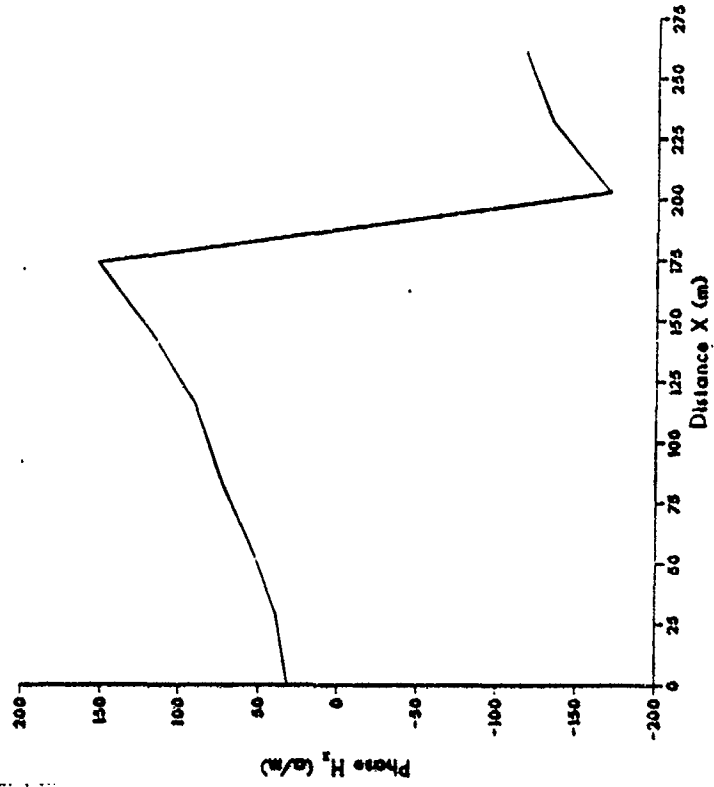
Standard Dipole Array - PHASE 4.38 MHz  
 3/8 lambda spacing, switched parallel feed



Standard Dipole Array - MAGNITUDE 4.88 MHz  
 3/8 lambda spacing, switched parallel feed

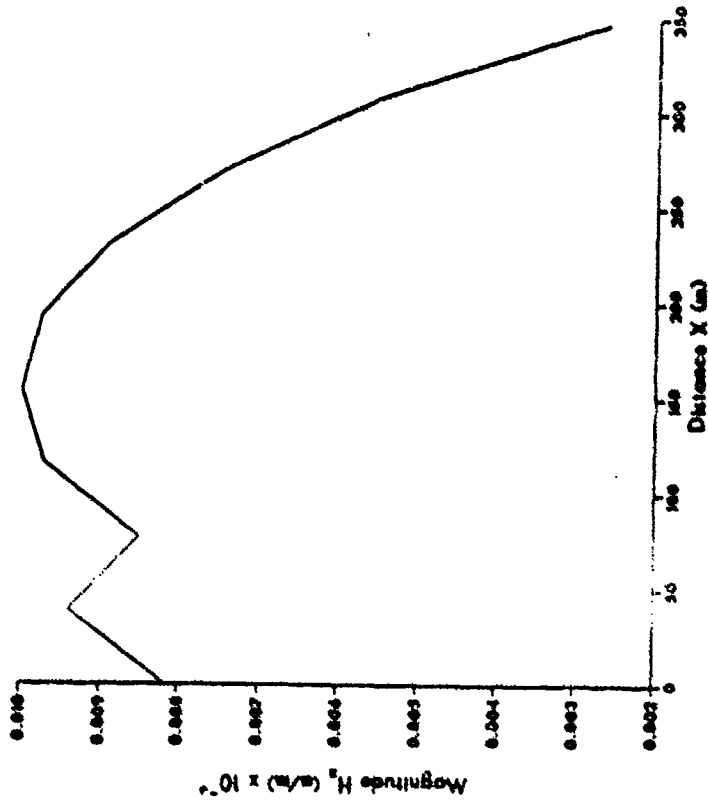


Standard Dipole Array - PHASE 4.88 MHz  
 3/8 lambda spacing, switched parallel feed



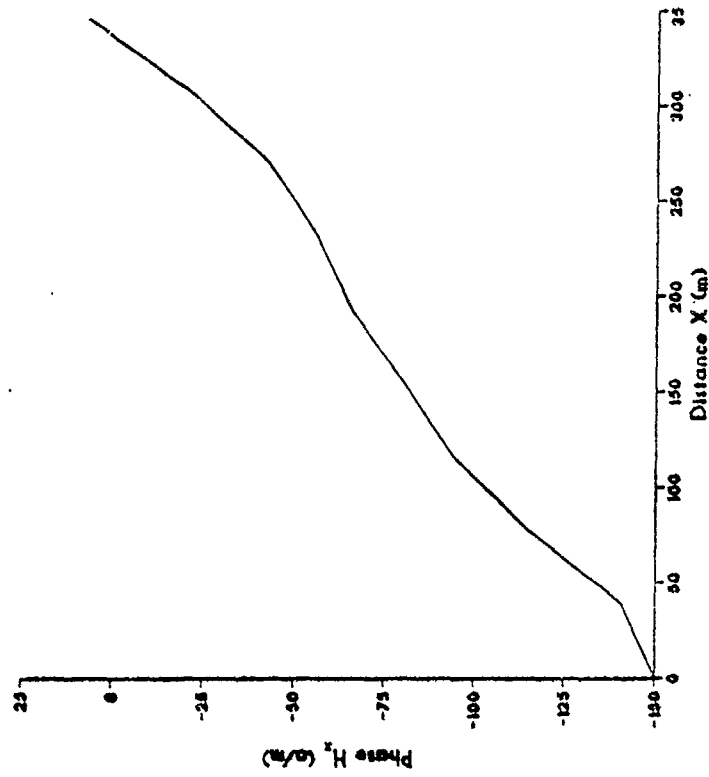
MAGNITUDE 2.88 MHz

1/2 lambda spacing, switched parallel feed



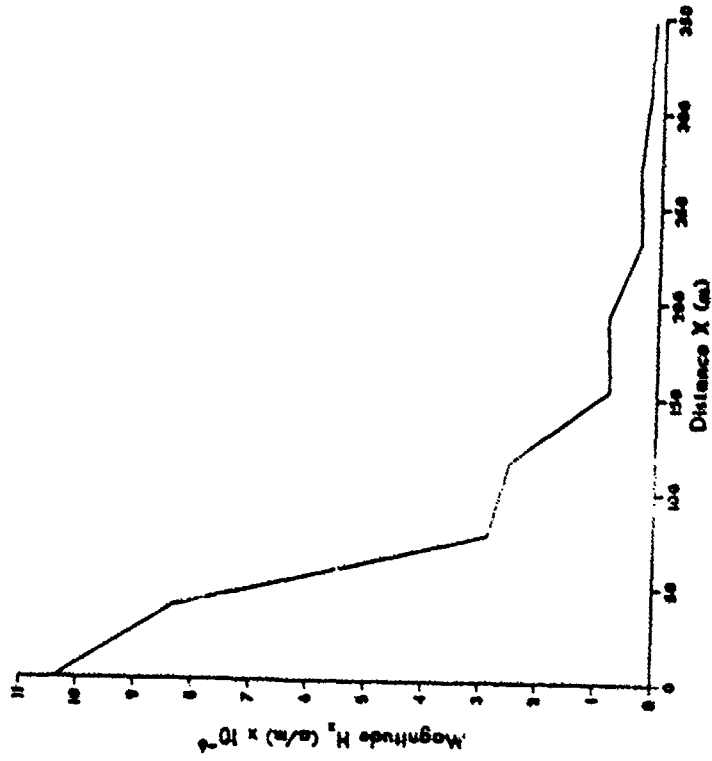
PHASE 2.88 MHz

1/2 lambda spacing, switched parallel feed



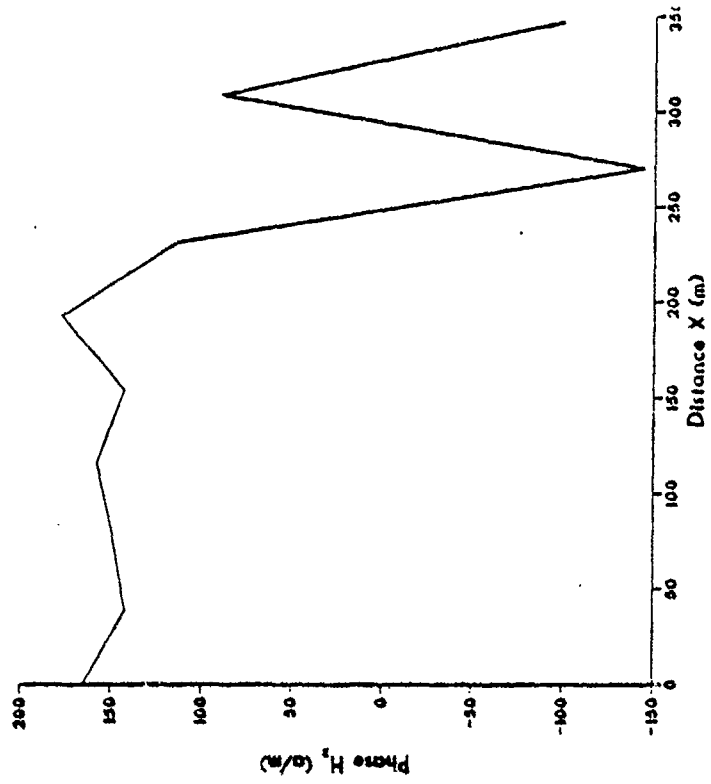
MAGNITUDE 3.38 MHz

1/2 lambda spacing, switched parallel feed

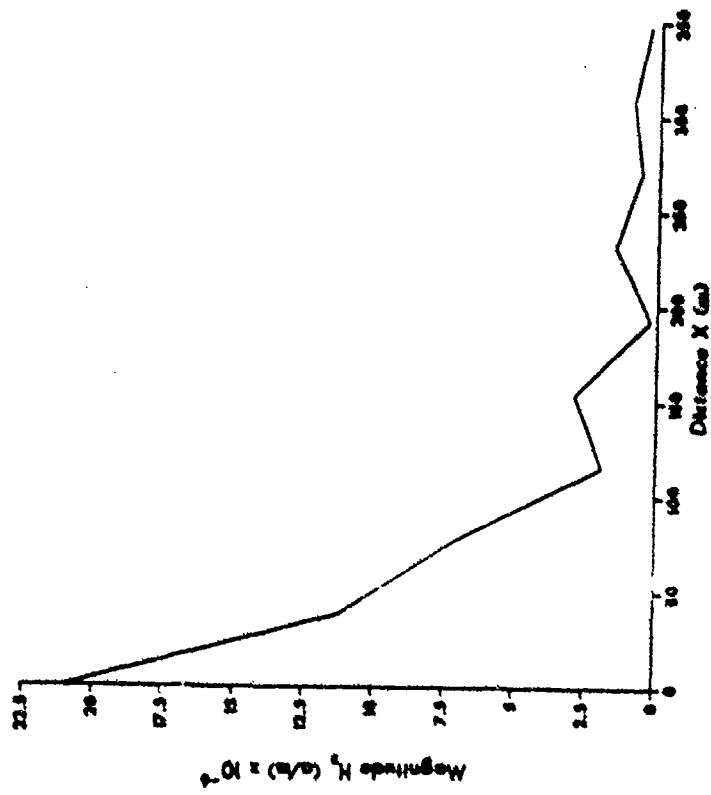


PHASE 3.38 MHz

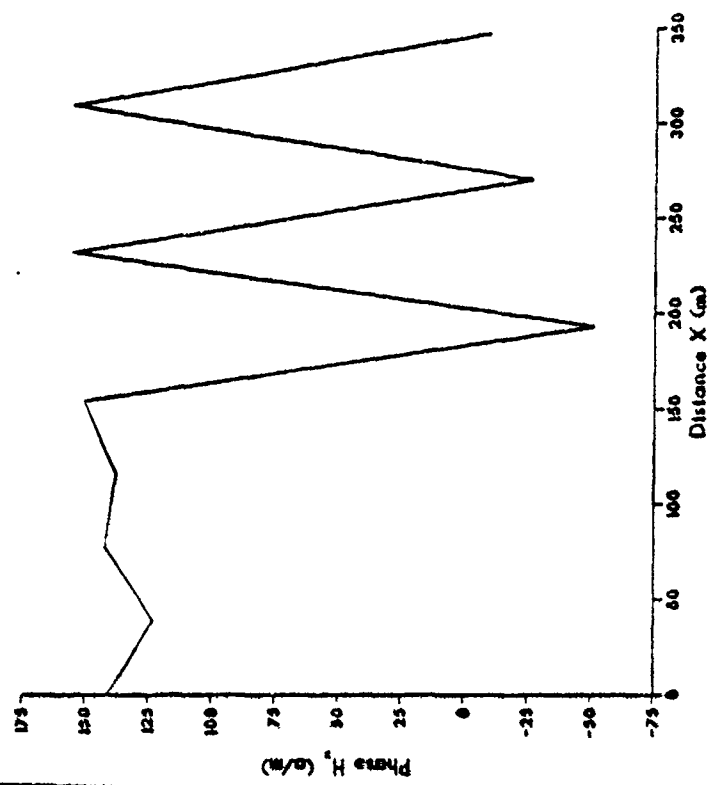
1/2 lambda spacing, switched parallel feed



MAGNITUDE 3.63 MHz  
 1/2 lambda spacing, switched parallel feed

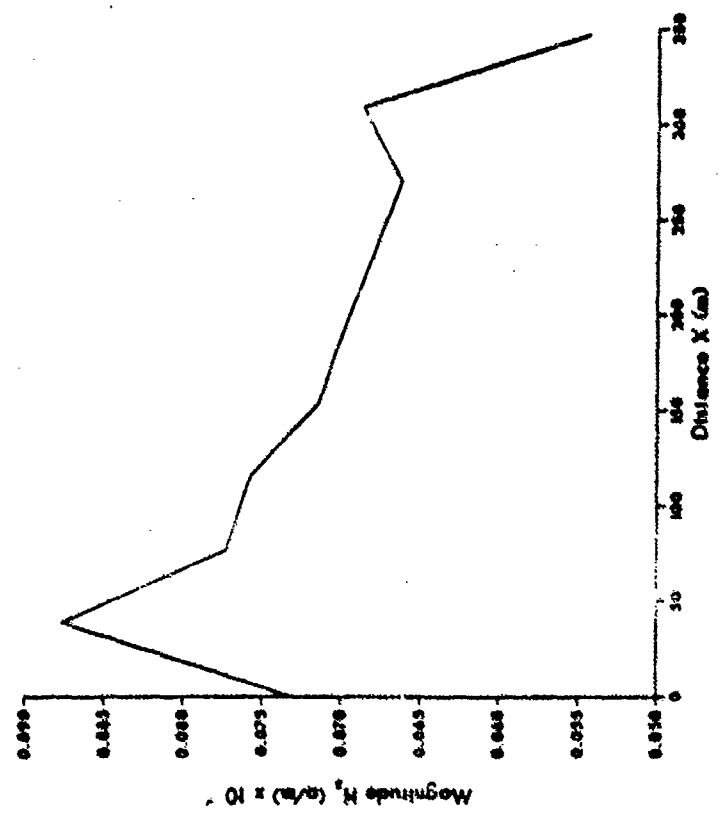


PHASE 3.63 MHz  
 1/2 lambda spacing, switched parallel feed



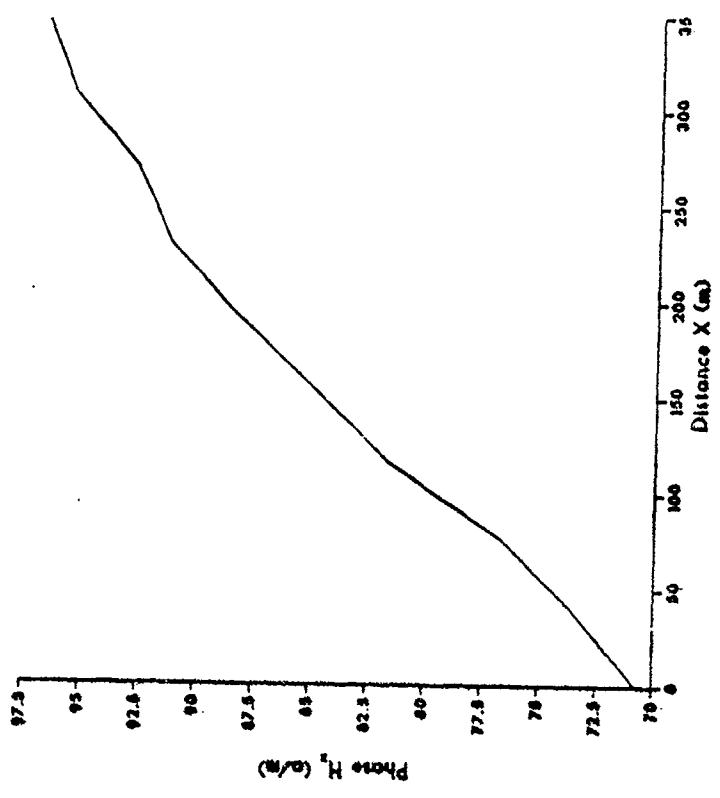
MAGNITUDE 3.86 MHz

1/2 lambda spacing, switched parallel feed



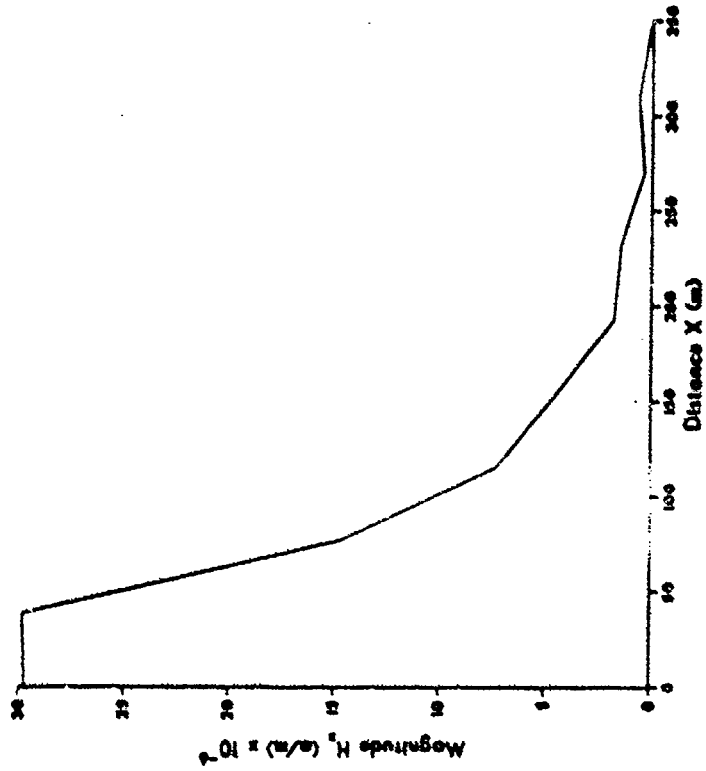
PHASE 3.86 MHz

1/2 lambda spacing, switched parallel feed



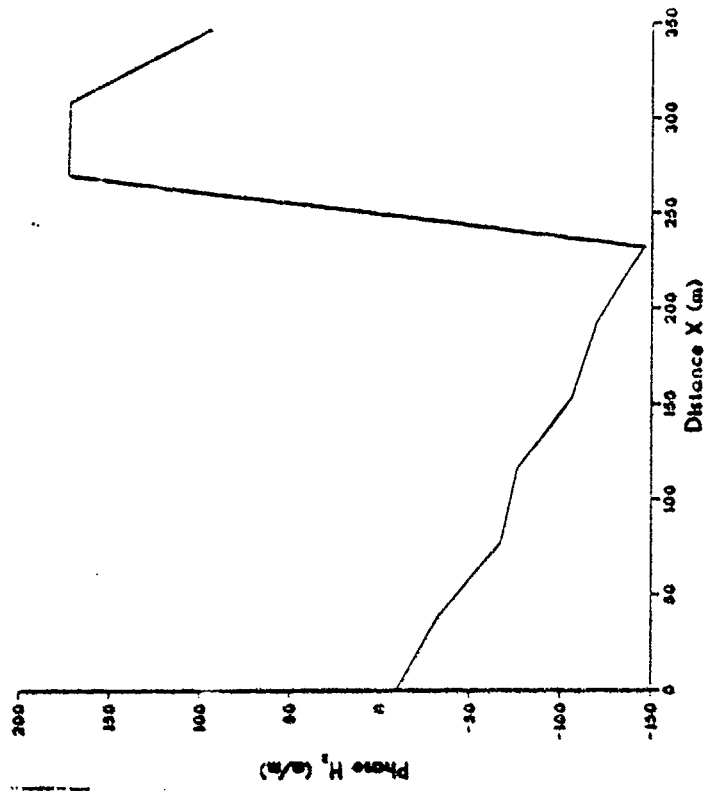
MAGNITUDE 4.04 MHz

1/2 lambda spacing, switched parallel feed



PHASE 4.04 MHz

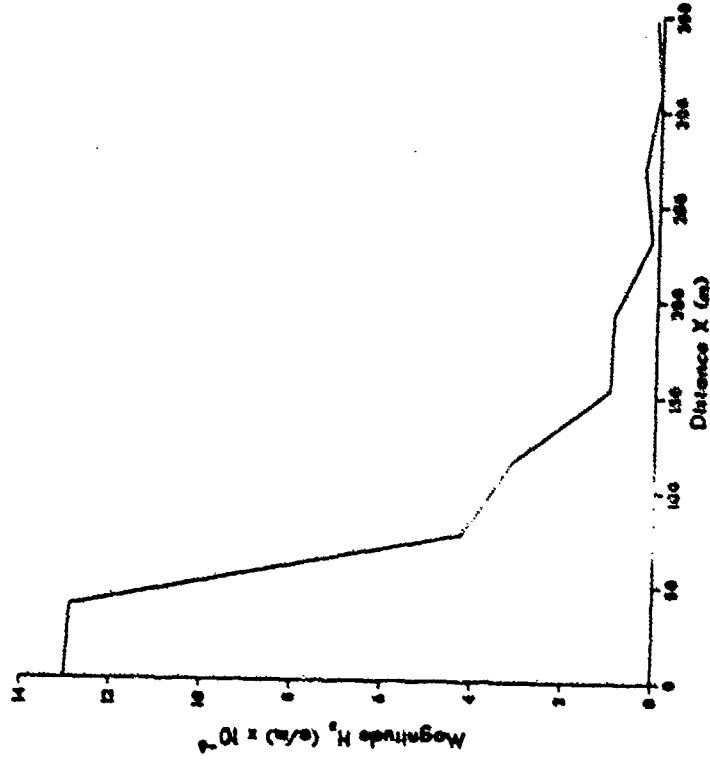
1/2 lambda spacing, switched parallel feed





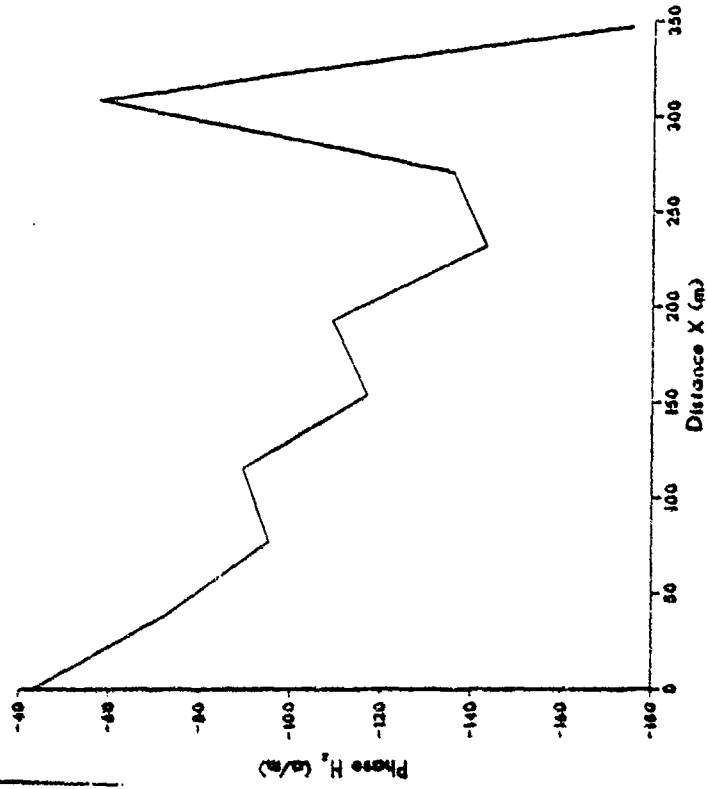
MAGNITUDE 4.38 MHz

1/2 lambda spacing, switched parallel feed



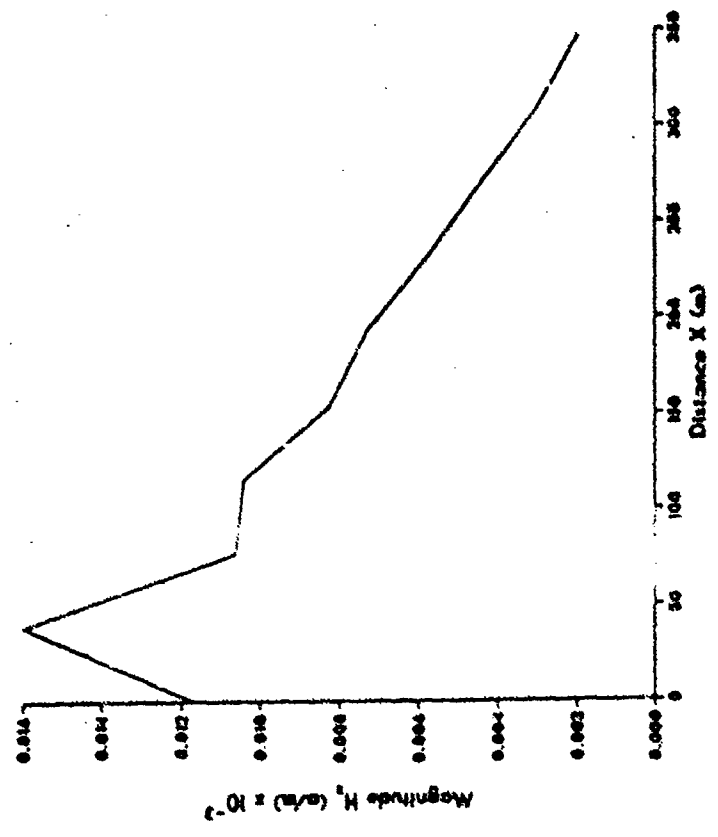
PHASE 4.38 MHz

1/2 lambda spacing, switched parallel feed



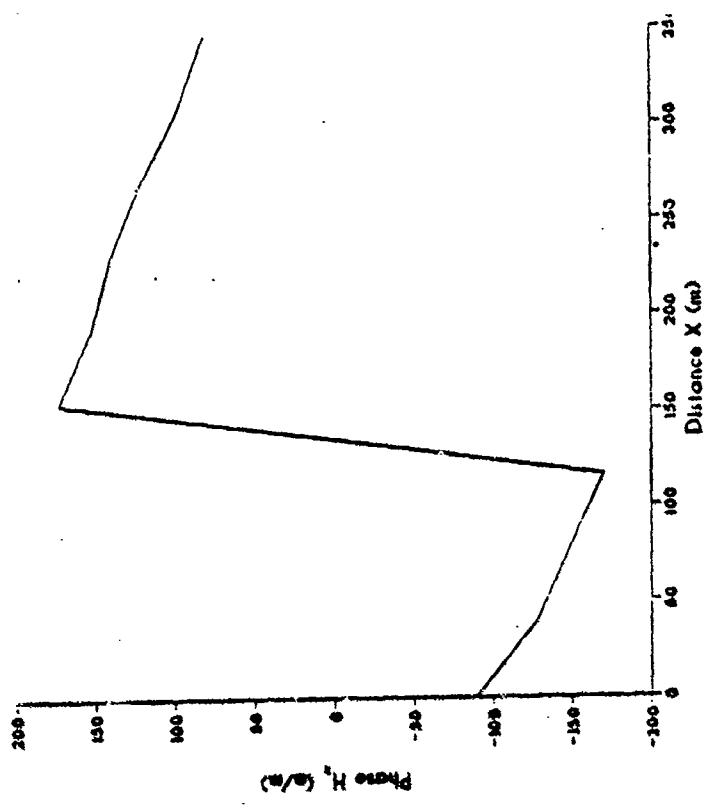
MAGNITUDE 4.88 MHz

1/2 lambda spacing, switched parallel feed



PHASE 4.88 MHz

1/2 lambda spacing, switched parallel feed



## LIST OF REFERENCES

1. Johnson, Richard C. and Jasik, Henry, *Antenna Engineering Handbook*, McGraw-Hill Book Company, New York, 1984.
2. Stutzman, Warren L., and Thiele, Gary A., *Antenna Theory and Design*, John Wiley and Sons, New York, 1981.
3. Rumsey, Victor H., *Frequency Independent Antennas*, Academic Press, New York, 1966.
4. Johnsen, John Richard, *An Investigation into the Potential for Developing a Successful Log-periodic Half Square Antenna with Dual-feed*, MSEE Thesis, Naval Postgraduate School, Monterey, California, December 1986.
5. Snyder, Richard D., *Broadband Antennae Employing Coaxial Transmission Line Sections*, U.S. Patent 4,479,130, 23 October 1984.
6. Naval Ocean Systems Center Technical Document 116 volume 2, *Numerical Electromagnetics Code (NEC)-Method of Moments*, January 1981.
7. Hansen, Robert C., "Evaluation of the Snyder Dipole", *IEEE Transactions on Antennas and Propagation*, vol. AP-35, no. 2, February 1987.
8. Collin, Robert E., and Zucker, Francis J., *Antenna Theory Part 2*, McGraw-Hill Book Company, New York, 1969.
9. Mitra, Raj and Jones, Kenneth E., "How to Use  $k$ - $\beta$  Diagrams in Log-Periodic Antenna Design", *Microwaves*, pp: 18-26, June 1965.

## INITIAL DISTRIBUTION LIST

		No. Copies
1.	Defense Technical Information Center Cameron Station Alexandria, VA 22304-6145	2
2.	Library, Code 0142 Naval Postgraduate School Monterey, CA 93943-5002	2
3.	Dr. J.P. Powers, Code 62 Chairman, Dept. of Electrical and Computer Engineering Naval Postgraduate School Monterey, CA 93943-5000	1
4.	Director Research Administration, Code 012 Naval Postgraduate School Monterey, CA 93943-5000	1
5.	Director, Development Center ATTN: Major P. Dulin, 3-C Division MCDEC Quantico, VA 22134-5080	1
6.	Naval Technical Training Dept. ATTN: RMCM Ken Farwell Keesler AFB, MS 39354-5000	1
7.	Commander 127th Signal Battalion ATTN: ADSO Fort Ord, CA 93941	1
8.	Commander U.S. Army Signal Center and Ft. Gordon ATTN: ATZH-PO-ACS (CPT MAYES) Ft. Gordon, GA 30905-5300	1
9.	U.S. Army DECOM ATTN: AMSEL-RD-COM-TA-1 Ken Loffer) Ft. Monmouth, NJ 07703-5202	1
10.	Air Force Communications and Communication Engineering Institute Center EIE/EIEUS Air Force Base Oklahoma City, OK 73145	1

11. Dr. R. W. Adler, Code 62Ab 8  
Naval Postgraduate School  
Monterey, CA 93943-5000
12. Mr. Harold Askins 1  
NESEC/Charleston  
4600 Goer Road  
N. Charleston, SC 29406
13. Capt. W. P. Averill 1  
U. S. Naval Academy  
Department of Electrical Engineering  
Annapolis, MD 21402
14. Barker and Williamson 1  
ATTN: Sr. Antenna Design Engineer  
10 Canal Street  
Briston, PA 19007
15. Mr. Lawrence Behr 1  
Lawrence Behr Assoc., Inc.  
P.O. Box 8026  
210 W. 4th  
Greenville, NC 27834
16. Mr. Ross Bell 1  
DHV/Antenna Production Division  
P.O. Box 520  
Mineral Wells, TX 76067
17. Mr. J. Belrose 1  
Communication Research Center  
Box 11490, Sta. H  
Ottawa, Ontario, Canada K2H8S2
18. Mr. R.L. Bibey 1  
Comm Engineering Service  
1600 Wilson Blvd. #1003  
Arlington, VA 22209
19. Mr. Edwin Bramel 1  
P.O. Box 722  
Ft. Huachuca, AZ 85613
20. Mr. J. K. Breakall 1  
Lawrence Livermore National Laboratories  
P. O. Box 5504, L-156  
Livermore, CA 94550
21. Mr. D. Campbell 1  
TRW Military Electronics Division  
RC2/265 7x  
San Diego, CA 92128

22. Mr. Al Christman / Rodger Radcliff 2  
Ohio University  
Clippenger Research Laboratory  
Athens, OH 45701
23. Mr. R. Corry 1  
USACEEIA  
CCC-CE-TP  
Ft. Huachuca, AZ 85613
24. Mr. Lee W. Corrington 1  
Commander USAISEIC  
ATTN: ASBI-STS  
Ft. Huachuca, AZ  
85613-7300
25. Dr. Roger A. Cox 1  
TELEX Communications, Inc.  
8601 Northeast Hwy 6  
Lincoln, NE 68505
26. Mr. Pete Cunningham 1  
DRSEL-COM-RN-4  
CENCOM-CENCOMS  
Ft. Monmouth, NJ 07703-5202
27. Mr. W. Decormier 1  
Dielectric Products  
Tower Hill Road  
Raymond, ME 04071
28. Mr. E. Domning 1  
Lawrence Livermore National Laboratory  
P. O. Box 5504, L-153  
Livermore, CA 94550
29. Mr. R.P. Eckert 1  
FED COMM COMM  
2025 M Street, NW  
Washington, D.C. 20554
30. Mr. D. Faust 1  
Eyring Research Institute  
1455 W. 820 N.  
Provo, UT 84601
31. Dr. A.J. Ferraro 1  
Penn State Univ.  
Ionosphere Res. Lab  
University Park, PA 16802
32. D. Fessenden 1  
Naval Underwater Systems Ctr

New London Laboratory  
New London, CT 06320

33. G. H. Hagn 1  
SRI International  
1611 N. Kent Street  
Arlington, VA 22209
34. Mr. R.C. Hansen 1  
Box 215  
Tarzana, CA 91336
35. Mr. Lawrence Harnish 1  
SRI International  
1611 N. Kent Street  
Arlington, VA 22209
36. Mr. J.B. Hatfield 1  
Hatfield & Dawson  
4226 Sixth Avenue, N. W.  
Seattle, WA 98107
37. Jackie Ervin Hipp 1  
S W Research Institute/EMA  
P.O. Drawer 28510  
San Antonio, TX 78284
38. Mr. H. Hochman/MS 4G12 1  
GTE Sylvania  
Box 7188  
Mountain View, CA 94039
39. Mr. R. T. Hoverter 1  
U. S. Army CECOM  
AMSEL-COM-RN-R  
Ft. Monmouth, NJ 07703
40. Mr. Dwight Isbell 1  
Boeing Company  
Box 3999, Mail Stop 47-35  
Seattle, WA 98124
41. Dr. A. Jennetti 1  
ESL Inc.  
Box 510  
Sunnyvale, CA 94086
42. S.W. Kershner 1  
Kershner & Wright  
5730 Gen. Washington Drive  
Alexandria, VA 22312
43. Mr. M. King 1  
Eyring Research Institute

- 1455 W. 820 N.  
Provo, UT 84601
44. H. Kobayashi 1  
1607 Cliff Drive  
Edgewater, MD 21037
45. Dr. H. M. Lee, Code 62Lh 1  
Naval Postgraduate School  
Monterey, CA 93943-5000
46. Mr. George Lane 1  
Voice of America/ESBA  
601 D. Street, NW  
Washington, DC 20547
47. Mr. Jim Lily 1  
Litton/Amecon  
5115 Calvert Road  
College Park, MD 20740
48. Mr. J. Logan, Code 822 (T) 1  
Naval Ocean System Center  
271 Catalina Boulevard  
San Diego, CA 92152
49. R. Luebbers 1  
Penn State University  
EE Department  
University Park, PA 16802
50. Ms. Janet McDonald 1  
USAISESA  
ASBH-SET-P  
Ft. Huachuca, AZ 85613-5300
51. Mr. B. John Meloy 1  
333 Ravenswood /Bldg. G  
Menlo Park, CA 94025
52. E.K. Miller 1  
Rockwell Science Center  
Box 1085  
Thousand Oaks, CA 91365
53. Mr. L.C. Minor 1  
IIT Research Inst./ECAC  
185 Admiral Cochrane Dr.  
Annapolis, MD 21401
54. J. Molnar 1  
Space and Naval Warfare Systems Command  
Code G141  
National Center #1



- Washington, DC 20363
55. Mr. Wes Olsen 1  
2005 Yacht Defender  
Newport Beach, CA 92660
56. Mr. D. J. Pinion 1  
74 Harper Street  
San Francisco, CA 94131
57. C.E. Poole 1  
FCC/Field Póns Bur  
555 Battery Street Rm. 323A  
San Francisco, CA 94111
58. Mr. J. J. Reaves Jr. 1  
Naval Elec. System Engineering Center  
4600 Marriott Drive  
N. Charleston, SC 29413
59. Mr. A. Resnick 1  
Capital Cities Communication / ABC Radio  
1345 Avenue of Americas / 26th Floor  
New York, NY 10705
60. R.B. Riegel 1  
8806 Crandall Road  
Lanham, MD 20801
61. Dr. J. W. Rockway, Code 8112 (T) 1  
Naval Ocean System Center  
271 Catalina Boulevard  
San Diego, CA 92152
62. Mr. Joseph R. Romanosky 1  
National Security Agency/R632  
Electronic Engineer  
Ft. Meade, MD 20755
63. R. Royce 1  
Naval Research Laboratory  
Washington, DC 20375
64. Dr. Jacob Z. Schanker 1  
Scientific Radio Systems  
367 Orchard Street  
Rochester, NY 14606
65. Mr. T.B. Sullivan 1  
108 Market Street  
Newburgh, IN 47630
66. T. Simpson 1  
Univ. of S. Carolina  
College of Engineering

- Columbia, SC 29208
67. Mr. N. Skousen 1  
Zyring Research Institute Inc.  
1455 W. 820 N.  
Provo, UT 84601
  68. Space and Naval Warfare Systems Command 1  
Code PD70-33C  
National Center #1  
Washington, DC 20363
  69. Dr. Eric Stoll, P.E. 1  
117 Hillside Ave.  
Teaneck, NJ 07666
  70. Mr. W. D. Stuart 1  
IIT Research Institute  
185 Admiral Cochrane Drive  
Annapolis, MD 21402
  71. Sylvania Systems Group/West Division 1  
100 Ferguson Drive  
Mountain View, CA 94042
  72. Mr. L.J. Blum/R. Tanner 2  
Technology Communications Intl.  
1625 Stierlin Road  
Mountain View, CA 94043
  73. Mr. R.E. Tarleton, Jr. 1  
1152 E. 12th Street  
Casa Grande, AZ 85222
  74. E. Thowless 1  
NOSC Code 822 (T)  
271 Catalina Blvd.  
San Diego, CA 92152
  75. Mr. W.R. Vincent 1  
Code 62Ja  
Naval Postgraduate School  
Monterey, CA 93943-5000
  76. Mr. Robert Word 1  
Technology Communications Intl.  
1625 Stierlin Road  
Mountain View, CA 94043